AIRCRAFT ACCIDENT

FINAL REPORT

A 03/24

Air Accident Investigation Bureau (AAIB)

Ministry of Transport Malaysia

Fixed-Wing Aircraft Blackshape BK 160TR, Registration I-POOC

at Kapar, Selangor

on 13 February 2024

Air Accident Investigation Bureau
Ministry of Transport
No. 26, Jalan Tun Hussein, Precinct 4
Federal Government Administrative Centre
62100 PUTRAJAYA
Phone: +603-8892 1072
Fax: +603-8888 0163
E-mail: AAIB@mot.gov.my
Website: http://www.mot.gov.my/en

Issued on 7 April 2025
MOT.(S).600-5/4/104

AIR ACCIDENT INVESTIGATION BUREAU (AAIB)
MALAYSIA

FINAL REPORT NO: A 03/24

OPERATOR	**: AVIATION SAFETY TECHNOLOGY PTE LTD, SINGAPORE (PRIVATE OPERATOR)**[1]
AIRCRAFT TYPE	**: BLACKSHAPE BK 160TR**
NATIONALITY	**: ITALY**
REGISTRATION	**: I-POOC**
PLACE OF OCCURRENCE	**: KAMPUNG TOK MUDA, KAPAR, SELANGOR MALAYSIA**
DATE AND TIME	**: 13 FEBRUARY 2024 AT 1336 LT (0536 UTC)**

The sole objective of the investigation is the prevention of accidents and incidents. In accordance with Annex 13 to the Convention on International Civil Aviation, it is not the purpose of this investigation to apportion blame or liability.

All times in this report are Local Time (LT) unless stated otherwise. LT is Coordinated Universal Time (UTC) + 8 hours.

[1] Aviation Safety Technology Pte Ltd (AST) is a private operator based in Singapore. AST does not hold any certificate or approval from the Civil Aviation Authority of Malaysia (CAAM) as an aircraft operator under Malaysian regulations. Furthermore, as far as can be determined, AST does not hold an operator certificate from the civil aviation authorities of Singapore or any other country.

For convenience, AST will be referred to as the operator of the aircraft throughout this report. This reference does not imply ownership of the I-POOC aircraft.

INTRODUCTION

The Air Accident Investigation Bureau (AAIB) is the authority responsible for investigating air accidents and incidents in Malaysia, operating under the Ministry of Transport. The AAIB's mission is to promote aviation safety through independent and objective investigations into air accidents and serious incidents.

All investigations by the AAIB are conducted in accordance with Annex 13 to the Convention on International Civil Aviation (ICAO Annex 13) and the Civil Aviation Regulations 2016. It is important to note that AAIB reports are not intended to apportion blame or determine liability, as neither the investigations nor the reporting processes are designed for those purposes. The sole objective of this investigation and the Final Report is the prevention of accidents and incidents.

In accordance with ICAO Annex 13, the accident was notified to the *Agenzia Nazionale per la Sicurezza del Volo* (ANSV) of Italy, as the State of Registry, Design, and Manufacture, on 14 February 2024. The Preliminary Report was submitted on 13 March 2024 to ANSV, the Civil Aviation Authority of Malaysia (CAAM), and the aircraft operator, and was also shared with the United States National Transportation Safety Board (NTSB), which provided technical assistance. The Draft Final Report was sent on 21 November 2024 to these organisations, inviting significant and substantiated comments. The initial 60-day consultation period was set to end on 20 January 2025 but was extended to 19 February 2025 due to delays and multiple extension requests. An Interim Statement was issued on 13 February 2025, marking the accident's anniversary and updating the investigation's progress. Following this, a further request extended the consultation period to 26 March 2025.

The AAIB extends its deepest appreciation to the ANSV and NTSB for their valuable technical assistance in the investigation of this accident.

Unless otherwise indicated, recommendations in this report are addressed to the investigating or regulatory authorities of the State responsible for the matters concerning the recommendations. It is up to those authorities to decide what actions to take.

TABLE OF CONTENTS

LIST OF APPENDICES

GLOSSARY OF ABBREVIATIONS

A

AAIB	Air Accident Investigation Bureau
AAFC	Air Adventure Flying Club
Accrep	Accredited Representative
AD	Airworthiness Directive
ADS-B	Automatic Dependent Surveillance–Broadcast
ANSV	*Agenzia Nazionale per la Sicurezza del Volo* (National Agency for the Safety of Flight) (Italy)
ARC	Airworthiness Review Certificate
Arr	Arrival
AST	Aviation Safety Technology Pte Ltd (Singapore)
ATC	Air Traffic Control
AVGAS	Aviation Gasoline

B

baro	Barometer
BAC	Blood Alcohol Concentration
BrAC	Breath Alcohol Concentration

C

C	Celsius
CAAM	Civil Aviation Authority Malaysia
CAMO	Continuing Airworthiness Management Organisation
CAS	Calibrated Airspeed
CFRP	Carbon Fibre Reinforced Plastic
CHT	Cylinder Head Temperature
CO	Carbon Monoxide
CoA	Certificate of Airworthiness
COHb	Carboxyhaemoglobin
CPL (A)	Commercial Pilot Licence (Aeroplane)
CS-VLA	Certification Specification – Very Light Aircraft
CVR	Cockpit Voice Recorder

D

deg	degree
Demo	Demonstration
Dept	Departure
DETRESFA	Distress Phase (ICAO emergency phase)
DGAC	*Direction Générale de l'Aviation Civile* (Directorate General of Civil Aviation) (France)
DSC	Differential Scanning Calorimetry

E

E	East
EAD	Emergency Airworthiness Directive
EAS	Equivalent Airspeed
EASA	European Union Aviation Safety Agency
EDNY	Friedrichshafen Airport, Germany
EFIS	Electronic Flight Instrument System
EGT	Exhaust Gas Temperature
ENAC	*Ente Nazionale per l'Aviazione Civile* (Italian Civil Aviation Authority)

F

F	Fahrenheit
FDR	Flight Data Recorder
FI (A)	Flight Instructor (Aeroplane)
FIS N	Flight Information Service North
Flt	Flight
FR24	Flightradar24
ft	feet
FTIR	Fourier Transform Infrared
FWD	Forward

G

g	Measurement unit for force per unit mass
G/S	Ground speed
GH	General Handling
GPS	Global Positioning System

I

IATA	International Air Transport Association
IAS	Indicated Airspeed
ICAO	International Civil Aviation Organisation
IFR	Instrument Flight Rules
IR	Instrument Rating
IR/SE	Instrument Rating/Single-Engine

J

JBPM	*Jabatan Bomba Dan Penyelamat Malaysia* (Fire and Rescue Department of Malaysia)

K

kg	kilogramme
KIAS	Knots Indicated Airspeed
KLATCC	Kuala Lumpur Air Traffic Control Centre
kts	knots (nautical miles per hour)

L

L/l	litres
lbs	pounds
LDG	Landing
LG	Landing Gear
LH	Left-Hand
LIBD	Bari Karol Wojtyła Airport. Italy
LIBG	Taranto-Grottaglie Airport, Italy
LIKO	Guglielmo Zamboni Airfield, Italy
LT	Local Time

M

m	metre
MAC	Mean Aerodynamic Chord
Max	Maximum
MCP	Maximum Continuous Power
MEP Land	Multi-Engine Piston Aeroplane
METAR	Meteorological Aerodrome Report
MLG	Main Landing Gear
mm	millimetre
MOR	Mandatory Occurrence Report
MTOW	Maximum Take-off Weight

N

N	North
n	Load Factor
NDI	Non-Destructive Inspection
NLG	Nose Landing Gear
NOSAS	Non-Scheduled Application System (CAAM)
NTSB	National Transportation Safety Board (United States of America)

O

OEM	Original Equipment Manufacturer
OSHA	Occupational Safety and Health Administration

P

Pax	Passenger
Perf	Performance
P/N	Part Number
POB	Persons on Board
ppm	parts per million
PPL	Private Pilot License

R

RH	Right-Hand
ROI	Region of Interest
RPM	Revolution per Minute
RWD	Rear

S

SEM	Scanning Electron Microscopy
SEP Land	Single-Engine Piston Aeroplane
SIB	Safety Information Bulletin
S/N	Serial Number
S.p.A.	*Società per Azioni* (Joint-Share Company) (Italy)
SZB	Sultan Abdul Aziz Shah Airport, Subang (IATA Designator)

T

TA	Technical Advisor
TAS	True Airspeed
temp	temperature
T_g	Glass Transition Temperature
TGA	Thermogravimetric Analysis
T/O	Take-off
TOW	Take-off Weight

U

und	Undetermined
unk	Unknown
UTC	Coordinated Universal Time

V

V_A	Design Manoeuvring Speed
$V_{FE\text{-}LND}$	Maximum Flaps Extended Speed
$V_{FE\text{-}T/O}$	Maximum Flaps Take-Off Speed
V_{LE}	Maximum Speed with Landing Gear Extended
V_{LO}	Maximum Speed for Landing Gear Operation
V_{NE}	Never Exceed Speed
V_{NO}	Maximum Structural Cruising Speed
VDL	Valid only with correction for defective distant vision
VFR	Visual Flight Rules
VLA	Very Light Aircraft
VTBD	Don Mueang International Airport, Bangkok, Thailand
VTCC	Chiang Mai International Airport, Thailand

VTPH	Hua Hin Airport, Thailand
VTPP	Phitsanulok Airport, Thailand
VTSB	Surat Thani International Airport, Thailand
VTSP	Phuket International Airport, Thailand
VTSS	Hat Yai International Airport, Thailand
VTSW	Phuket Airpark, Thailand
VYNT	Naypyidaw International Airport, Myanmar

W

WIDD	Hang Nadim International Airport, Batam, Indonesia
WIDN	Raja Haji Fisabilillah Airport, Tanjungpinang, Indonesia
WIHH	Halim Perdanakusuma International Airport, Jakarta, Indonesia
WIPP	Sultan Mahmud Badaruddin II Airport, Palembang, Indonesia
WMSA	Sultan Abdul Aziz Shah Airport, Subang
WMKI	Sultan Azlan Shah Airport, Ipoh
WMKP	Penang International Airport
WMKJ	Senai International Airport
WSSL	Seletar Airport, Singapore
w/v	Wind Velocity

Z

ZZZZ	Chiang Mai Air Sports Airfield (nominal designation in this report)

SYNOPSIS

On 13 February 2024, at approximately 1328 LT, a Blackshape Gabriél BK 160TR, bearing the registration mark I-POOC, with the callsign ADV429 and operated by Aviation Safety Technology Pte Ltd (AST), Singapore, departed Sultan Abdul Aziz Shah Airport (WMSA), Subang, Selangor, Malaysia, for a recreational flight to the area west of Kapar. The flight was routine until about 1336 LT, when ADV429 tragically crashed into a small oil palm plantation located at the village of Kampung Tok Muda, near Kapar, Selangor. The aircraft was destroyed upon impact with ground, and both occupants on board sustained fatal injuries.

As required by regulations, a Mandatory Occurrence Report (MOR) was submitted by AST, the operator of the aircraft, to the Air Accident Investigation Bureau (AAIB) Malaysia, officially notifying them of the accident. In addition, the Civil Aviation Authority of Malaysia (CAAM) also submitted a MOR to the AAIB to provide formal notification of the event. This triggered an immediate investigation into the circumstances of the crash.

1.0 FACTUAL INFORMATION

1.1 History of the Flight

At approximately 1300 LT, ADV429 filed a flight plan for a recreational flight, departing from Sultan Abdul Aziz Shah Airport (WMSA) to the area west of Kapar, with an expected flight duration of about one hour before returning to WMSA. The aircraft had two persons on board (POB) and was reported to have a flight endurance of 3.5 hours.

Earlier that morning, the pilot and passenger had flown together, completing two dual flights on a Piper PA28 aircraft under the callsign ADV891. In addition, the passenger performed a solo flight between the two dual flights. The pilot, a flight instructor at the Air Adventure Flying Club (AAFC), was providing instruction to the passenger, who was a student pilot (callsign ADV891). The third and final ADV891 flight of the day landed at WMSA at 1152 LT.

ADV429, with the pilot and the passenger onboard, departed WMSA at 1328 LT. The aircraft was cleared for take-off from Runway 15, with instructions to turn right after departure and climb to 1,500 feet. At 1335 LT, ADV429 reported to the Flight Information Service North (FIS N), the air traffic service unit responsible for the area, that it was operating at 1,500 feet and below, west of Kapar. This was the last radio transmission from ADV429; no distress call was received.

At 1357 LT, the Subang Tower controller at WMSA was informed by the Malaysian Fire and Rescue Department (JBPM) that an aircraft had crashed near Kapar. Subang Tower immediately notified FIS N of the report. Despite multiple attempts by FIS N to re-establish contact with ADV429, no response was received. At 1411 LT, DETRESFA (Distress Phase) was declared by FIS N.

The wreckage of ADV429 was discovered in a small oil palm plantation in Kampung Tok Muda, Kapar (coordinates 3° 07' 56.9"N, 101° 20' 18.7"E). Both the pilot and the passenger sustained fatal injuries.

1.1.1 Flight Path

The flight path of ADV429 was reconstructed using Automatic Dependent Surveillance –Broadcast (ADS-B) data[2], Air Traffic Control (ATC) radar data[3], and Garmin G3X GDU 460 flight display data[4], as shown in Figure 1.

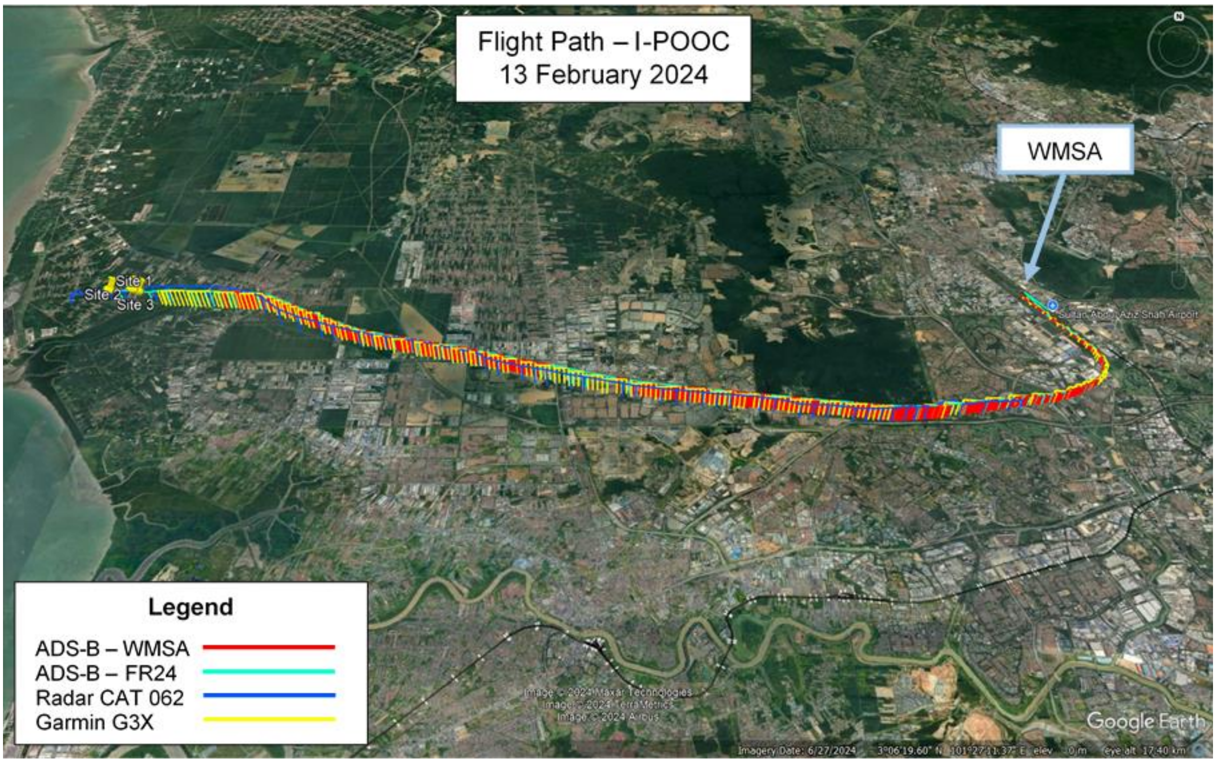

Figure 1. ADV429 Flight Path

The flight paths from all four data sources are well-aligned. Although the Garmin G3X display shows a jagged path due to unsmoothed data points, its overall trajectory is consistent with the other sources.

According to the data, after departing WMSA, ADV429 turned westward towards Kapar, maintaining an altitude of about 1,500 feet (+/- 200 feet). The Garmin G3X recording stopped at 13:35:52 LT, capturing a rapid descent of 2,830 feet per minute, with an increasing airspeed of 155 KIAS (145 knots ground speed) as the aircraft

[2] Sources: ADS-B WMSA and ADS-B Flightradar24 (FR24).

[3] Kuala Lumpur Air Traffic Control Centre (KLATCC) fused radar data (CAT 062).

[4] Recovered flight data from the rear Garmin G3X GDU 460 retrieved from the aircraft wreckage.

descended to 1,367 feet.[5] At this point, the aircraft was heading 279°, with wind velocity at 287/09. Due to data buffering on the G3X device, the final seconds of the flight were not captured.

ADS-B data from Flightradar24 (FR24) recorded two additional data points after the G3X recording ceased: at 13:35:54 LT, the aircraft was at an altitude of 1,250 feet with a ground speed of 150 knots on a track of 276°; and at 13:36:04 LT, it was at 1,150 feet, 139 knots, on a track of 277°.

The ATC radar (CAT 062) plots beyond the point where the other data sources terminate—particularly those beyond the aircraft's ground impact point—are considered unreliable, as these fused data plots were generated by the ATC radar system algorithm after the aircraft's transponder transmission was lost.

The following Figures 2 dan 3 illustrate the final phase of the flight with locations of where the wreckage and debris were found.

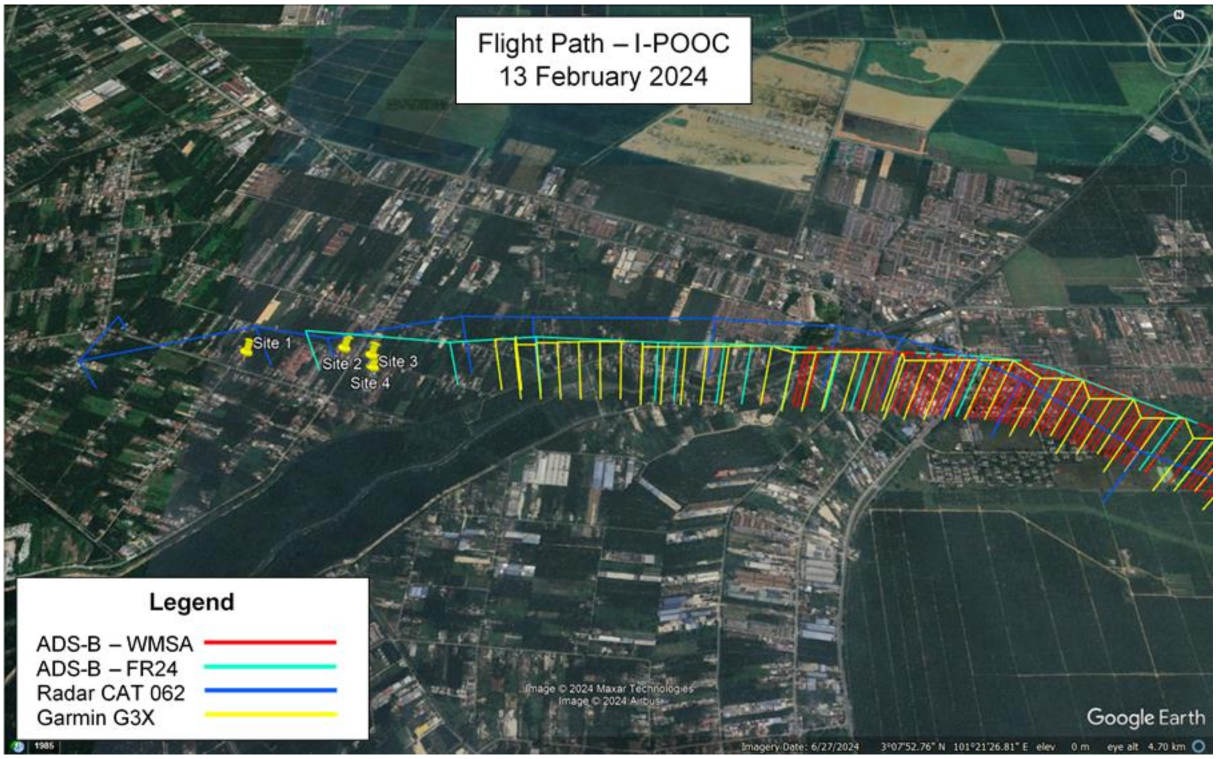

Figure 2. Final Phase of Flight and Wreckage/Debris Locations

[5] Pressure altitude is used for consistent comparison with ADS-B altitude data.

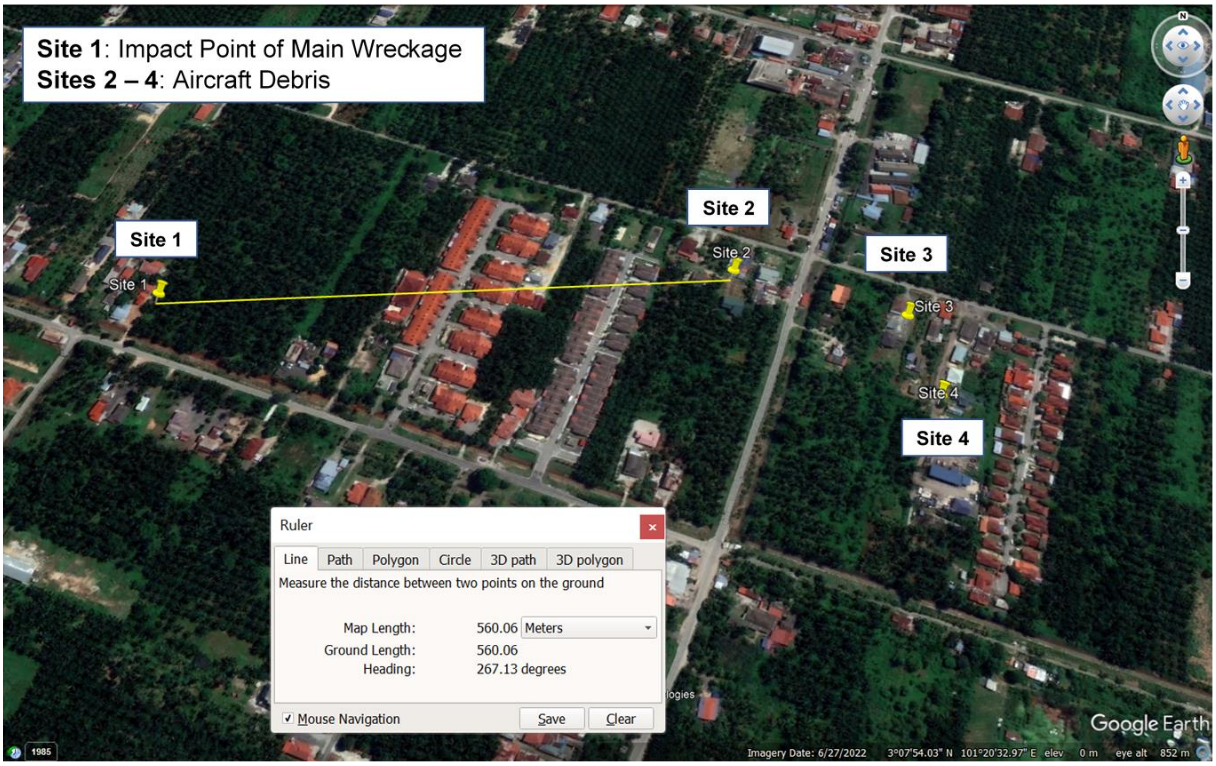

Figure 3. Wreckage and Debris Locations

1.1.2 Wreckage and Debris Distribution

Figures 4 to 7 show the locations of the wreckage and debris. Site 1 marks the location of the main wreckage, including the bodies of the pilot and passenger. Sites 2 to 4 are within an area approximately 250 to 300 metres in diameter, where various aircraft debris were scattered. Before investigators arrived, most of the scattered debris were found by local villagers, who had collected and pooled much of it, particularly at Sites 3 and 4. Site 2, the closest of the three debris sites to the main wreckage, is located about 560 metres east of Site 1.

Site 1. Oil Palm Plantation – Main Wreckage – 3° 07' 56.9"N 101° 20' 18.7"E

Figure 4. Site 1

Site 2. Next to House Kitchen – Right Wing – 3°07'57.8"N 101°20'36.8"E

Figure 5. Site 2

Site 3. Uninhabited House – Various Debris & Cap – 3°07'56.1"N 101°20'42.1"E

Figure 6. Site 3

Site 4. Front of House – Left Wing Parts – 3°07'53.3"N 101°20'42.7"E

Figure 7. Site 4

1.1.3 Flight and Engine Parameters

Figures 8 to 11 illustrate the plots of the aircraft’s basic flight and engine parameters during the flight on 13 February 2024.[6] These charts were generated using data recovered from the aircraft’s rear Garmin G3X GDU 460 flight display, retrieved from the wreckage at the crash site. The flight data was recovered with assistance from the Vehicle Recorder Laboratory of the National Transportation Safety Board (NTSB). Details of the flight data recovery process are provided in Section 1.11.

[6] The flight and engine parameter data, as well as the charts, are extracted from the NTSB Specialist’s Factual Report on the Cockpit Display – Recorded Flight Data (ENG24WA011), dated 26 June 2024. The plots in Figures 8 to 11 are provided with the courtesy of the NTSB.

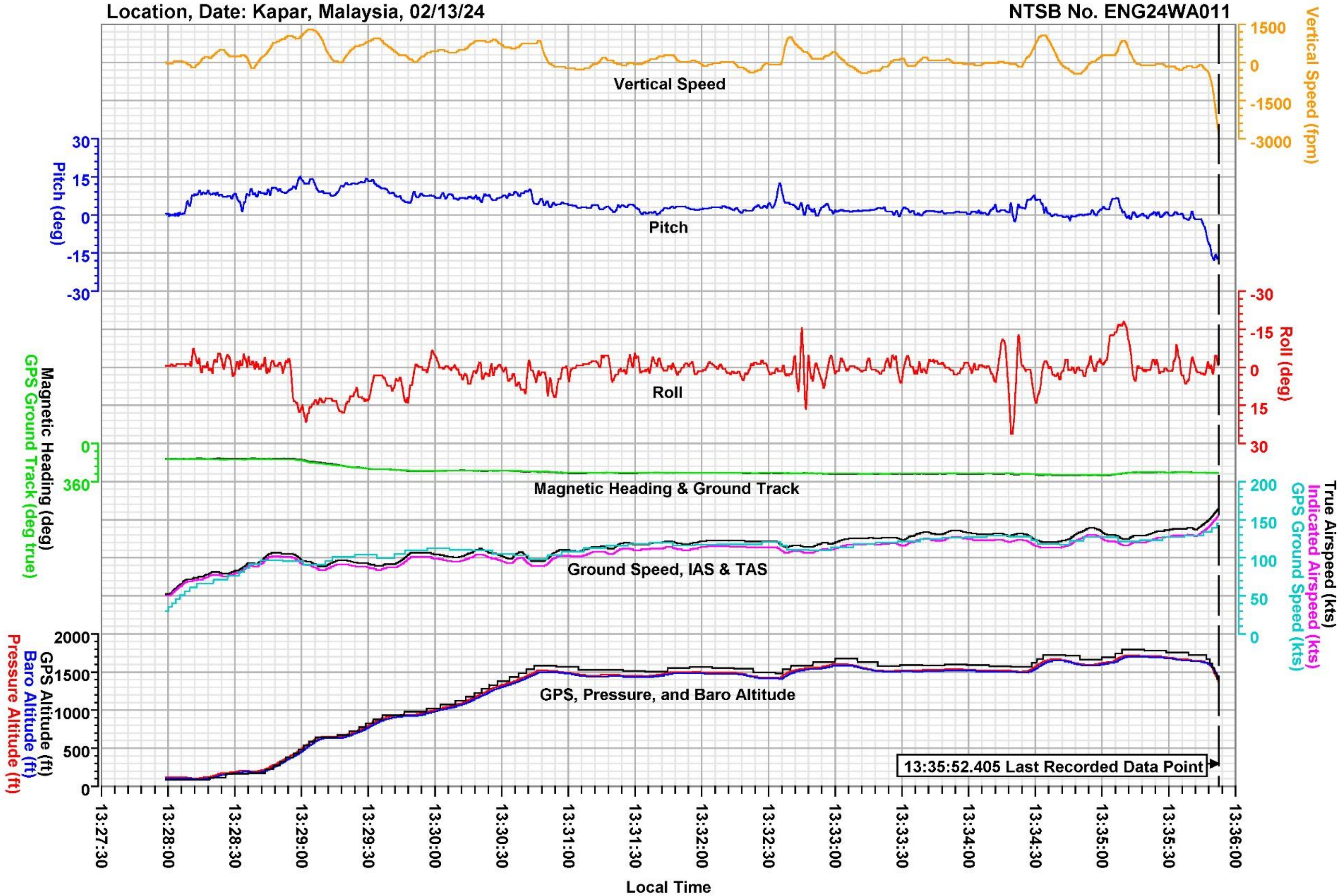

Figure 8. Plot of Basic Parameters for the Entire Accident Session (Courtesy of the NTSB)

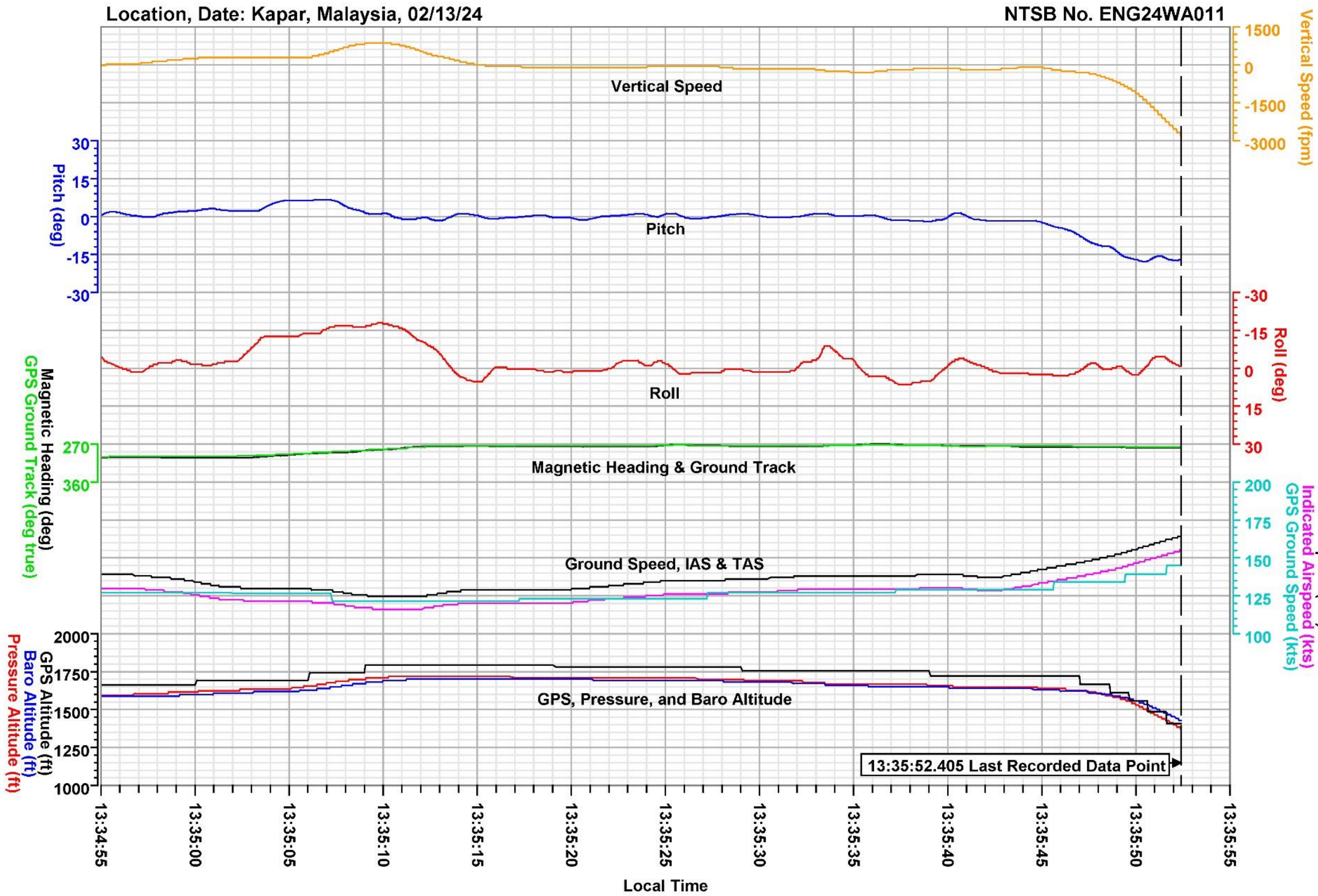

Figure 9. Plot of Basic Parameters at the End of the Accident Session (Courtesy of the NTSB)

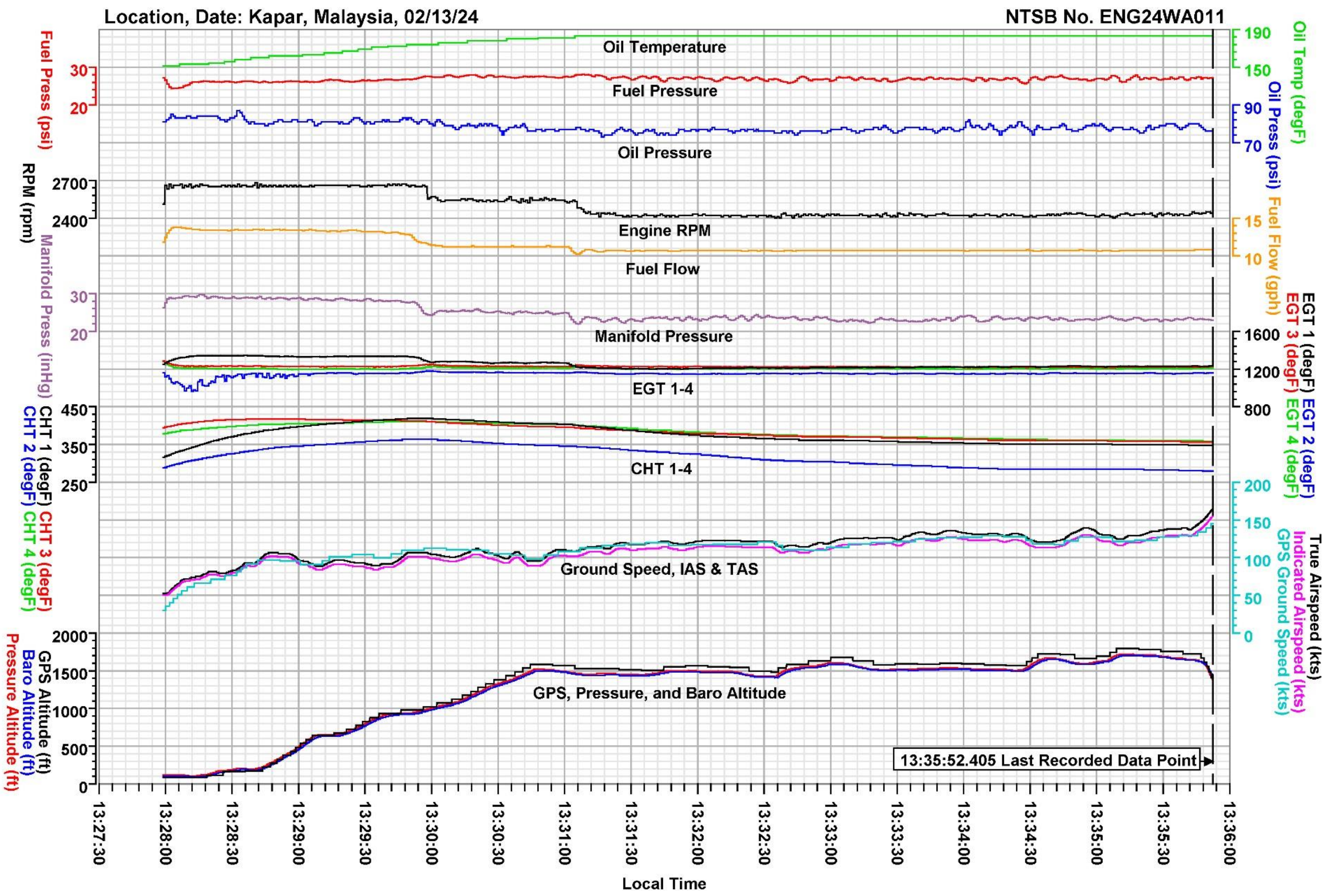

Figure 10. Plot of Engine Parameters for the Entire Accident Session (Courtesy of the NTSB)

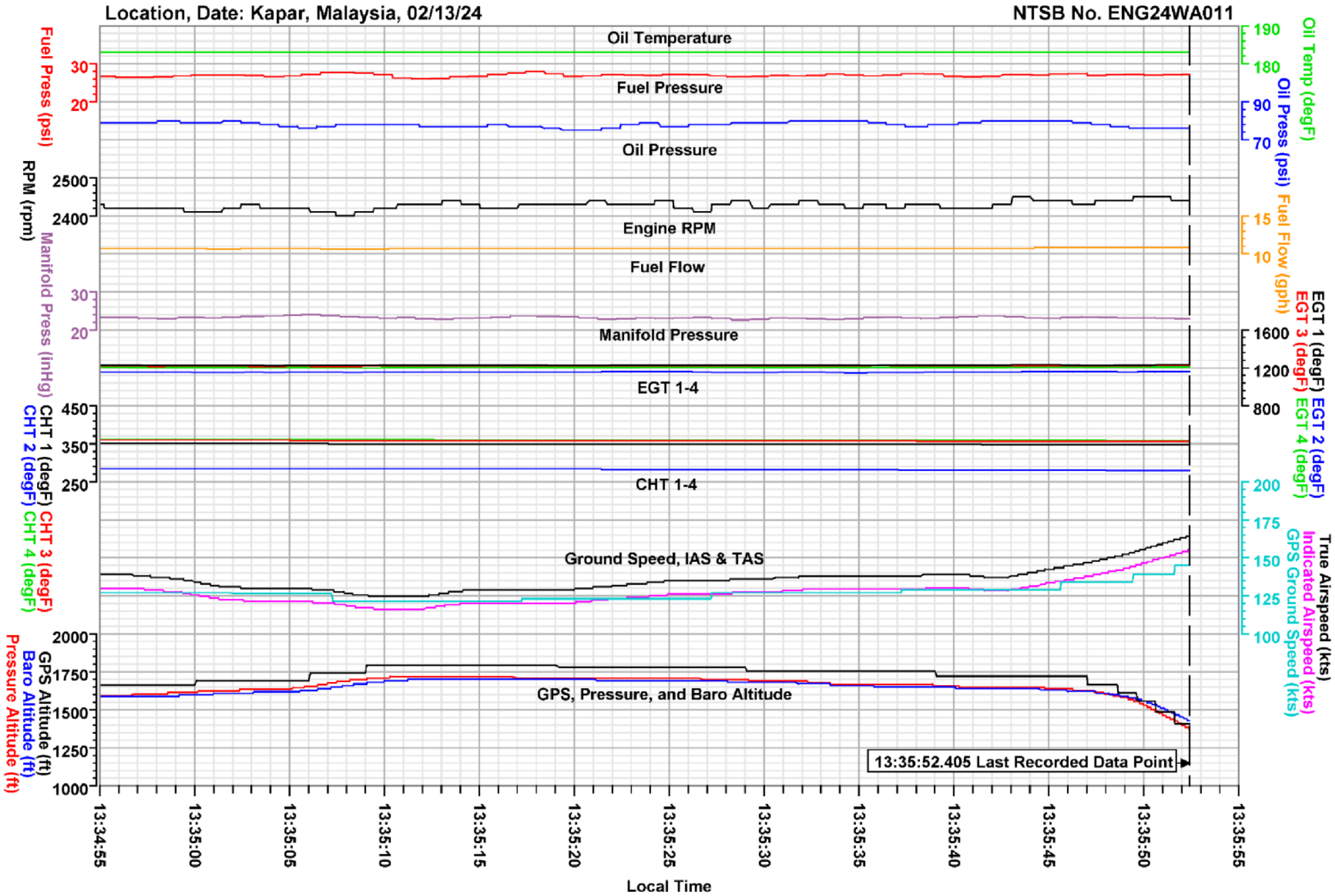

Figure 11. Plot of Engine Parameters at the End of The Accident Session (Courtesy of the NTSB)

1.2 Injuries to Persons

Injuries	Crew	Passengers	Others	Total
Fatal	1	1	-	**2**
Serious	-			**-**
Minor/None	-	-	-	**-**
Total	**1**	**1**	**-**	**2**

Table 1. Injuries to Persons

1.3 Damage to Aircraft

The aircraft was destroyed. A damage assessment of the I-POOC was conducted following the accident, with assistance from the Accredited Representative (Accrep) from the National Agency for the Safety of Flight, Italy (ANSV), and three Technical Advisers (TA) from Blackshape S.p.A. The team was dispatched from Italy to Kuala Lumpur, Malaysia, to provide technical assistance for the investigation. The report on the damage assessment is included in **Appendix A**.

1.4 Other Damage

Minor damage occurred to the oil palm plantation, with some oil palm trees damaged at the main wreckage impact site. Otherwise, there was no notable damage to public or private property, nor any significant impact on the environment.

1.5 Personnel Information

1.5.1 Pilot

Nationality	Malaysian
Age	30
Gender	Male

License Type	CPL (A) by DGAC France Issued on 2 February 2021	
Medical Certificate	Class 1 Issued on 3 May 2023 Expiry on 31 May 2024	
Aircraft Ratings	MEP Land (Including IR) valid until 30 November 2023 SEP Land valid until 30 November 2024 IR/SE valid until 30 November 2023	
Instructor Rating	FI (A) valid until 30 November 2024	
Flying Hours	Total Hours	1680.0 hours
	Total on Type (BK 160TR)	80.1 hours
	Last 24 Hours	6.0 hours
	Last 7 Days	33.5 hours
	Last 90 Days	211.8 hours

Table 2. Personnel Information – Pilot

At the time of the accident, the pilot held a valid CPL (A) licence with an SEP Land rating and was appropriately endorsed by a test pilot from Blackshape S.p.A., the manufacturer, to operate the BK 160TR. Thus, he was properly licensed and qualified to operate this aircraft. However, the pilot's IR/SE had expired on 30 November 2023, yet he had filed IFR flight plans for I-POOC flights after this expiry date.

Additionally, the pilot held a valid FI (A) rating, qualifying him to conduct flight instruction on the Piper PA28 and Cessna 172; however, he was not certified to instruct on the BK 160TR, nor did he hold an aerobatic rating.

1.5.2 Passenger

The 42-year-old passenger was a student pilot in training for a Private Pilot Licence (PPL) at the AAFC. On the morning of the accident flight, he had flown three flights, including two dual flights with his assigned flight instructor—the pilot of ADV429—and one solo flight, all under his personal AAFC callsign, ADV891. The pilot of ADV429 was the passenger's sole flight instructor at AAFC.

The passenger had accumulated a total of 27.6 hours on the Piper PA28 aircraft. To the best of available knowledge, the passenger had not flown on the BK 160TR prior to the accident flight.

1.6 Aircraft Information

1.6.1 Aircraft General Information

The BK 160TR aircraft (S/N BCV.21010) was manufactured in Italy by Blackshape S.p.A. and registered in Italy under the registration mark I-POOC on 2 August 2022 (refer to **Appendix B**). The aircraft was exported and shipped to Singapore in October 2022 and subsequently transferred from Singapore to Malaysia in July 2023.

In addition to operations in Singapore and Malaysia, the aircraft had also undertaken long-distance trips with multiple stops in Myanmar and Thailand, as well as an aborted trip to the Philippines, during which the aircraft returned to Kuala Lumpur after encountering an in-flight fuel transfer indication system issue in Indonesian airspace. The aircraft was scheduled to participate in the Singapore Airshow 2024 in February 2024. Prior to the accident, it had logged approximately 85.5 total flight hours.

Aircraft Type / Model	Blackshape BS 115 / BK 160TR
Manufacturer	Blackshape S.p.A.
Year of Manufacture	2022
EASA Type Certification	14 June 2022
Owner	Blackshape S.p.A.
Certificate of Registration	Issued on 2 August 2022
Registration Number	I-POOC
Aircraft Serial Number	BCV.21010

Certificate of Airworthiness	Issued on 26 August 2022
Airworthiness Review Certificate	Issued on 18 October 2023 Expiry on 18 October 2024
Total Flight Hours	85.5 hours

Table 3. Aircraft General Information

The BK 160TR is a single-engine, low-wing monoplane with a tandem two-seat layout. It has retractable landing gear, a variable-pitch, constant-speed propeller, and a 160 shp Lycoming IO-320 engine, giving a maximum structural cruise speed of 155 KIAS.

Its airframe, constructed from Carbon Fibre Reinforced Plastic (CFRP), offers a combination of lightness and durability. Certified as a Very Light Aircraft (CS-VLA) by the European Union Aviation Safety Agency (EASA), the BK 160TR is primarily designed for recreational, light sport flying and limited training purposes. It is not certified for aerobatics.

The aircraft's Garmin G3X glass cockpit offers comprehensive flight and engine data for improved situational awareness for pilots, though the CS-VLA certification restricts its operation to specific weather and flight conditions.

1.6.2 General Technical Data and Operational Limitations

<table>
<tr><td>Aircraft Dimensions</td><td colspan="2">Span: 9.000 m (29.53 ft)
Length: 7.437 m (24.40 ft)
Height: 2.455 m (8.05 ft)
Wing Area: 10.31 m^2 (111.00 ft^2)</td></tr>
<tr><td rowspan="5">Load Factors</td><td>Flaps UP/Landing Gear UP</td><td>Flaps EXTENDED/T/O & Land</td></tr>
<tr><td colspan="2">Symmetric Flight</td></tr>
<tr><td>Max positive: +4.4 g
Max negative: -2.0 g</td><td>Max positive: +2.0 g
Max negative: 0 g</td></tr>
<tr><td colspan="2">Asymmetric / Rolling</td></tr>
<tr><td>Max positive: +2.9 g
Max negative: 0 g</td><td>Max positive: +1.3 g
Max negative: 0 g</td></tr>
</table>

Air Speeds	Never Exceed Speed (V_{NE}): 180 KIAS Max. Structural Cruising Speed (V_{NO}): 155 KIAS Design Manoeuvring Speed (V_{A}): 128 KIAS Max. speed with landing gear extended (V_{LE}): 115 KIAS Max. speed for landing gear operation (V_{LO}): 115 KIAS Max. flaps extended speed ($V_{FE\text{-}LND}$): 105 KIAS Max. flaps take-off speed ($V_{FE\text{-}T/O}$): 115 KIAS
Maximum Operating Altitude	11,500 ft – Density Altitude
Maximum Masses	Max. Take-off: 850 kg (1874 lbs) Max. Landing: 850 kg (1874 lbs)
Centre of Gravity Range	23% MAC – 28.5% MAC at 850 Kg 19% MAC – 28.5% MAC at 800 Kg
Mean Aerodynamic Chord	1360.26 mm (4,46 ft)
Datum	800 mm aft of composite bulkhead. 165 mm up from airplane fuselage centreline.
Minimum Flight Crew	1 pilot seated at the front seat
Maximum Passenger Seating Capacity	1
Baggage/Cargo Compartment	33 kg capacity, 2.5 m aft of datum

Table 4. General Technical Data and Operational Limitations

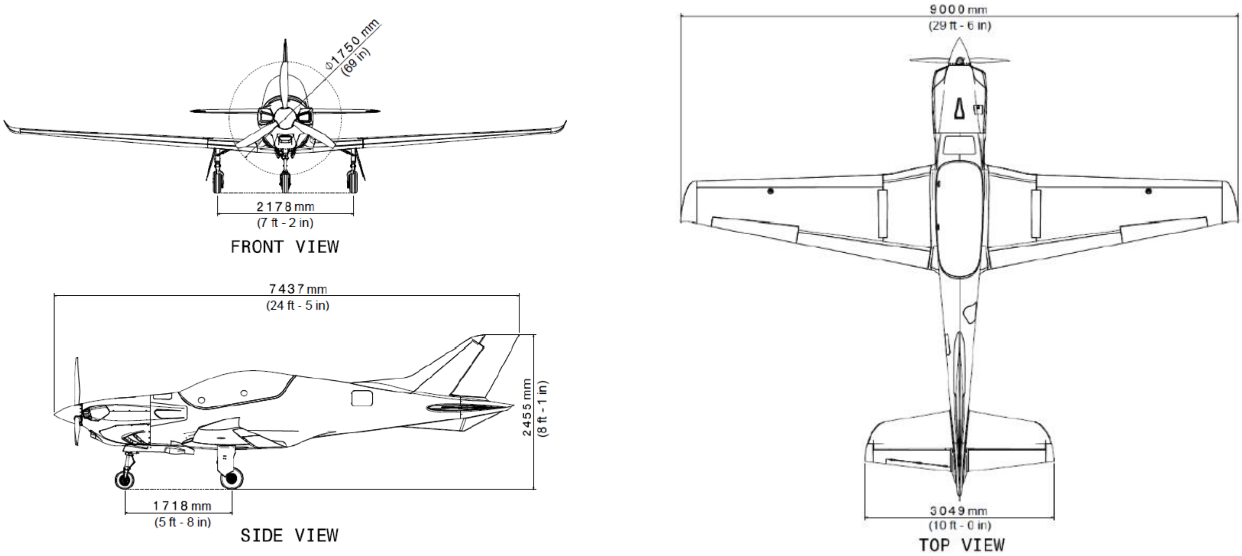

Figure 12. Aircraft Dimensions

1.6.3 Overall Aircraft Flight History

A comprehensive flight history of the I-POOC aircraft, from its maiden flight in March 2022 to its final flight in December 2023, prior to the accident on 13 February 2024, was compiled from various sources.[7] This compilation covers two distinct periods: factory flights from March to June 2022 and all flights following the aircraft's delivery from November 2022 to December 2023. Detailed information is provided in **Appendix C**. A summary of the overall flight history is presented in Table 5 below.

Factory flight hours	25:20 hours
Flight hours after aircraft delivery	60:12 hours
Total flight hours	85:32 hours
Number of factory flights	31 flights
Number of flights after aircraft delivery (excluding accident flight)	54 flights
Total flights (excluding accident flight)	85 flights

Table 5. Summary of Aircraft Overall Flight History

1.6.4 Aircraft Airworthiness

The aircraft was issued a Certificate of Airworthiness (CoA) by the Italian Civil Aviation Authority (ENAC) on 26 August 2022. The CoA was attached with an Airworthiness Review Certificate (ARC) that was issued on 18 October 2023 and it was valid until 18 October 2024 (refer to **Appendix D**). As such, the aircraft had valid airworthiness certification at the time of the accident.

1.6.5 Aircraft Grounding Instructions

On 25 October 2023, Blackshape S.p.A. notified the EASA of a fuel selector indication system issue in the BK 160TR aircraft (registration I-POOC), which is owned by

[7] Sources: Aircraft logbook, technical logs, pilot logbooks, digital flight logs, and witness statements.

Blackshape. As only one BK 160TR had been delivered at the time, Blackshape stated that this aircraft would be grounded pending identification of the root cause and resolution of the issue.

An earlier grounding instruction was issued by Blackshape on 27 May 2023 concerning the transfer of ownership and registration of the aircraft to its purchaser, Sky Media Ltd, Hong Kong. The adequacy of communication and understanding of these grounding instructions—issued on 27 May and 25 October 2023—remains disputed among the relevant parties, with the issue still unresolved.

Despite these instructions, available evidence shows that the BK 160TR (I-POOC) continued to be operated during the grounding period. The potential impact of this on safe operations will be examined in Section 2.

The Civil Aviation Authority of Malaysia (CAAM) was unaware of any grounding instructions that could have affected the airworthiness status of the BK 160TR aircraft (I-POOC) during its operations in Malaysia.

1.6.6 Aircraft Maintenance

Evidence suggests that irregular maintenance activities were conducted on the aircraft (I-POOC). These included the installation of uncertified or non-conforming parts and maintenance by unauthorised personnel who were not properly qualified. The known irregular maintenance activities are as follows:

- **Nose Landing Gear (NLG) Replacement**. The aircraft's NLG was removed and replaced with a new unit by unauthorised personnel in February 2024. This replacement was completed, with assistance from the pilot, shortly before the accident flight on 13 February 2024, which was apparently intended as a test of the newly installed NLG.

Figure 13. Old NLG Found at AAFC Hangar (Left)
and Newly Installed NLG on Wreckage (Right)

- **Installation of Non-Certified Tie-Down Rings**. Non-certified 'tie-down ring' parts were installed on the underside of each wing, near the main landing gear wheel well. These were bolted through the composite wing skin onto the joint of the wing fitting with the main spar. Witness testimony indicates these parts were installed by the pilot on 23 November 2023.

Figure 14. Tie-Down Ring on the Underside of the RH Wing Near Wheel Well (Left);
Tie-Down Ring Bolted to the LH Wing Joint (Centre);
Two New Similar Parts Found at the Pilot's Locker at AAFC (Right)

- **Routine Maintenance by Unauthorised Personnel**. In late November 2023, unauthorised personnel performed routine maintenance activities such as replacing spark plugs and the air filter element. The maintenance log kept by the late pilot suggests other irregular maintenance activities may have occurred.

The impact of irregular maintenance activities, along with the results of material testing on the aircraft's structural parts, will be discussed in analysis section as they relate to the cause of the accident.

1.6.7 Weight and Balance

Evidence indicates that the I-POOC aircraft exceeded its Maximum Take-Off Weight (MTOW) limit of 850 kg during the accident flight on 13 February 2024. The estimated take-off weight for this flight is as follows:

Aircraft (S/N BCV.21010) Empty Weight[8]	653.4 kg	Weight Limits: Max. Take-off Weight Max. Landing Weight
Aircraft Fuel Upload – 129 litres[9]	92.9 kg	
Pilot's Weight[10]	87 kg	
Passenger's Weight[11]	92 kg	
Minus Nominal Start-Up and Taxy Fuel	– 4 kg	
TOTAL (Take-Off Weight)	**921.3 kg**	**850 kg**

Table 6. Aircraft Weight Calculation

Assuming no luggage and no significant changes in the pilot or passenger's weights since their last recorded measurements, the aircraft's take-off weight exceeded the MTOW limit by approximately 8.4% on the accident flight.

[8] As recorded in the aircraft (S/N BCV.21010) weighing form by Blackshape dated 12 July 2022, that is attached in Appendix E.

[9] Aircraft was fully fuelled based on witness account. The pilot also reported an aircraft endurance of 3.5 hours before departure from WMSA, indicating a full fuel load. Fuel density: 0.72 kg/L.

[10] Based on medical examination record, weight reading taken on 3 May 2023.

[11] Based on medical examination record, weight reading taken on 5 July 2023.

The BK 160TR is relatively weight-sensitive, and evidence indicates that the pilot likely exceeded operating weight limitations on previous flights, particularly during long-distance trips to Myanmar, the Philippines, and Thailand. Similar instances were also observed on certain local flights with two persons onboard and heavy fuel loads, conditions consistent with those on 13 February 2024.

To assess the frequency of overweight operations, additional evidence was gathered on the take-off weights of all I-POOC flights, with a compiled record in **Appendix F**. Before aircraft delivery to Singapore in July 2022, 31 factory flights were recorded between March and June 2022. Records indicate that 20 of these test flights exceeded the 850 kg MTOW, ranging from 0.4% to 5.2% over the limit, within the weight tolerance permitted for factory test flights.

Of the 55 flights conducted after the aircraft's delivery, it is probable that 30 exceeded the MTOW limit, in addition to the accident flight, which was confirmed to have exceeded this limit. Some flights could not be assessed due to insufficient weight data. This suggests that at least 56.4% of I-POOC flights since November 2022 were either likely or confirmed to have been overweight at take-off, with excess weight ranging from 7.6% to 8.5% above the MTOW limit.

1.6.8 Carbon Monoxide (CO) Contamination

The pilot reported to Blackshape that the aircraft's Master Caution and CO Master Caution alerts on the Garmin G3X flight display occasionally activated during flight. Additionally, the CO indicator strip in the front cockpit was observed to be partially black, suggesting elevated levels of CO in the cockpit.

To monitor CO levels, the pilot improvised with two portable CO detectors, placing one in the front and the other in the rear of the cockpit. The pilot reported that CO levels peaked at 285 ppm during the climb phase and reached 45 ppm during cruise.

The accident flight on 13 February 2024 lasted approximately eight minutes, involving a brief climb followed by a cruise at around 1,500 feet. The relatively short duration of the climb and overall flight will be considered when assessing the potential impact of CO exposure on the pilot and passenger in Section 1.13.3.

Figure 15. Jury-Rigged Portable CO Detector

1.7 Meteorological Information

The accident occurred during daylight hours. At WMSA, the weather at 1300 LT was clear, with visibility exceeding 10 km and variable winds at 4 knots. By 1400 LT, winds at WMSA had increased, gusting up to 20 knots and varying between 340° and 150°. The following METARs were active:

- 130500Z VRB04KT 9999 FEW018 33/21 Q1013
- 130600Z 06007G20KT 340V150 9999 FEW018 34/22 Q1012

Garmin G3X data indicate that the wind direction was backing from north-westerly to westerly at 8 to 9 knots at an altitude of about 1,500 feet during the latter half of the ADV429 flight. No significant local meteorological conditions were reported in the Kapar area at the time of the accident that might have affected the ADV429 flight.

1.8 Aids to Navigation

Navigation aids in the area were operating normally.

1.9 Communications

All ATC communication frequencies were operating normally.

1.10 Aerodrome Information

Airfield	Sultan Abdul Aziz Shah Airport, Subang (WMSA)
Runway	15 / 33
Length	3782 m
Width	45 m
ICAO Designator	WMSA
IATA Designator	SZB
Elevation	21.5 m

Table 7. WMSA Aerodrome Information

1.11 Flight Recorders

The aircraft was not equipped with either a Flight Data Recorder (FDR) or a Cockpit Voice Recorder (CVR). However, it was fitted with two Garmin G3X GDU 460 primary flight displays, one in each cabin. Following the accident, the GX3 GDU 460 unit from the rear cockpit was recovered in heavily damaged condition and sent to the NTSB in the United States for data recovery and analysis. The details of the unit are as follows:

- Device: Garmin G3X Flight Display
- Model: GDU 460
- Part No.: 011-02920-05
- Serial No. 350008350

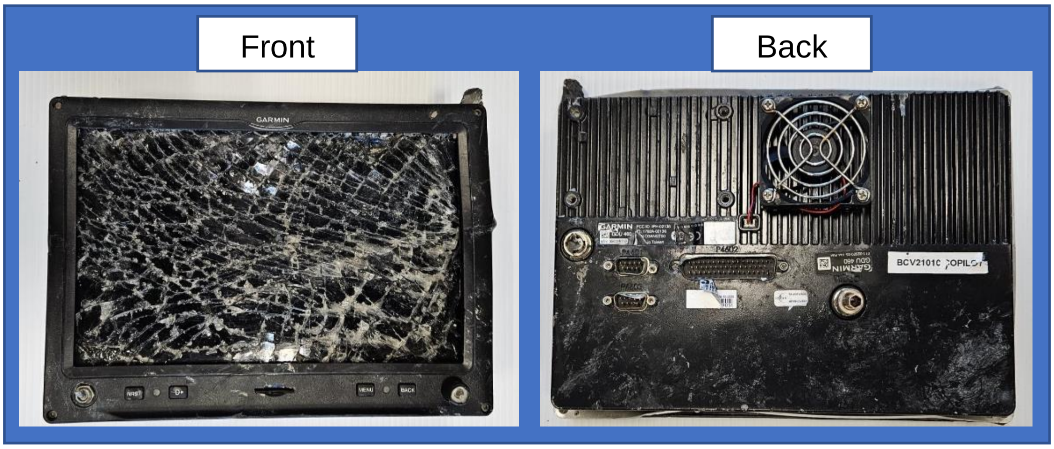

Figure 16. Damaged Garmin G3X GDU 460

1.11.1 Garmin G3X GDU 460 Data Recovery

Upon receipt at the NTSB Vehicle Recorder Laboratory, the device was carefully examined. Although the unit was damaged, internal components were largely intact, and laboratory surrogate parts were used to successfully power on the device. Data extraction followed manufacturer-recommended procedures.

1.11.2 Recorded Data Description

The recovered data spanned the last 13 flights of the I-POOC aircraft, covering a total duration of 12 hours and 44 minutes with 29.08 million recorded data counts, from 8 December 2023 to 13 February 2024.

For the accident flight on 13 February, data recording began at 13:27:59 LT and ended at 13:35:52 LT, just before the crash. Due to data buffering limitations, the final seconds of the flight were not captured by the G3X recording.

Key recorded parameters included pressure altitude, GPS altitude, ground speed, indicated and true airspeeds, magnetic heading, pitch and roll angles, vertical speed, load factor, cylinder head and exhaust gas temperatures, manifold pressure, engine RPM, fuel flow, fuel pressure, oil pressure, and oil temperature.

A summary of the data analysed by the AAIB from the Garmin G3X GDU 460, as recovered by the NTSB, is provided in **Appendix G**.

1.11.3 Flight and Engine Parametric Data and Charts

The NTSB provided visual and tabular analyses, including a Google Earth overlay showing the recorded flight path, which reveals variations in critical flight and engine parameters, particularly in the final moments. Detailed plots of the flight path, including flight and engine parameters (Figures 8 to 11), illustrate both the entire accident flight session and critical parameter changes during the last minute of recorded data.

Data retrieved from the Garmin G3X GDU 460 provides valuable insights into the accident flight's dynamics, including key flight and engine performance parameters. This information is crucial for reconstructing the flight path on 13 February 2023 and understanding the operational conditions leading up to the accident. Additionally, the recorded parametric data from the last 13 flights of I-POOC offer critical information and valuable insights into the aircraft's recent operational history, aiding in the analysis of factors contributing to the accident.

1.12 Wreckage and Impact Information

1.12.1 In-Flight Separation of Aircraft Structural Parts

Section 1.1 above includes illustrations of the general area (Figures 2 and 3) and the geographical locations of the main aircraft wreckage and debris sites (Figures 4 to 7). Site 1 contained the main wreckage along with the bodies of the pilot and passenger. Sites 2 to 4 contained various aircraft debris, including large structural parts scattered over an area extending at least 500 metres east of the main wreckage impact point.

Notably, debris found at or near Site 3 included fragments of the cockpit canopy in various sizes, along with the passenger's baseball cap, suggesting that the canopy had broken up in-flight prior to the aircraft's ground impact at Site 1.

The distribution of debris around Sites 2, 3, and 4 strongly indicates that large structural parts separated from the aircraft while it was in flight, before impacting the ground in the oil palm plantation. No evidence of pre-crash or post-crash fire was found on any debris at these sites.

Figure 17 below displays the major separated structural parts found after the accident. Smaller debris, such as canopy fragments at Site 3, are not included in the illustration. Notable damage includes the left (LH) aileron, which detached from its hinges, and the aileron connecting rod, which separated from the bellcrank. The right (RH) wing, which detached at both the front and rear spars, was found at Site 2. The RH wing's inner upper skin, detached along with the inner rib, was found at Site 3. The LH wing's upper skin was located at Site 4, while the lower skin was found at Site 3.

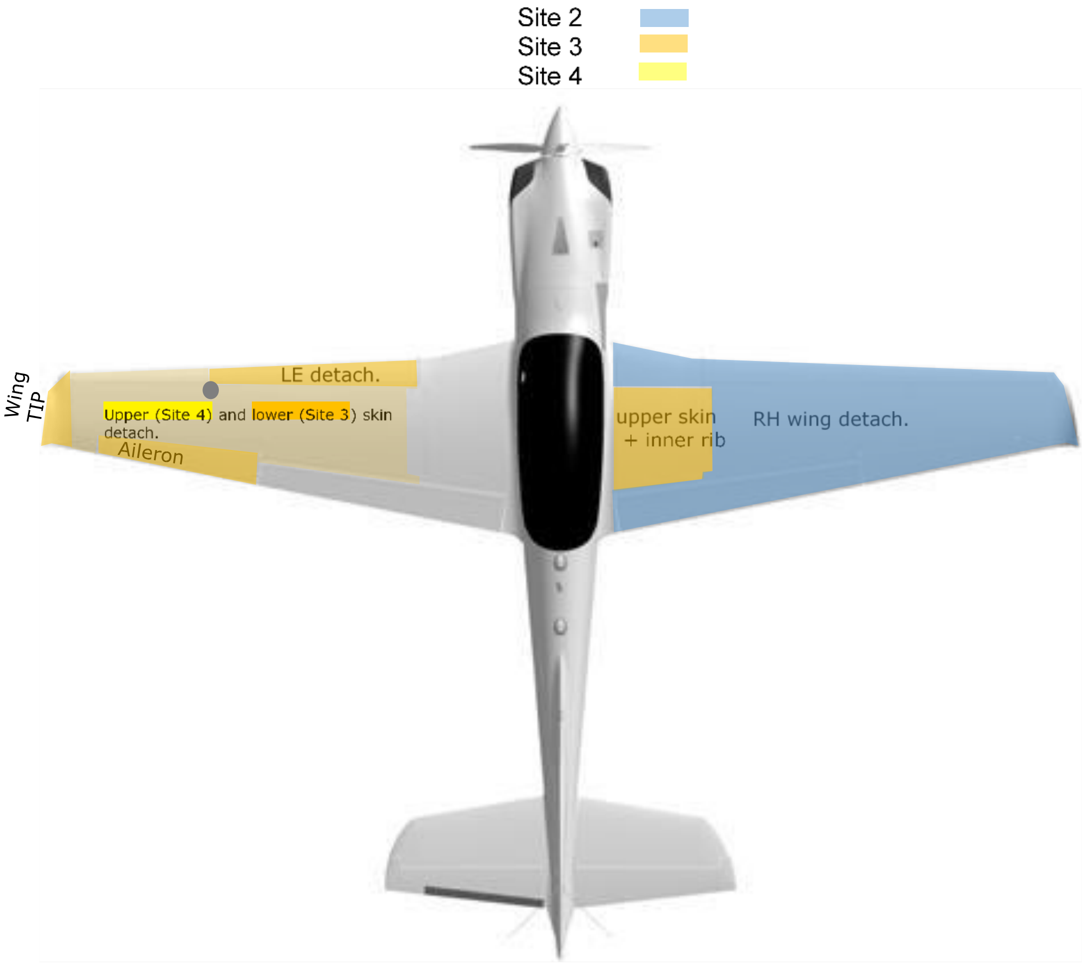

Figure 17. Structural Parts Recovered from Various Sites

Figure 18. Layout of the Aircraft Wreckage

1.12.2 Impact Point of Main Wreckage

The front portion of the main aircraft wreckage, including the engine and forward section of the cockpit, was buried approximately two metres deep in the relatively soft ground of the oil palm plantation. The rear section of the fuselage, with the tail and vertical stabiliser, remained above ground.

Numerous debris and aircraft parts were scattered around the impact site, within a radius of approximately 50 metres. No evidence of pre-crash or post-crash fire was found on the wreckage at or around the impact point.

Figure 19. Impact Point of Main Wreckage

Based on the orientation of the partially buried fuselage, ground markings near the wreckage, and freshly broken branches at the top of an adjacent palm tree, the aircraft impacted the ground at an approximate heading of 292°. The vertical angle from the impact point on the ground to the top of the broken branches indicates that the aircraft struck the ground at an approximate 45° downward trajectory.

Figure 20. Impact Point of Main Wreckage
and Travel Direction of Aircraft Impacting Ground

Figure 21. Broken Palm Branches (Left)
and Aircraft Downwards Trajectory (Right)

1.13 Medical and Pathological Information

Two individuals were fatally injured in this accident—the pilot in the front seat and the passenger in the rear seat. Witnesses indicated to investigators that the pilot was not experiencing any financial, social, or familial difficulties.

1.13.1 Cause of Death

Post-mortem examinations concluded that both the pilot and the passenger died from multiple injuries sustained in the crash.

1.13.2 Toxicology Information

The post-mortem report indicated the pilot's blood alcohol concentration (BAC) at 32 milligrams per 100 millilitres (0.032 g/dL or 0.032%). This exceeds the regulatory BAC limit set by CAAM[12] as well as the maximum limit recommended by EASA[13], which is 0.02 g/dL (0.02%). As the body was refrigerated within 24 hours post-accident, post-mortem changes are unlikely to have influenced this finding, indicating that the pilot was under the influence of alcohol while operating the aircraft.

INVESTIGATION RESULTS

Chemistry results from Chemistry Department Malaysia (24-FR-B-04775)

Blood for common drugs of abuse	:	No drugs detected
Blood for ethyl alcohol	:	Detected at a level of 32 milligram per 100 milliliter

Figure 22. Excerpt from the Pilot's Report of Post Mortem Examination[14]

1.13.3 Carbon Monoxide (CO) Contamination in the Cockpit

The pilot previously reported a CO level of 285 parts per million (ppm) during the climb phase of an earlier flight—equivalent to 0.0285% (285 x 0.0001). This level decreased to 45 ppm during the cruise phase. Haemoglobin's high affinity for CO enables even

[12] Civil Aviation Directive (CAD) 6007 – Operator Alcohol and Drug Testing Programme prohibits flight crew from operating under the influence of alcohol and sets a regulatory BAC limit of 0.02%, equivalent to 0.02 g/dL (grams per decilitre).

[13] Commission Regulation (EU) No 965/2012 prohibits flight crew from operating under the influence of alcohol. EASA SIB 2018-07 recommends a maximum BAC limit of 0.02% or the national statutory limit, whichever is lower. In Italy, the national statutory limit set by ENAC enforces a zero-tolerance policy, stipulating that breath alcohol concentration (BrAC) must not exceed a level equivalent to 0.0 g/L of BAC during alcohol testing (ENAC General Director Provision DG-15/02/2021-0000012-P).

[14] Report reference: Bil. (36) dlm. HTAR/KLG/RP/Am 12/15 Pt. 4/2024) dated 13 March 2024.

low atmospheric concentrations to cause significant Carboxyhaemoglobin (COHb) saturation. The Occupational Safety and Health Administration (OSHA) recommends a maximum permissible exposure limit of 35 ppm over an 8-hour period.

A CO level of 285 ppm (0.0285%) during the accident flight would not have reached immediate incapacitation levels. Exposure to this concentration would require approximately 5 to 6 hours to reach the incapacitating threshold of 23-30% COHb (see Figure 23). Therefore, the brief exposure duration during the climb—approximately 2 minutes—during the accident flight on 13 February 2024 was insufficient to result in significant COHb accumulation.

Similarly, a CO level of 45 ppm (0.0045%) sustained for approximately 6 minutes during cruise before the accident was also insufficient to result in significant COHb accumulation.

Table 14.1 Time Required for Various Concentrations of Carbon Monoxide to Produce 80% Equilibrium Value of Blood Saturation

Concentration of CO in air (%)	Blood Saturation (%)	Time
0.02-0.03	23-30	5-6 h
0.04-0.06	36-44	4-5 h
0.07-0.10	47-53	3-4 h
0.11-0.15	55-60	1.5-3 h
0.16-0.20	61-64	1-1.5 h
0.20-0.30	64-68	30-45 min
0.30-0.50	68-73	20-30 min
0.50-1.00	73-76	2-15 min

Reproduced from Von Oettingen WF, *Carbon Monoxide: Its Hazards and the Mechanism of Its Action,* U.S. Public Health Service, Bulletin 290. Washington, D.C., U.S. Government Printing Office.

Figure 23. Exposure Time of CO Concentration to Produce Blood Saturation

1.13.4 Medical Fitness Status of Pilot and Passenger

The pilot held a valid Class One Medical Certificate issued by the Directorate General of Civil Aviation, France (DGAC), with a limitation of “VDL – Valid only with correction for defective distant vision.” He also held a CAAM Class One Medical Certificate with the same VDL limitation. A review of the medical documentation showed no significant medical concerns, and the attending Designated Medical Examiner found no notable conditions on physical examination. Based on available medical history and examinations, the pilot had no known medical conditions that could have posed significant flight safety hazards.

The passenger, seated in the rear, held a valid Class Two Medical Certificate issued by CAAM without any limitations. The medical review revealed no significant health issues, and the Designated Medical Examiner noted no significant findings during the physical examination. Thus, the passenger had no known medical conditions that could have impacted flight safety.

1.14 Fire

There was no evidence of pre-crash or post-crash fire.

1.15 Survival Aspects

There were no survivors in this catastrophic accident.

1.15.1 Analysis of Aircraft Crashworthiness and Post-Crash Survivability

Crash survivability and human tolerance to impact are analysed using the reference tool C.R.E.E.P (Container, Restraint, Environment, Energy Absorption, and Post-crash factors). The following factors are assessed to determine the causes of injuries and the survivability of the aircraft's occupants.

1.15.2 Container

The container refers to the space occupied by the aircrew, including both the cockpit and cabin areas. It is designed to be robust to withstand deformation, as any reduction in occupiable space can cause injury or death.

Due to the high-energy impact, the container of the I-POOC aircraft was shattered into pieces, failing to prevent intrusion by external objects and leading to fatal injuries for the occupants.

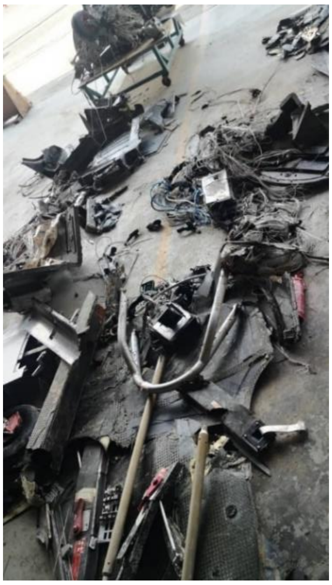

Figure 24. Location of Cockpit

Figure 25. Container Shattered into Debris Survivability Almost Impossible

1.15.3 Restraint

The restraint system is intended to keep individuals secure within their workspace, maintaining control over the aircraft and equipment, attenuating crash dynamics, and limiting occupant movement to reduce impact with aircraft structures.

The I-POOC aircraft was equipped with a four-point restraint system, which was found intact and functional. However, examination showed that only the left side of the front seat belt was cut during the pilot's extrication, suggesting that the pilot may have fastened the seat belt to only two points. This was consistent with the pilot's posture observed as "submarining" through the seat during search and rescue.

The restraint system for the passenger was lost, so no inspection was possible.

1.15.4 Environment

This refers to the internal space of the container. Even if the container maintains its integrity, occupants may still suffer injuries from collision with cabin structures. The brace position can reduce body movement, protect vital parts from injury, and stabilise occupants. However, in this accident, the energy environment was lethal, making survivability unlikely.

Interaction between the cockpit structure, control levers, and human body parts caused various injuries and fracture patterns. A detailed analysis of these injuries may provide insights into which pilot was flying the aircraft at the time of the accident.

Figure 26. Rear Seat Rudder Pedal Relatively Intact

Figure 27. Pilot's Rudder Pedal Broken into Two Pieces

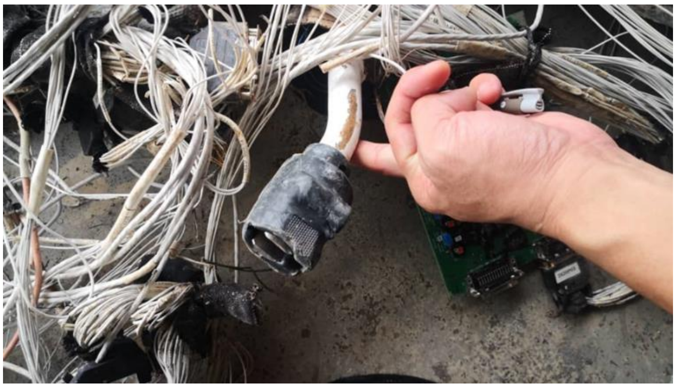

Figure 28. Pilot's Control Column Broken into Half.

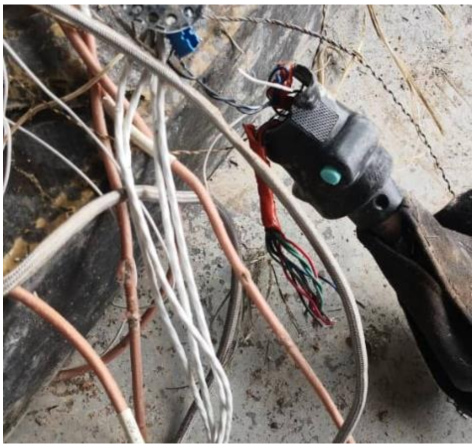

Figure 29. Rear Seat Control Column Broken into Half

1.15.5 Energy Absorption

Crumple zones are designed to deform in a controlled manner upon impact, increasing stopping distance and reducing deceleration forces on occupants. In this accident, the landing gear was in a stowed position and did not absorb impact forces. Additionally, the aircraft struck the ground at a 45° downward angle, with only the engine and its housing acting as a crumple zone to extend deceleration time.

Figure 30. Nose Wheel Retracted; Impact Not Absorbed by Landing Gear.

1.15.6 Post-Crash Factor

This encompasses hazards present after the initial impact that could affect cabin occupants. No post-crash hazards were identified that would have diminished survivability.

1.16 Tests and Research

1.16.1 Fuel System Components Tests

From the outset of the investigation, there were clear indications of in-flight separation of aircraft structural parts. One initial consideration for this in-flight separation was fuel tank overpressure, which may have caused the aircraft wing’s skin to detach from the wing spars. A possible cause of this overpressure was blockages in the fuel vent and fuel vent lines. Consequently, relevant fuel system components were identified, recovered, and sent to ANSV for testing.

Figure 31. Fuel Components Tested by ANSV (Courtesy of ANSV)
Fuel Valve (Centre); Inner and Outer Fuel Vent Lines (Left – LH; Right – RH)

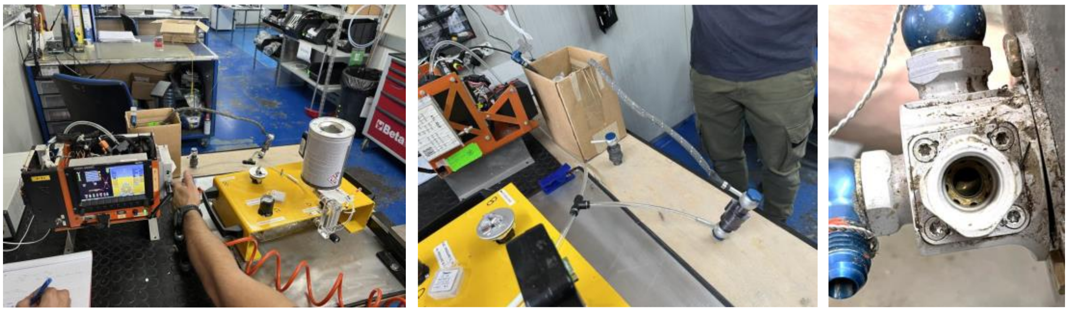

Figure 32. Fuel System Components Tests and Inspection (Courtesy of ANSV)

ANSV conducted technical tests on the fuel valve and both inner and outer fuel vent lines (left and right) of the BK 160TR (I-POOC) at Blackshape's facility in Italy. Testing, performed by Blackshape technicians under ANSV supervision, utilised a simulated "dummy tank" setup with a rollover valve and pressure measurement tools.[15] Key findings were as follows:

- **Fuel Vent Lines Inspection**. The vent lines showed no structural damage aside from minor impact marks and were confirmed to be unobstructed, with stable pressure observed during all flight simulations, including inverted flight.

[15] Reference: ANSV 0048/24 dated 28 July 2024 – ANSV Technical Analysis of Components (ref: ACC BK1260TR Reg: I-POOC of: 13 February 2024 Malaysia). Testing was conducted on 2 July 2024.

- **Fuel Valve Alignment and Functionality**. A minor misalignment in the fuel valve assembly—about 30 degrees of rotation and a 5 mm offset—was noted, likely due to accident impact, but was determined to have no significant effect on functionality. Flow through the valve was confirmed to be correct, with the selected tank identified as the LH tank.

- **Disassembly and Examination**. Internal examination showed that the valve moved freely with proper flow in each tank selection, and the electric motor operated normally, allowing unrestricted selector movement.

- **Conclusion**. The fuel valve and vent lines were found to be in good condition, without malfunctions or deviations from standards. These components remain in ANSV custody for any future needs by AAIB.

This analysis indicates that neither the fuel valve nor the vent lines contributed to the accident through mechanical failure.

1.16.2 Fuel Storage Temperature Checks and Fuel Quality Tests

Due to the consideration that fuel tank overpressure might have been caused by blockages in the fuel vent and vent lines, Petronas Dagangan Berhad (PDB) Subang Aviation Fuel Terminal was requested to conduct checks and tests on AVGAS fuel storage conditions and fuel quality.

No temperature records were available from 4th to 13th February 2024, in line with JIG Standard 1 and 2 (Issue 13, Sept 2021), which does not require daily temperature recording. Following a request from AAIB, a temperature check was conducted on 28th May 2024 under similar conditions and at approximately the same time as the refuelling of the I-POOC aircraft on 13th February 2024. Results indicated:

- **Bowser AVGAS BA203**: Outside air temperature 34.5°C;
Fuel sample temperature 35.5°C.

- **Storage Tank AVGAS T20**: Outside air temperature 34.5°C;
  Fuel sample temperature 32.0°C.

Routine checks and tests during the period included daily water and dirt precaution checks on storage tanks and refuelling equipment in accordance with JIG Standard 2 requirements. On 13th February 2024, tests for water detection, particulate contamination, and fuel appearance were conducted on the AVGAS storage tanks and fueller, with results showing:

- **Water Detector Test**: Negative for both tanks and fueller.
- **Undissolved Water and Particulate Contamination**: Clear.
- **Appearance**: Bright and clear, with the AVGAS colour confirmed as blue.

These results indicate that the fuel met quality standards for contamination and appearance on the day of the accident.

1.16.3 Non-Destructive Inspection on Factory Aircraft

Following the accident, Blackshape S.p.A. conducted thermographic and visual inspections on two company aircraft—S/N BCV.001 and S/N BCV.21012—at Blackshape facilities.

- **Aircraft S/N BCV.001**. A model BK 160 manufactured in 2016, BCV.001 has accumulated 250 flight hours (FH), including limit envelope tests during initial type investigation. This aircraft provides a relevant comparison due to its extensive use and testing.

- **Aircraft S/N BCV.21012**. A model BK 160TR manufactured in 2022, BCV.21012 has accumulated 30 FH and closely matches the accident aircraft, BCV.21010, in terms of configuration, including empty mass distribution, cockpit layout, and systems.

The six-year difference between these models allowed for a comparison that could reflect consistency in the manufacturing process. The inspections aimed to verify the structural integrity and condition of the aircraft and rule out potential degradation from operational use.

The non-destructive inspection (NDI) by Blackshape included wing disassembly, thermographic scans of the fuselage and wing assemblies focused on bonding lines, and detailed visual assessments of all bonded joints and accessible parts. The NDI results are as follows:

- **Aircraft S/N BCV.001**. Minor defects, primarily holes from removed installations and patches on the lower fuselage skin, were observed. These defects were within acceptable limits per standards SPEC.BS-PRC-003 and SPEC.BS-PRC-001, with no delamination or dis-bonding found.

- **Aircraft S/N BCV.21012**. No thermal anomalies were detected, confirming the structural integrity of composite parts and bonding lines.

Blackshape concluded that the inspections revealed no critical structural issues or anomalies related to the accident, indicating that both aircraft met structural integrity standards.[16]

1.16.4 Composite Material Tests

Sixteen composite material samples from the I-POOC wreckage were selected and sent for analysis to the SIRIM QAS International Sdn Bhd test facility. This analysis aimed to investigate potential material degradation, with a specific focus on the in-flight separation of components prior to the aircraft crash. The samples sent to SIRIM are detailed in Table 8 below.

[16] Reference: Blackshape S.p.A report: Root Cause Analysis Report BK 160TR - S/N BCV.21010 I-POOC (OAC-01-2024 Rev. 2) dated 15.04.2024.

Sample ID	Location on Aircraft	Wreckage Location	Description	Quantity
BSKU/IPOOC/001(S4)	Left Wing (Upper Skin, near refuelling point)	Site 4	Composite material near refuelling point	1 piece
BSKU/IPOOC/002(S3)	Right Wing (Upper Skin, near fuselage)	Site 3	Composite material on upper skin	1 piece
BSKU/IPOOC/003(S1)	Left Wing (near wheel well)	Site 1	Composite part near wheel well	1 piece
BSKU/IPOOC/004(S2)	Right Wing (near wheel well)	Site 2	Composite part near wheel well	1 piece
BSKU/IPOOC/005(S1)	Left Wing Spar	Site 1	Structural component of left wing	1 piece
BSKU/IPOOC/006(S1)	Left Wing – Studbox	Site 1	Two small structural parts	2 pieces
BSKU/IPOOC/007(S1)	Rudder	Site 1	Composite part of rudder	1 piece
BSKU/IPOOC/008(S4)	Left Wing	Site 4	Additional composite sample from left wing	1 piece
BSKU/IPOOC/009(S4)	Left Wing	Site 4	Another sample from left wing	1 piece
Small parts and spars	Left Inner Wing (trailing edge)	Various Locations	Component near inspection panel	1 piece
	Right Inner Rib		Structural rib	1 piece
	Vertical Fin (lower)		Part of lower vertical fin	1 piece
	Left Lower Wing Skin Piece		Section of wing skin	1 piece
	Left Wing Tip (upper)		Tip component of left wing	1 piece
	Left Stabiliser Upper Leading Edge		Part of stabiliser leading edge	1 piece

Table 8. Composite Material Samples Sent to SIRIM

Key tests conducted included Fourier Transform Infrared (FTIR) analysis, Thermogravimetric Analysis (TGA), Differential Scanning Calorimetry (DSC) for resin matrix analysis, and Scanning Electron Microscopy (SEM) for failure mode analysis.

Mechanical tests assessed tensile and compressive properties. A detailed report by SIRIM is in **Appendix H**, with key findings summarised below:

- The epoxy resin matrix used in the tested carbon fibre reinforced plastic (CFRP) composite material has likely experienced significant degradation due to hydrolysis from exposure to a high-humidity environment, leading to increased moisture ingress.

- The resin material's glass transition temperature (T_g) was found to be higher than reported values in Blackshape's compliance report (Doc No BCV-04-64-02). This discrepancy may be due to post-curing effects, thermal aging, and residual stress reduction.

- The tested CFRP composite components[17] contain microcracks and voids that likely weakened the component's overall structural integrity. Under conditions outside of the approved flight envelope, these defects may propagate, leading to significant cracking and delamination that further compromise the composite's mechanical properties.

- Man-made holes observed at the composite material near the wheel well of the RH wing found at Site 2[18] and the material near the wheel well of the LH wing found at Site 1[19] have induced severe cracking on the surface of the component and across the thickness of the component, along with layer delamination. This likely reduced the material's resistance to tensile forces in flight, as evidenced by fibre pull-out in tension-mode at the failed areas.

- The composite matrix's resin-to-fibre ratio of 3:2 was consistent with Blackshape's compliance report (Doc No BCV-04-64-02), aligning with standard values for similar materials.

[17] Sample ID: 1. BSKU/IPOOC/004(S2) – Right Wing: Cut sections A (front spar), B (rear spar), and C (near the man-made hole).
2. BSKU/IPOOC/003(S1) – Left Wing: Cut section D (near the man-made hole).

[18] Sample ID: BSKU/IPOOC/004(S2) – Right Wing.

[19] Sample ID: BSKU/IPOOC/003(S1) – Left Wing.

- The void content in the tested composite component, composed of alternating fabric plies with 90° and 45° orientations, was found to be about 1.2%. The void content falls within the normal range as specified in the original material qualification reports.

- A wide range of tensile and compressive strengths and moduli were observed across component samples of the same design structure. This variability suggests that hydrolysis, delamination, or both may have damaged the CFRP composite samples.

In conclusion, the SIRIM analysis indicates that the CFRP composite material in the I-POOC airframe likely suffered significant degradation due to hydrolysis, thermal aging, and internal defects such as microcracks and voids. These factors diminished structural integrity and led to variabilities in mechanical properties. The presence of cracking and delamination, particularly around the man-made holes, highlighted the root cause of failure under operational overload.[20]

1.17 Organisational and Management Information

1.17.1 Blackshape S.p.A.

The manufacturer of the BK 160TR aircraft (S/N BCV.21010, registration mark I-POOC) is Blackshape S.p.A., an Italian company. According to the Certificate of Registration issued by *Ente Nazionale per l'Aviazione Civile* (ENAC), Blackshape is also the registered owner of this BK 160TR aircraft (refer to **Appendix C**).

1.17.2 Sky Media Ltd

Sky Media Ltd, based in Hong Kong, is the distributor for Blackshape aircraft in the Southeast Asia region under an exclusive distribution agreement with Blackshape

[20] The SIRIM test samples, taken from accident wreckage, had experienced significant operational stresses, crash impact damage, and environmental exposure, contributing to degradation not present in factory-prepared samples used for qualification testing. Results may not fully reflect the pristine material properties as tested by the manufacturer.

S.p.A., signed in 2022. Sky Media ordered and paid for the BK 160TR aircraft (S/N BCV.21010, registration mark I-POOC), which was shipped from Italy to Singapore on 11 October 2022.

However, the aircraft's ownership has not yet been transferred or registered to Sky Media. A business dispute between Blackshape and Sky Media regarding the ownership transfer, registration, and related issues remains unresolved.

Evidence suggests that Sky Media was aware of the aircraft grounding instructions and the irregular maintenance activities conducted on the aircraft, as discussed in Sections 1.6.5 and 1.6.6 respectively. Additionally, Sky Media supplied the non-certified 'tie-down ring' parts installed by the pilot on the underside of the aircraft wings. The Director of Sky Media (referred to hereafter as the distributor for convenience)[21] was a frequent passenger on many of the I-POOC flights, particularly on long-distance overseas journeys, which would have made the distributor well aware of how the aircraft was operated by the pilot.

The impact of the ongoing disputes between Blackshape S.p.A. and Sky Media Ltd, as well as the potential roles of each party in the aircraft's airworthiness and safe operation, will be examined in the analysis section.

1.17.3 Aviation Safety Technology Pte Ltd (AST)

Sky Media Ltd had appointed Aviation Safety Technology Pte Ltd (AST), a Singapore-based company, to provide marketing and promotional services for the BK 160TR aircraft. AST subsequently engaged the pilot of the accident aircraft to operate it for promotional activities aimed at attracting potential customers.

AST was identified or implied as the owner and/or operator of the aircraft in various documents, including business and contract records, insurance policies, property leases, service agreements, business correspondence, flight permit applications

[21] Sky Media Ltd will be referred to as the aircraft distributor for convenience in this report. This reference does not imply ownership of the I-POOC aircraft.

submitted to CAAM through the Non-Scheduled Application System (NOSAS), and in both the Mandatory Occurrence Report (MOR) and the Accident Notification submitted to the AAIB for the I-POOC accident.

Figure 33. AST Logo on the Aircraft

1.17.4 Aurotel Sdn Bhd (Aurotel) and Air Adventure Flying Club (AAFC)

The I-POOC aircraft was based at WMSA and operated from a hangar facility sub-leased through a contractual agreement between AST and Aurotel. Aurotel, closely affiliated with AAFC, leased aircraft to AAFC for leisure and flight training for its members. In AAFC's NOSAS account, Aurotel is listed in the "Airline/Operator" field, while AAFC appears in the "Trading Name" field for I-POOC's flight permit application. Consequently, according to CAAM records, Aurotel/AAFC were identified as the operator of the I-POOC aircraft.

Aurotel/AAFC also operates another foreign-registered aircraft, a Cessna 172M with registration number N1188U, based at WMSA.

The pilot of the I-POOC was a member and flight instructor at AAFC, using his personal AAFC callsign (ADV429) when filing ATC flight plans with CAAM for I-POOC flights. Additionally, the pilot used AAFC's NOSAS account to apply for non-scheduled flight permits with CAAM for I-POOC flights, thereby explicitly identifying both AAFC and Aurotel as the aircraft operator. The AAFC logo was also prominently displayed on the aircraft.

In addition to the hangar facility sub-lease, flight permit applications, and flight plan submissions, evidence suggests that Aurotel provided further operational support for the I-POOC aircraft, including refuelling and servicing. However, Aurotel was not a certified maintenance organisation for the BK 160TR aircraft.

Figure 34. AAFC Logo on the Aircraft

1.18 Additional Information

1.18.1 EASA Emergency Airworthiness Directive

Following the issuance of the Preliminary Report for the accident by the AAIB on 13 March 2024, the European Union Aviation Safety Agency (EASA) issued the Emergency Airworthiness Directive (AD) No. 2024-0074-E on 18 March 2024. This AD applied to BS 115, BK 160, BK 160-200, and BK 160TR aeroplanes and became effective on 20 March 2024.

The directive was issued in response to two fatal accidents involving BS 115 aeroplanes. While investigations were ongoing to determine the exact causes, structural failure of the wing was identified as a possible contributing factor in the second accident (I-POOC case).

EASA determined that further action might be necessary to ensure the continued airworthiness of BS 115 aeroplanes. Pending further information, EASA decided to suspend all flight operations of BS 115 aeroplanes, instructing operators to ground the aircraft from the effective date of this AD.

1.18.2 EASA Airworthiness Directive Cancellation Notice

On 13 June 2024, EASA issued an AD cancellation notice for Emergency AD 2024-0074-E. In the cancellation notice (No.: 2024-0074-CN), EASA stated that while the investigations were not yet completed, additional data indicated that the aeroplane involved in the second accident (I-POOC case) may have been operated beyond its certified envelope and subjected to loads exceeding ultimate limits.

As a result, the suspension of all BS 115 aeroplane operations was no longer deemed necessary, leading to the cancellation of EASA Emergency AD 2024-0074-E.

1.18.3 Alcoholic Beverages Found at AAFC

During the field investigation, alcoholic and non-alcoholic beverages were found near the I-POOC pilot’s storage locker at the AAFC. Witness statements at AAFC could not determine the ownership of these beverages.

Figure 35. Alcoholic (6 Cans) And Non-Alcoholic (5 Cans) Beverages Discovered at AAFC Premises

1.19 Useful or Effective Investigation Techniques

Not applicable.

2.0 ANALYSIS

2.1 Analysis Framework

The analysis framework for the accident involving the BK 160TR aircraft (I-POOC) is structured to provide clear and actionable insights into the accident's causes and contributing factors. The approach begins by identifying and eliminating aspects that evidently did not contribute to the accident, followed by a focused examination of factors likely to have influenced its occurrence. Non-causal factors are reviewed to consider any consequences, outcomes, or other impacts related to the accident.

Key areas of analysis include an assessment of aircraft airworthiness, covering a review of airworthiness certification, maintenance activities, testing of fuel system components, and evaluation of structural integrity. This is followed by a review of the aircraft operational history and a detailed analysis of the accident flight to identify circumstances and probable causes. Human factors are then examined, along with an assessment of organisational influences that may have impacted operational safety.

The investigation benefited from comprehensive data sources, including operational and technical records, maintenance logs, witness statements, forensic examination of the wreckage, and particularly the recovered Garmin G3X flight data and SIRIM's analysis of the aircraft composite material. This structured framework supports a thorough analysis to identify root causes and contributing factors, offering insights for enhancing future aviation safety.

2.2 Summary of Non-Causal Factual Information

2.2.1 Flight Details

The I-POOC aircraft (ADV429), carrying the pilot and a passenger, departed WMSA at approximately 1328 LT for a leisure flight to the area west of Kapar, Selangor. Communication with ATC confirmed normal aircraft operations, with the last recorded transmission from the pilot at 13:35:34 LT, reporting that the aircraft was operating at or below 1,500 feet at the west of Kapar. No distress call was received.

2.2.2 Ground Impact

The I-POOC aircraft subsequently crashed into an oil palm plantation near Kampung Tok Muda, Kapar. The distribution of wreckage across multiple sites suggests in-flight separation of structural parts prior to ground impact.

2.2.3 Injuries and Fatalities

Both occupants—the pilot and the passenger—sustained fatal injuries. There were no additional injuries or fatalities on the ground.

2.2.4 Aircraft and Other Damage

The aircraft was destroyed by the impact. The front section, including the engine and cockpit, was buried approximately two metres in soft ground, while the tail section remained above ground. No additional property damage was reported, and there was no indication of pre- or post-crash fire.

2.2.5 Pilot Information

The pilot held a valid CPL (A) licence with an SEP Land rating, though his IR/SE rating had expired on 30 November 2023. He was not certified to instruct on the BK 160TR but held an FI (A) rating for other aircraft types.

2.2.6 Meteorological Information

Weather conditions were favourable at the time of the accident, with visibility exceeding 10 kilometres and variable winds at 4 knots at WMSA. No adverse weather was reported enroute, and meteorological factors are not considered contributory.

2.2.7 Navigational Aids and Communication

All navigation aids and ATC communications were functioning normally. ATC records confirm the last communication from ADV429 showed no indication of distress.

2.2.8 Flight Recorders

The aircraft was not equipped with an FDR or CVR. However, data from the recovered Garmin G3X GDU 460 primary flight display provided critical parametric information, offering significant insight into both the aircraft's recent operational history and the flight profile during the accident.

2.2.9 Wreckage and Impact Information

Examination of the wreckage revealed significant in-flight structural separation, with debris scattered over multiple locations. Evidence suggests structural components detached prior to impact.

2.2.10 Medical and Pathological Information

Both the pilot and passenger were identified through standard procedures. Medical records and post-mortem reports revealed no incapacitating medical conditions for either individual. Additionally, analysis of likely carbon monoxide (CO) levels in the cockpit indicated exposure insufficient to cause incapacitation and is not considered to have contributed to the accident. However, the blood alcohol analysis in the pilot's post-mortem report showed a positive blood alcohol concentration (BAC) result, which will be further examined in the human factors analysis section.

2.2.11 Fire

No fire occurred before or after the crash, and no signs of burning or thermal damage were observed on the wreckage.

2.2.12 Survival Aspects

The accident was deemed non-survivable due to the high-energy impact. The cockpit and fuselage shattered upon impact, with forces exceeding survivable limits.

2.3 Aircraft Airworthiness

2.3.1 Airworthiness Status

At the time of the accident, the BK 160TR aircraft (I-POOC) held a valid Certificate of Airworthiness (CoA), issued by the Italian Civil Aviation Authority (ENAC) on 26 August 2022. An Airworthiness Review Certificate (ARC) was subsequently issued by Cantor Air, the authorised Continuing Airworthiness Management Organisation (CAMO), on 18 October 2023, valid until 18 October 2024. This confirmed the aircraft's compliance with applicable airworthiness standards under ENAC oversight. This documentation verified that the aircraft met the necessary safety and maintenance standards at the time of the accident and was considered airworthy.

However, grounding instructions issued by Blackshape S.p.A. both before and after the ARC was granted introduce additional considerations regarding the aircraft's operational status and potential safety implications. Irregular maintenance activities were also conducted after the ARC issuance. These grounding notifications and maintenance irregularities will be further examined, as they may have influenced the aircraft's airworthiness during its operational period in Malaysia.

2.3.2 Aircraft Grounding Instructions and Irregular Maintenance Activities

Blackshape S.p.A. issued two grounding instructions for the BK 160TR aircraft, both of which may have had implications for the aircraft's operational and airworthiness status. The first grounding instruction, issued on 27 May 2023, was due to unresolved issues concerning the transfer of ownership and aircraft registration to Sky Media Ltd., its intended purchaser. The second instruction, issued on 25 October 2023, followed Blackshape's notification to the EASA about a fuel selector indication system issue. Blackshape specified that the aircraft should remain grounded until the root cause was identified and rectified.

Despite these grounding instructions, evidence indicates that the aircraft continued to operate during both grounding periods, potentially compromising its safe operational status. Additionally, irregular maintenance activities were carried out on the aircraft, including the installation of uncertified components, such as 'tie-down rings' on the wings by the pilot, and the replacement of the nose landing gear (NLG) by personnel lacking proper authorisation or qualifications, with assistance from the pilot.

Most significantly, the installation of non-compliant ‘tie-down rings’ through man-made holes in the wings, combined with operational stresses, had serious implications for the aircraft’s structural integrity and directly affected its airworthiness. The impact of these factors on the aircraft's airworthiness is further examined in Section 2.3.4.

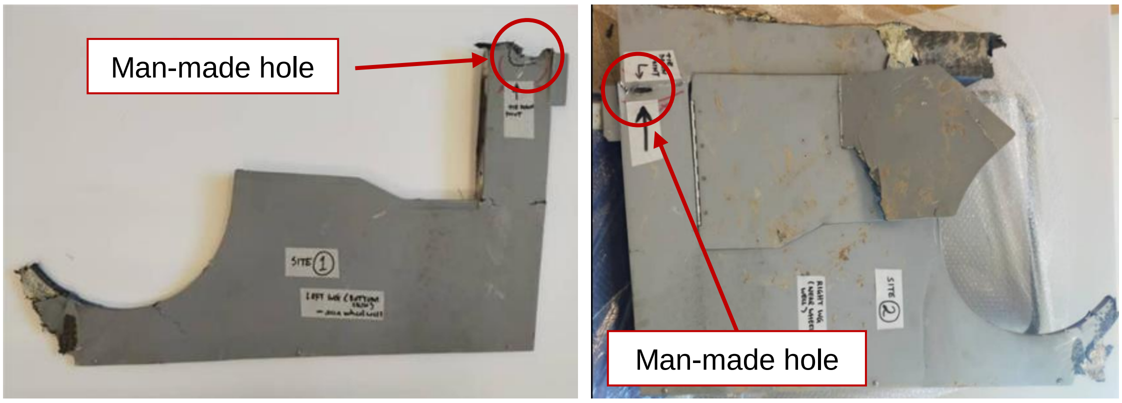

Figure 36. Man-Made Holes on The Underside of The Aircraft Wings, Near the Wheel Wells (Left Picture: LH Wing; Right Picture: RH Wing)

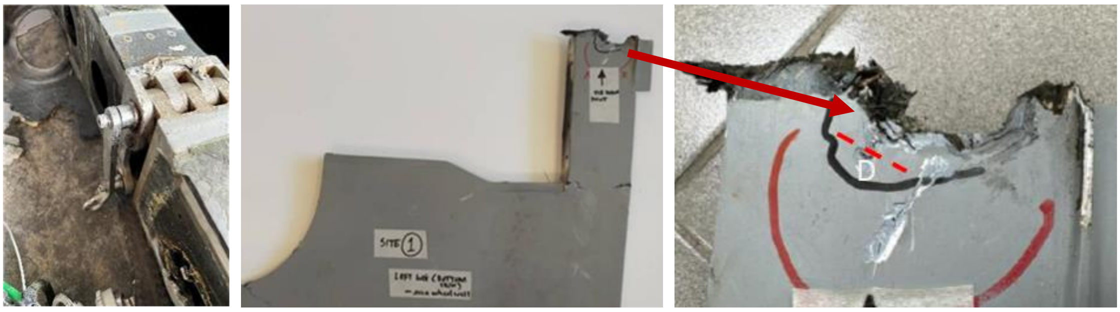

Figure 37. LH Wing – Tie-Down Ring and Man-Made Hole (Fragmented Portion)

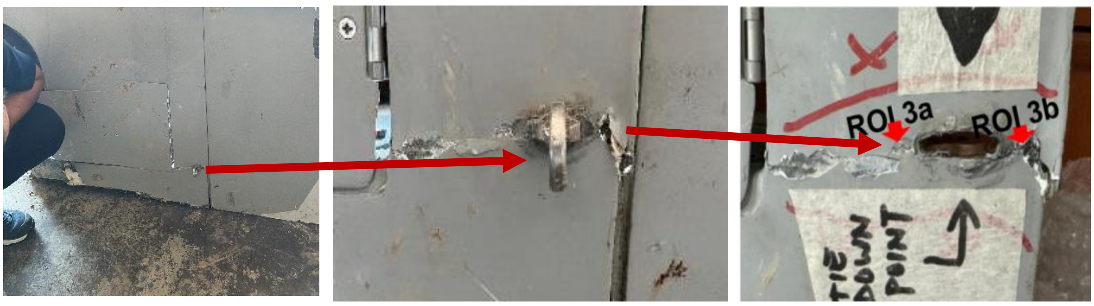

Figure 38. RH Wing – Tie-Down Ring and Man-Made Hole

2.3.3 Fuel System Components Analysis and Fuel Quality Checks

In response to concerns about potential fuel tank overpressure contributing to the in-flight structural separation, key fuel system components were retrieved from the wreckage and sent to ANSV for detailed testing. Technical analysis conducted at Blackshape’s facilities confirmed that the fuel vent lines and fuel valve exhibited no blockages or structural defects that could have caused overpressure in the fuel tank.

A minor misalignment was observed in the fuel valve, attributed to impact forces from the accident. This misalignment, however, was determined not to have affected the valve’s functionality. Inlet/outlet flow verification identified the selected tank as the LH tank. Additionally, AVGAS fuel quality tests and storage temperature checks by Petronas at Subang found no issues, including no significant temperature differences between ambient air and fuel, that could have caused fuel tank overpressure.

In summary, the fuel system components were confirmed to be in working order, with no indication that they contributed to the accident.

2.3.4 Composite Material Analysis

SIRIM conducted analyses of composite samples from the I-POOC airframe to assess structural integrity and identify degradation factors that may have contributed to the in-flight separation of components. Samples were taken from critical sections of the aircraft, including the wings and areas around man-made holes, and tested using FTIR, TGA, DSC, SEM, structure design verification tests, and mechanical testing for tensile and compressive properties.

SIRIM's findings provide valuable insights into the condition of the I-POOC material. However, the tested samples were subjected to operational overload and crash impact damage, and the composite wreckage parts were exposed to severe environmental conditions. Consequently, the tested samples may not fully reflect the characteristics of factory-prepared samples used in qualification testing or an undamaged structure. The key findings from the SIRIM tests are summarised below:

- **Material Degradation**. FTIR and TGA analyses indicated hydrolytic degradation in the epoxy resin matrix of the CFRP material, likely due to prolonged exposure to high humidity. While post-accident cleaning and conservation may have contributed, pre-existing factors—such as operational overload causing microcracking and delamination, along with man-made holes compromising the protective barrier and exposing unsealed material—could have allowed moisture ingress before the accident. This degradation weakened the resin's structure.

- **Thermal Properties**. DSC analysis showed a glass transition temperature (T_g) slightly higher than the values reported in the original material qualification. However, T_g values can vary depending on the test standard used, and this slight increase may also result from normal thermal aging.

- **Structural Defects and Degradation**. SEM analysis of the RH wing's front and rear spars, and areas near man-made holes, identified fibre pull-out, breakage, debonding, and matrix cracking. Microsection analysis also revealed voids and microcracks, suggesting compromised bonding. The recovered flight data indicate that the aircraft was routinely operated beyond the certified flight envelope, strongly suggesting that these damage mechanisms resulted from such operations. The observed damage is consistent with the stresses associated with exceeding operational limits, which likely contributed to the degradation of the material's structural integrity.

- **Man-Made Holes and Associated Damage**. The installation of uncertified tie-down rings around man-made holes on the aircraft wings introduced localised stress concentrations, weakening the structure. Samples near the wheel wells showed severe cracking, delamination, and fibre pull-out, suggesting heightened vulnerability to tensile forces in these areas.

- **Resin-to-Fibre Ratio and Void Content**. The composite's resin-to-fibre ratio of 3:2 met the documented requirements. The average void content in the compliance report was 0.5%, while the measured void content was 1.2%.

However, this value remains within the acceptable range outlined in the original material qualification reports.

- **Mechanical Property Variability**. Tensile and compressive testing revealed high variability in strength across the samples tested. This is likely due to repeated exceedances of the certified flight envelope, which caused progressive material degradation through microcracking and delamination. Additionally, the abnormal loads experienced during the accident and post-accident environmental exposure could have further contributed to the observed variability in structural properties.

The analysis of the I-POOC airframe’s composite materials identified several factors that likely compromised its structural integrity, including degradation from hydrolysis and thermal aging, variability in mechanical properties, and internal defects such as voids and microcracks. These findings must be considered alongside operational overload, crash impact damage, and post-accident environmental exposure. Also, stresses from uncertified modifications, such as tie-down rings installed through man-made holes, likely exacerbated these weaknesses, accelerating the failure of critical components and contributing to the in-flight separation. While this investigation has identified these contributing factors, a more detailed assessment would be needed to determine their precise impact on the pre-crash airframe condition.

It is important to note that the SIRIM composite material test samples, taken from the accident wreckage, had been subjected to operational overload, crash impact damage, and environmental exposure. These factors likely contributed to material degradation not present in factory-prepared samples used for qualification testing. While the SIRIM results provide valuable insights into the real-world durability of the I-POOC composite material, they may not fully reflect the properties of pristine samples used in the manufacturer’s qualification tests. Additionally, structural damage from man-made perforations in the aircraft wings, including cracking and delamination, further complicates direct comparison with factory test results.

2.4 Aircraft Operational History

2.4.1 General Flight History

The BK 160TR aircraft, registration I-POOC (S/N BCV.21010), was delivered to Singapore in October 2022, where it logged 25.3 hours before transfer. In July 2023, it was relocated to Malaysia and subsequently undertook various local and long-distance flights, including multi-stop trips through Myanmar and Thailand. Additionally, a planned journey to the Philippines was aborted due to a fuel transfer system issue encountered in Indonesian airspace, after which the aircraft returned to Kuala Lumpur.

By February 2024, I-POOC had accumulated approximately 85.5 flight hours and was scheduled to participate in the Singapore Airshow. Operational records, detailed in **Appendix C**, document 54 flights from November 2022 to December 2023, totalling 60.2 hours and 59 landings (excluding factory flights).

2.4.2 Aircraft Overweight Operation

A review of I-POOC's operational history, supported by multiple data sources, reveals frequent instances of the aircraft exceeding its MTOW limit of 850 kg, particularly on long-distance flights with full fuel loads and two occupants. Of the 55 flights conducted since November 2022, at least 30 (56.4%) likely exceeded the MTOW at take-off, including the accident flight, which was confirmed to be overweight. Some flights could not be assessed due to incomplete weight data.

Before the aircraft's delivery to Singapore in July 2022, records show that 20 out of 31 test flights conducted between March and June 2022 exceeded the MTOW by 0.4% to 5.2%. These factory test flights were carried out under controlled conditions with defined objectives and flight profiles. Such deviations fall within the weight tolerance allowances permitted under CS-VLA 21,[22] which allows limited exceedances during development and compliance demonstration flights.

[22] CS-VLA 21 Proof of Compliance is part of EASA's Certification Specifications for Very Light Aircraft (CS-VLA). This regulation permits weight tolerances during development and compliance demonstration flights, allowing limited deviations beyond the certified MTOW. General tolerances

However, while controlled test flights have specific allowances, repeated overweight operations outside a test environment pose a significantly greater risk. Frequent MTOW exceedances in routine operations meant the aircraft was consistently flown beyond its approved flight envelope, subjecting it to loads exceeding its certified structural limits. The accident flight on 13 February 2024 had an estimated take-off weight of 921.3 kg, approximately 8.4% above the maximum allowable weight. Prolonged overweight operations increase structural stress, accelerate fatigue, and reduce safety margins. When combined with excessive g-loading, speed exceedances, and prohibited manoeuvres, these factors would have further compromised the aircraft's airworthiness.

2.4.3 Operation Outside the Approved Flight Envelope

Flight data retrieved from the Garmin G3X GDU 460 system, encompassing the last 13 flights conducted between December 2023 and February 2024, revealed numerous alarming instances of prohibited manoeuvres (**see Appendix I** for a complete record). (**Appendix J** provides the list of approved and prohibited manoeuvres.)

- **Airspeed Limit Exceedances**. The Never Exceed Speed (V_{NE}) of 180 KIAS was exceeded twice, and the Maximum Structural Cruising Speed (V_{NO}) of 155 KIAS was exceeded 41 times, often combined with high load factors and steep bank angles (15 occurrences), indicating significant operational stress.

- **Load Factor Exceedances**. The symmetrical load factor limit of 4.4 g was exceeded once, and the asymmetrical load factor limit of 2.9 g was exceeded 32 times, including 11 occurrences with excessive roll angles, indicating repeated high-stress manoeuvres beyond approved limits.

- **360-Degree Rolls**. Ten prohibited 360-degree rolls were performed, with four instances exceeding the asymmetrical load factor limit.

allow up to +5% for weight, with additional allowances for specific test conditions. In this case, the manufacturer slightly exceeded this tolerance, reaching up to 5.2% over MTOW during factory test flights. These deviations were documented in the Safety of Flight submission to EASA for Flight Conditions approval. The resulting EASA Permit to Fly authorised controlled test operations but not routine overweight flights.

- **Steep Turns Exceeding 60°**. Seventy-five (75) instances of rolls exceeding 60° bank angle were recorded, six of which involved load factors beyond the asymmetrical limit.

Notably, these manoeuvres were mostly conducted at Chiang Mai Air Sports Airfield and Phuket Airpark in December 2023, apparently as part of air displays at these locations. The manoeuvres involved aggressive pull-ups, steep turns, and rolls under high load factors, evidencing frequent operations outside approved parameters. Specific instances of high-speed, high-load manoeuvres are detailed in **Appendix K**, including repeated aileron rolls and pull-ups that exceeded approved load factor limits.

In summary, I-POOC's recent operational history—marked by frequent exceedances in airspeed and load factor, along with repeated prohibited manoeuvres—reveals a very concerning pattern of sustained stress on a non-aerobatic aircraft. Combined with consistent breaches of weight limitations, this pattern likely caused a progressive compromise in the aircraft's structural integrity over time.

2.4.4 Impact of Prohibited Manoeuvres on Structure

I-POOC's history of prohibited manoeuvres and flight envelope exceedances significantly compromised its structural integrity. SIRIM's composite material analysis indicates that prolonged exposure to excessive loads accelerates fatigue, particularly in composite structures, weakening the airframe's resistance to stress and raising the risk of undetected degradation, which could lead to in-flight structural failure.

- **Structural Fatigue and Potential Undetected Damage**. High load factors and repeated exceedances of V_{NE} and V_{NO} stressed critical areas like wing roots and control attachments beyond design tolerances. This accelerated fatigue, likely causing hidden cracks, delamination, and composite material weakening, as supported by the SIRIM analysis. Over time, these factors cumulatively compromised the airframe's structural integrity.

- **Potential for Structural Deformation**. Excessive operational stress can lead to deformation of the airframe. In I-POOC's case, the detection of carbon monoxide (CO) in the cockpit may indicate structural changes that created leaks or gaps, allowing exhaust gases to enter the cabin, which posed further safety risks to the crew.

- **Impaired Handling and Control Response**. For a non-aerobatic aircraft, performing prohibited 360-degree rolls and extreme bank angles under high loading subjected the control surfaces and linkages to abnormal forces. These forces could compromise handling stability and reduce control predictability, particularly under high loading and speeds, increasing the risk of instability even during normal flight conditions.

- **Increased Likelihood of Maintenance Oversight**. High-stress operations can cause microscopic or internal damage that is difficult to detect during routine inspections. For example, Cantor Air's inspection prior to issuing the ARC in October 2023 (when high-stress events may have already occurred) could have missed hidden damage, particularly if prior exceedances were not accounted for, leaving critical components vulnerable to unexpected failure.

- **Reduced Safety Margins and Compounded Risk**. Frequent operation outside the prescribed flight envelope reduces the aircraft's safety margin, making it more susceptible to structural failure. Over time, cumulative wear likely contributed to the accident, as even minor deviations could lead to cascading failures due to accumulated stress and fatigue.

The combined effect of repeated prohibited manoeuvres and operational exceedances likely compromised I-POOC's structural integrity, increasing its vulnerability to failure. These degraded conditions, along with potential maintenance oversight, significantly contributed to the circumstances surrounding the accident.

2.4.5 Composite Material Integrity and Potential Defects

Prolonged exposure to excessive loads accelerates fatigue in composite structures, highlighting the importance of adhering to operational limits to ensure structural longevity and safety. Repeated prohibited manoeuvres and operational exceedances placed undue stress on the I-POOC's composite structure, contributing to accelerated fatigue in the CFRP material. While CFRP is generally resilient, excessive loading can lead to delamination, micro-cracking, and other forms of fatigue-related damage, as identified in SIRIM's analysis.

It is important to acknowledge that the SIRIM test samples, taken from the accident wreckage, were subjected to post-accident environmental exposure, including water contamination, which may have further contributed to the observed material degradation. These factors complicate the interpretation of the results, as the samples may not fully reflect the properties of factory-prepared material. While the analysis provides valuable insights into potential real-world degradation mechanisms, the observed structural degradation must be viewed in the context of the specific conditions to which the wreckage was exposed.

While operational stresses played a significant role in the degradation of the composite material, the possibility of potential manufacturing defects, such as incomplete curing or voids in the laminate, cannot be entirely ruled out. However, the available evidence strongly suggests that operational exceedances were the primary contributors to the material degradation.

In summary, excessive loads accelerate fatigue in composite materials and repeated operational exceedances contributed significantly to the degradation of the I-POOC's CFRP material. While the investigation indicates that operational stresses were the dominant factor in the material's compromised structural integrity, potential manufacturing defects—however slight—cannot be entirely ruled out. Given these conclusions, it is crucial to ensure that appropriate measures are in place to maintain the continued safety and airworthiness of the existing BK 160TR fleet.

2.5 Accident Flight Analysis

2.5.1 Flight Preparation and Operational Overview

On 13 February 2024, at approximately 1300 LT, the pilot of ADV429 filed a flight plan for a one-hour recreational flight from WMSA to an area west of Kapar, reporting an endurance of 3.5 hours (indicating a full fuel load). The aircraft, a BK 160TR (I-POOC), had two persons on board: the pilot, a flight instructor at the AAFC, and a student pilot. The student pilot was on board as a passenger and was not receiving instruction during this flight. The pilot, an AAFC member, had used the club's NOSAS account to apply for a non-scheduled flight permit from the CAAM, listing AAFC and Aurotel as the operators for the I-POOC flight.

ADV429 departed WMSA at 13:27:59 LT, according to Garmin G3X data. The aircraft was cleared from Runway 15 to turn right and climb to 1,500 feet. At 13:35:34 LT, the pilot reported to FIS N that the aircraft was operating at or below 1,500 feet, west of Kapar. This was the last communication from ADV429; no distress call was received.

Garmin G3X and ADS-B data show that ADV429 turned westward after departure, maintaining approximately 1,500 feet (+/- 200 feet). At 13:35:52 LT, the G3X recorded a rapid descent of 2,830 feet per minute, with an increasing airspeed of 155 KIAS and a heading of 279°, before the recording ceased. Wind velocity was 287°/09 knots. Further ADS-B data indicates continued descent: at 13:35:54 LT, the aircraft was at 1,250 feet with a ground speed of 150 knots on a track of 276°, and by 13:36:04 LT, it had descended to 1,150 feet with a ground speed of 139 knots, tracking 277°.

The estimated aircraft take-off weight was 921.3 kg, approximately 8.4% over the maximum allowable weight. Additionally, a new nose landing gear had been installed by unauthorised personnel shortly before the flight.

2.5.2 Flight Profile Analysis

Recorded flight data indicate that the accident flight profile involved a series of controlled, intentional manoeuvres performed at a relatively low altitude. Figures 8 to

11 illustrate key parameters captured by the aircraft's Garmin G3X flight display, recording primary flight and engine data up to 13:35:52 LT.

At 13:35:45 LT—around 7:46 minutes into the flight and shortly after the pilot's final ATC radio transmission at 13:35:34 LT—the data show the initiation of a controlled dive manoeuvre, with stable roll and yaw angles and a gradual pitch decrease to approximately -17 degrees, which was then held steady. Roll remained within ±5 degrees, indicating wings-level flight, and there was no sign of instability in yaw.

During this descent, the power setting was recorded at approximately 75% maximum continuous power (MCP), beginning from a pressure altitude of 1,650 feet and descending to 1,367 feet. Airspeed increased from 130 KIAS to 155 KIAS, and the controlled parameters of roll, pitch, yaw, and power suggest an intentional, stable descent within the aircraft's operational limits (although the airspeed had reached the V_{NO} limitation of 155 KIAS). No signs of instability or aerodynamic stall were observed, and the aircraft appeared responsive to control inputs.

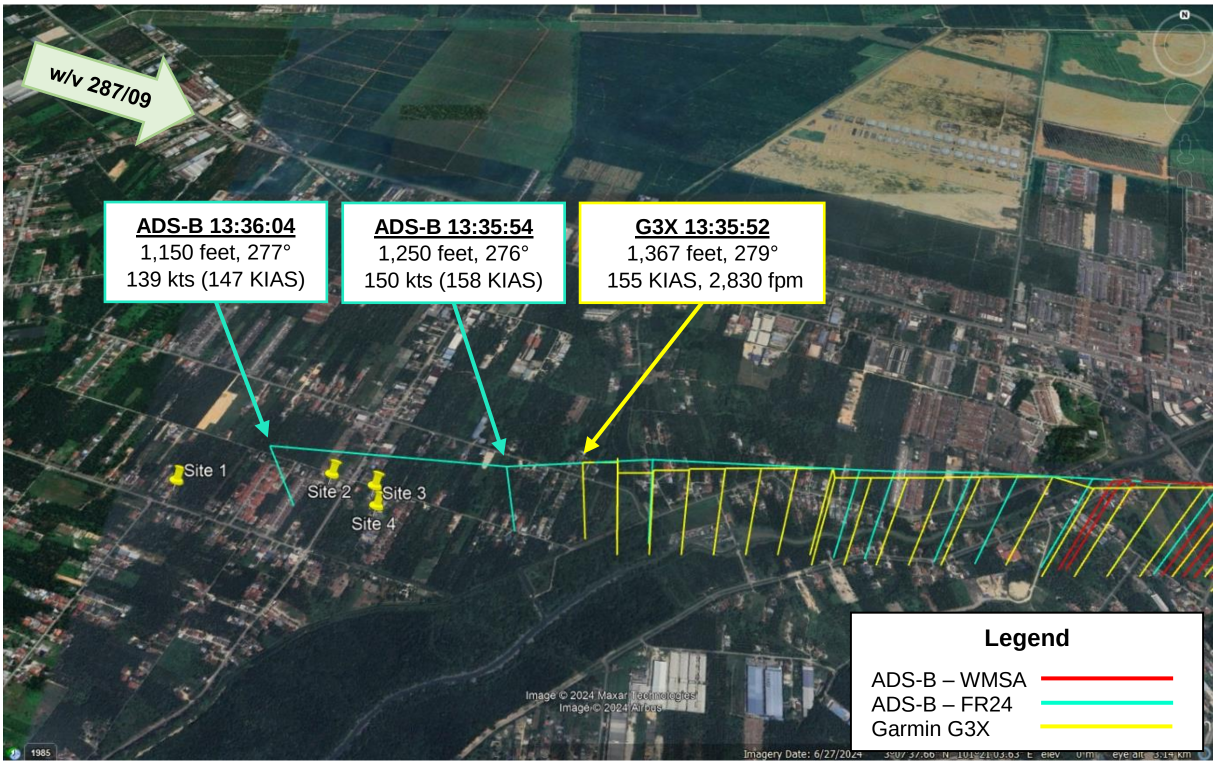

Figure 39. Final Phase of ADV429 Flight

Following the loss of G3X data at 13:35:52 LT, ADS-B data provided two additional points tracking the descent. At 13:35:54 LT, the aircraft was recorded at 1,250 feet with a ground speed of 150 knots (approximately 158 KIAS)[23] on a westerly track of 276°. By 13:36:04 LT, the altitude had decreased to 1,150 feet, with a ground speed of 139 knots (approximately 147 KIAS) on a track of 277°. These points indicate a continued descent from the controlled dive, with decreasing altitude and speed.

However, fluctuating descent rates—ranging from 2,830 fpm at 13:35:52 LT, peaking at approximately 3,510 fpm at 13:35:54 LT, and then reducing to about 600 fpm by 13:36:04 LT—suggest an aerodynamic response to either a controlled or uncontrolled manoeuvre, providing clues to the likely sequence of events.

Fuel readings from the G3X during the flight revealed a discrepancy between the LH and RH fuel tanks. The LH tank recorded a stable 15 US gallons throughout, while the RH tank showed a constant reading of 4 US gallons, which appears erroneous. Previous flights also recorded consistently low and likely inaccurate readings for the RH tank, indicating a possible malfunction in the RH fuel level indicator.

Furthermore, although the LH tank's 15-gallon reading aligns with pre-flight records and evidence noting a full tank, this reading also appears inaccurate. The ANSV fuel valve test results indicated that fuel was selected to be drawn from the LH tank, so its fuel quantity should have gradually decreased over time. Similar discrepancies in fuel quantity readings were observed on other recorded I-POOC flights. Despite these inconsistencies, all other engine and fuel system parameters remained normal, with no evidence of a technical malfunction impacting the flight.

In summary, the controlled descent manoeuvre and stable flight parameters indicate a deliberate, managed descent within the aircraft’s flight envelope up to the final G3X data point. This flight profile suggests the pilot maintained control, actively managing descent rate and airspeed to stay within operational limits, despite reaching or possibly exceeding the Maximum Structural Cruising Speed (V_{NO}), as indicated by the second-

[23] Conversion to KIAS at corresponding pressure altitude, wind velocity of 287°/09 knots and outside air temperature of 36.4 deg Celsius (G3X data).

to-last ADS-B data point (158 KIAS). Stability in roll, yaw, and power settings further supports the interpretation of intentional control up to the last G3X data point at 13:35:52 LT. Subsequently, the decrease in altitude and ground speed, along with fluctuating descent rates in the final ADS-B points, may reflect an aerodynamic response to either a controlled or unexpected manoeuvre.

2.5.3 Structural Separation and Contributing Factors

The separation of structural parts from the I-POOC aircraft, observed after the final recorded G3X data point, can only be hypothesised due to limitations in the available data. Unlike the G3X, which provides comprehensive parametric information, ADS-B captures only limited flight profile data, lacking details on aircraft attitude and engine performance. Additionally, potential discrepancies between the recorded positions from the G3X and ADS-B systems—and between these recorded points and the actual impact location and wreckage distribution sites—could stem from factors such as data buffering, recording algorithms, and transmission lags. Despite these limitations, a probable and credible sequence of events can be constructed by examining other available data and circumstantial evidence.

To construct a plausible sequence of events leading to the aircraft's structural separation and subsequent crash, several contributing factors must be considered:

- **Excessive Take-off Weight**. The aircraft's estimated take-off weight was 921.3 kg, approximately 8.4% above the maximum allowable weight. This excess weight placed undue stress on the airframe, especially when combined with the dynamic forces encountered in flight. Operating above the weight limit compounded the vulnerability of an already compromised structure, increasing the likelihood of structural failure under high-stress conditions.

- **Overstressed Airframe and Reduced Safety Margins**. Prior to this incident, the I-POOC airframe had been subjected to significant operational stress. Previous overloads had likely weakened the composite materials, diminishing the airframe's overall safety margins. With added stress from the excess weight, the airframe's capacity to withstand forces was further compromised, making even routine operations riskier and creating dangerous conditions for high-stress manoeuvres or extreme flight conditions.

- **Pilot's Operational History**. The pilot had a recorded history of performing prohibited manoeuvres and exceeding the aircraft's operational limits. This habitual overstressing of the aircraft compounded previous structural strains. Given that the pilot brought along a passenger on this flight, it is likely he may have planned to demonstrate similar manoeuvres, as he had on recent flights with passengers on board in Chiang Mai and Phuket. This operational pattern significantly increased the risk of a structural failure.

Given the significant combination of excess weight, an overstressed airframe, and the pilot's operational habits, these factors created conditions that likely led to structural separation. Based on the available data and circumstantial evidence, the following is the most probable sequence of events that led to the accident.

- **Flight Path and Control**. Up until the final recorded G3X data point, the pilot appeared to maintain control of the aircraft. The rapid descent brought the aircraft to and then beyond V_{NO}, suggesting it may have operated outside the approved flight envelope—particularly if it had not been flown cautiously in smooth air without abrupt manoeuvres or full control surface deflections.[24] The speed reduction and fluctuating descent rates observed in the final ADS-B data points indicate the aircraft could have been responding to an aerodynamic manoeuvre, whether intentional or otherwise.

- **Pilot's Manoeuvres**: Considering the pilot's history of performing aggressive manoeuvres, such as steep pull-ups and excessive rolls after a dive, as observed in this instance, it is plausible that the pilot initiated a similar manoeuvre after the last recorded stable control point at 13:35:52 LT. Such a manoeuvre would have placed the aircraft outside the approved flight envelope,

[24] The BK 160TR's V_{NO} (155 KIAS) is the Maximum Structural Cruising Speed, which should not be exceeded except in smooth air and only with caution. The Design Manoeuvring Speed (V_A) is 128 KIAS, above which full or abrupt deflection of any flight control surfaces must be avoided.

exceeding both V_A and V_{NO}. Combined with the already structurally weakened and overloaded airframe, this could have led to the separation of critical components, resulting in sharp, uncontrollable flight.

- **Failure and Separation of the LH Wing Skin**: One of the likely failure points in the compromised I-POOC airframe was the area around the man-made hole in the LH wing. Severe cracking and significant material damage observed in the corresponding area of the recovered RH wing suggest that similar damage could have affected the LH wing as well. Material examination and failure analysis indicate that a rupture likely occurred near the LH man-made hole, leading to a cascading debonding and detachment of larger sections of the LH wing's skin, which were subsequently found at Site 4 and Site 3. Aerodynamic forces and airflow likely contributed to the separation, as evidenced by debris dispersed across multiple wreckage sites.

- **LH Wing Loss of Lift and Asymmetry**: Following the LH wing skin failure in an already structurally compromised airframe, the LH wing experienced a rapid loss of lift, initiating a roll to the left. The pilot likely responded with RH aileron input and pulled back on the stick in an attempt to counteract the roll and regain altitude. However, the resulting lift asymmetry would have intensified the roll, exposing the RH wing to extreme aerodynamic loads, which ultimately led to its structural failure.

  Calculations by Blackshape S.p.A. on the RH wing load distribution in the event of LH wing skin failure (see **Appendix L**) confirmed that these loads could have approached or exceeded ultimate certification limits, particularly in a weakened structure with reduced safety margins. This finding is consistent with the observed in-flight break-up and wreckage analysis, which indicated upward bending of the RH wing (see **Appendix A**). Furthermore, Blackshape's analysis suggests that the left aileron may have failed due to unexpected flight loads during the pilot's recovery attempts, aligning with its discovery at Site 3.

- **RH Wing Failure and Cockpit Impact**: The RH wing likely experienced critical structural failure due to excessive aerodynamic loads generated by the aircraft's rolling motion and the pilot's recovery attempts. Examination of the RH wing flap connecting rod indicates upward bending, consistent with stress applied during the roll. This failure, combined with extreme forces on an already weakened airframe, likely resulted in the wing's separation. The wreckage distribution supports this theory; fragments of the cockpit canopy and passenger cap found at Site 3 suggest that the RH wing bent upward, detached, and struck the canopy. This impact would have caused significant destruction to the cockpit structure, contributing to the overall catastrophic failure.

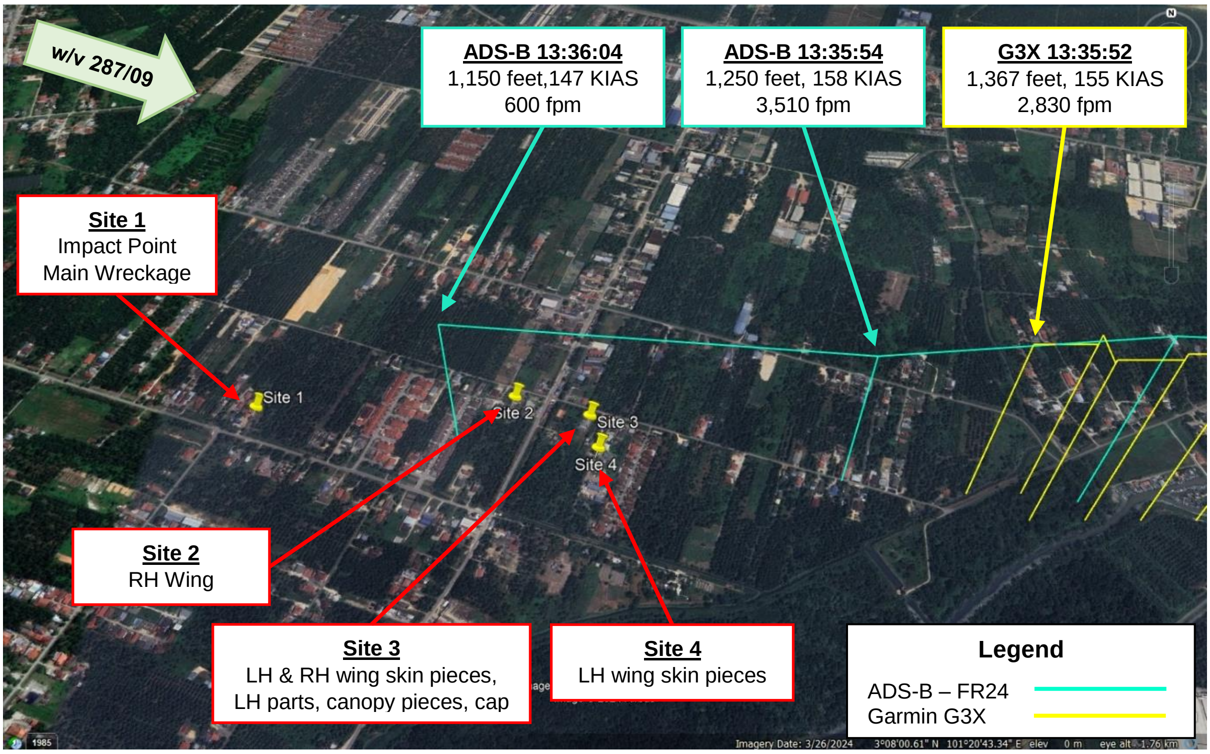

Figure 40. Flight Parameters Changes and Wreckage Distribution

- **Wreckage Distribution and Sequence of Events:** The wreckage distribution provides important clues to the sequence of the breakup. Large sections of the LH wing skin were located at Site 4, the farthest wreckage site to the east of the main impact area, indicating that the LH wing skin was likely the first component to detach. Additional smaller fragments, including the LH wing lower skin, RH wing inner upper skin, LH aileron, and LH wing tip, along with cockpit canopy fragments and the passenger cap, were found at Site 3, positioned slightly west of Site 4.

Further west, the separated RH wing was discovered at Site 2, while the main wreckage, including the cockpit and fuselage, was located at Site 1, marking the final impact point. This pattern of wreckage distribution aligns with the hypothesised sequence of events leading to the aircraft's structural separation and supports the assumed direction of travel of the aircraft. It also reflects the influence of the prevailing wind, which likely affected the drift and final resting positions of various separated components.

The separation of the aircraft's structural components likely occurred between the final two ADS-B data points, recorded between 13:35:54 LT and 13:36:04 LT, as suggested by changes in flight parameters during this brief interval. This event followed the pilot's last radio transmission to ATC at 13:35:34 LT, reporting the aircraft's position west of Kapar. This hypothesis is supported by the understanding of the weakened structural integrity of the aircraft, the pilot's operational history, available flight data, and the wreckage distribution across multiple sites.

The sequence of events suggests that the structural failure of the I-POOC began with the detachment of the LH wing skin, likely originating from the area around a man-made hole, which led to the rapid separation of larger sections. This caused a loss of lift on the LH wing, initiating a left roll. The pilot's recovery attempts exacerbated the stress on the RH wing, which subsequently failed under extreme aerodynamic loads and struck the cockpit canopy, resulting in catastrophic destruction. The wreckage distribution, with LH wing fragments located furthest east, and cockpit remains and RH wing found further west, supports this sequence and reflects the aircraft's direction of travel and the influence of wind effects:

- **13:35:34 LT**: Pilot reported being established west of Kapar.
- **13:35:45 LT**: Initiation of a controlled dive manoeuvre.
- **13:35:54 – 13:36:04 LT**: Structural separation sequence likely commenced within this window, as indicated by changes in flight parameters.

- **Flight Beyond Limits**: The aircraft likely operated outside the approved envelope with minimal safety margin due to its weakened structure.
- **LH Wing Failure**: The initial failure of the LH wing led to rotation and a subsequent loss of control.
- **RH Wing Failure**: The RH wing separated due to stresses induced by the roll.
- **Cockpit Impact**: The RH wing impacted the cockpit.
- **Wreckage Pattern**: The wreckage distribution supports the sequence and the breakup direction of the aircraft.

2.5.4 Summary of Flight Analysis

In conclusion, while the exact sequence of events leading to the in-flight breakup cannot be definitively determined, the evidence strongly indicates that the I-POOC aircraft was critically compromised, with structural weaknesses rendering it effectively unairworthy. The aircraft’s frequent operations beyond its approved flight envelope, combined with severe degradation of its composite materials, had significantly diminished its structural integrity. Without drastic intervention to address these issues, catastrophic failure became inevitable. Each flight pushed the aircraft beyond its remaining safety margins, ultimately leading to this unavoidable accident.

2.6 Human Factors Analysis

This analysis examines the pilot's actions, decisions, and personal circumstances that contributed to the accident. Key elements include the pilot’s operational history, risk-taking behaviours, the impact of alcohol consumption on performance, and irregular maintenance practices. Notably, the pilot’s installation of uncertified tie-down rings—a critical factor in the aircraft’s structural failure—is also addressed.

2.6.1 Pilot Experience and Operational History

The pilot’s operational history indicates a moderate level of experience, particularly with the BK 160TR type, but also a tendency to operate the aircraft beyond its approved limits. Frequent aggressive manoeuvres and exceeding operational boundaries likely accelerated the wear of the aircraft's composite materials, ultimately compromising its structural integrity. This pattern reflects a high-risk tolerance and an apparent underestimation of the associated consequences.

A critical aspect of the pilot's decision-making was the installation of the uncertified tie-down rings, which weakened the wing structure and directly contributed to the in-flight breakup. Despite the clear risks involved, the pilot proceeded with installing this unapproved component, demonstrating a serious lapse in judgment and a disregard for safety protocols.

Additionally, the pilot conducted maintenance activities, including assisting uncertified personnel in the installation of a new nose landing gear, despite lacking the necessary qualifications to perform such tasks. This further highlights a pattern of unsafe practices and decision-making.

2.6.2 Alcohol Influence and Performance

The post-mortem report revealed that the pilot's blood alcohol level exceeded the regulatory limit, indicating that the pilot was under the influence of alcohol while operating the aircraft. Alcohol consumption can impair cognitive and motor functions, affecting judgment, reaction times, and overall performance. It is likely that the pilot's ability to assess the situation accurately and respond appropriately during the critical moments of flight was compromised. The presence of alcohol, combined with the pilot's aggressive flying style, may have contributed to the failure to recognise the aircraft's structural distress in time, further exacerbating the situation.

2.6.3 Risk Awareness and Safety Culture

The pilot's history of operating the aircraft beyond its limits and the installation of uncertified tie-down rings reflect a culture of risk-taking and disregard for safety protocols. Installing an uncertified component undermines the aircraft's airworthiness and represents a critical oversight in maintaining safety standards. Coupled with alcohol consumption, this indicates a failure to fully appreciate the associated risks.

Additionally, inadequate supervision by from all involved organisations—Sky Media, AST, and AAFC—allowed these unsafe practices to persist. This lack of effective oversight and enforcement of safety standards fostered a broader issue of operational complacency, where safety boundaries were routinely breached, culminating in the aircraft's catastrophic failure.

2.6.4 Summary of Human Factors

The key human factors contributing to the accident are rooted in the pilot's overconfidence, risk tolerance, and impaired decision-making. The pilot's consistent tendency to operate the aircraft beyond its safety limits, combined with alcohol consumption, diminished his ability to assess risks accurately during critical flight operations. Additionally, the pilot's installation of uncertified tie-down rings, which compromised the structural integrity of the wings, played a pivotal role in the in-flight breakup. This decision, alongside other unsafe maintenance practices, demonstrated a disregard for safety protocols and operational limits, ultimately weakening the aircraft's overall airworthiness.

The pilot's actions, compounded by the absence of effective oversight by Sky Media, AST, and AAFC, contributed to a culture of operational complacency. This lack of supervision enabled the pilot to operate the aircraft beyond its safe limits. Furthermore, the pilot's alcohol impairment significantly compromised his judgment, resulting in critical failures to recognise and respond to the aircraft's structural distress. These factors, combined with the aircraft's already compromised condition, culminated in the catastrophic accident.

2.7 Organisational Factors Analysis

The organisational factors contributing to the accident stemmed from systemic shortcomings in oversight, maintenance practices, and operational procedures across multiple entities, including Blackshape, Sky Media, AST, Aurotel, and AAFC. Each organisation's involvement revealed gaps in ensuring the safe and airworthy operation of the I-POOC aircraft. These shortcomings collectively contributed to the conditions under which the accident occurred.

2.7.1 Blackshape S.p.A.

As the manufacturer and registered owner of the BK 160TR aircraft (I-POOC), Blackshape held a responsibility to ensure the aircraft's ongoing safety and operational integrity. Business disputes with Sky Media, however, resulted in a lack of operational support and oversight. Blackshape did not facilitate the effective transfer of ownership or implement mechanisms to address maintenance and operational risks associated with the aircraft. While indirect, these unresolved issues created gaps that were later exacerbated by actions—or inactions—of other organisations involved in the aircraft's operations.

2.7.2 Sky Media Ltd and Aviation Safety Technology Pte Ltd (AST)

Sky Media, as the regional distributor, was positioned to play a critical role in ensuring the airworthiness of the I-POOC aircraft but did not fulfil this responsibility effectively. Ongoing disputes with Blackshape over ownership and registration created ambiguity in accountability. Despite being aware of grounding instructions, Sky Media allowed the aircraft to continue operating. Furthermore, they supplied and permitted the installation of non-certified tie-down ring parts, compromising the aircraft's structural integrity. The organisation's failure to address these safety concerns and implement corrective actions highlighted significant deficiencies in oversight.

AST, identified as the aircraft's operator in official documentation, did not undertake adequate operational monitoring or enforce safety standards. This lack of diligence extended to oversight of the pilot's actions and compliance with operational limits. Irregular maintenance practices and insufficient inspections of the aircraft compounded these risks, reflecting a broader absence of accountability in ensuring the aircraft was operated within safe parameters.

2.7.3 Aurotel Sdn Bhd and Air Adventure Flying Club (AAFC)

Aurotel, which sub-leased the hangar space to AST and provided operational support services—including aircraft refuelling and servicing—permitted uncertified personnel to perform maintenance on the I-POOC aircraft. This practice likely compromised the aircraft's airworthiness. Aurotel's role at Subang highlighted systemic weaknesses in enforcing compliance with proper maintenance standards.

AAFC, where the pilot was both a member and an instructor, exhibited significant lapses in safety management. Although the I-POOC aircraft bore the AAFC logo and the pilot utilised the club's resources—such as the NOSAS account for flight permits and the club callsign—AAFC distanced itself from responsibility for the aircraft's operation. While AAFC did not directly manage the I-POOC, it failed to exercise oversight over an instructor who was actively involved in its operations.

Furthermore, while not explicitly prohibited, the presence of alcoholic beverages on AAFC premises raised concerns about the club's safety culture. More critically, evidence that an AAFC-affiliated flight instructor operated an aircraft under the influence of alcohol highlighted a significant lapse in maintaining a safety-conscious environment. This instructor had also conducted AAFC flight training sorties earlier in the day before the accident flight, underscoring insufficient organisational control and a failure to enforce safety protocols.

2.7.4 Summary of Organisational Factors

The accident was influenced by systemic shortcomings across multiple organisations, each contributing to an environment of reduced safety margins. Blackshape S.p.A. failed to provide adequate operational support or oversight, while Sky Media supplied non-certified parts and neglected to address safety concerns. AST, responsible for the aircraft's operation, did not enforce critical safety protocols or adequately monitor the pilot's actions.

Aurotel allowed uncertified maintenance, undermining the aircraft's airworthiness. AAFC demonstrated significant lapses in safety management, particularly in overseeing instructors and flight operations. This was evidenced by insufficient oversight, including the discovery of practices inconsistent with promoting a strong safety culture. The cumulative effect of these organisational factors created conditions under which the accident became inevitable, highlighting the need for systemic improvements to prevent future occurrences.

3.0 CONCLUSION

3.1 Findings

The investigation into the accident involving the Blackshape BK 160TR aircraft, registration mark I-POOC, revealed the following key findings:

3.1.1 Aircraft

3.1.1.1 The aircraft held valid airworthiness certification at the time of the accident.

3.1.1.2 The aircraft's take-off weight (921.3 kg) on the accident flight exceeded the maximum allowable take-off weight (850 kg).

3.1.1.3 The aircraft had a history of being operated above its maximum take-off weight limitation, which likely contributed to increased structural fatigue.

3.1.1.4 Uncertified maintenance activities were performed on the aircraft by non-qualified personnel.

3.1.1.5 Non-certified parts, particularly tie-down ring components, were installed on the aircraft, compromising its structural integrity.

3.1.1.6 The aircraft's composite materials were likely weakened by prolonged exposure to excessive operational loads, as well as modifications such as the installation of uncertified tie-down rings.

3.1.1.7 Evidence of delamination and micro-cracking in the composite materials suggests cumulative structural degradation.

3.1.1.8 The man-made hole in the LH wing, created to accommodate the tie-down ring, significantly weakened the wing's structural integrity and possibly contributed to the failure sequence.

3.1.1.9 The aircraft's Maximum Structural Cruising Speed (V_{NO}) was likely exceeded during the descent, contributing to structural stresses beyond design limits.

3.1.1.10 Potential manufacturing defects in the composite materials could not be definitively determined due to the degraded condition of test samples, which were subjected to sustained operational overload, crash impact forces, and environmental exposure.

3.1.1.11 Maintenance records were incomplete, with gaps in compliance regarding modifications and repairs, impacting the aircraft's airworthiness.

3.1.2 Pilot

3.1.2.1 The pilot was properly licensed and qualified for the flight.

3.1.2.2 The pilot had a history of performing aggressive manoeuvres that exceeded operational limits.

3.1.2.3 The pilot's flying style and decisions during the flight likely contributed to excessive loading on the aircraft's structure.

3.1.2.4 The pilot participated in maintenance activities on the aircraft despite not being certified to do so, compromising airworthiness and safety, and exhibiting a lack of adherence to standard procedures and safety protocols.

3.1.2.5 The pilot ignored operational limits, including the aircraft's weight limitations and other operational restrictions, performing numerous prohibited manoeuvres that compromised the safe operation of the aircraft and contributed to excessive stresses on the aircraft's structure.

3.1.2.6 The pilot was operating the aircraft under the influence of alcohol on the accident flight.

3.1.3 Flight Operations

3.1.3.1 The accident flight was probably operated outside the approved flight envelope, with the aircraft reaching and likely exceeding V_{NO}.

3.1.3.2 The aircraft frequently exceeded its flight envelope, surpassing V_{NE}, V_{NO}, and load factor limits, including exceedances of 4.4 g symmetrical and 2.9 g asymmetrical load limits, while performing steep turns, 360-degree rolls, and other manoeuvres beyond approved limits.

3.1.3.3 Unsafe operational behaviour, including disregard for weight and airspeed limits, and repeated prohibited manoeuvres, highlighted a failure to follow safe flying practices.

3.1.4 Organisation

3.1.4.1 Unresolved disputes between **Blackshape S.p.A.** and **Sky Media Ltd** resulted in gaps in accountability for the aircraft's maintenance and condition, affecting operational safety oversight.

3.1.4.2 **Sky Media Ltd** supplied non-certified parts compromising the aircraft's structural integrity, and operated the aircraft despite grounding instructions, without ensuring proper corrective action for maintenance issues.

3.1.4.3 **Aviation Safety Technology Pte Ltd**, listed as the operator, did not monitor or enforce safe operational practices.

3.1.4.4 **Aurotel Sdn Bhd**, although uncertified for maintenance, permitted uncertified personnel to perform maintenance, impacting airworthiness.

3.1.4.5 **Air Adventure Flying Club** distanced itself from operational accountability, failing to enforce safety oversight despite the pilot's use of its resources and close association with the operation of I-POOC.

3.1.5 Flight Recorders

3.1.5.1 The aircraft was not equipped with an FDR or CVR, as neither was required by regulation.

3.1.5.2 The Garmin G3X GDU 460 data provided key flight and engine parameters, aiding the reconstruction of the accident flight and analysis of the aircraft's operational history over its last 13 flights.

3.1.5.3 ADS-B data complemented the G3X data, offering final descent tracking points and contributing to the understanding of the probable sequence of events during the final moments of the flight.

3.1.6 Medical

3.1.6.1 The pilot’s blood alcohol concentration (BAC) was found to be 0.032%, which is above the prescribed legal limit (0.02%) and may have impaired the pilot’s performance during the flight.

3.1.6.2 Apart from the BAC result, no other medical factors were identified that contributed to the pilot’s performance or the accident.

3.1.6.3 Post-mortem examinations determined that both the pilot and passenger sustained fatal injuries from the crash.

3.1.7 Survivability

3.1.7.1 The accident was not survivable due to the magnitude of the deceleration forces involved upon impact.

3.2 Causes/Contributing Factors

3.2.1 Causes of the Accident

The accident was primarily caused by the failure and in-flight separation of structural parts due to excessive operational stresses on the aircraft's weakened composite materials. The aircraft's structural integrity was compromised by repeated operation outside its approved flight envelope, including exceeding maximum airspeeds, load factors, and structural limits, which placed undue strain on its structure. Furthermore, the installation of non-certified parts, specifically the tie-down rings, further weakened the aircraft's integrity, contributing to the failure.

3.2.2 Contributing Factors

Several contributing factors to the accident have been identified:

- **Pilot Performance**: The pilot engaged in aggressive flying manoeuvres beyond the aircraft's approved limits that contributed to excessive loading that compromised the aircraft's structural integrity, leading to the in-flight separation of parts.

- **Aircraft Maintenance**: The aircraft was subjected to unapproved maintenance practices, including the installation of non-certified parts by unqualified personnel, compromising the aircraft's structural integrity, making it more susceptible to in-flight failure.

- **Organisational Failures**: The aircraft operator, along with the distributor, failed to ensure adherence to proper operation, maintenance and safety protocols, contributing to an unsafe operational environment.

- **Operational Oversight**: There were no procedures in place to monitor and enforce safe operational limits, resulting in a lack of oversight of the aircraft's condition and performance during flight operations.

3.2.3 Occurrence Category

This aviation occurrence is coded as **System/Component Failure or Malfunction (Non-Power Plant) (SCF-NP)**.

4.0 SAFETY RECOMMENDATIONS

4.1 Civil Aviation Authority of Malaysia (CAAM)

4.1.1 CAAM is recommended to implement enhanced measures for scrutinising non-scheduled flight operations within Malaysia, particularly those involving foreign-registered aircraft and foreign-licensed aircrew. These measures should include more stringent vetting of NOSAS applications and conducting ramp inspections of foreign aircraft operations to ensure regulatory compliance and maintain safe operations.

4.1.2 CAAM is recommended to strengthen its oversight of approved training organisations by ensuring strict adherence to safety standards through regular audits, inspections, and closer monitoring of operational and maintenance practices.

4.2 Aviation Safety Technology Pte Ltd (AST)

4.2.1 In the event that AST resumes aircraft operations, it is recommended that the operator strengthen its internal procedures for monitoring and assessing pilot performance, particularly concerning aggressive flying manoeuvres and the risks of exceeding operational limits.

4.3 Aurotel Sdn Bhd and Air Adventure Flying Club (AAFC)

4.3.1 AAFC is recommended to implement a strict policy on substance and alcohol use to ensure the fitness and safety of flight instructors, students, and staff.

4.3.2 Aurotel and AAFC are recommended to strengthen oversight of operations and maintenance for their aircraft, including the foreign-registered Cessna 172M (N1188U). This should involve ensuring maintenance is conducted exclusively by certified personnel and performing regular audits to ensure compliance with airworthiness standards.

4.4 Blackshape S.p.A.

4.4.1 Blackshape is recommended to adopt a cautious approach in reviewing the structural integrity of the BK 160TR aircraft, particularly concerning the composite material used in the I-POOC. While the likelihood of material issues may be low, a thorough assessment of potential airworthiness concerns is essential to ensure the continued structural integrity of the existing fleet.

5.0 COMMENTS ON DRAFT FINAL REPORT

In accordance with ICAO Annex 13, paragraph 6.3, the Draft Final Report was sent to the State of Registry, Design, and Manufacturer (ANSV), the State that participated in the investigation (NTSB), CAAM, AAFC, and AST, inviting their significant and substantiated comments. The NTSB's comments were agreed upon and incorporated into the report. Comments from ANSV were partially accepted, while comments from AST were not accepted. The substance of the agreed portions of ANSV's comments have been incorporated into the report. In accordance with paragraph 6.3 of ICAO Annex 13, ANSV requested that any disagreed comments be appended to the report, which has been done in **Appendix M**. AST did not indicate any such desire. CAAM and AAFC did not provide any comments on the Draft Final Report.

CONCLUDING STATEMENT

This investigation has identified many instances of non-compliance and operational deficiencies. However, in accordance with ICAO Annex 13 principles, it must be emphasised that these findings are not intended to apportion blame or liability, but rather to facilitate the prevention of future accidents and enhance overall aviation safety. The adoption of the recommended safety measures will help address the identified shortcomings, strengthen the aviation safety framework, and mitigate risks associated with operational lapses and regulatory gaps. All stakeholders are urged to prioritise safety and collaborate in implementing the necessary measures to prevent recurrence.

INVESTIGATOR IN-CHARGE

Air Accident Investigation Bureau

Ministry of Transport Malaysia

Appendix A

Aircraft Damage Assessment

1 Introduction

This damage assessment report on the BK 160TR aircraft (S/N BCV.21010, registration mark I-POOC) is based on the report prepared by the Blackshape Technical Advisers (TA) to the ANSV Accredited Representative (Accrep).

2 Left Hand (LH) Wing

The LH wing main spar, aft spar and ribs were found at Site 1, the main wreckage area. The front and rear spar breaking points are compatible with high energy impact.

Figure 1. LH Wing

The wing upper skin, the lower skin with part of the wing leading edge and wing tip were detached. The wing upper skin was detached from the front and rear spar. The failure mode seems to be interlaminar failure of the skin. Part of the wing leading edge, i.e. from the wing fitting to the fuel cap location, was detached. The failure mode is also in this case interlaminar failure, in correspondence of the bonding flange.

3 LH Aileron

The LH aileron was found bent almost in the middle of its span. The aileron was detached from the hinges. The connecting rod was detached from the bellcrank.

Figure 2. LH Aileron Connecting Rod, and Bellcrank

4 Right Hand (RH) Wing and Main Landing Gear (MLG)

The whole RH wing (except for the inner upper skin) was found at Site 2, about 560 metres to the east of the main wreckage. The RH wing inner upper skin, together with the inner rib, was found at Site 3. Refer to paragraph 5 below for the failure mode of the upper skin. The failure mode of the inner rib is interlaminar failure. The RH flap and aileron were found connected to the wing.

Figure 3. RH Wing

The MLG was found installed in the wing box in its retracted position. The forward (FWD) and rear (RWD) wing spars were totally cracked at the intersection with the fuselage monocoque, where the lower side fuselage spars are installed.

Figure 4. RH MLG

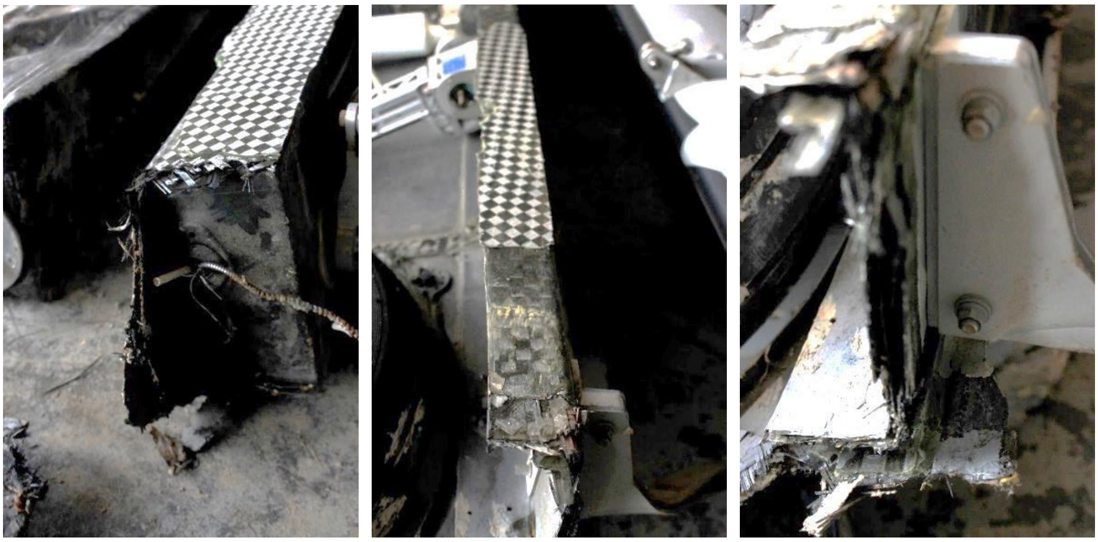

Figure 5. RH Wing Main and Rear Spar Crack

5 Skin/Spar Failure Mode

The failure of the skin/spar junction seems to be an interlaminar failure. The portion of laminate bonded to the wing spar remained attached to the spar cap revealing no failure of the bonding. The inner ribs of the wing box seem to have experienced the same failure mode.

Figure 6. Skin/Spar Failure Mode

6 Main Spar Fuselage

The web of the main spar is totally lost.

Figure 7. Main Spar Fuselage

7 Fuel Tank

7.1 LH Fuel Tank. The bladder of the LH fuel tank appears to be torn apart in correspondence of the filler cap. The rest of the damage is probably due to the ground impact with the main wreckage.

Figure 8. LH Fuel Tank

7.2 RH Fuel Tank. The RH fuel tank appears in good condition. There is no sign of collapse. Signs of rupture are found in the inner part of the tank.

Figure 9. RH Fuel Tank

8 Engine Compartment

The engine compartment was found two metres under the ground. All damages appear to be caused by the high energy ground impact. Two blades where found cracked around the root. One blade is missing from the rotating shaft.

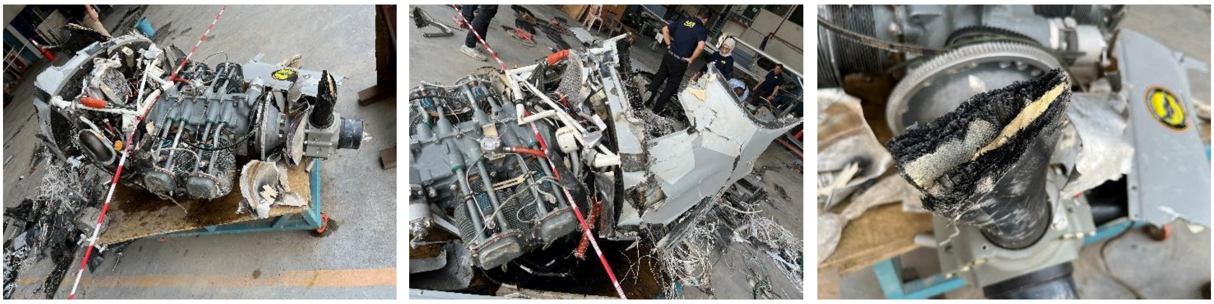

Figure 10. Engine Compartment and Propeller

9 Cockpit

Both cockpits were found destroyed by the high energy ground impact. The roll bar and the seat cushions are retrieved as shown below.

Figure 11. Cockpit (Destroyed)

10 Electro-Avionics Components

The following are the main electro-avionics components that were retrieved from the wreckage:

- Rear only EFIS / Garmin GDU 460

- Front and rear Garmin G5
- Front and rear LG panel
- Front and rear audio panel PM8000 and radio GNC255a
- Battery box
- Mode selector switch
- Alternator

Figure 12. Rear EFIS / Garmin GDU 460

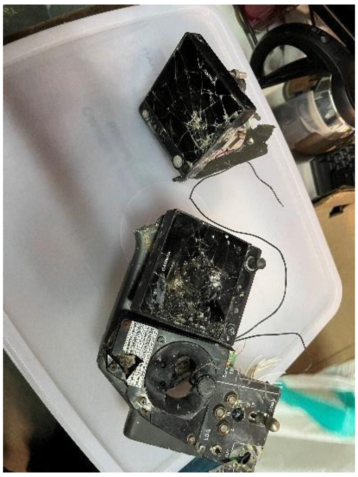

Figure 13. Front and Rear Garmin G5, Rear LG Panel

Figure 14. Front LG Panel

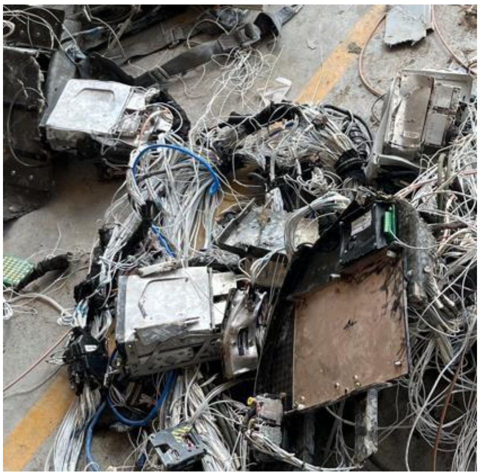

Figure 15. Front and Rear Audio Panel PM8000 and Radio GNC255a

Figure 16. Battery Box

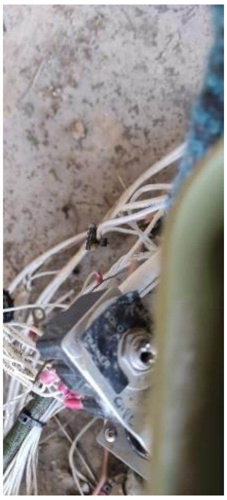

Figure 17. Mode Selector
(Passenger Mode Selected)

Figure 18. Alternator

11 Aircraft Tail

The rudder was found detached from the vertical stabiliser through the hinges. The horizontal stabiliser was found detached from the fuselage. The elevator was partially detached from the horizontal stabiliser through the hinges. The elevator trim was found detached from the elevator through the hinges. The lever to the trim motor was found in place.

Figure 19. Tail Destroyed (Left), Tail Reconstructed (Middle),
Trim Tab (Right)

12 Flight Controls

12.1 Longitudinal. All connecting rods are found disconnected from the forks (weakest elements).

Figure 20. Longitudinal Control: Control Column (Top Left),
First Connecting Rod (Top Right), Last Connecting Rod (Bottom)

12.2 Lateral. The connecting forks to the control column are broken, probably due to high energy impact. The end connecting rod is detached from the bellcrank (refer to paragraph 3).

Figure 21. RH and LH Aileron Connecting Forks to The Control Column

12.3 Directional control. The forward and aft pedal systems, and their connecting elements are found broken, compatible with the high energy impact,

Figure 22. Front and Rear Pedal Assembly

12.4 Flap Control. The flap motor is found detached from the rear spar, compatible with high energy impact. The RH connecting rod is disconnected from the gear motor and from the wing flap actuator by the rotating joints. The RH connecting rod is bent, probably due to the in-flight RH wing detachment.

Figure 23. Flap Control System: Flap Motor and Connecting Rods

13 Landing Gear

The RH Main Landing Gear (MLG) was found installed in its compartment (RH wing box) apparently in retracted position. The LH MLG was found attached on the LH wing main spar only. The Nose Landing Gear (NLG) was found installed in its position (engine mount), apparently in retracted position.

Figure 24. Main Landing Gear (LH and RH)

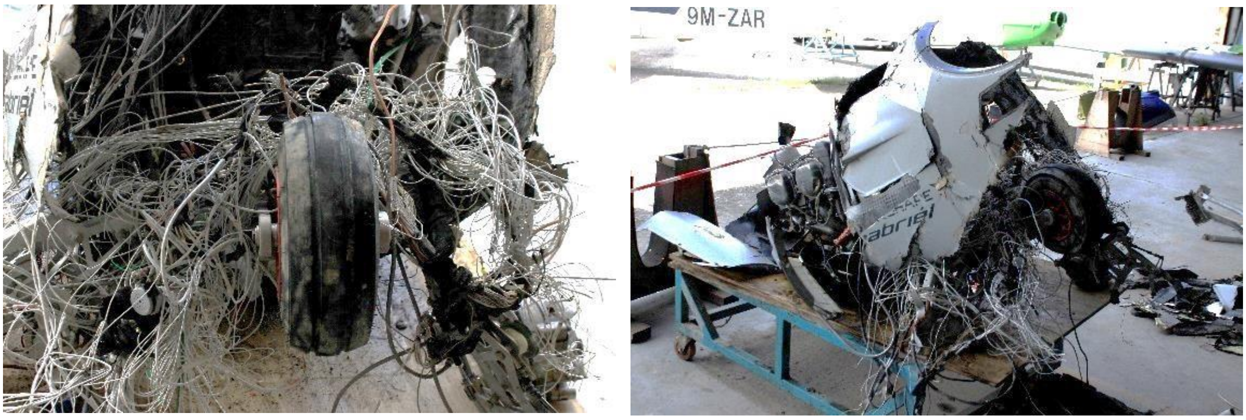

Figure 25. Nose Landing Gear

14 Canopy

Fragments of the canopy was found at or around Site 3. The front canopy handle was retrieved. The position of the handle was not closed. However, the opening system was broken.

Figure 26. Fragments of Canopy Found at or Around Site 3

Figure 27. Front Canopy Opening Handle

15 Non-Conforming / Non-Certified Parts

As discussed in section 1.6.6, two ‘tie-down ring’ parts were installed at the joints of the wing fitting and main spar, i.e. one ‘tie-down ring’ on each wing. These parts are not part of the approved aircraft configuration.

Figure 28. Non-Conforming Parts Installed on The LH And RH Wing Fitting

A fire extinguisher was found together with the wreckage. It was not part of the approved configuration. There is no provision of a storage place in the cabin for the fire extinguisher.

Figure 29. Fire Extinguisher

16. Additional Wreckage Assessment – RH Flap Connecting Rod

An additional wreckage assessment was conducted on the RH flap connecting rod to evaluate the bending of the right wing. The RH flap rod joint was re-connected onto the shaft of the flap actuator (wing side), as depicted in Figure 30 below. The shaft has a key that ensures a precise positioning within the joint. Assessing the bending of this flap rod indicates that the direction of wing bending was up.

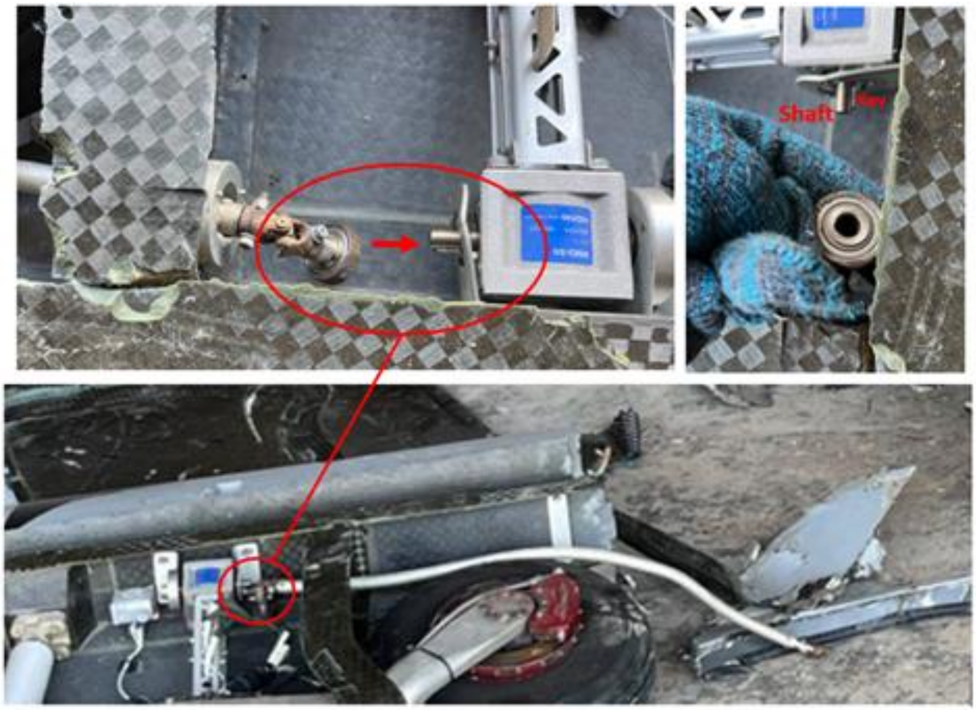

Figure 30. RH flap connecting rod joint re-connected to flap actuator shaft

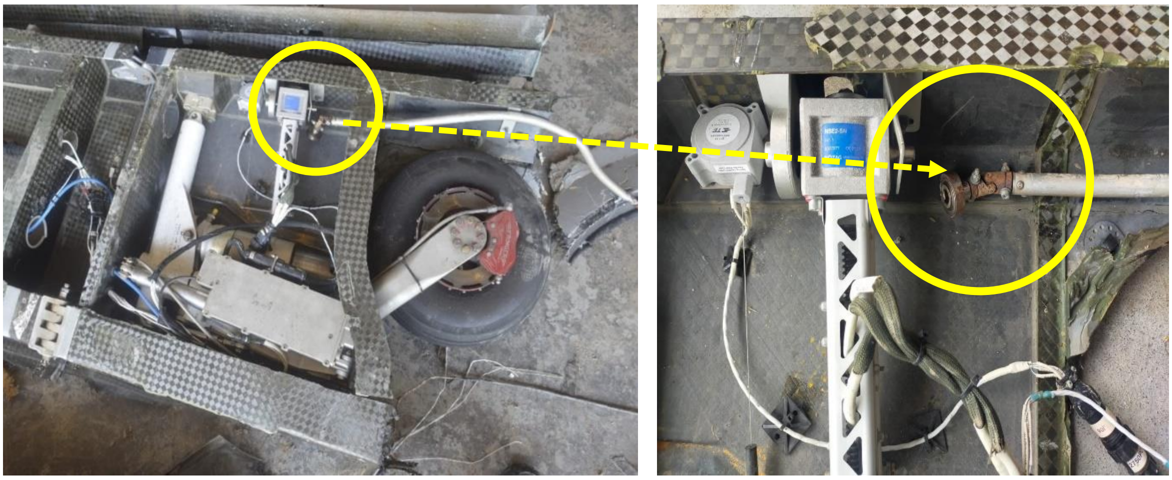

Figure 31. Physical condition of the connecting rod and shaft inside the RH wing (After recovery from the crash site – Site 2)

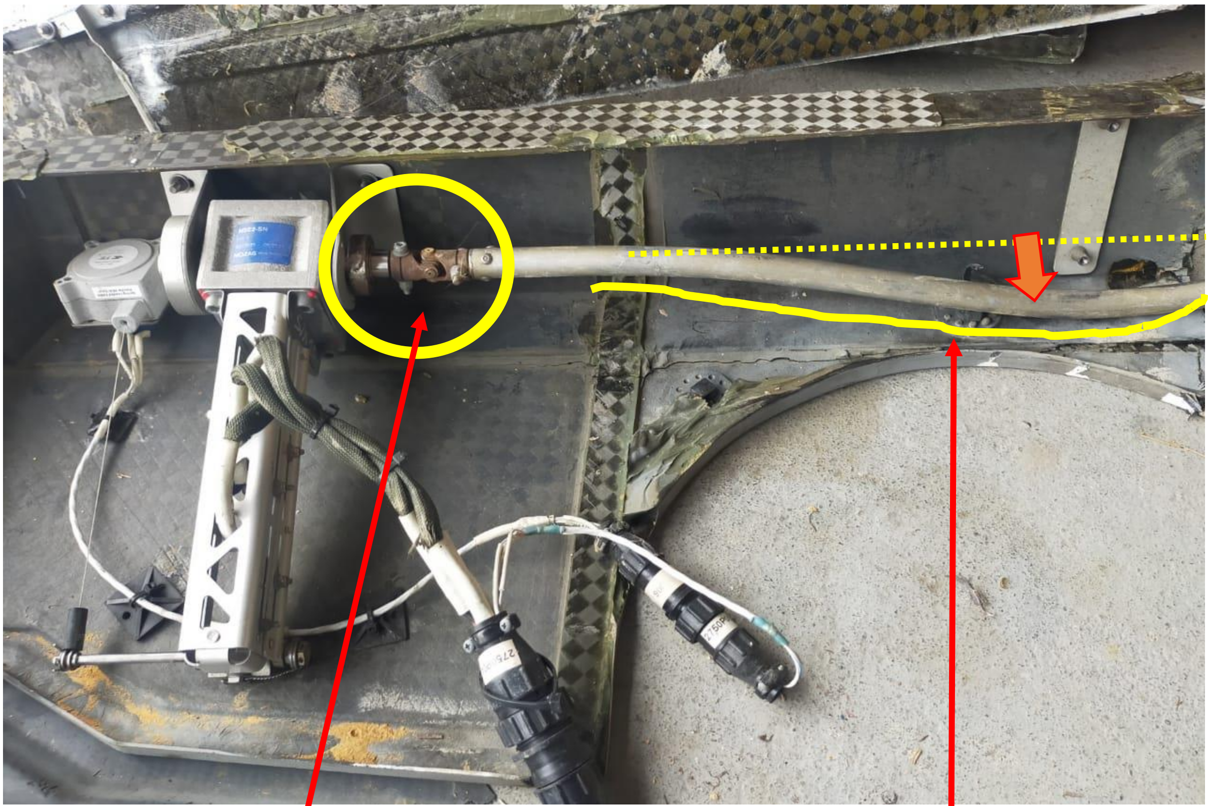

The RH flap connecting rod reconnected to the shaft of the flap actuator (wing side)

Observations:
1. The rod bent direction: **DOWN**
2. The wing bent direction: **UP**

Figure 32. Wing Bent Direction

Appendix B

Aircraft Certificate of Registration

ENAC
ENTE NAZIONALE PER L'AVIAZIONE CIVILE

Funzione Organizzati
RAN-ENG

Spett.le
BLACKSHAPE SPA
Pec: blackshapeaircraft@legalmail.it

ENAC - DIREZIONE OPERAZIONI SUD
ENAC - FUNZIONE ORGANIZZATIVA FATTURAZIONE

Oggetto: BK160TR - S/N BCV.21010 - MARCHE I-POOC
Immatricolazione Autocostruito

Si comunica che in data 02 Agosto 2022 l'aeromobile in oggetto è stato immatricolato nel Registro Aeronautico Nazionale.

Si allega il Certificato di Immatricolazione n.12921 rev.0.

Cordiali saluti

Il Responsabile
Eugenia Mannelli

documento informatico firmato digitalmente
ai sensi dell'art. 24 D.Lgs. 82/2005 e ss.mm.ii.

sede legale: Viale Castro Pretorio, 118
sede operativa: Via Gaeta, 3
00185 Roma
centr. +39 06 445961
c.f. 97158180584
ERN

tel. +39 06 44596219
RAN :registro.aeromobili@enac.gov.it
ENGA : gente.aria@enac.gov.it
protocollo@pec.enac.gov.it
www.enac.gov.it

REPUBBLICA ITALIANA ENAC ENTE NAZIONALE PER L'AVIAZIONE CIVILE *ITALIAN CIVIL AVIATION AUTHORITY*	**CERTIFICATO DI IMMATRICOLAZIONE** CERTIFICATE OF REGISTRATION	**N.12921** del (dated) 02/08/2022 **Rev. N.** 0 del (dated) 02/08/2022
1. Marche di nazionalità e di immatricolazione *Nationality and registration marks* **I - POOC**	2. Costruttore e tipo dell'aeromobile *Manufacturer and manufacturer's designation of aircraft* **BLACKSHAPE SPA - BK160TR**	3. Numero di serie *Serial number* **BCV.21010**

4. Proprietario
Owner

BLACKSHAPE SPA
S.S. 16 kM 841+900 Z.I. - 70043 Monopoli (BA) - Italia

5. Il presente Certificato attesta che il sopra indicato aeromobile è stato iscritto nel Registro Aeronautico Nazionale in accordo con le disposizioni contenute nella Convenzione per l'Aviazione Civile Internazionale del 7 Dicembre 1944 e nel Codice della Navigazione

It is hereby certified that the above described aircraft has been duly entered on the Italian Civil Aircraft Register in accordance with the Convention on International Civil Aviation dated 7 December 1944 and with the Italian Air Navigation Code.

Data *date*	02/08/2022	Firma *signature*	Funzione Organizzativa RAN-ENGA Il Responsabile Eugenia Mannelli	Bollo assolto in modo virtuale aut. Direz. Reg. Entrate Lazio n. 135047/98 del 30/11/1998

Esercente *(authorized operator):*
Ipoteche *(mortgage):*
NESSUNA / NONE
Atti esecutivi o provvedimenti cautelari *(executive deed / interim injunction):*
NESSUNO / NONE

Appendix C

I-POOC Flight History* – March 2022 to December 2023

Flt No	Date	Dept	Arr	Blk Off	T/O	LDG	Blk On	Flt Time	Block Time	Daily Total	VRF IFR	LDG	Fuel Uplift	Avg Fuel Burn	POB	Pilot & Pax	Remarks
I-POOC Factory Flights - March 2022 to June 2022 (Flown as I-RAIA, BCV.21010's former Registration Mark)																	
F1	31/3/2022							00:20	00:27						2	Pilot 2	Maiden flight
F2	31/3/2022							00:32	00:35						2	Pilot 2 & unk	Stall handling. High speed stability
F3	31/3/2022							00:42	00:44	01:34					2	Pilot 2 & unk	Lateral stability
F4	6/4/2022							00:49	00:55						2	Pilot 2 & unk	Lateral stability
F5	6/4/2022							00:37	00:44						1	Pilot 2	Fwd CG controllability. Stall
F6	6/4/2022							01:28	01:36						2	Pilot 2 & unk	Night VFR evaluation
F7	6/4/2022							00:38	00:47	03:32					2	Pilot 2 & unk	Night VFR evaluation
F8	7/4/2022	LIBD	LIBG					00:24	00:34						2	Pilot 2 & unk	Transfer LIBD - LIBG. Production tests
F9	7/4/2022							01:10	01:14	01:34					2	Pilot 2 & unk	Avionic test flight
F10	11/4/2022							00:17	00:21	00:17					2	Pilot 2 & unk	Demo flight
F11	12/4/2022							01:00	01:04						2	Pilot 2 & unk	Avionic test flight. LG warning test
F12	12/4/2022							01:03	01:08	02:03					2	Pilot 2 & unk	Avionic test flight. LG/GPS
F13	22/4/2022							00:17	00:22						1	Pilot 2	Demo flight/perf check/shake-down
F14	22/4/2022							00:20	00:26	00:37					2	Pilot 2 & unk	Demo flight
F15	24/2/2022	LIBG	LIKO					02:46	02:50						1	Pilot 2	LIBG - LIKO
F16	24/2/2022	LIKO	EDNY					02:15	02:20	05:01					1	Pilot 2	LIKO - EDNY
F17	1/5/2022	EDNY	LIKO					02:32	02:40						1	Pilot 2	EDNY - LIKO
F18	1/5/1022	LIKO	LIBG					02:40	02:45	05:12					1	Pilot 2	LIKO - LIBG
F19	12/5/2022	LIBG	(Esprt)					00:11	00:13						2	Pilot 2 & unk	LIBG - Esperti
F20	12/5/2022	(Esprt)	LIBD					01:41	01:45	01:52					2	Pilot 2 & unk	Esperti - LIBD. Anti-collision
F21	13/5/2022	LIBD	(Esprt)					00:27	00:30	00:27					1	Pilot 2	LIBD - Esperti
F22	8/6/2022	(Esprt)	LIBG					00:09	00:12	00:09					2	Pilot 2 & unk	Esperti - LIBG
F23	9/6/2022							00:17	00:20	00:17					2	Pilot 2 & unk	Market survey
F24	16/6/2022	LIBG	(Esprt)					00:22	00:26	00:22					2	Pilot 2 & unk	LIBG - Esperti

Flt No	Date	Dept	Arr	Blk Off	T/O	LDG	Blk On	Flt Time	Block Time	Daily Total	VRF IFR	LDG	Fuel Uplift	Avg Fuel Burn	POB	Pilot & Pax	Remarks
F25	23/6/2022	(Esprt)	LIBG					00:14	00:19						1	Pilot 2	Esperti - LIBG
F26	23/6/2022	LIBG	LIBG					00:14	00:19	00:28					2	Pilot 2 & unk	LIBG - LIBG. Test unusable
F27	24/6/2022							00:48	00:53						2	Pilot 2 & unk	Test unusable
F28	24/6/2022							00:09	00:13	00:57					2	Pilot 2 & unk	Test unusable
F29	29/6/2022							00:09	00:16						2	Pilot 2 & unk	Test unusable
F30	29/6/2022							00:15	00:19						2	Pilot 2 & unk	ADS-B In Test
F31	29/6/2022							00:34	00:37	00:58					2	Pilot 2 & unk	ADS-B In Test
	Total for I-POOC Factory Flights (I-RAIA/BCV.21010)							**25:20**	**27:54**	**25:20**							

Flt No	Date	Dept	Arr	Blk Off	T/O	LDG	Blk On	Flt Time	Block Time	Daily Total	VRF IFR	LDG	Fuel Uplift	Avg Fuel Burn	POB	Pilot & Pax	Remarks
I-POOC Flights After Aircraft Delivery - November 2022 to December 2023																	
1	01/11/2022	WSSL	WSSL	02:15	02:30	03:50	04:00	01:20	01:45		V	1			2	Pilot 2 & Pilot 1	Pilot 2 and Pilot 1 - Training flight
2	01/11/2022	WSSL	WSSL	06:45	07:00	07:25	07:35	00:25	00:50		V	3			1	Pilot 2	
3	01/11/2022	WSSL	WSSL	08:00	08:10	08:15	08:20	00:05	00:20	01:50	V	1			1	Pilot 2	
4	02/11/2022	WSSL	WIPP	00:35	00:50	02:50	03:00	02:00	02:25		I	1			2	Pilot 2 & Pilot 1	Pilot 2 and Pilot 1 - Training flight
5	02/11/2022	WIPP	WIHH	04:05	04:20	06:15	06:25	01:55	02:20	03:55	I	1			2	Pilot 2 & Pilot 1	Pilot 2 and Pilot 1 - Training flight
6	05/11/2022	WIHH	WIPP	01:00	01:15	02:50	03:00	01:35	02:00		I	1			2	Pilot 2 & Pilot 1	Pilot 2 and Pilot 1 - Training flight
7	05/11/2022	WIPP	WSSL	03:40	03:55	05:40	05:50	01:45	02:10	03:20	I	1			2	Pilot 2 & Pilot 1	Pilot 2 and Pilot 1 - Training flight
8	28/11/2022	WSSL	WMSA	01:00	01:15	02:20	02:30	01:05	01:30	01:05	I	1			2	Pilot 1 & Pax 1	Shell 100 mineral oil uplift: 8 qt Probable maximum fuel load
9	29/11/2022	WMSA	WMKP	00:50	01:00	02:00	02:10	01:00	01:20		I	1	48L	9.5	2	Pilot 1 & Pax 1	Probable maximum fuel load
10	29/11/2022	WMKP	VTSP	03:30	03:40	05:10	05:20	01:30	01:50		I	1	66L	9.5	2	Pilot 1 & Pax 1	Probable maximum fuel load
11	29/11/2022	VTSP	VTPH	06:40	06:50	08:30	08:40	01:40	02:00	04:10	I	1	64L	8.5	2	Pilot 1 & Pax 1	Probable maximum fuel load
12	30/11/2022	VTPH	VTPP	01:05	01:15	02:40	02:50	01:25	01:45		I	1	67L		2	Pilot 1 & Pax 1	Probable maximum fuel load
13	30/11/2022	VTPP	VTCC	03:35	03:45	04:40	04:50	00:55	01:15		I	1	34L		2	Pilot 1 & Pax 1	Probable maximum fuel load
14	30/11/2022	VTCC	VYNT	05:35	05:45	06:35	06:45	00:50	01:10	03:10	I	1			2	Pilot 1 & Pax 1	Probable maximum fuel load
15	01/12/2022	VYNT	VYNT	02:00	02:05	02:30	02:35	00:25	00:35		V	1			2	Pilot 1 & unk Pax	Probable demonstration flight
16	01/12/2022	VYNT	VYNT	03:00	03:05	03:25	03:30	00:20	00:30		V	1			2	Pilot 1 & unk Pax	Probable demonstration flight

Flt No	Date	Dept	Arr	Blk Off	T/O	LDG	Blk On	Flt Time	Block Time	Daily Total	VRF IFR	LDG	Fuel Uplift	Avg Fuel Burn	POB	Pilot & Pax	Remarks
17	01/12/2022	VYNT	VYNT	05:00	05:05	05:35	05:40	00:30	00:40	01:15	V	1	63L		2	Pilot 1 & unk Pax	Probable demonstration flight
18	02/12/2022	VYNT	VTCC	02:15	02:25	03:35	03:45	01:10	01:30		I	1	42L		2	Pilot 1 & Pax 1	Probable maximum fuel load
19	02/12/2022	VTCC	VTPP	04:25	05:25	05:35	05:35	00:50	01:10		I	1			2	Pilot 1 & Pax 1	Probable maximum fuel load
20	02/12/2022	VTPP	VTPH	06:05	06:15	07:50	08:00	01:35	01:55		I	1	39L		2	Pilot 1 & Pax 1	Probable maximum fuel load
21	02/12/2022	VTPH	VTSP	09:45	09:55	11:45	11:55	01:50	02:10	05:25	I	1	70L	8.5	2	Pilot 1 & Pax 1	Probable maximum fuel load
22	03/12/2022	VTSP	WMKP	04:15	04:25	06:05	06:15	01:40	02:00		I	1			2	Pilot 1 & Pax 1	Probable maximum fuel load
23	03/12/2022	WMKP	WMSA	06:35	06:45	07:45	07:55	01:00	01:20		I	1	48L	9.5	2	Pilot 1 & Pax 1	Oil uplift: 2 qt; Avg 0.09 qt per hour Probable maximum fuel load
24	03/12/2022	WMSA	WSSL	08:25	08:35	10:00	10:10	01:25	01:45	04:05	I	1	54L	8.2	2	Pilot 1 & Pax 1	Probable maximum fuel load
	03/02/2023	WSSL	WSSL													Pax 1	Engine ground run: 00:35 hr
25	27/03/2023	WSSL	WSSL	02:45	03:00	03:25	03:30	00:25	00:45	00:25	V	2	19L		2	Pilot 1 & Pax 2	Circuits with Pax 2
	19/05/2023	WSSL	WSSL													Pilot 1	Engine ground run: 1:00 hr
26	28/07/2023	WSSL	WMSA	02:15	02:30	04:15	04:20	01:45	02:05	01:45	I	1			2	Pilot 1 & Pax 3	Ferry flight
	10/09/2023	WMSA	WMSA													Pilot 1	Engine ground run: 00:35 hr
27	17/10/2023	WMSA	WMSA	10:00	10:05	10:50	10:55	00:45	00:55	00:45	V	1	93L		1	Pilot 1	Test flight. Oil uplift: 8 qt
28	18/10/2023	WMSA	WMSA	03:15	03:23	03:32	03:40	00:09	00:25		V	1	30L		1	Pilot 1	Test flight
29	18/10/2023	WMSA	WMSA	07:30	07:40	08:11	08:15	00:31	00:45	00:40	I	1	36L		2	Pilot 1 & Pax 4	GH with Pax 4
30	20/10/2023	WMSA	WMKJ	00:30	00:42	02:16	02:25	01:34	01:55		I	1	63L		2	Pilot 1 & Pax 1	Probable maximum fuel load
31	20/10/2023	WMKJ	WIDD	03:20	03:37	04:07	04:15	00:30	00:55		I	1			2	Pilot 1 & Pax 1	Probable maximum fuel load
32	20/10/2023	WIDD	WIDN	04:35	04:41	04:57	05:05	00:16	00:30		I	1			2	Pilot 1 & Pax 1	Probable maximum fuel load
33	20/10/2023	WIDN	WIDN	06:40	06:46	08:19	08:30	01:33	01:50	03:53	I	1			2	Pilot 1 & Pax 1	Probable maximum fuel load
34	21/10/2023	WIDN	WIDD	03:20	03:30	03:51	03:55	00:21	00:35		I	1			2	Pilot 1 & Pax 1	Probable maximum fuel load
35	21/10/2023	WIDD	WMKJ	09:30	09:42	10:54	11:00	01:12	01:30	01:33	I	1			2	Pilot 1 & Pax 1	Probable maximum fuel load
36	22/10/2023	WMKJ	WMSA	02:45	02:53	04:17	04:25	01:24	01:40	01:24	I	1	58L		2	Pilot 1 & Pax 1	Probable maximum fuel load
37	29/11/2023	WMSA	WMSA	08:40	08:50	09:25	09:30	00:35	00:50	00:35	V	1	56L		2	Pilot 1 & Pax 5	Test flight with Pax 5
38	30/11/2023	WMSA	WMKI	01:45	02:10	03:10	03:15	01:00	01:30		I	1	29L		2	Pilot 1 & Pax 6	
39	30/11/2023	WMKI	WMSA	05:40	06:00	06:40	06:50	00:40	01:10	01:40	I	1	66L		2	Pilot 1 & Pax 6	
40	06/12/2023	WMSA	VTSS	00:12	00:29	02:35	02:38	02:06	02:26		I	1			2	Pilot 1 & Pax 4	Probable maximum fuel load
41	06/12/2023	VTSS	VTSB	03:47	03:57	05:06	05:10	01:09	01:23		I	1			2	Pilot 1 & Pax 4	Probable maximum fuel load
42	06/12/2023	VTSB	VTBD	06:50	06:53	09:22	09:26	02:29	02:36	05:44	I	1	91L		2	Pilot 1 & Pax 4	Probable maximum fuel load
43	08/12/2023	VTBD	ZZZZ	02:46	02:58	05:14	05:16	02:16	02:30		I	1	92L		2	Pilot 1 & Pax 4	ZZZZ - Chiang Mai Airsport airfield
44	08/12/2023	ZZZZ	ZZZZ	10:03	10:06	10:17	10:19	00:11	00:16	02:27	V	1			2	Pilot 1 & Pax 7	Pax 7 - Siam Scenic
45	09/12/2023	ZZZZ	ZZZZ	10:00	10:05	10:40	10:40	00:35	00:40	00:35	V	1			2	Pilot 1 & Pax 8	Oil uplift: 1 qt. Pax 8 - Siam Scenic
46	10/12/2023	ZZZZ	ZZZZ	03:18	03:23	03:32	03:33	00:09	00:15		I	1			2	Pilot 1 & unk Pax	Probable maximum fuel load

Flt No	Date	Dept	Arr	Blk Off	T/O	LDG	Blk On	Flt Time	Block Time	Daily Total	VRF IFR	LDG	Fuel Uplift	Avg Fuel Burn	POB	Pilot & Pax	Remarks
47	10/12/2023	ZZZZ	VTPP	03:40	03:42	04:45	04:48	01:03	01:08		I	1			2	Pilot 1 & Pax 4	Probable maximum fuel load
48	10/12/2023	VTPP	VTPH	05:24	05:28	07:24	07:26	01:56	02:02		I	1			2	Pilot 1 & Pax 4	Probable maximum fuel load
49	10/12/2023	VTPH	VTSW	07:53	08:00	10:29	10:33	02:29	02:40	05:37	I	1			2	Pilot 1 & Pax 4	VTSW - Phuket Airpark
50	11/12/2023	VTSW	VTSW	06:40	06:50	07:10	07:11	00:20	00:31		V	1			2	Pilot 1 & Pax 9	Pax 9 - Lessure ride
51	11/12/2023	VTSW	VTSW	10:31	10:37	11:05	11:07	00:28	00:36	00:48	V	1			2	Pilot 1 & Pax 10	Pax 10 - Lessure ride
52	13/12/2023	VTSW	VTSS	00:25	00:34	01:44	01:47	01:10	01:22		I	1			2	Pilot 1 & Pax 4	Probable maximum fuel load
53	13/12/2023	VTSS	WMSA	02:36	02:40	04:32	04:36	01:52	02:00	03:02	I	1			1	Pilot 1 & Pax 4	Probable maximum fuel load
54	24/12/2023	WMSA	WMSA	01:33	01:49	02:53	02:58	01:04	01:25	01:04	V	3	70L		2	Pilot 1 & Pax 6	Circuits/GH with Pax 6
		Total for I-POOC (Nov 2022 to Dec 2023)						**60:12**	**75:25**	**60:12**		**59**					
		Grand Total I-POOC (Plus Factory Flt Times)						**85:32**									
		Pilot 1's Total for I-POOC (Minus Pilot 2's Flt Times)							74:15								
		Pilot 1's Total for BK160 (I-POOC + I-PDVK)							**80:05**								
	22/4/2023	EDNY	LIKO	14:40			17:00		02:20		V	1				Yee D.	Aircraft Reg. I-PDVK. Aero Show
	23/4/2023	LIKO	LIBG	08:35			11:15		02:40		V	1				Yee D.	Aircraft Reg. I-PDVK. Aero Show
	23/4/2023	LIBG	(BROG)	13:40			14:30		00:50		V	1				Yee D.	Aircraft Reg. I-PDVK. Aircraft Check
		Pilot 1's Total for I-PDVK (Apr 2023)							**05:50**			**3**					

Notes:

1. * The flight history of I-POOC was compiled using data extracted from a range sources, that include the aircraft logbook, technical logs, pilot logbooks, digital flight logs, and witness statements.
2. unk – Unknown

Appendix D

Certificate of Airworthiness and Airworthiness Review Certificate

BOLLO ASSOLTO IN MODO VIRTUALE
AUT. DIREZ. REG. ENTRATE LAZIO
N. 135047/98 DEL 30/11/1998

CERTIFICATO DI AERONAVIGABILITA'
(CERTIFICATE OF AIRWORTHINESS)

ENAC

Certificato N. *(Certificate no.)* **POOC20220826/a**	**REPUBBLICA ITALIANA ENTE NAZIONALE PER L'AVIAZIONE CIVILE**	Edizione N. *(Edition no.)* **1**
1. Marche di nazionalità e di immatricolazione *(Nationality and registration marks)* **I-POOC**	2. Costruttore e designazione dell'aeromobile a cura del costruttore *(Manufacturer and manufacturer's designation of aircraft)* **Blackshape BK 160TR**	3. Numero di serie dell'aeromobile *(Aircraft Serial Number)* **BCV.21010**

4. Categorie *(Categories)* **Very Light Aeroplane**

5. Il presente Certificato di Aeronavigabilità è rilasciato ai sensi della Convenzione sull' Aviazione Civile Internazionale del 7 Dicembre 1944 e del Regolamento (CE) No 216/2008, articolo 5(2)(c) in relazione all'aeromobile summenzionato che si considera navigabile se mantenuto ed impiegato in accordo con le precedenti disposizioni ed i limiti operativi applicabili.

(This Certificate of Airworthiness is issued pursuant to the Convention on International Civil Aviation dated 7 December 1944 and Regulation (EC) No 216/2008, Article 5(2)(c) in respect of the abovementioned aircraft which is considered to be airworthy when maintained and operated in accordance with the foregoing and the pertinent operating limitations.)

Limitazioni/Note
(Limitations/remark)

Data di rilascio: **26 Agosto 2022**
(Date of Issue) *26th August 2022*

Firma: **Direzione Operazioni Sud**
(Signature) **Il Direttore Alessandro Scialla**

6. Il presente Certificato di Aeronavigabilità è valido a meno che non sia revocato dall'ENAC. Un Certificato di Revisione della Aeronavigabilità valido deve essere allegato al presente certificato

(This Certificate of Airworthiness is valid unless revoked by ENAC. A current Airworthiness Review Certificate shall be attached to this Certificate)

Modello AESA 25 versione 2 (EASA Form 25 issue 2) **Marzo 2010**
Il presente Certificato deve essere conservato a bordo durante tutti i voli (This certificate shall be carried on board during all flights)

REPUBBLICA ITALIANA

Stato Membro dell'Unione Europea
[a Member of the European Union]

CERTIFICATO DI REVISIONE DELL'AERONAVIGABILITà

(ARC - per aeromobili conformi alla Parte ML)
(AIRWORTHINESS REVIEW CERTIFICATE (ARC))
(for aircraft complying with Part-ML)

RIFERIMENTO ARC (CRA): [ARC Reference]: **2023-0095-1810-I-POOC**

A norma del regolamento (UE) 2018/1139 del Parlamento Europeo e del Consiglio:
(Pursuant to Regulation (EC) 2018/1139 of the European Parliament and of the Council:)

CANTOR AIR

Cantor Air - CAMO
Riferimento Approvazione: **EASA IT.CAMO.1041**
(Approval Reference):

certifica di aver effettuato una revisione dell'aeronavigabilità in conformità al Regolamento (EU) 1321/2014 sull'aeromobile seguente:
(Hereby certifies that it has performed an airworthiness review in accordance with Regulation (EU) No 1321/2014 on the following aircraft:)

Fabbricante dell'aeromobile: (Aircraft Manufacturer)	**Blackshape**	**Registrazione dell'aeromobile:** (Aircraft Registration)	**I-POOC**
Designazione dell'aeromobile a cura del fabbricante: (Manufacturer's Designation)	**BK160TR**	**Numero di serie dell'aeromobile:** (Aircraft Serial Number)	**BVC.21010**

e che l'aeromobile in questione è ritenuto aeronavigabile alla data della revisione.
(and this considered airworthy at the time of the review.)

Data di rilascio: (Date of issue)	**18 Ottobre 2023** 18 October 2023	Data di scadenza: (Date of expiry)	**18 Ottobre 2024** 18 October 2024

Ore di volo della cellula (FH) alla data della revisione: **53:50** (TSN)
(Aiframe Flight Hours at date of review)

Firma: (Signed)	Dott. Luigi Fruggiero	Autorizzazione n.: (Authorisation No.)	IT-TSU-ARS-VC1041-001-D

Primo rinnovo: l'aeromobile è conforme alle condizioni di cui al punto ML.A.901 lettera c), dell'Allegato Vter (Parte-ML).
(First extension: the aircraft complies with the conditions of ML.A.901(c) of Annex Vb (Part-ML).

Data di rilascio: (Date of issue)		Data di scadenza: (Date of expiry)	

Ore di volo della cellula (FH) alla data della revisione: (TSN)
(Aiframe Flight Hours at date of review)

Firma: (Signed)		Autorizzazione n.: (Authorisation No.)	
Nome dell'impresa: (Company Name)		Riferimento dell'approvazione: (Approval Reference)	

Secondo rinnovo: l'aeromobile è conforme alle condizioni di cui al punto ML.A.901 lettera c), dell'Allegato Vter (Parte-ML).
(Second extension: the aircraft complies with the conditions of ML.A.901(c) of Annex Vb (Part-ML).

Data di rilascio: (Date of issue)		Data di scadenza: (Date of expiry)	

Ore di volo della cellula (FH) alla data della revisione: (TSN)
(Aiframe Flight Hours at date of review)

Firma: (Signed)		Autorizzazione n.: (Authorisation No.)	
Nome dell'impresa: (Company Name)		Riferimento dell'approvazione: (Approval Reference)	

Modello AESA 15c versione 4 [EASA Form 15c Issue 4] - Ed. Maggio 2021

Appendix E

BS115 Weighing Form – BK 160TR S/N BCV.21010

BLACKSHAPE EASA 21J.550	PRODUCT SPECIFICATION **BS115 WEIGHING**	N° SPEC.BS-PRD-015 Issue 2 dtd 31/03/2017 Page 7 of 7

BLACKSHAPE

A/C: B3115 BK160TR	S/N: BCV.21010	Reg. Mark: I-RA1A (TEMPORARY REGISTRATION, NOW I-[illegible]) 28/07/2022

MEASURING EQUIPMENT

DESCRIPTION	PART NUMBER	S/N (if applicable)	EXPIRATION DATE
SCALE	DFWL	0100919343	04/2023
SCALE	DFWL	0100919491	04/2023
SCALE	DFWL	0100919692	04/2023

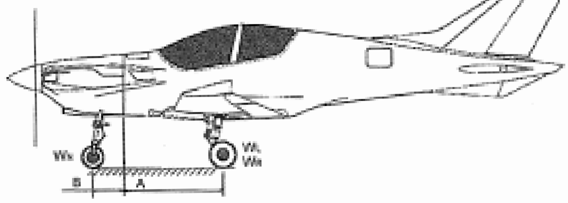

Figure A-1

Refer to a/c configuration and to current appl. AFM for proper equipment list

WEIGHING POINT	SCALE READING (kg)	TARE (kg)	NET WEIGHT (kg)	ARM (m)	MOMENT** (kgm)
N	177.1	0.0	177.1	B −0.42	−74.382
L	237.0	0.0	237.0	A_L +1.31	+310.470
R	239.3	0.0	239.3	A_R +1.31	+313.483
TOTAL			WEIGHT	C.G. (%MAC)***	MOMENT
			653.4	0.841 ≡ 17.0%	+549.571

$$^{*}Net\ Weight = SCALE\ READING - TARE$$

$$^{**}Moment = Net\ Weight \times Arm$$

$$^{***}C.G.(\%MAC) = \frac{\frac{Moment}{Weight} - 0.61}{1.36} \times 100$$

Note: A_L and A_R are the left and right main landing gear arms that in the Figure A-1 are indicated as A

PLACE	DATE	AUTHORIZING STAMP	AUTHORIZING SIGNATURE
MONOPOLI	12/07/2022	OP N.RUOTOLO BS 28	OP BS 28
		QC N.RUOTOLO BS 08	QC BS 08

Form A-2: Weighing Form

mod. PS00-DO-R0 Issue 2 - dated 31/03/2017

Appendix F

I-POOC Flight History (With Aircraft Take-off Weights) – March 2022 to February 2024

Flt No	Date	Dept	Arr	T/O	LDG	Flt Time	POB	Pilot & Pax	Pilot Weight (kg)	Pax Weight (kg)	Probable Fuel Load (lt)	Probable Fuel Wt (kg)*	Ac Empty Wt (kg)	Ac TOW (kg)	% Over-Weight	Remarks
Factory Flights from March 2022 to June 2022																
F1	31/3/2022					00:20	2	Pilot 2	87	unk	unk	unk	653.4	821.0		
F2	31/3/2022					00:32	2	Pilot 2 & unk	87	unk	unk	unk	653.4	**887.0**	4.35%	Exceeded maximum TOW
F3	31/3/2022					00:42	2	Pilot 2 & unk	87	unk	unk	unk	653.4	**887.0**	4.35%	Exceeded maximum TOW
F4	6/4/2022					00:49	2	Pilot 2 & unk	87	unk	unk	unk	653.4	**874.0**	2.82%	Exceeded maximum TOW
F5	6/4/2022					00:37	1	Pilot 2	87	unk	unk	unk	653.4	809.0		
F6	6/4/2022					01:28	2	Pilot 2 & unk	87	unk	unk	unk	653.4	**894.0**	5.18%	Exceeded maximum TOW
F7	6/4/2022					00:38	2	Pilot 2 & unk	87	unk	unk	unk	653.4	**894.0**	5.18%	Exceeded maximum TOW
F8	7/4/2022	LIBD	LIBG			00:24	2	Pilot 2 & unk	87	unk	unk	unk	653.4	**894.0**	5.18%	Exceeded maximum TOW
F9	7/4/2022					01:10	2	Pilot 2 & unk	87	unk	unk	unk	653.4	**892.0**	4.94%	Exceeded maximum TOW
F10	11/4/2022					00:17	2	Pilot 2 & unk	87	unk	unk	unk	653.4	**892.0**	4.94%	Exceeded maximum TOW
F11	12/4/2022					01:00	2	Pilot 2 & unk	87	unk	unk	unk	653.4	**883.0**	3.88%	Exceeded maximum TOW
F12	12/4/2022					01:03	2	Pilot 2 & unk	87	unk	unk	unk	653.4	**883.0**	3.88%	Exceeded maximum TOW
F13	22/4/2022					00:17	1	Pilot 2	87	unk	unk	unk	653.4	841.2		
F14	22/4/2022					00:20	2	Pilot 2 & unk	87	unk	unk	unk	653.4	**894.0**	5.18%	Exceeded maximum TOW
F15	24/2/2022	LIBG	LIKO			02:46	1	Pilot 2	87	unk	unk	unk	653.4	841.2		
F16	24/2/2022	LIKO	EDNY			02:15	1	Pilot 2	87	unk	unk	unk	653.4	841.2		
F17	1/5/2022	EDNY	LIKO			02:32	1	Pilot 2	87	unk	unk	unk	653.4	841.2		
F18	1/5/1022	LIKO	LIBG			02:40	1	Pilot 2	87	unk	unk	unk	653.4	841.2		
F19	12/5/2022	LIBG	(Esprt)			00:11	2	Pilot 2 & unk	87	unk	unk	unk	653.4	**894.0**	5.18%	Exceeded maximum TOW
F20	12/5/2022	(Esprt)	LIBD			01:41	2	Pilot 2 & unk	87	unk	unk	unk	653.4	**894.0**	5.18%	Exceeded maximum TOW
F21	13/5/2022	LIBD	(Esprt)			00:27	1	Pilot 2	87	unk	unk	unk	653.4	787.2		
F22	8/6/2022	(Esprt)	LIBG			00:09	2	Pilot 2 & unk	87	unk	unk	unk	653.4	780.0		
F23	9/6/2022					00:17	2	Pilot 2 & unk	87	unk	unk	unk	653.4	**871.2**	2.49%	Exceeded maximum TOW
F24	16/6/2022	LIBG	(Esprt)			00:22	2	Pilot 2 & unk	87	unk	unk	unk	653.4	**871.2**	2.49%	Exceeded maximum TOW

Flt No	Date	Dept	Arr	T/O	LDG	Flt Time	POB	Pilot & Pax	Pilot Weight (kg)	Pax Weight (kg)	Probable Fuel Load (lt)	Probable Fuel Wt (kg)*	Ac Empty Wt (kg)	Ac TOW (kg)	% Over-Weight	Remarks
F25	23/6/2022	(Esprt)	LIBG			00:14	1	Pilot 2	87	unk	unk	unk	653.4	787.2		
F26	23/6/2022	LIBG	LIBG			00:14	2	Pilot 2 & unk	87	unk	unk	unk	653.4	**853.0**	0.35%	Exceeded maximum TOW
F27	24/6/2022					00:48	2	Pilot 2 & unk	87	unk	unk	unk	653.4	**866.0**	1.88%	Exceeded maximum TOW
F28	24/6/2022					00:09	2	Pilot 2 & unk	87	unk	unk	unk	653.4	**866.0**	1.88%	Exceeded maximum TOW
F29	29/6/2022					00:09	2	Pilot 2 & unk	87	unk	unk	unk	653.4	849.0		
F30	29/6/2022					00:15	2	Pilot 2 & unk	87	unk	unk	unk	653.4	**855.0**	0.59%	Exceeded maximum TOW
F31	29/6/2022					00:34	2	Pilot 2 & unk	88	unk	unk	unk	654.4	**853.0**	0.35%	Exceeded maximum TOW

Flt No	Date	Dept	Arr	T/O	LDG	Flt Time	POB	Pilot & Pax	Pilot Weight (kg)	Pax Weight (kg)	Probable Fuel Load (lt)	Probable Fuel Wt (kg)*	Ac Empty Wt (kg)	Ac TOW (kg)	% Over-Weight	Remarks
Flights After Aircraft Delivery from November 2022 to February 2024																
1	01/11/2022	WSSL	WSSL	02:30	03:50	01:20	2	Pilot 2 & Pilot 1	87	87	unk	unk	653.4	und		
2	01/11/2022	WSSL	WSSL	07:00	07:25	00:25	1	Pilot 2	87	-	unk	unk	653.4	und		
3	01/11/2022	WSSL	WSSL	08:10	08:15	00:05	1	Pilot 2	87	-	unk	unk	653.4	und		
4	02/11/2022	WSSL	WIPP	00:50	02:50	02:00	2	Pilot 2 & Pilot 1	87	87	unk	unk	653.4	und		
5	02/11/2022	WIPP	WIHH	04:20	06:15	01:55	2	Pilot 2 & Pilot 1	87	87	unk	unk	653.4	und		
6	05/11/2022	WIHH	WIPP	01:15	02:50	01:35	2	Pilot 2 & Pilot 1	87	87	unk	unk	653.4	und		
7	05/11/2022	WIPP	WSSL	03:55	05:40	01:45	2	Pilot 2 & Pilot 1	87	87	unk	unk	653.4	und		
8	28/11/2022	WSSL	WMSA	01:15	02:20	01:05	2	Pilot 1 & Pax 1	87	93	129	88.9	653.4	**922.3**	8.51%	Probably exceeded maximum TOW
9	29/11/2022	WMSA	WMKP	01:00	02:00	01:00	2	Pilot 1 & Pax 1	87	93	129	88.9	653.4	**922.3**	8.51%	Probably exceeded maximum TOW
10	29/11/2022	WMKP	VTSP	03:40	05:10	01:30	2	Pilot 1 & Pax 1	87	93	129	88.9	653.4	**922.3**	8.51%	Probably exceeded maximum TOW
11	29/11/2022	VTSP	VTPH	06:50	08:30	01:40	2	Pilot 1 & Pax 1	87	93	129	88.9	653.4	**922.3**	8.51%	Probably exceeded maximum TOW
12	30/11/2022	VTPH	VTPP	01:15	02:40	01:25	2	Pilot 1 & Pax 1	87	93	129	88.9	653.4	**922.3**	8.51%	Probably exceeded maximum TOW
13	30/11/2022	VTPP	VTCC	03:45	04:40	00:55	2	Pilot 1 & Pax 1	87	93	129	88.9	653.4	**922.3**	8.51%	Probably exceeded maximum TOW
14	30/11/2022	VTCC	VYNT	05:45	06:35	00:50	2	Pilot 1 & Pax 1	87	93	129	88.9	653.4	**922.3**	8.51%	Probably exceeded maximum TOW
15	01/12/2022	VYNT	VYNT	02:05	02:30	00:25	2	Pilot 1 & unk	87	unk	unk	88.9	653.4	und		
16	01/12/2022	VYNT	VYNT	03:05	03:25	00:20	2	Pilot 1 & unk	87	unk	unk	88.9	653.4	und		
17	01/12/2022	VYNT	VYNT	05:05	05:35	00:30	2	Pilot 1 & unk	87	unk	unk	88.9	653.4	und		

Flt No	Date	Dept	Arr	T/O	LDG	Flt Time	POB	Pilot & Pax	Pilot Weight (kg)	Pax Weight (kg)	Probable Fuel Load (lt)	Probable Fuel Wt (kg)*	Ac Empty Wt (kg)	Ac TOW (kg)	% Over-Weight	Remarks
18	02/12/2022	VYNT	VTCC	02:25	03:35	01:10	2	Pilot 1 & Pax 1	87	93	129	88.9	653.4	**922.3**	8.51%	Probably exceeded maximum TOW
19	02/12/2022	VTCC	VTPP	05:25	05:35	00:10	2	Pilot 1 & Pax 1	87	93	129	88.9	653.4	**922.3**	8.51%	Probably exceeded maximum TOW
20	02/12/2022	VTPP	VTPH	06:15	07:50	01:35	2	Pilot 1 & Pax 1	87	93	129	88.9	653.4	**922.3**	8.51%	Probably exceeded maximum TOW
21	02/12/2022	VTPH	VTSP	09:55	11:45	01:50	2	Pilot 1 & Pax 1	87	93	129	88.9	653.4	**922.3**	8.51%	Probably exceeded maximum TOW
22	03/12/2022	VTSP	WMKP	04:25	06:05	01:40	2	Pilot 1 & Pax 1	87	93	129	88.9	653.4	**922.3**	8.51%	Probably exceeded maximum TOW
23	03/12/2022	WMKP	WMSA	06:45	07:45	01:00	2	Pilot 1 & Pax 1	87	93	129	88.9	653.4	**922.3**	8.51%	Probably exceeded maximum TOW
24	03/12/2022	WMSA	WSSL	08:35	10:00	01:25	2	Pilot 1 & Pax 1	87	93	129	88.9	653.4	**922.3**	8.51%	Probably exceeded maximum TOW
25	27/03/2023	WSSL	WSSL	03:00	03:25	00:25	2	Pilot 1 & Pax 2	87	unk	unk	unk	653.4	und		
26	28/07/2023	WSSL	WMSA	02:30	04:15	01:45	2	Pilot 1 & Pax 3	87	80	unk	unk	653.4	und		
27	17/10/2023	WMSA	WMSA	10:05	10:50	00:45	1	Pilot 1	87	-	unk	unk	653.4	und		
28	18/10/2023	WMSA	WMSA	03:23	03:32	00:09	1	Pilot 1	87	-	unk	unk	653.4	und		
29	18/10/2023	WMSA	WMSA	07:40	08:11	00:31	2	Pilot 1 & Pax 4	87	85	unk	unk	653.4	und		
30	20/10/2023	WMSA	WMKJ	00:42	02:16	01:34	2	Pilot 1 & Pax 1	87	93	129	88.9	653.4	**922.3**	8.51%	Probably exceeded maximum TOW
31	20/10/2023	WMKJ	WIDD	03:37	04:07	00:30	2	Pilot 1 & Pax 1	87	93	129	88.9	653.4	**922.3**	8.51%	Probably exceeded maximum TOW
32	20/10/2023	WIDD	WIDN	04:41	04:57	00:16	2	Pilot 1 & Pax 1	87	93	129	88.9	653.4	**922.3**	8.51%	Probably exceeded maximum TOW
33	20/10/2023	WIDN	WIDN	06:46	08:19	01:33	2	Pilot 1 & Pax 1	87	93	129	88.9	653.4	**922.3**	8.51%	Probably exceeded maximum TOW
34	21/10/2023	WIDN	WIDD	03:30	03:51	00:21	2	Pilot 1 & Pax 1	87	93	129	88.9	653.4	**922.3**	8.51%	Probably exceeded maximum TOW
35	21/10/2023	WIDD	WMKJ	09:42	10:54	01:12	2	Pilot 1 & Pax 1	87	93	129	88.9	653.4	**922.3**	8.51%	Probably exceeded maximum TOW
36	22/10/2023	WMKJ	WMSA	02:53	04:17	01:24	2	Pilot 1 & Pax 1	87	93	129	88.9	653.4	**922.3**	8.51%	Probably exceeded maximum TOW
37	29/11/2023	WMSA	WMSA	08:50	09:25	00:35	2	Pilot 1 & Pax 5	87	unk	unk	unk	653.4	und		
38	30/11/2023	WMSA	WMKI	02:10	03:10	01:00	2	Pilot 1 & Pax 6	87	48	unk	unk	653.4	und		
39	30/11/2023	WMKI	WMSA	06:00	06:40	00:40	2	Pilot 1 & Pax 6	87	48	unk	unk	653.4	und		
40	06/12/2023	WMSA	VTSS	00:29	02:35	02:06	2	Pilot 1 & Pax 4	87	85	129	88.9	653.4	**914.3**	7.56%	Probably exceeded maximum TOW
41	06/12/2023	VTSS	VTSB	03:57	05:06	01:09	2	Pilot 1 & Pax 4	87	85	129	88.9	653.4	**914.3**	7.56%	Probably exceeded maximum TOW
42	06/12/2023	VTSB	VTBD	06:53	09:22	02:29	2	Pilot 1 & Pax 4	87	85	129	88.9	653.4	**914.3**	7.56%	Probably exceeded maximum TOW
43	08/12/2023	VTBD	ZZZZ	02:58	05:14	02:16	2	Pilot 1 & Pax 4	87	85	129	88.9	653.4	**914.3**	7.56%	Probably exceeded maximum TOW
44	08/12/2023	ZZZZ	ZZZZ	10:06	10:17	00:11	2	Pilot 1 & Pax 7	87	unk	unk	unk	653.4	und		ZZZZ - Chiang Mai Airsports airfield
45	09/12/2023	ZZZZ	ZZZZ	10:05	10:40	00:35	2	Pilot 1 & Pax 8	87	unk	unk	unk	653.4	und		
46	10/12/2023	ZZZZ	ZZZZ	03:23	03:32	00:09	2	Pilot 1 & unk	87	unk	unk	unk	653.4	und		
47	10/12/2023	ZZZZ	VTPP	03:42	04:45	01:03	2	Pilot 1 & Pax 4	87	85	129	88.9	653.4	**914.3**	7.56%	Probably exceeded maximum TOW
48	10/12/2023	VTPP	VTPH	05:28	07:24	01:56	2	Pilot 1 & Pax 4	87	85	129	88.9	653.4	**914.3**	7.56%	Probably exceeded maximum TOW

Flt No	Date	Dept	Arr	T/O	LDG	Flt Time	POB	Pilot & Pax	Pilot Weight (kg)	Pax Weight (kg)	Probable Fuel Load (lt)	Probable Fuel Wt (kg)*	Ac Empty Wt (kg)	Ac TOW (kg)	% Over-Weight	Remarks
49	10/12/2023	VTPH	VTSW	08:00	10:29	02:29	2	Pilot 1 & Pax 4	87	85	129	88.9	653.4	**914.3**	7.56%	Probably exceeded maximum TOW
50	11/12/2023	VTSW	VTSW	06:50	07:10	00:20	2	Pilot 1 & Pax 9	87	unk	unk	unk	653.4	und		
51	11/12/2023	VTSW	VTSW	10:37	11:05	00:28	2	Pilot 1 & Pax 10	87	unk	unk	unk	653.4	und		
52	13/12/2023	VTSW	VTSS	00:34	01:44	01:10	2	Pilot 1 & Pax 4	87	85	129	88.9	653.4	**914.3**	7.56%	Probably exceeded maximum TOW
53	13/12/2023	VTSS	WMSA	02:40	04:32	01:52	2	Pilot 1 & Pax 4	87	85	129	88.9	653.4	**914.3**	7.56%	Probably exceeded maximum TOW
54	24/12/2023	WMSA	WMSA	01:49	02:53	01:04	2	Pilot 1 & Pax 6	87	48	unk	unk	653.4	und		
55	13/2/2024	WMSA	-	05:28	05:35	00:07	2	Pilot 1 & Pax 11	87	92	129	88.9	653.4	**921.3**	8.39%	Exceeded maximum TOW

Notes:

1. Compiled data are based on various flight records, Garmin G3X data, medical records and witness statements, with the data assessed as the most accurate being used for the compilation.
2. **OEM Test Flight Weight Tolerances**. During development and compliance flights, the CS-VLA 21 regulation permits weight tolerances beyond MTOW within set limits. In this case, the manufacturer recorded a slight exceedance of the general +5% tolerance, reaching 5.18% over MTOW during test flights. These tolerances were documented in the Safety of Flight submission to EASA for Flight Conditions approval. Based on this approval, EASA issued a Permit to Fly, allowing operations within controlled test parameters but not authorising routine overweight operations.
3. Body weight information was obtained from medical records and witness statements.
4. Probable fuel weight: Minus 4 kg of nominal fuel used for start-up and taxy.
5. Shaded rows (Flights 43 - 55): Flight data were recovered for these flights from Garmin G3X GDU 460 recording.
6. TOW – Take-off weight
7. unk – Unknown
8. und – Undetermined

Appendix G

Summary of Recovered Data from Garmin G3X GDU 460 – 8 Dec 2023 to Feb 2024 (13 Flights)

Flt No	Date	Flight Log						Summary of Garmin G3X Recorded Data							
		Dept	Arr	T/O (UTC)	LDG (UTC)	Flt Time	Probable TOW (kg)	Time Start (UTC)	Time End (UTC)	Duration (h:mm:ss)	Data Count (million)	Max Airspeed (KIAS)	Max Load Factor (g)	Average Fuel Flow (gal/hr)
43	08/12/2023	VTBD	ZZZZ	02:58	05:14	02:16	914.3	8/12/2023 4:07:17	8/12/2023 5:14:59	1:07:42	2.4363	174.2	3.81	9.2
44	08/12/2023	ZZZZ	ZZZZ	10:06	10:17	00:11	und	8/12/2023 10:06:56	8/12/2023 10:17:12	0:10:16	0.5691	168.3	3.88	11.5
45	09/12/2023	ZZZZ	ZZZZ	10:05	10:40	00:35	und	9/12/2023 10:04:41	9/12/2023 10:39:57	0:35:16	1.7306	159.2	4.30	9.7
46	10/12/2023	ZZZZ	ZZZZ	03:23	03:32	00:09	und	10/12/2023 3:23:43	10/12/2023 3:33:09	0:09:26	0.5509	149.5	3.44	10.2
47	10/12/2023	ZZZZ	VTPP	03:42	04:45	01:03	914.3	10/12/2023 3:42:36	10/12/2023 4:47:56	1:05:20	2.3601	**180.2**	1.68	9.8
48	10/12/2023	VTPP	VTPH	05:28	07:24	01:56	914.3	10/12/2023 5:28:10	10/12/2023 7:25:31	1:57:21	3.7995	179.9	2.48	9.1
49	10/12/2023	VTPH	VTSW	08:00	10:29	02:29	914.3	10/12/2023 8:00:30	10/12/2023 10:30:58	2:30:28	5.4219	**186.1**	3.21	9.3
50	11/12/2023	VTSW	VTSW	06:50	07:10	00:20	und	11/12/2023 6:51:00	11/12/2023 7:11:55	0:20:55	1.1191	161.3	4.01	9.8
51	11/12/2023	VTSW	VTSW	10:37	11:05	00:28	und	11/12/2023 10:37:08	11/12/2023 11:06:22	0:29:14	1.3720	160.7	4.26	9.8
52	13/12/2023	VTSW	VTSS	00:34	01:44	01:10	914.3	13/12/2023 0:34:13	13/12/2023 1:45:51	1:11:38	2.6672	173.9	**4.59**	9.6
53	13/12/2023	VTSS	WMSA	02:40	04:32	01:52	914.3	13/12/2023 2:40:18	13/12/2023 4:33:52	1:53:34	3.9581	179.3	1.92	9.3
54	24/12/2023	WMSA	WMSA	01:49	02:53	01:04	und	24/12/2023 1:49:47	24/12/2023 2:55:17	1:05:30	2.6850	160.1	4.20	9.8
55	13/2/2024	WMSA	-	05:28	05:35	00:07	921.3	13/2/2024 5:27:59	13/2/2024 5:35:52	0:07:53	0.4100	155.0	1.58	11.5
									Total	**12:44:33**	**29.0799**			

Notes:

1. The Garmin G3X GDU 460 data was recovered by the NTSB, and the above table provides a summary of the recovered data as analysed by the AAIB.
2. The load factor recorded by the Garmin G3X is zero (0.0) under a 1.0 g condition (as indicated by the G-meter in the EFIS display). Therefore, for load factor analysis, a value of 1.0 g is added to G3X recorded values.
3. und – Undetermined.

Appendix H

SIRIM Test Report No 2024CE2314

SIRIM QAS International Sdn. Bhd.
(Company No.: 199601037981 (410334-X))
No.1, Persiaran Dato' Menteri, P.O.BOX 7035, Section 2,
40700 Shah Alam, Selangor Darul Ehsan, Malaysia
Tel: 012-662 0261
Fax: 03-55446688
www.sirim-qas.com.my

TEST REPORT

REPORT NO : 2024CE2314	PAGE : 1 OF 44

THIS TEST REPORT IS ISSUED IN SECURED PDF SOFTCOPY

Applicant	: BIRO SIASATAN KEMALANGAN UDARA, KEMENTERIAN PENGANGKUTAN MALAYSIA Biro Siasatan Kemalangan Udara D/A Kementerian Pengangkutan Malaysia Tingkat 8, Presint 4, Pusat Pentadbiran Kerajaan Persekutuan 62100 Putrajaya Wilayah Persekutuan Malaysia
Manufacturer	: - NA -
Product	: COMPOSITE FIBRE-RESIN, COMPOSITE POLYMER-FIBRE, COMPOSITE FIBRE MATERIALS
Reference Standard / Method of Test	: Failure Analysis on Failed Aircraft Components - Refer to Pages 6 to 9 of this test report.
Description of sample	: Refer to Pages 2 to 5 of this test report.
Date Received of Complete Application	: 15 August 2024
Job No.	: J20243671588
Description of Test Results	: The test results of the submitted test samples are described on Pages 10 to 43 of this test report.
Issued Date	: 28 October 2024

Approved Signatory;

(Ir. ZARINA BINTI RASMIN)
Principal Testing Engineer

SIRIM QAS International Sdn. Bhd.
CHEMICAL, POLYMER AND COMPOSITE SECTION (CPCT)

(DALHA BIN KATNI @ RAHMAT)
Head
Chemical, Polymer and Composite Section
Testing Services Department

SIRIM QAS International Sdn. Bhd.
(Company No.: 199601037981 (410334-X))
No.1, Persiaran Dato' Menteri, P.O.BOX 7035, Section 2,
40700 Shah Alam, Selangor Darul Ehsan, Malaysia
Tel: 012-662 0261
Fax: 03-55446688
www.sirim-qas.com.my

TEST REPORT

REPORT NO : 2024CE2314	PAGE : 1 OF 44
This Test Report refers only to samples submitted by the applicant to SIRIM QAS International Sdn. Bhd. and tested by SIRIM QAS International Sdn. Bhd. This Test Report shall not be reproduced, except in full and shall not be used for any purpose by any means or forms (including but not limited to advertising purposes) without written approval from the Head of Quality, Occupational Safety and Health & Environment (QOSHE), SIRIM QAS International Sdn. Bhd. Please refer to the last page of this Test Report for Conditions Relating to the Use of Test Report.	

THIS TEST REPORT IS ISSUED IN SECURED PDF SOFTCOPY

Applicant	: BIRO SIASATAN KEMALANGAN UDARA, KEMENTERIAN PENGANGKUTAN MALAYSIA Biro Siasatan Kemalangan Udara D/A Kementerian Pengangkutan Malaysia Tingkat 8, Presint 4, Pusat Pentadbiran Kerajaan Persekutuan 62100 Putrajaya Wilayah Persekutuan Malaysia
Manufacturer	: - NA -
Product	: COMPOSITE FIBRE-RESIN, COMPOSITE POLYMER-FIBRE, COMPOSITE FIBRE MATERIALS
Reference Standard / Method of Test	: Failure Analysis on Failed Aircraft Components - Refer to Pages 6 to 9 of this test report.
Description of sample	: Refer to Pages 2 to 5 of this test report.
Date Received of Complete Application	: 15 August 2024
Job No.	: J20243671588
Description of Test Results	: The test results of the submitted test samples are described on Pages 10 to 43 of this test report.
Issued Date	: 28 October 2024

Approved Signatory;

(Ir. ZARINA BINTI RASMIN)
Principal Testing Engineer

SIRIM QAS International Sdn. Bhd.
CHEMICAL, POLYMER AND COMPOSITE SECTION (CPCT)

(DALHA BIN KATNI @ RAHMAT)
Head
Chemical, Polymer and Composite Section
Testing Services Department

1. Introduction

A total of sixteen (16) aircraft components, shown in Pages 2 to 5 of this test report, were received on 23 April 2024.

No.	Photograph & ID No.	Wreckage Location (Site No.)	Descriptions of Parts/Debris/Materials, (location on the aircraft) & Quantity
1	ID No: **BSKU/IPOOC/001(S4)** 	**Site 4**	Left wing (upper skin) - near to the refuelling point. (Qty: 1 piece)
2	ID No: **BSKU/IPOOC/002(S3)** 	**Site 3**	Right wing (upper skin) - near to fuselage. (Qty: 1 piece)
3	ID No: **BSKU/IPOOC/003(S1)** 	**Site 1**	Left wing - near to the wheel well. (Qty: 1 piece) 

Note: ROI indicates region of interest

SIRIM QAS International Sdn. Bhd.
CHEMICAL, POLYMER AND COMPOSITE SECTION (CPCT)

No.	Photograph & ID No.	Wreckage Location (Site No.)	Descriptions of Parts/Debris/Materials, (location on the aircraft) & Quantity
4	ID No: **BSKU/IPOOC/004(S2)**  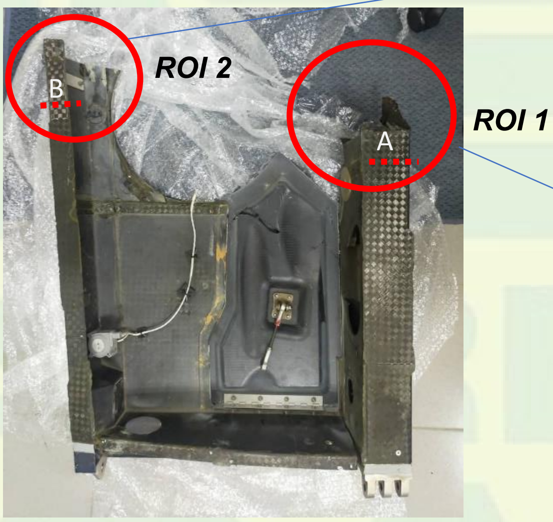	**Site 2**	Right wing - near to the wheel well. (Qty: 1 piece)   

Note: ROI indicates region of interest

SIRIM QAS International Sdn. Bhd.
CHEMICAL, POLYMER AND COMPOSITE SECTION (CPCT)

No.	Photograph & ID No.	Wreckage Location (Site No.)	Descriptions of Parts/Debris/Materials, (location on the aircraft) & Quantity
5	ID No: **BSKU/IPOOC/005(S1)** 	**Site 1**	Left wing spar. (Qty: 1 piece)
6	ID No: **BSKU/IPOOC/005(S1)** – upper photo ID No: **BSKU/IPOOC/006(S1)** – lower photo 	**Site 1**	Left wing - studbox. (Qty: 2 pieces)
7	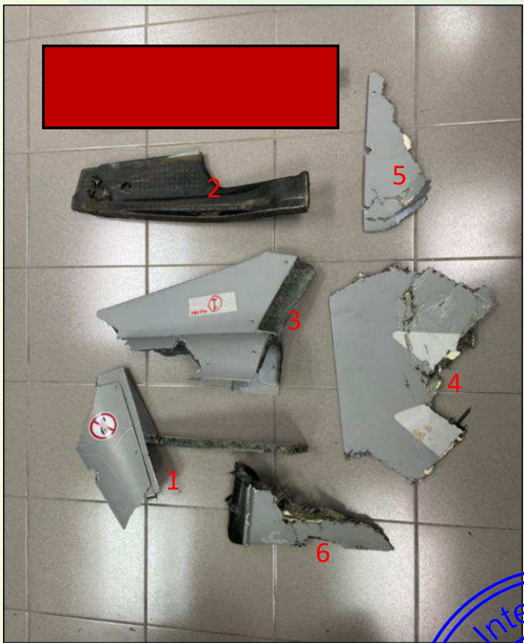	**Various Locations**	Small parts & spar: (Total qty: 6 pieces) 1. Left inner wing trailing edge corner including inspection panel 2. Right Inner Rib 3. Vertical fin (lower) 4. Left Lower wing skin peace 5. Left wing tip (upper) peace 6. Left stabilizer upper leading edge (or Right lower)

SIRIM QAS International Sdn. Bhd.
CHEMICAL, POLYMER AND COMPOSITE SECTION (CPCT)

No.	Photograph & ID No.	Wreckage Location (Site No.)	Descriptions of Parts/Debris/Materials, (location on the aircraft) & Quantity
8	ID No: **BSKU/IPOOC/007(S1)** 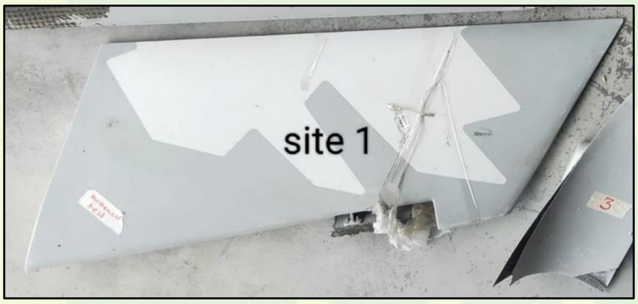	**Site 1**	Rudder (Site 1) (Qty: 1 piece)
9	ID No: **BSKU/IPOOC/008(S4)**  	**Site 4**	Left wing. (Qty: 1 piece)
10	ID No: **BSKU/IPOOC/009(S4)** 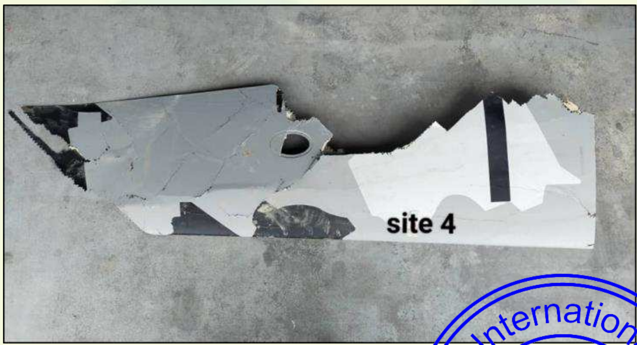	**Site 4**	Left wing. (Qty: 1 piece)

The aircraft components are made up the carbon fibre reinforced plastics (CFRP) composite material. The requests were as follows:

i. To analyse the resin matrix and investigate for possibility of material degradation of the matrix material
ii. To verify the structure design of the component
iii. To carry out mechanical testing on the CFRP composite material

2. Analysis

The analysis was conducted with reference to ICAO Doc No 9756 AN/965 – First Edition – 2011 – Manual of Aircraft Accident and Incident Investigation – Part III Investigation. Data from the analysis (if applicable) were also compared against Blackshape DOA No. EASA 215.550 – Compliance Report – Toray 2510 Series Resin Material Equivalency Test Results (Doc Nº BCV-04-64-02).

The analyses techniques employed are as follows:

2.1 Material Analysis for Resin Material

2.1.1 Fourier Transform Infra-Red (FTIR) Analysis

The analysis was conducted in accordance with ASTM E1252:1998 (2021) - Standard Practice for General Techniques for Obtaining Infrared Spectra for Qualitative Analysis. A thinly sliced test specimen taken from the sample was placed directly onto the Golden Gate Diamond Attenuated Total Reflectance (ATR) accessory and scanned in reflectance mode for 16 times from 4000 cm^{-1} to 600 cm^{-1} using an FTIR spectrometer.

The analysis was conducted on the resin sample obtained on the following samples:

i. Site 1; Sample ID: BSKU/IPOOC/003(S1) - Left wing - near to the wheel well
ii. Site 2; Sample ID: BSKU/IPOOC/004(S2) - Right wing - near to the wheel well
iii. Site 3; Sample ID: BSKU/IPOOC/002(S3) - Right wing (upper skin) - near to the fuselage

SIRIM QAS International Sdn. Bhd.
CHEMICAL, POLYMER AND COMPOSITE SECTION (CPCT)

2.1.2 Differential Scanning Calorimetry (DSC)

The DSC analysis was conducted in accordance with ISO 11357-2:2020 - Plastics - Differential Scanning Calorimetry (DSC) - Part 2: Determination of Glass Transition Temperature and Step Height. Approximately (9 to 11) mg resin sample taken from Site 1; Sample ID: BSKU/IPOOC/003(S1) - Left wing - near to the wheel well; Site 2; Sample ID: BSKU/IPOOC/004(S2) - Right wing - near to the wheel well and Site 3; Sample ID: BSKU/IPOOC/002(S3) - Right wing (upper skin) - near to the fuselage, were heated using the following test parameters in a DSC analyser equipped with an auto sampler.

a) Temperature program:
   i. Isothermal at 10°C for 5 minutes in nitrogen
   ii. Heat from 10°C to 200°C at 20°C/minute in nitrogen
   iii. Isothermal at 200°C for 5 minutes
   iv. Cool from 200°C to 10°C at 50°C/minute in nitrogen
   v. Isothermal at 10°C for 5 minutes
   vi. Heat from 10°C to 200°C at 20°C/minute in nitrogen
b) Gas flow rate: 50 ml per minute

2.1.3 Thermogravimetry (TGA) Analysis

Approximately (12 to 13) mg of test specimen cut from composite sample taken from Site 1; Sample ID: BSKU/IPOOC/003(S1) - Left wing - near to the wheel well; Site 2; Sample ID: BSKU/IPOOC/004(S2) - Right wing - near to the wheel well and Site 3; Sample ID: BSKU/IPOOC/002(S3) - Right wing (upper skin) - near to the fuselage, were subjected to a TGA analysis in accordance with ASTM E1131:2020 - Standard Test Method for Compositional Analysis by Thermogravimetry. The samples were analysed using the following test parameters using a TGA thermogravimetric analyser:

- Temperature Program:
  i. Heat from 30°C to 600°C at 10°C/minute in nitrogen
  ii. Heat from 600°C to 800°C at 10°C/minute in oxygen
- Gas flow rate: 50 ml per minute

SIRIM QAS International Sdn. Bhd.
CHEMICAL, POLYMER AND COMPOSITE SECTION (CPCT)

2.2 Verification on Structure Design

2.2.1 Failure Mode Analysis

The mode of failure was analysed using Scanning Electron Microscopy (SEM) analysis at 500x and 5000x magnification factors. The SEM image was taken at 15kV voltage at the region of interests (ROIs) indicated on Site 2; Sample ID: BSKU/IPOOC/004(S2) - Right wing - near to the wheel well.

2.2.2 Microsection Analysis

Verification of laminate thickness and checking for resin starvation as well as poor bonding surfaces were carried out using microsection analysis technique. Test specimens taken from the cut sections indicated as A, B and C indicated on Site 2; Sample ID: BSKU/IPOOC/004(S2) - Right wing - near to the wheel well, and D indicated on Site 1; Sample ID: BSKU/IPOOC/003(S1) - Left wing - near to the wheel well, were cold mounted in an epoxy resin before being grounded and polish until mirror-like surface was obtained. The prepared test specimens were analysed under a stereo microscope at 10x magnification factor and compound microscope at 50x magnification factor.

2.2.3 Verification on Constituent Content, Fibre Ratio and Plies Orientation

The test was conducted in accordance with ASTM D2584:2018 - Standard Test Method for Ignition Loss of Cured Reinforced Resins. A muffle furnace was used to heat 3 test specimens taken from the cut section C indicated on Site 2; Sample ID: BSKU/IPOOC/004(S2) - Right wing - near to the wheel well, at 565°C for 5 hours.

2.2.4 Verification on Porosity/Void Content

The test was conducted in accordance with Agreed Test Method 021 - Microsection Analysis for Porosity Content. The entire cross-section thickness in ROI1 indicated on Site 2; Sample ID: BSKU/IPOOC/004(S2) - Right wing - near to the wheel well, were cold mounted in an epoxy resin and polished with fine grit media to produce a uniform mirror surface finish, until no visible scratch or artefacts from the cutting or polishing operations were seen when viewed at 50x magnification (minimum) under a compound microscope.

2.3 Mechanical Testing

2.3.1 Tensile Properties

The test was conducted in accordance with ASTM D3039/D3039M:2017 - Standard Test Method for Tensile Properties of Polymer Matrix Composite Materials using the following test parameters:

- Sample: Cut from Site 1; Sample ID: BSKU/IPOOC/003(S1) - Left wing - near to the wheel well (Sample 1); Site 2; Sample ID: BSKU/IPOOC/004(S2) - Right wing - near to the wheel well (Sample 2), Site 3; Sample ID: BSKU/IPOOC/002(S3) - Right wing (upper skin) - near to the fuselage (Sample 3) and Site 4; Sample ID: BSKU/IPOOC/001(S4) - Left wing (upper skin) - near to the refuelling point (Sample 4)
- Specimen type: Coupon without tab – width: 25 mm; length: 200 mm
- Number of specimens per sample: 5 pieces
- Speed: 2 mm/minute
- Gauge length: 50 mm

2.3.2 Compressive Properties

The test was conducted in accordance with ASTM D6641/D6641M:2016 - Test Method for Compressive Properties of Polymer Matrix Composite Materials Using a Combined Loading Compression (CLC) Test Fixture using the following test parameters:

- Sample: Cut from Site 1; Sample ID: BSKU/IPOOC/003(S1) - Left wing - near to the wheel well (Sample 1); Site 2; Sample ID: BSKU/IPOOC/004(S2) - Right wing - near to the wheel well (Sample 2), Site 3; Sample ID: BSKU/IPOOC/002(S3) - Right wing (upper skin) - near to the fuselage (Sample 3) and Site 4; Sample ID: BSKU/IPOOC/001(S4) - Left wing (upper skin) - near to the refuelling point (Sample 4)
- Specimen type: Coupon without tab – width: 25 mm; length: 120 mm
- Number of specimens per sample: 5 pieces
- Speed: 1.3 mm/minute
- Anvil height: 13 mm

SIRIM QAS International Sdn. Bhd.
CHEMICAL, POLYMER AND COMPOSITE SECTION (CPCT)

3. Results and Discussion

3.1 Material Analysis for Resin Material

3.1.1 Fourier Transform Infra-Red (FTIR) Analysis Results

FTIR spectrum of the resin material used for the carbon fibre reinforced plastic (CFRP) composite sample taken from Site 1; Sample ID: BSKU/IPOOC/003(S1) - Left wing - near to the wheel well; Site 2; Sample ID: BSKU/IPOOC/004(S2) - Right wing - near to the wheel well, Site 3; Sample ID: BSKU/IPOOC/002(S3) - Right wing (upper skin) - near to the fuselage, are shown in Figures 1, 2 and 3 respectively. While the overlaid FTIR spectra of each sample with the most matching spectrum when compared against the available commercial library database are given in Figures 4, 5 and 6 respectively.

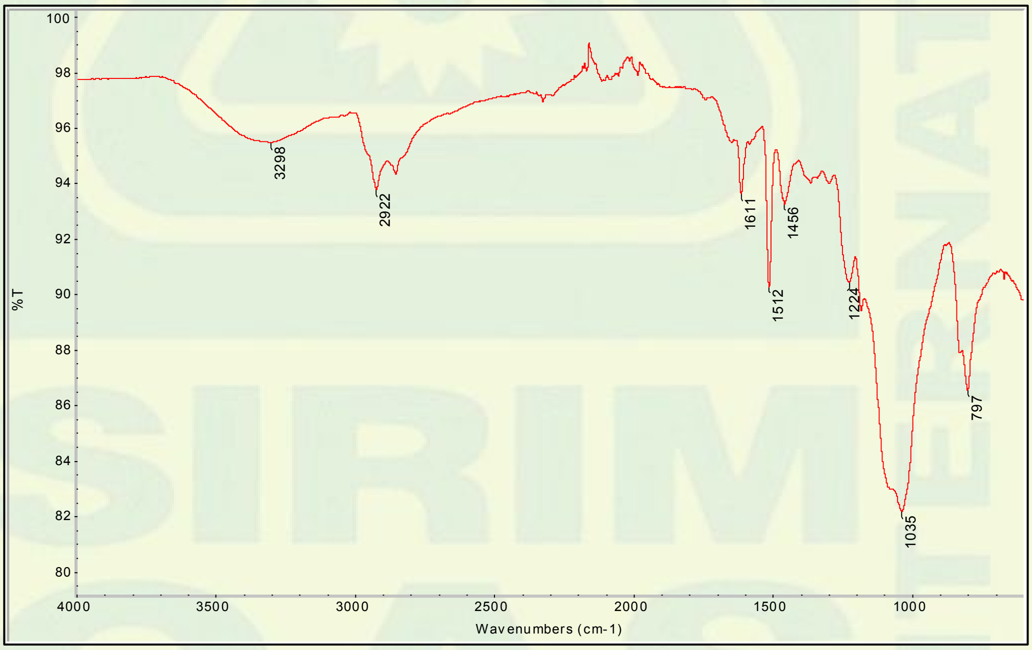

Figure 1. FTIR Spectrum of the resin sample collected from Site 1; Sample ID: BSKU/IPOOC/003(S1) - Left wing - near to the wheel well

CHEMICAL, POLYMER AND COMPOSITE SECTION (CPCT)
SIRIM QAS International Sdn. Bhd.

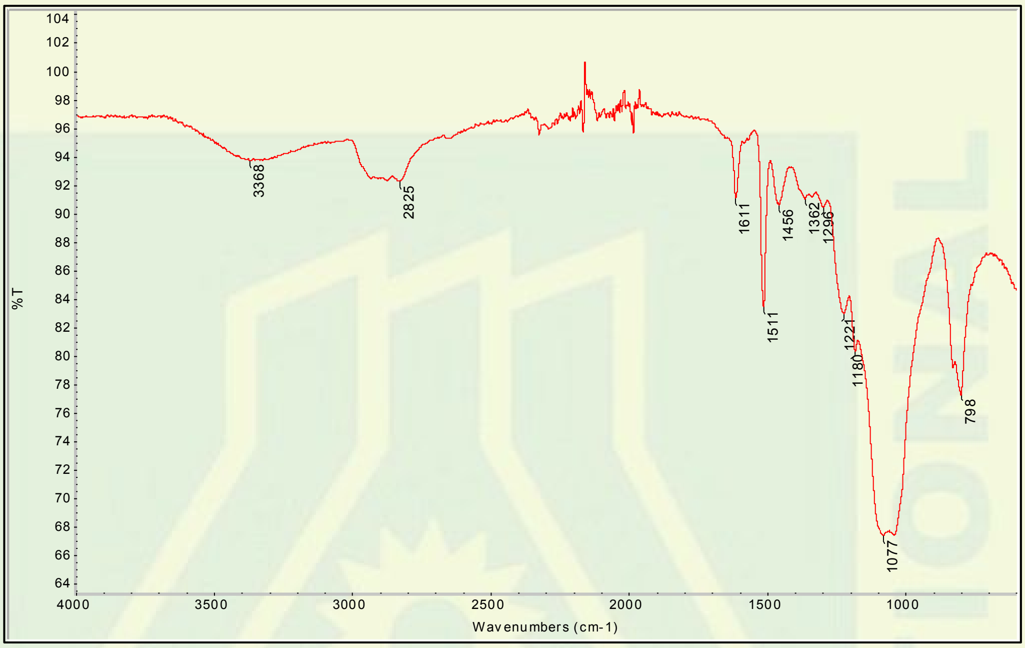

Figure 2. FTIR spectrum of the resin material collected from Site 2; Sample ID: BSKU/IPOOC/004(S2) - Right wing - near to the wheel well

Figure 3. FTIR spectrum of the resin material collected from Site 3; Sample ID: BSKU/IPOOC/002(S3) - Right wing (upper skin) - near to the fuselage

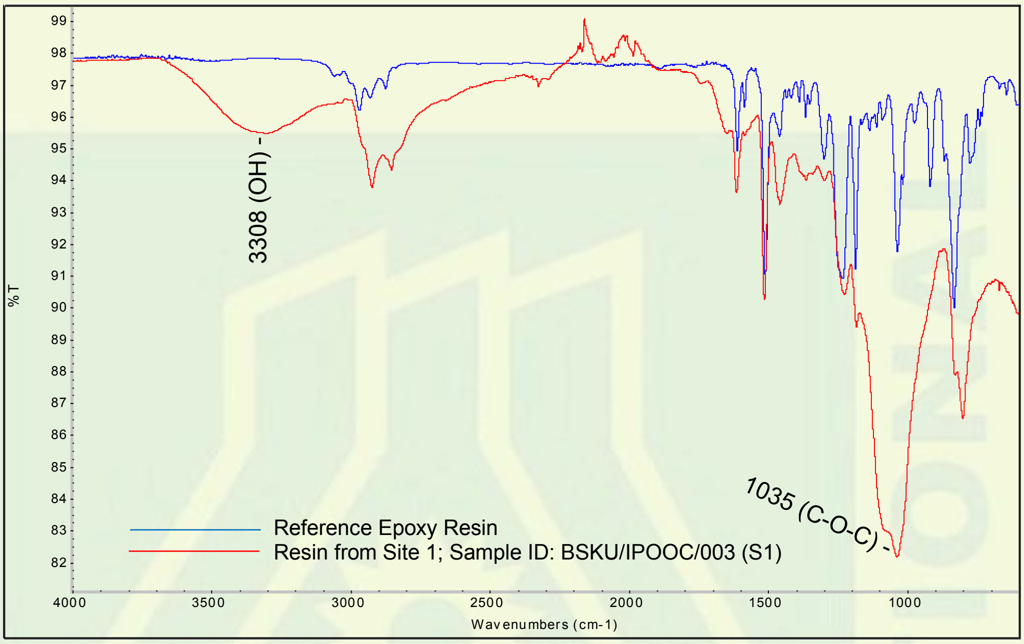

Figure 4. Overlaid FTIR spectra of the resin material collected from Site 1; Sample ID: BSKU/IPOOC/003(S1) - Left wing - near to the wheel well, with Reference Epoxy Resin

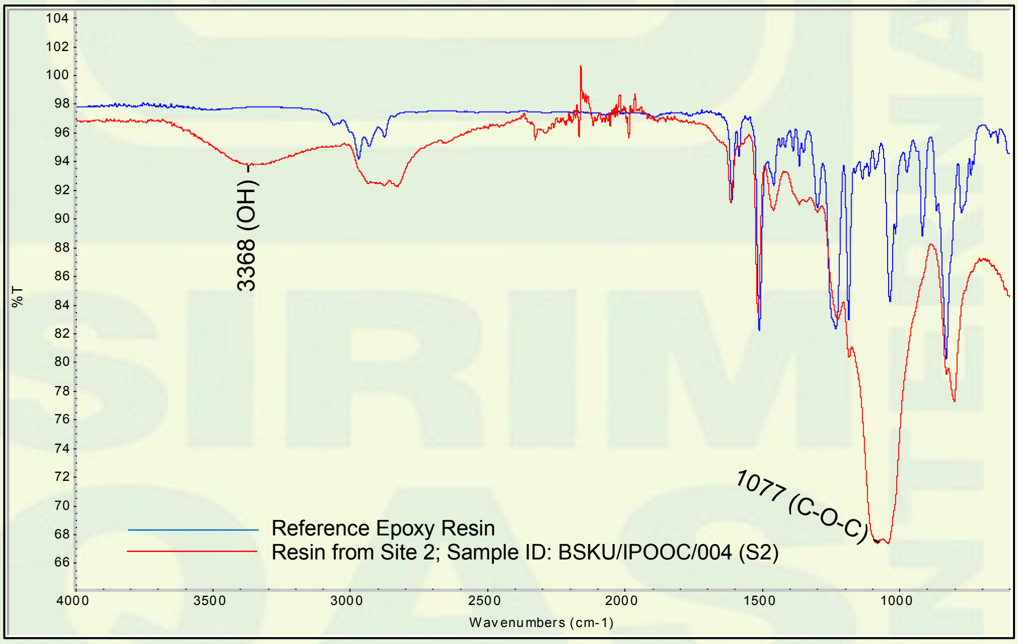

Figure 5. Overlaid FTIR spectra of the resin material collected from Site 2; Sample ID: BSKU/IPOOC/004(S2) - Right wing - near to the wheel well, with Reference Epoxy Resin

SIRIM QAS International Sdn. Bhd.
CHEMICAL, POLYMER AND COMPOSITE SECTION (CPCT)

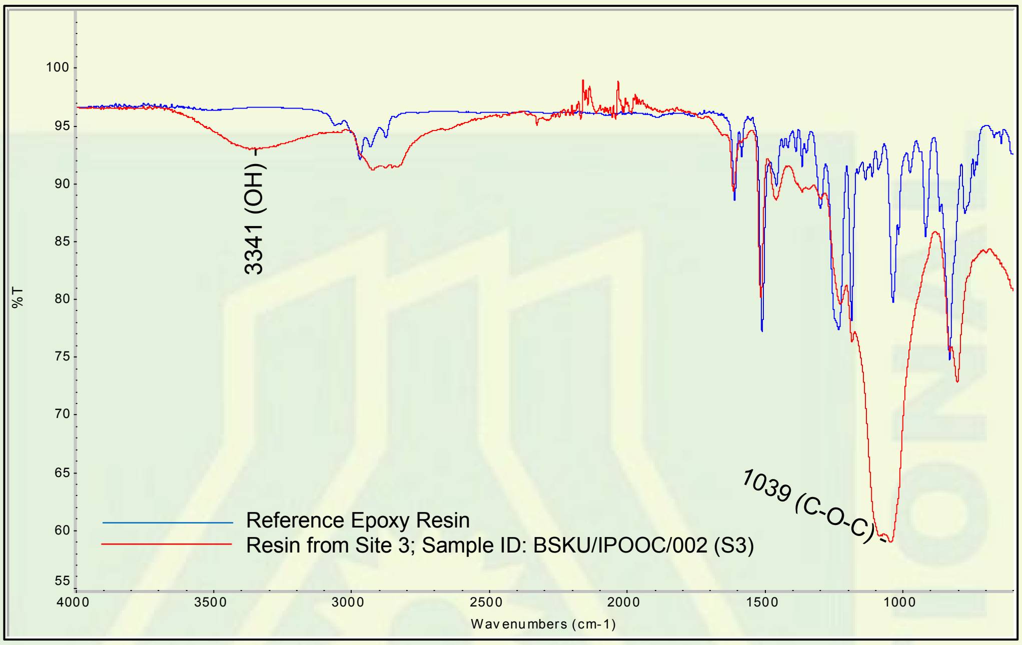

Figure 6. Overlaid FTIR spectra of the resin material collected from Site 3; Sample ID: BSKU/IPOOC/002(S3) - Right wing (upper skin) - near to the fuselage, with Reference Epoxy Resin

The overlaid FTIR spectra indicates that the FTIR spectrum of both tested samples are relatively similar to that of the reference epoxy resin except at the absorption peak at approximately (3308 – 3368) cm^{-1} and (1035 -1077) cm^{-1}. Explanation regarding these additional peaks are as follows:

- Peaks at about 3308 cm^{-1}, 3341 cm-1 and 3368 cm^{-1}: These peaks are often associated with O-H stretching vibrations, which can indicate the presence of hydroxyl groups. Hydroxyl groups can be formed as a result of material hydrolysis, especially in the case of water absorption or chemical breakdown involving water. In epoxy resins, this peak may suggest moisture uptake or possible hydrolytic degradation.

- Peaks at 1035 cm^{-1}, 1039 cm^{-1} and 1077 cm^{-1}: These peaks are commonly attributed to the C-O-C stretching vibrations of ether groups, which are part of the epoxy structure. It could also be indicative of aliphatic ether linkages, which are typical in many epoxy-based materials. This peak does not specifically suggest degradation but rather the inherent chemical bonds in the cured resin.

3.1.2 Differential Scanning Calorimetry (DSC) Analysis Results

DSC curves of the Site 1; Sample ID: BSKU/IPOOC/003(S1) - Left wing - near to the wheel well; Site 2; Sample ID: BSKU/IPOOC/004(S2) - Right wing - near to the wheel well, Site 3; Sample ID: BSKU/IPOOC/002(S3) - Right wing (upper skin) - near to the fuselage samples are shown in Figures 7 to 12, while the summary of the analysis results is given in Table 1.

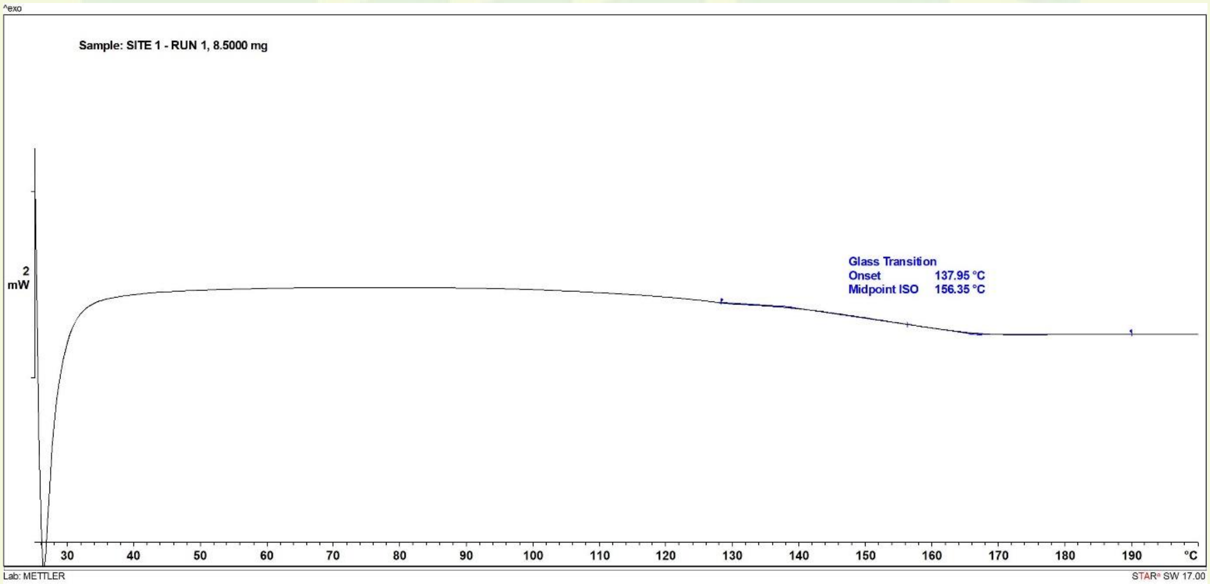

Figure 7. DSC Curve of The Resin Sample Taken from Site 1; Sample ID: BSKU/IPOOC/003(S1) - Left wing - near to the wheel well - Run #1

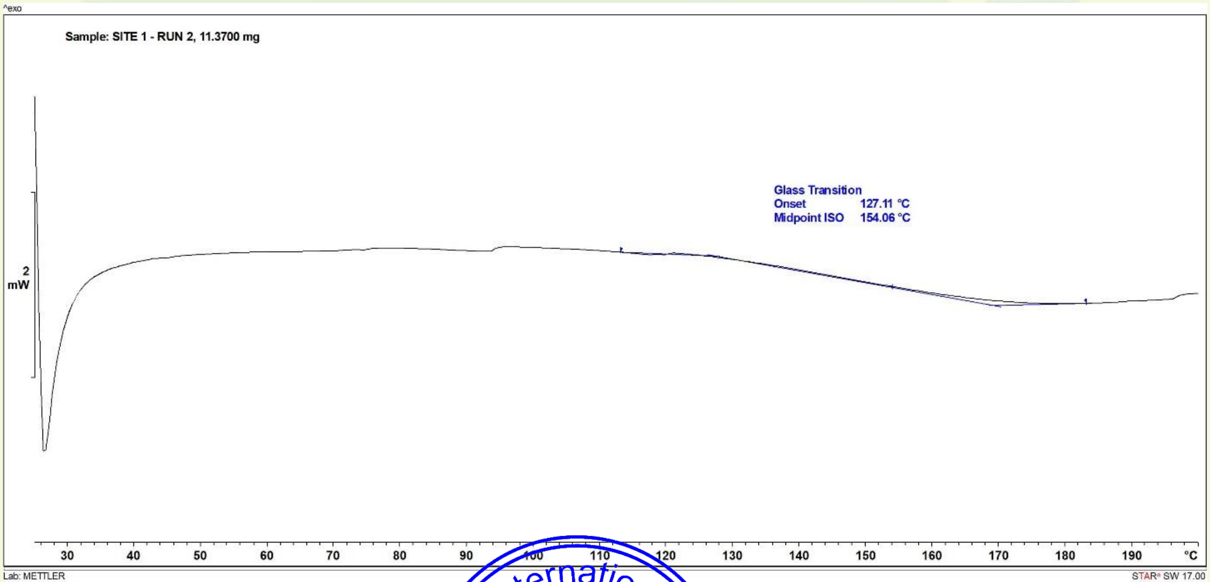

Figure 8. DSC Curve of The Resin Sample Taken from Site 1; Sample ID: BSKU/IPOOC/003(S1) - Left wing - near to the wheel well - Run #2

SIRIM QAS International Sdn. Bhd.
CHEMICAL, POLYMER AND COMPOSITE SECTION (CPCT)

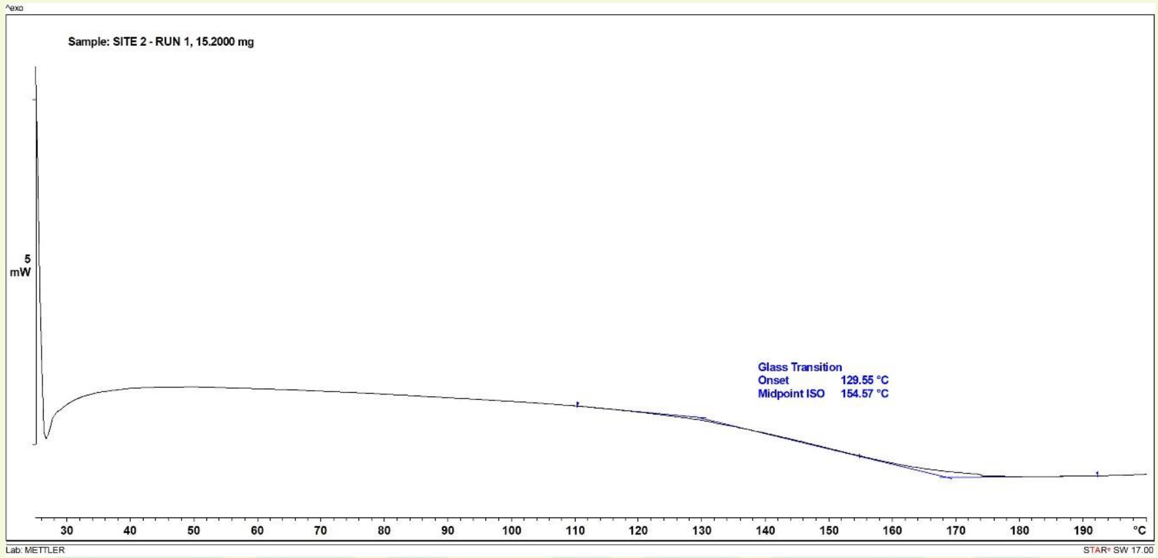

Figure 9. DSC Curve of The Resin Sample Taken from Site 2; Sample ID: BSKU/IPOOC/004(S2) - Right wing - near to the wheel well - Run #1

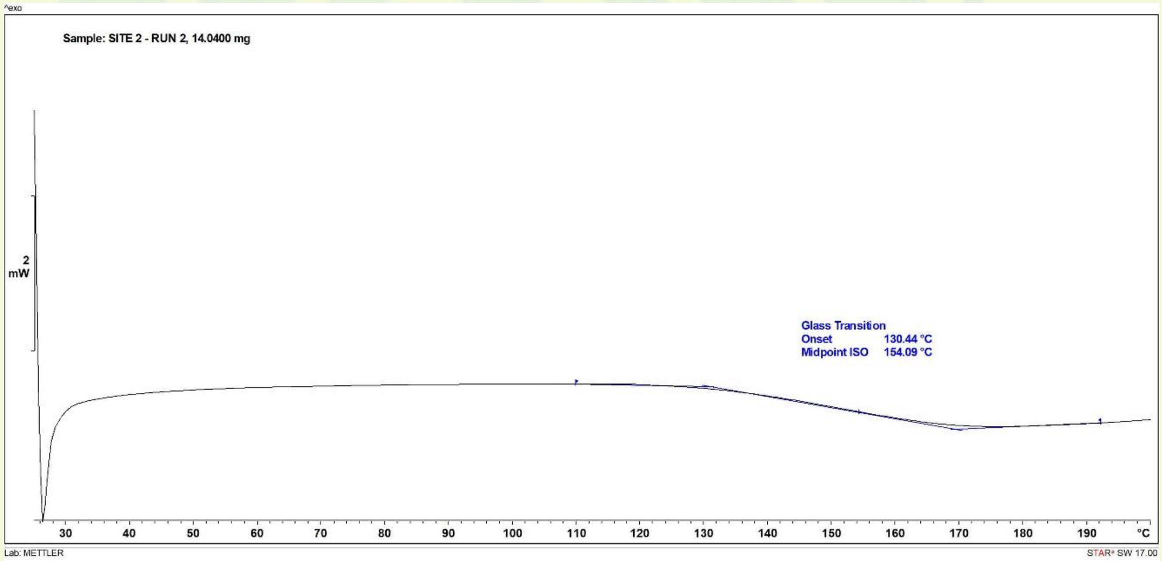

Figure 10. DSC Curve of The Resin Sample Taken from Site 2; Sample ID: BSKU/IPOOC/004(S2) - Right wing - near to the wheel well - Run #2

SIRIM QAS International Sdn. Bhd.
CHEMICAL, POLYMER AND COMPOSITE SECTION (CPCT)

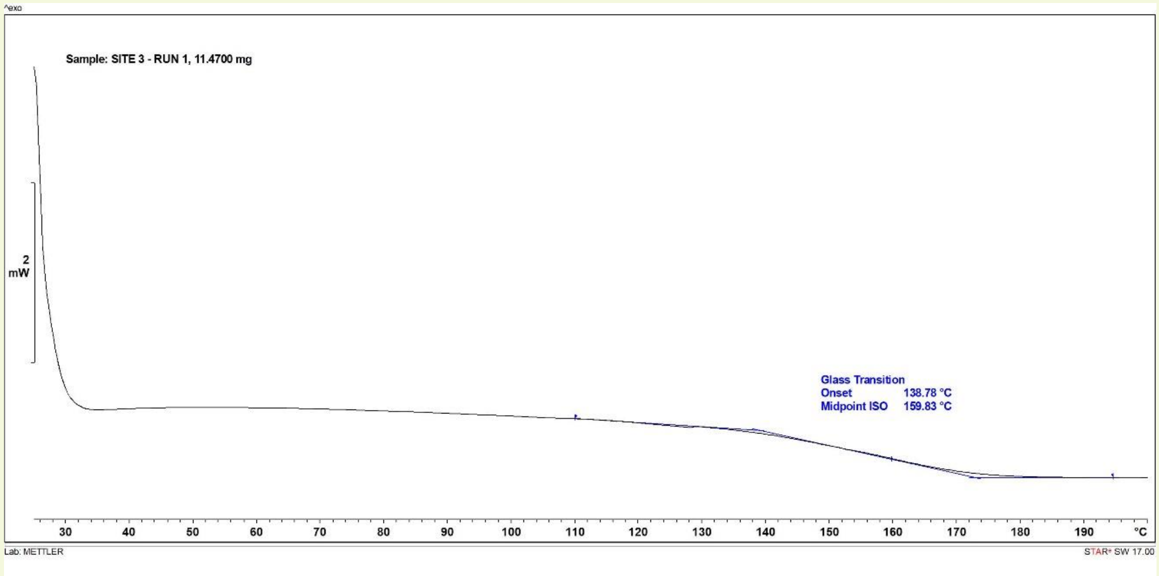

Figure 11. DSC Curve of The Resin Sample Taken from Site 3; Sample ID: BSKU/IPOOC/002(S3) - Right wing (upper skin) - near to the fuselage - Run #1

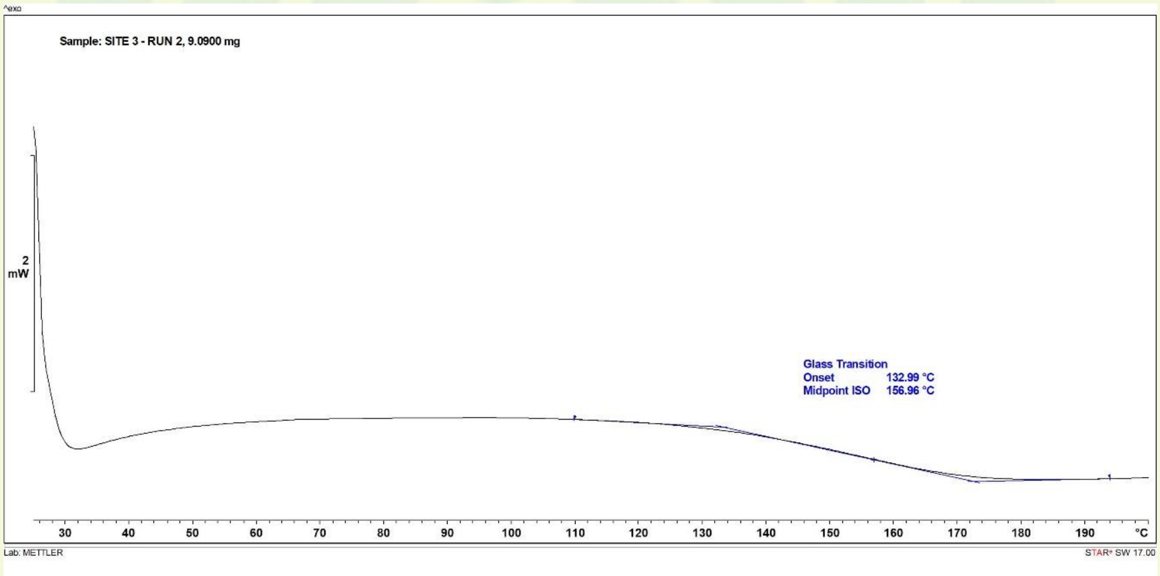

Figure 12. DSC Curve of The Resin Sample Taken from Site 3; Sample ID: BSKU/IPOOC/002(S3) - Right wing (upper skin) - near to the fuselage - Run #2

SIRIM QAS International Sdn. Bhd.
CHEMICAL, POLYMER AND COMPOSITE SECTION (CPCT)

Table 1. Glass Transition Temperature (T_g) of Resin Samples

RUN NO.	RESULT		
	Site 1; Sample ID: BSKU/IPOOC/003(S1) - Left wing - near to the wheel well	**Site 2; Sample ID: BSKU/IPOOC/004(S2)** - Right wing - near to the wheel well	**Site 3; Sample ID: BSKU/IPOOC/002(S3)** - Right wing (upper skin) - near to the fuselage
1	156°C	155°C	160°C
2	154°C	154°C	157°C
AVERAGE	**155°C**	**155°C**	**159°C**

The maximum and minimum T_g values of the resin sample in dry condition reported in Doc No: BCV-04-64-02; Table 18; Page 29 and Table 24; Page 37 of Compliance Report – Toray 2510 Series Resin Material Equivalency Test Results are approximately 137°C and 148°C respectively for unidirectional and approximately 140°C to 147°C respectively for the fabric sample.

In comparison to the above values, the T_g values of the tested samples are about 155°C and 159°C (see Table 1). Higher T_g values for an epoxy resin suggests the following:

i. **Post-Curing Effect:** The increase in Tg for the tested sample suggests that the material has undergone additional curing (post-curing) during service. Exposure to elevated temperatures over time can cause further cross-linking in the epoxy resin, leading to a higher T_g.

ii. **Thermal Aging:** The tested sample might have experienced thermal aging, which typically involves exposure to elevated temperatures over a long period. This could also explain the higher T_g, as thermal aging tends to enhance the cross-linking density in thermoset resins like epoxy.

iii. **Residual Stress Reduction:** In service, residual stresses in the epoxy might have relaxed due to prolonged exposure to heat, further cross-linking the polymer network and raising the T_g.

SIRIM QAS International Sdn. Bhd.
CHEMICAL, POLYMER AND COMPOSITE SECTION (CPCT)

3.1.3 TGA Analysis Results

TGA thermograms for the tested samples are shown in Figures 13 to 18, while the summary of the moisture content detected from the TGA analysis is given in Table 2.

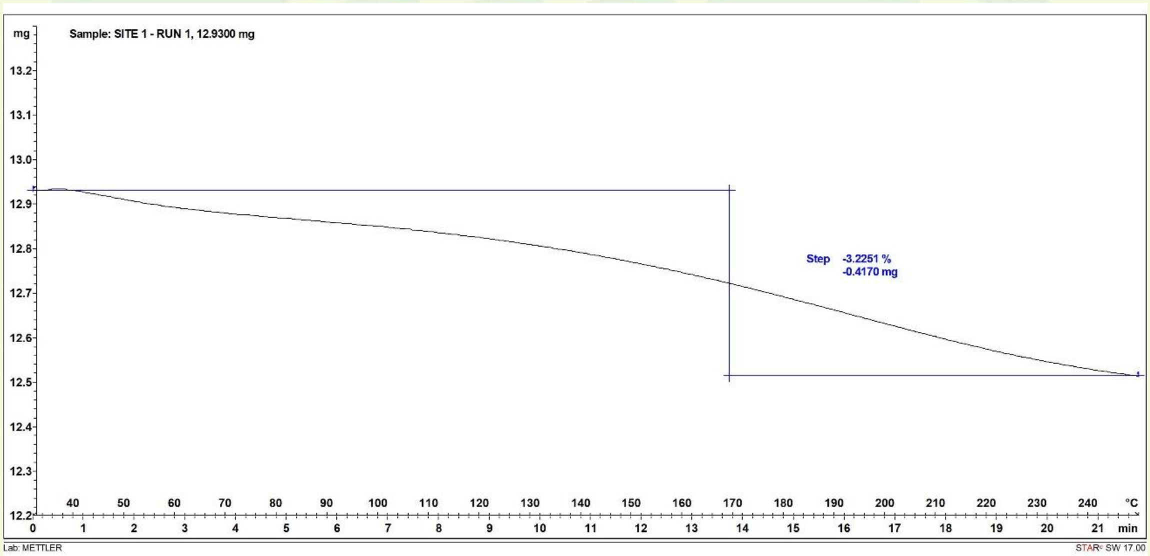

Figure 13. TGA Thermogram of Sample Taken from Site 1; Sample ID: BSKU/IPOOC/003(S1) - Left wing - near to the wheel well - Run #1

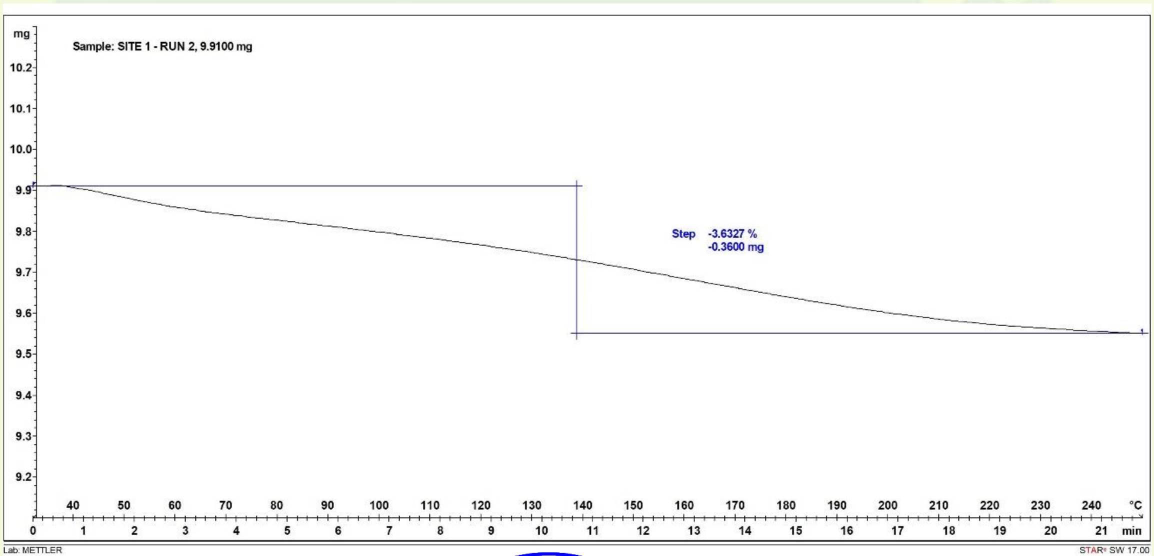

Figure 14. TGA Thermogram of Sample Taken from Site 1; Sample ID: BSKU/IPOOC/003(S1) - Left wing - near to the wheel well - Run #2

SIRIM QAS International Sdn. Bhd.
CHEMICAL, POLYMER AND COMPOSITE SECTION (CPCT)

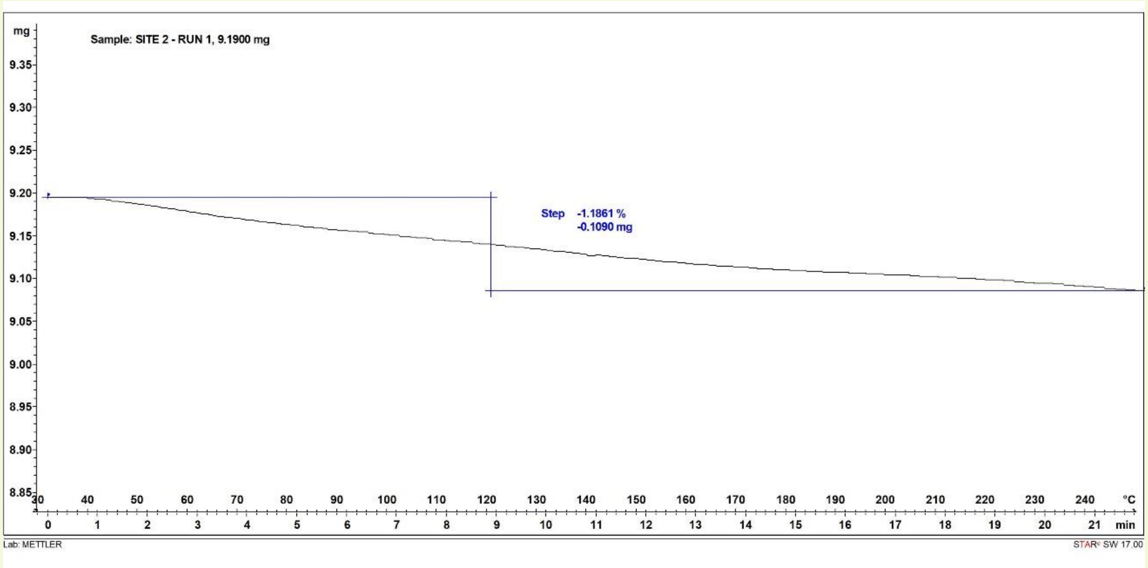

Figure 15. TGA Thermogram of Sample Taken from Site 2; Sample ID: BSKU/IPOOC/004(S2) - Right wing - near to the wheel well - Run #1

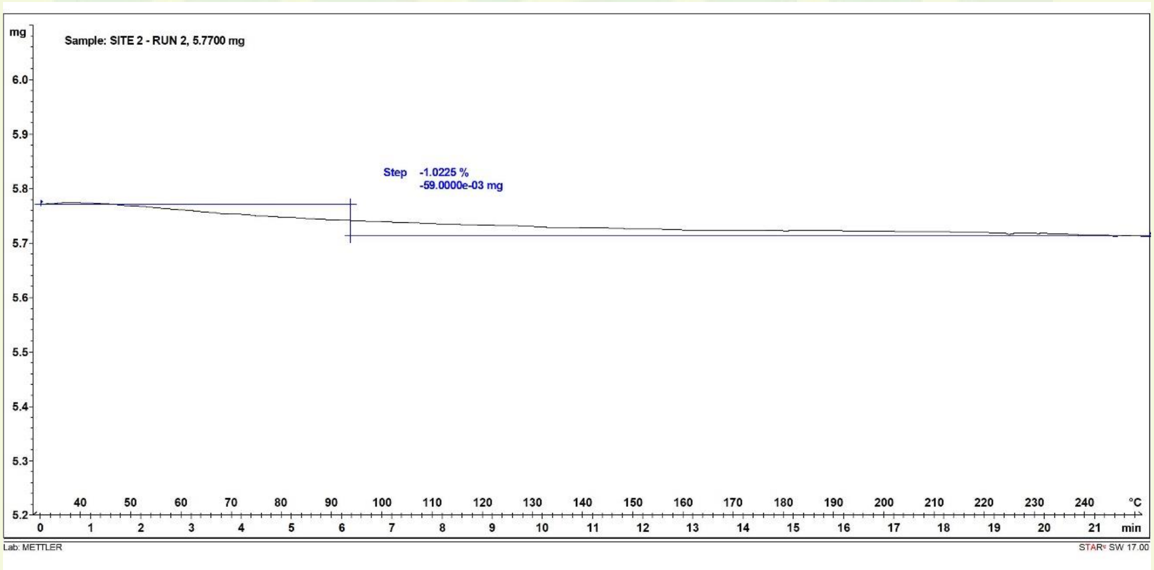

Figure 16. TGA Thermogram of Sample Taken from Site 2; Sample ID: BSKU/IPOOC/004(S2) - Right wing - near to the wheel well - Run #2

SIRIM QAS International Sdn. Bhd.
CHEMICAL, POLYMER AND COMPOSITE SECTION (CPCT)

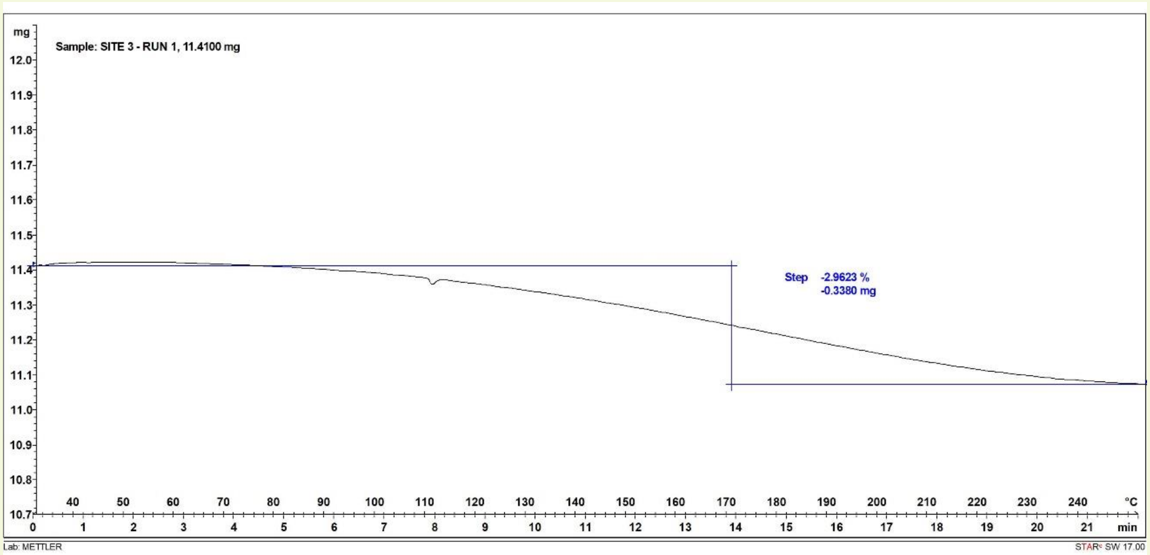

Figure 17. TGA Thermogram of Sample Taken from Site 3; Sample ID: BSKU/IPOOC/002(S3) - Right wing (upper skin) - near to the fuselage - Run #1

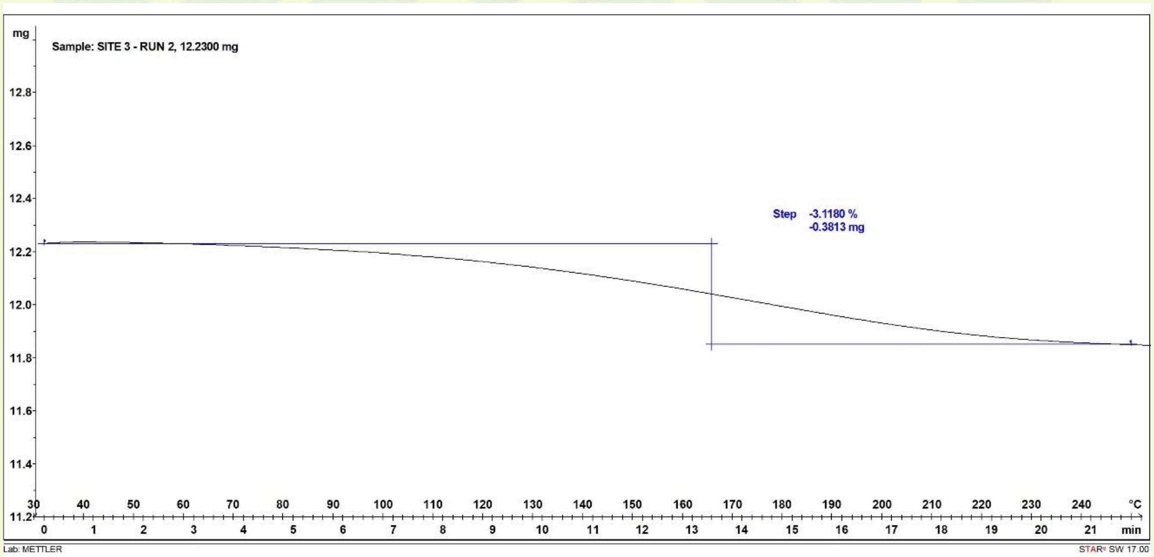

Figure 18. TGA Thermogram of Sample Taken from Site 3; Sample ID: BSKU/IPOOC/002(S3) - Right wing (upper skin) - near to the fuselage - Run #2

SIRIM QAS International Sdn. Bhd.
CHEMICAL, POLYMER AND COMPOSITE SECTION (CPCT)

Table 2. Summary of Moisture Content Analysis Results

RUN NO.	RESULT		
	Site 1; Sample ID: BSKU/IPOOC/003(S1) - Left wing - near to the wheel well	**Site 2; Sample ID: BSKU/IPOOC/004(S2)** - Right wing - near to the wheel well	**Site 3; Sample ID: BSKU/IPOOC/002(S3)** - Right wing (upper skin) - near to the fuselage
1	3 %	1 %	3 %
2	4 %	1 %	3 %
AVERAGE	**4 %**	**1 %**	**3 %**

Result from Table 2 indicates that the CFRP composite samples taken at Site 1, Site 2 and Site 3 contain about (1 to 4) % moisture. This result support the presence of the hydroxyl (OH) functional group observed from the FTIR analysis.

Since the matrix material in the CFRP composite material is epoxy, the presence of 1% to 4% moisture is particularly alarming. Epoxy resins are known to be somewhat hygroscopic, meaning they can absorb water from their environment. When moisture content reaches a certain threshold, it can cause hydrolysis of the epoxy network, specifically cleaving ester linkages, which leads to the formation of hydroxyl groups.

The hydroxyl groups detected in the FTIR analysis strongly suggest that hydrolysis is occurring, likely exacerbated by the absorbed moisture. This can negatively impact the mechanical properties of the CFRP composite, leading to issues such as reduced stiffness, strength, and long-term durability.

SIRIM QAS International Sdn. Bhd.
CHEMICAL, POLYMER AND COMPOSITE SECTION (CPCT)

3.2 Structure Design

3.2.1 Analysis Results for Failure Mechanism

The SEM images of cracked surfaces found at the ROIs in Site 2; Sample ID: BSKU/IPOOC/004(S2) - Right wing - near to the wheel well, are shown in Figures 19 to 23.

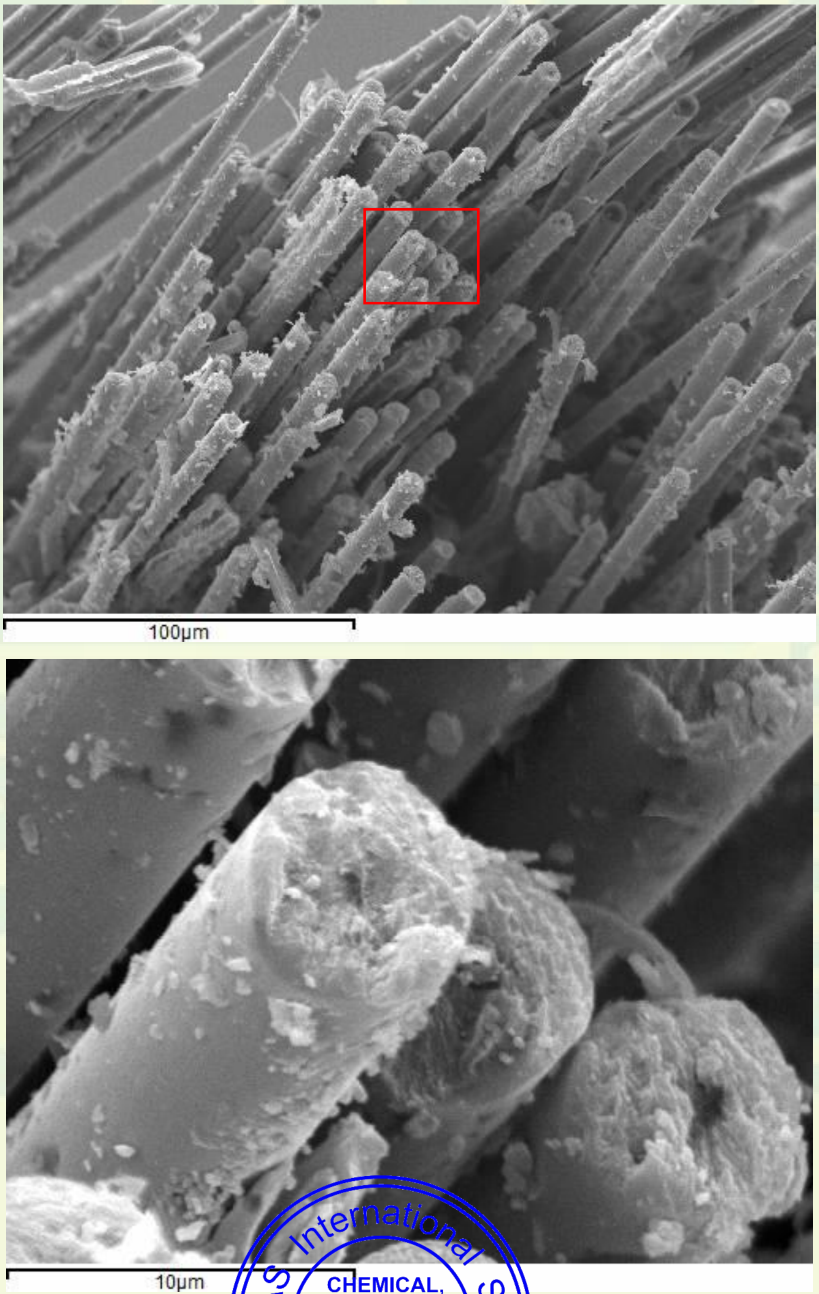

Figure 19. SEM Images at ROI 1(a) – Magnification: 500x (Top) and 5,000x (Bottom)

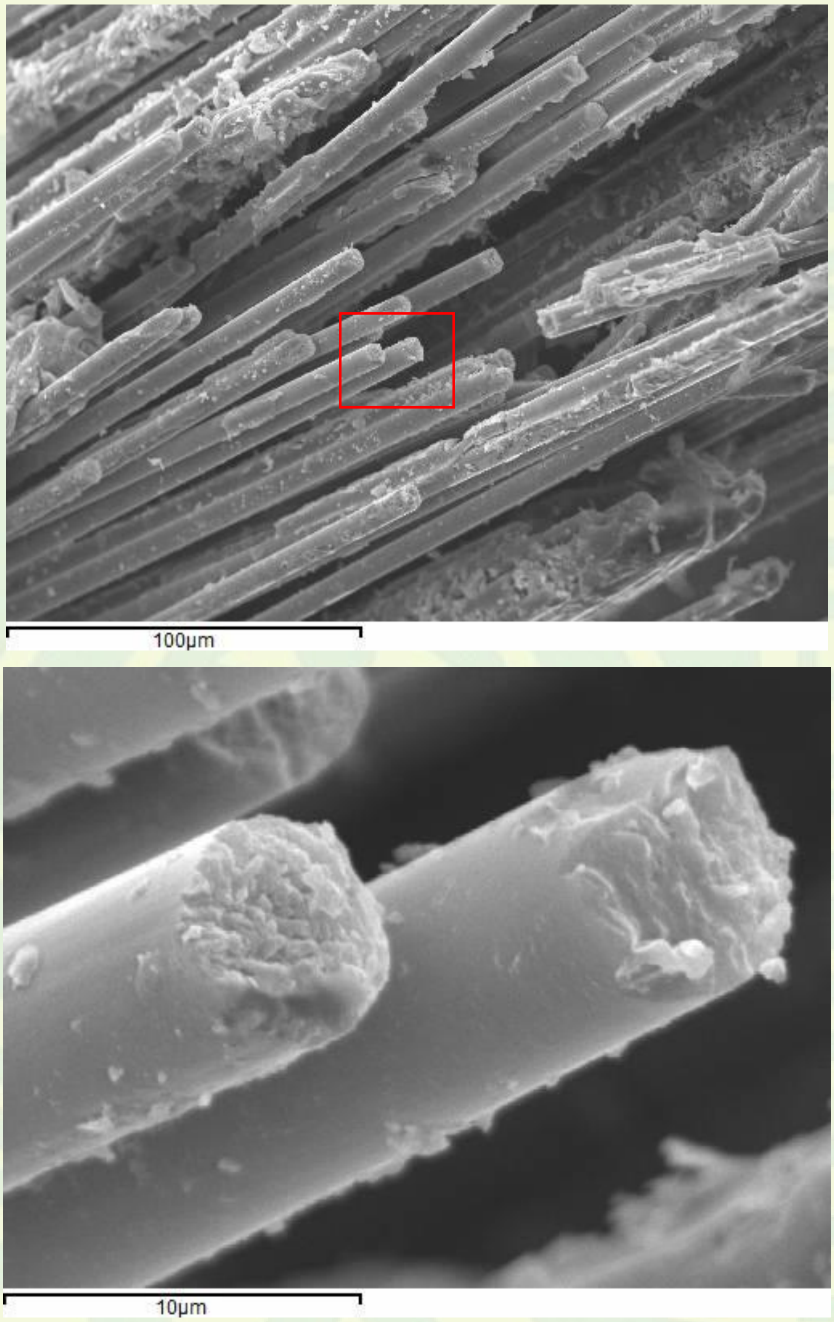

Figure 20. SEM Image at ROI 1(b) – Magnification: 500x (Top) and 5,000x (Bottom)

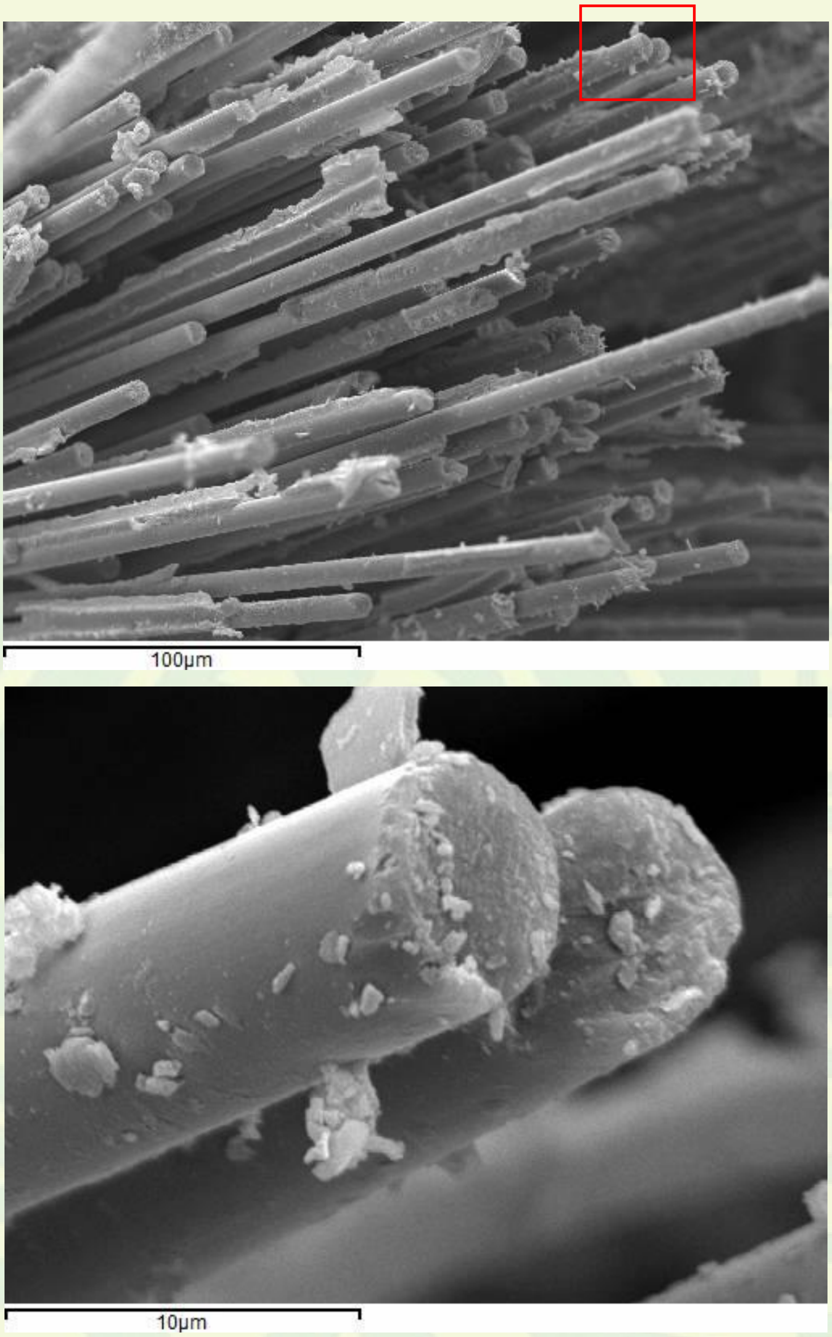

Figure 21. SEM Image at ROI 2 – Magnification: 500x (Top) and 5,000x (Bottom)

SIRIM QAS International Sdn. Bhd.
CHEMICAL, POLYMER AND COMPOSITE SECTION (CPCT)

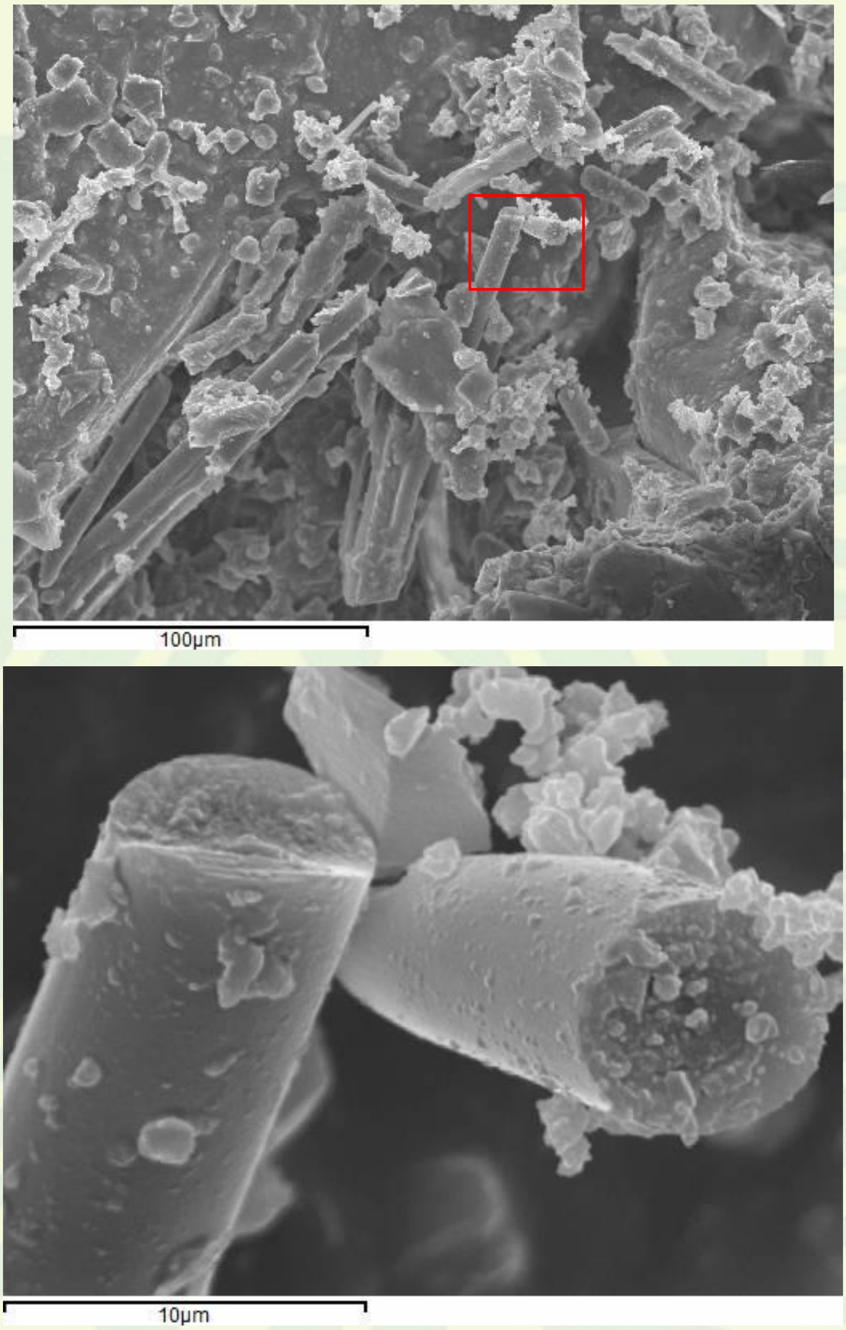

Figure 22. SEM Image at ROI 3(a) – Magnification: 500x (Top) and 5,000x (Bottom)

SIRIM QAS International Sdn. Bhd.
CHEMICAL, POLYMER AND COMPOSITE SECTION (CPCT)

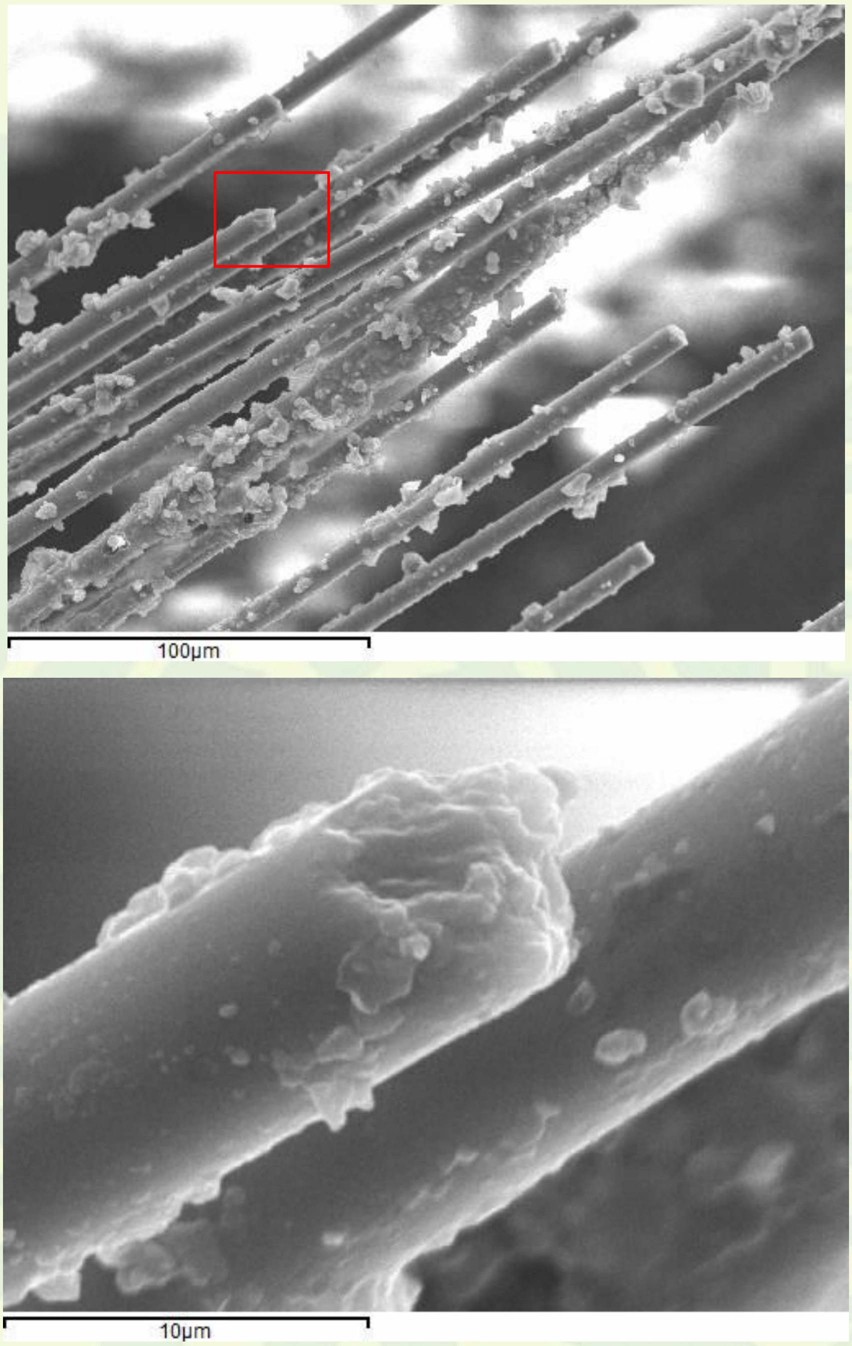

Figure 23. SEM Image at ROI 3(b) – Magnification: 500x (Top) and 5,000x (Bottom)

SIRIM QAS International Sdn. Bhd.
CHEMICAL, POLYMER AND COMPOSITE SECTION (CPCT)

The SEM images of the carbon fibres in the failed CFRP (Carbon Fiber Reinforced Polymer) component shows some key features that suggest certain failure mechanisms:

i. **Fiber Pull-out:** The exposed and partially separated fibres in the image indicate a weak fiber-matrix bond, which often leads to fibre pull-out. This could suggest that the failure initiated due to poor adhesion between the epoxy matrix and the carbon fibres, which is commonly caused by environmental factors like moisture (related to hydrolysis), poor curing, or degradation over time.

ii. **Fiber Breakage:** Some fibres appear to have rough, fractured ends, indicating they underwent brittle failure. This could be due to mechanical overload or a fatigue-related failure mechanism, where repeated stress leads to crack propagation through the fibres themselves.

iii. **Debonding and Surface Degradation:** The presence of debris on the surface of the fibres and the lack of continuous matrix around some of them suggests that environmental degradation, such as hydrolysis (from moisture absorption), might have led to debonding. This would cause a loss of load transfer between fibres and the matrix, leading to failure.

iv. **Matrix Cracking:** Although the matrix is not clearly visible, the combination of fibre pull-out and breakage suggests that matrix cracking or delamination likely occurred. This could have been initiated by environmental degradation (such as hydrolysis), mechanical stress, or thermal cycling.

The failure mechanism described above likely involves environmental degradation (hydrolysis) due to moisture absorption, leading to fibre-matrix debonding, and mechanical overload or fatigue, resulting in fibre breakage. This combination can cause the overall composite structure to weaken and fail under service loads.

SIRIM QAS International Sdn. Bhd.
CHEMICAL, POLYMER AND COMPOSITE SECTION (CPCT)

Photomicrographs taken using a stereo and compound microscope at cross sectioned area indicated as Section A are shown in Figures 24 and 25 respectively, while that at cross sectioned area indicated as Section B are shown in Figures 26 and 27 respectively.

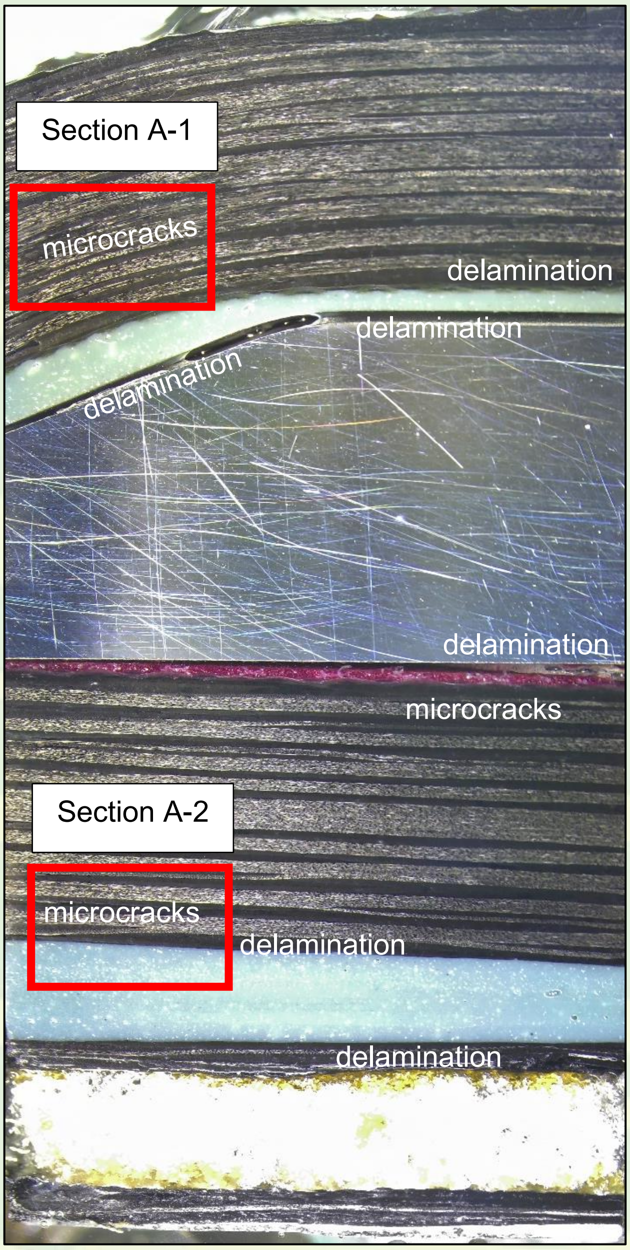

Figure 24. Cross Sectioned Image at Cut Section A – Using Stereo Microscope; Magnification: 10x

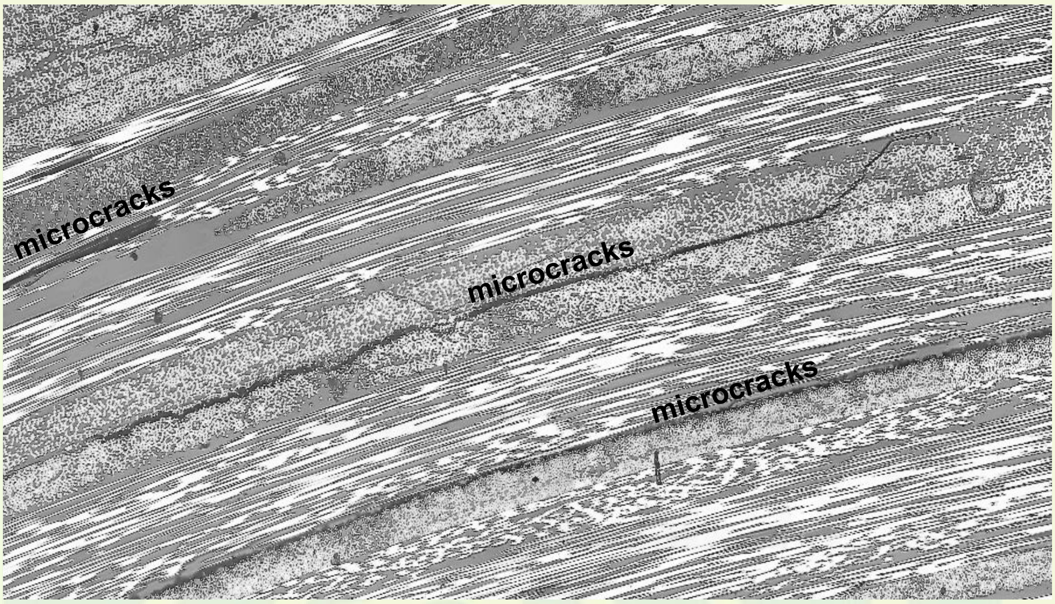

Section A-1

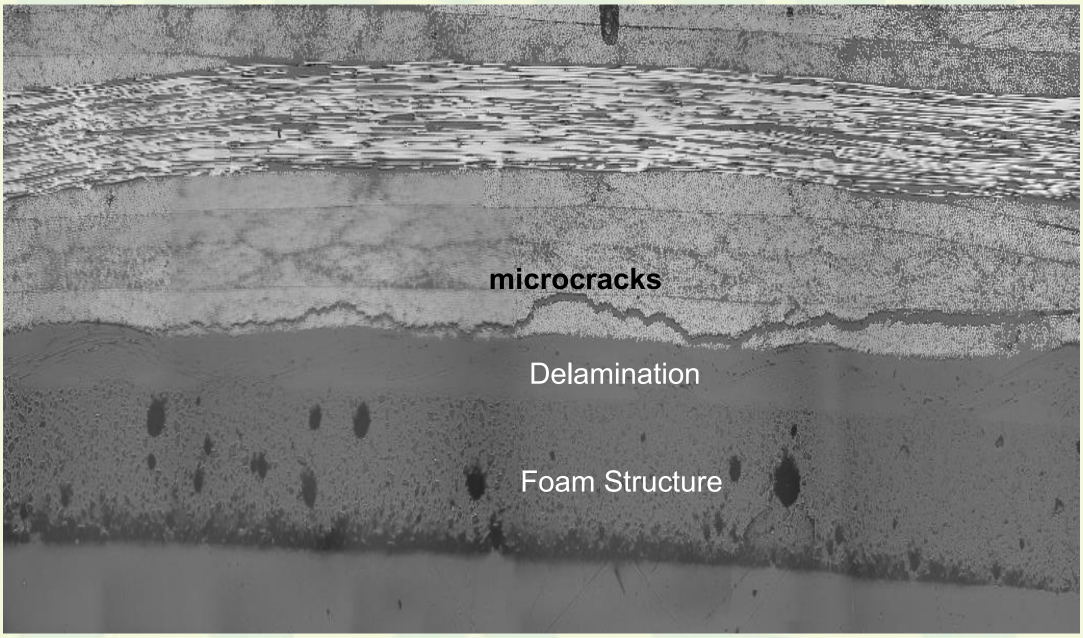

Section A-2

Figure 25. Cross Sectioned Image at Cut Section A – Using Compound Microscope; Magnification: 50x

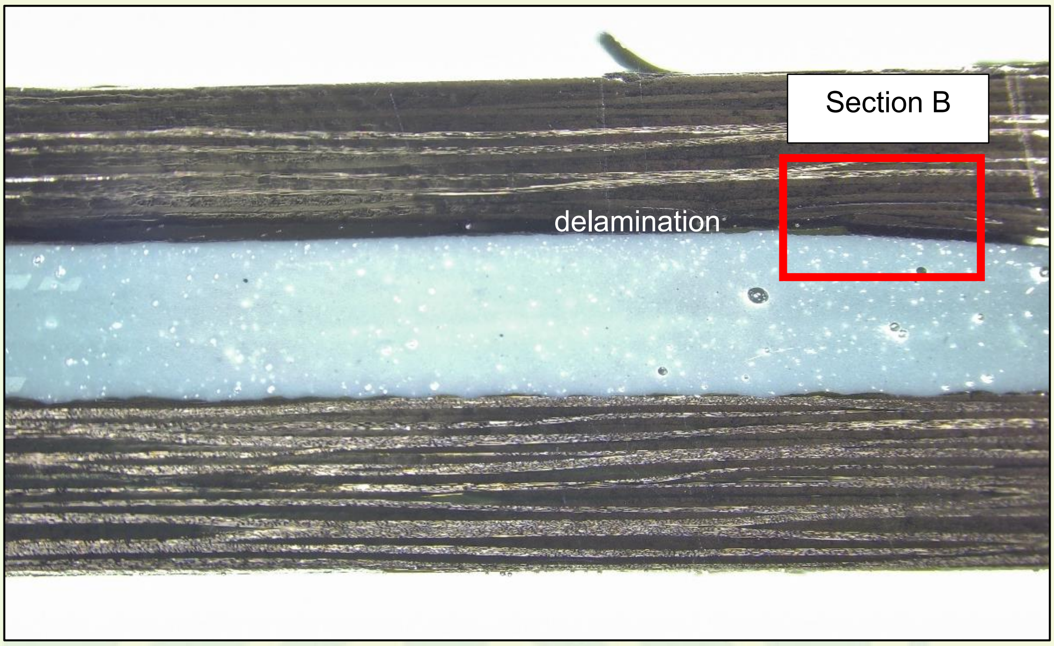

Figure 26. Cross Sectioned Image at Section B – Using Stereo Microscope; Magnification: 10x

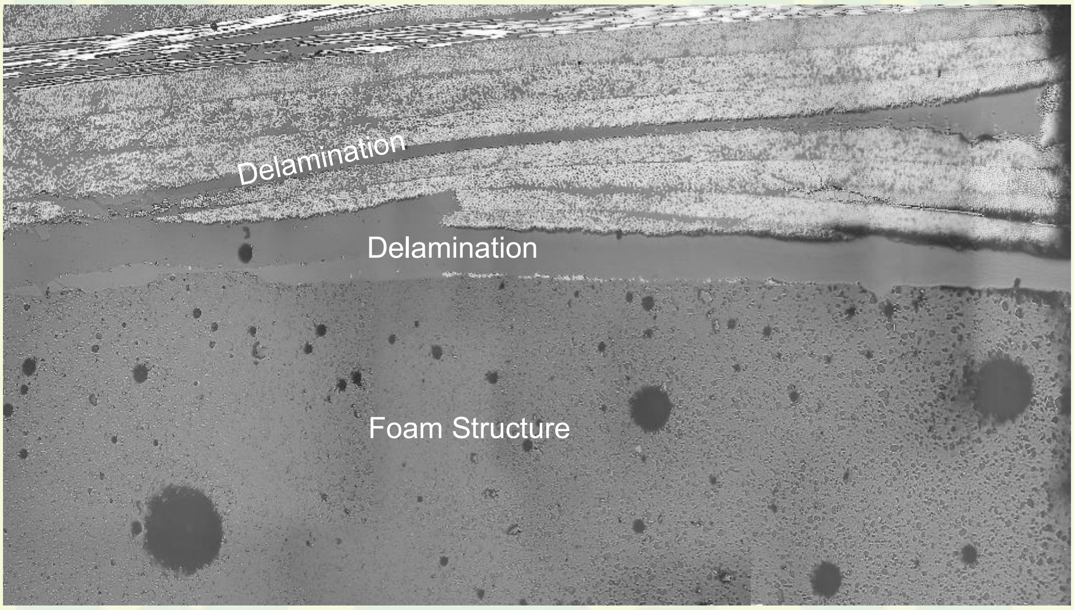

Figure 27. Cross Sectioned Image at Section B – Using Compound Microscope; Magnification: 50x

SIRIM QAS International Sdn. Bhd.
CHEMICAL, POLYMER AND COMPOSITE SECTION (CPCT)

The cross-section image of the carbon fibre-reinforced polymer (CFRP) composite component, displaying a series of layers and microcracks within the matrix. The key observations are as follows:

i. **Microcracks in the Matrix**: The microcracks appear between the fibre layers, particularly within the resin matrix. Microcracks can form due to several reasons such as thermal cycling, mechanical stress, or chemical degradation (e.g. hydrolysis as found the FTIR and TGA analysis). The presence of microcracks can lead to:
   - **Reduced Load Transfer**: Microcracks reduce the ability of the matrix to transfer loads effectively between the fibers. This can weaken the overall structural integrity.
   - **Delamination**: If these cracks propagate, they could result in delamination, which is a significant failure mode in composite structures. Delamination can drastically reduce the strength and stiffness of the component.

ii. **Crack Propagation Direction**: The orientation of the cracks relative to the fibres seems parallel or slightly inclined. If these cracks align with the primary stress directions or continue to propagate under operational loads (such as in-flight mechanical stresses), they could contribute to material failure over time.

While the microcracks are not catastrophic on their own, they are a sign of underlying issues that could eventually lead to failure. The accumulation of these cracks under repeated load cycles can result in:

i. **Fatigue Failure**: Over time, cyclic stresses could propagate these microcracks, leading to larger fractures.

ii. **Moisture Ingress**: In composite structures, microcracks can allow moisture to penetrate, leading to hydrolysis or other chemical degradation (especially in the epoxy matrix).

Photomicrographs taken using a stereo and compound microscope at cross sectioned area indicated as Section C are shown in Figures 28 and 29 respectively, while that indicated as Section D are shown in Figures 30 and 31 respectively.

SIRIM QAS International Sdn. Bhd.
CHEMICAL, POLYMER AND COMPOSITE SECTION (CPCT)

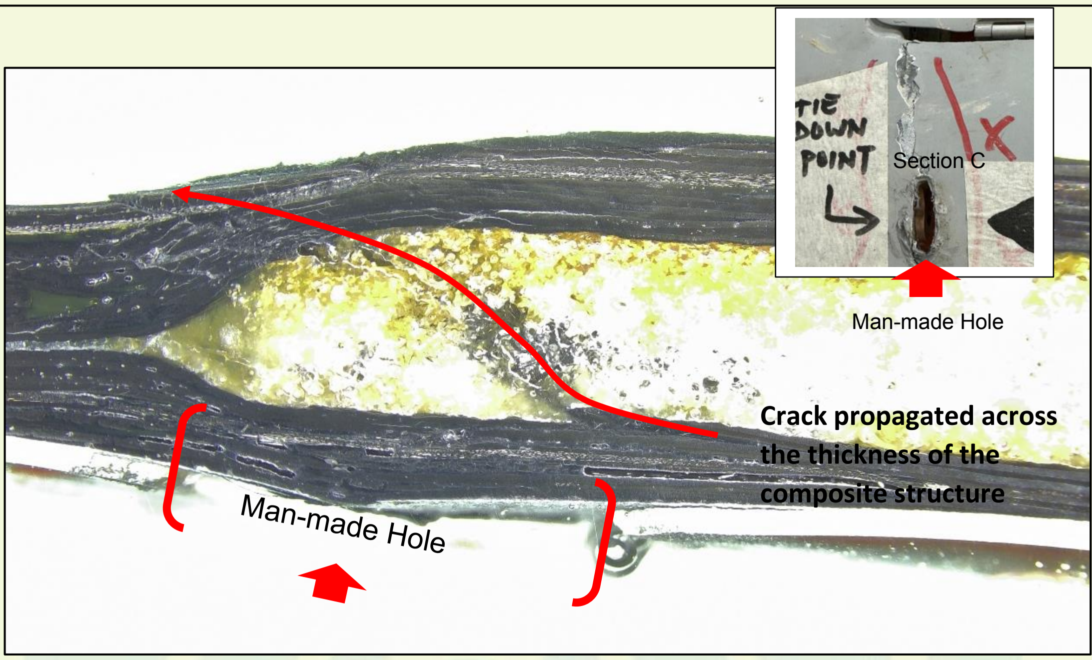

Figure 28. Cross Sectioned Image at Section C – Using Stereo Microscope; Magnification: 10x

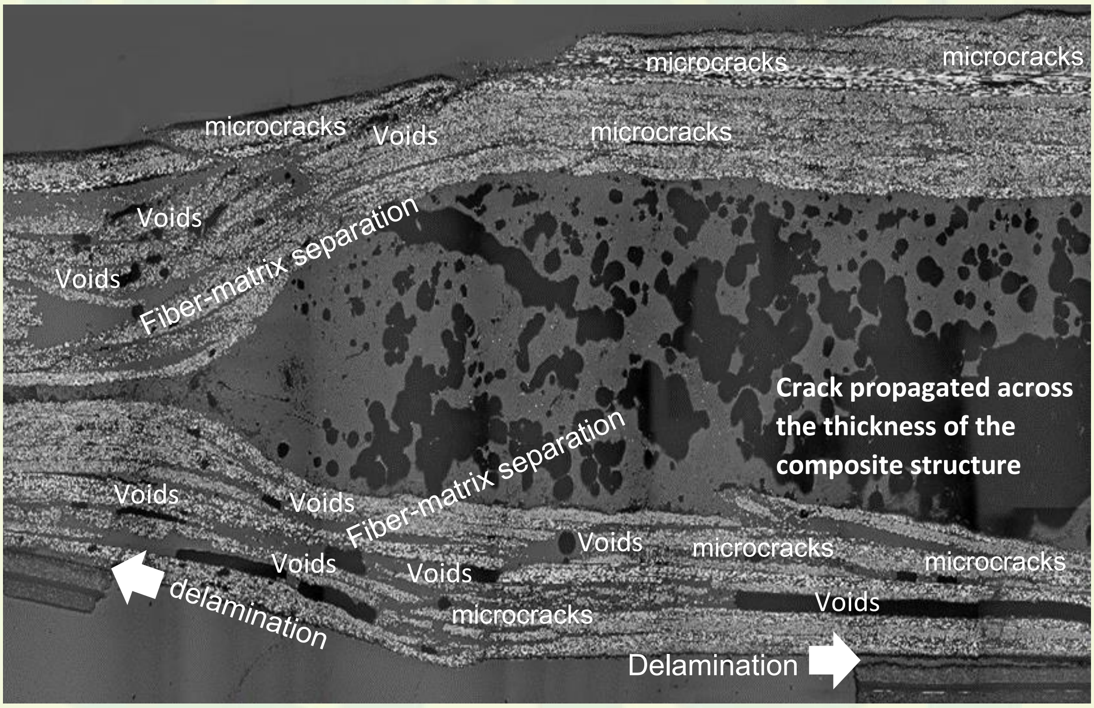

Figure 29. Cross Sectioned Image at Section C – Using Compound Microscope; Magnification: 50x

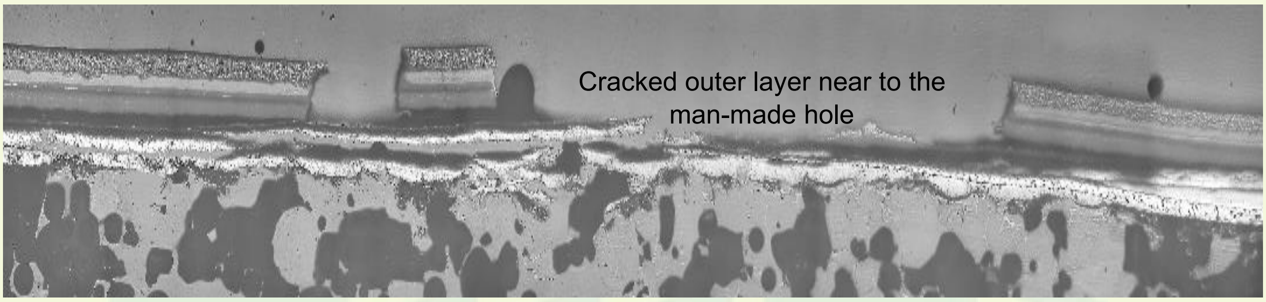

Figure 30. Cross Sectioned Image at Section D – Using Stereo Microscope; Magnification: 10x

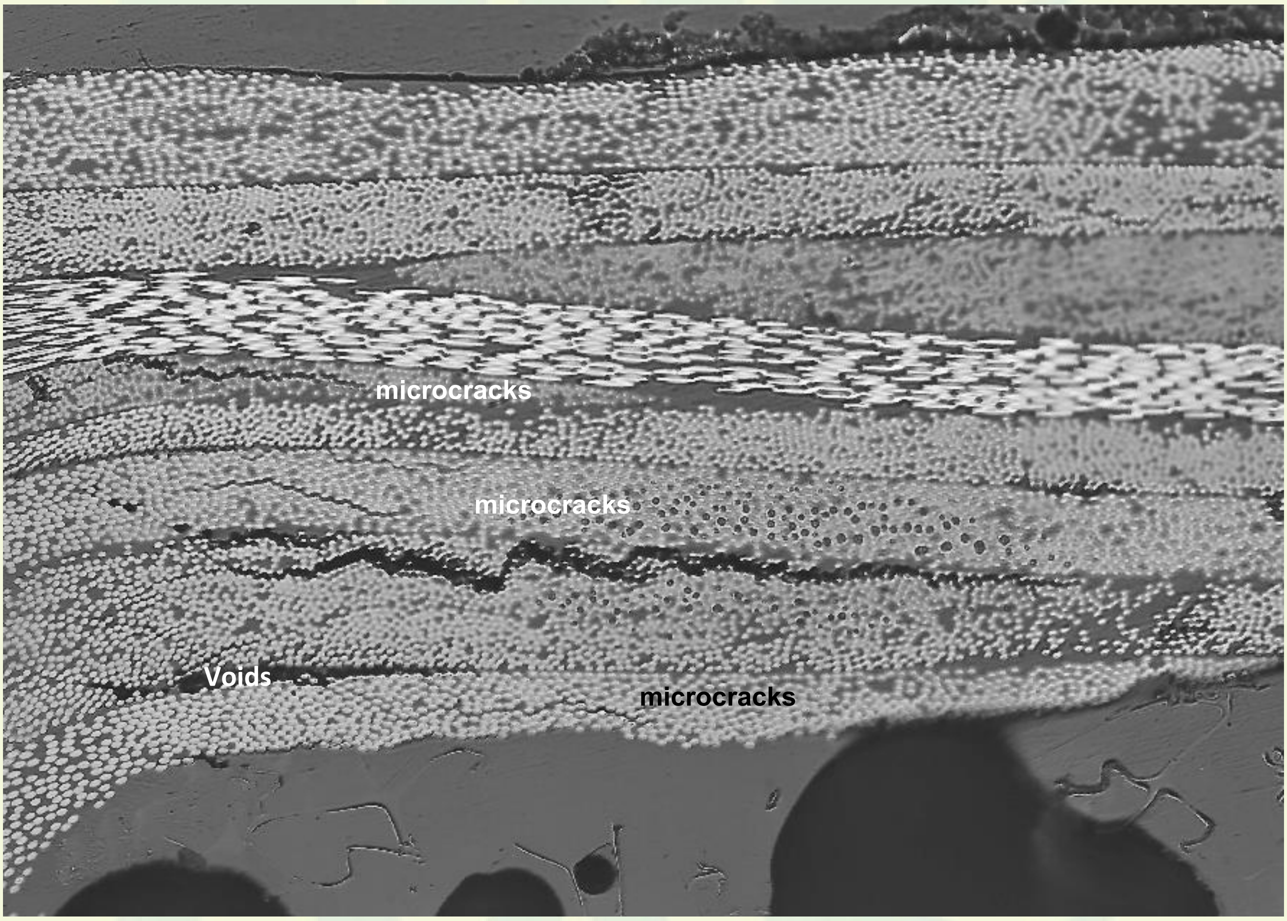

Figure 31. Cross Sectioned Image at Section D – Using Compound Microscope; Magnification: 50x

The surface morphology shown in Figure 28 to 31 present more significant signs of damage than the previous one. They key observations that can be made from these images are as follows:

i. **Voids**:
- **Size and Distribution**: The large dark area marked on the composite layers are voids, indicating porosity or incomplete curing of the resin during the manufacturing process. Voids can severely reduce the mechanical performance of the composite, as they disrupt the load-bearing capacity of the matrix and fibres.
- **Impact on Mechanical Strength**: The presence of these voids creates stress concentrations, meaning that even small loads (e.g. drilling a hole) can cause localized stress peaks around the voids, potentially leading to crack initiation and propagation. This dramatically increases the likelihood of failure under service conditions.

ii. **Microcracks**:
- Similar to the previous images, microcracks are visible near the fibre layers. However, the extent of these cracks appears more severe, particularly in areas adjacent to the voids. This suggests that microcracks have developed as a result of the stress concentrations induced by the voids.

iii. **Fiber-Matrix Separation**:
- The image shows areas where the fibre and matrix appear to be separating. This fibre-matrix debonding could have occurred due to:
  - Poor bonding during the manufacturing process (due to the voids).
  - Cyclic loading causing the cracks to spread, leading to further separation.
  - Environmental factors such as moisture ingress (particularly relevant if hydrolysis or chemical degradation is present).

iv. **Layer Delamination**:
- There is evidence of interlayer delamination, which is a typical failure mode in composite materials. The delamination is likely exacerbated by the presence of voids and microcracks, causing the material to lose cohesion between the composite layers.

SIRIM QAS International Sdn. Bhd.
CHEMICAL, POLYMER AND COMPOSITE SECTION (CPCT)

The combined presence of **voids, extensive microcracks, and fiber-matrix separation** points to significant material degradation. The voids alone could cause a major reduction in mechanical strength, while the presence of microcracks further compromises the material's structural integrity especially after it has been exposed to external load during drilling process to make the man-made hole which has led to formation of severe cracking across the thickness of the composite structure.

The observed damage (voids, microcracks, and debonding) is significant enough to cause failure, especially in high-performance applications like aircraft components. The voids create stress concentrations that amplify the effect of microcracks, eventually leading to larger cracks, delamination, and catastrophic failure.

3.2.2 Results for Constituent Content, Fibre Ratio and Plies Orientation

Results for the constituent content and fibre ratio for the structural frame and skin samples are shown in Table 3.

Table 3. Constituent Content and Fibre Ratio for the Structural Frame for Site 2; Sample ID: BSKU/IPOOC/004(S2) - Right wing – near to the wheel well

Specimen No.	Fibre Content, %	Resin Content, %	Fibre Ratio
1	59	41	3:2
2	61	39	
3	63	37	
Average	**61**	**39**	

The result for resin content value reported in Doc No: BCV-04-64-02; Table 17, Page 29 and Table 23, Page 36 of Compliance Report – Toray 2510 Series Resin Material Equivalency Test Results is about 36% for unidirectional sample and 42% for fabric sample. The resin content values reported in Tables 6 are in between these two values and the calculated fibre:resin ratio is 3:2.

SIRIM QAS International Sdn. Bhd.
CHEMICAL, POLYMER AND COMPOSITE SECTION (CPCT)

It was also observed from the analysis that the CFRP composite material comprises of alternating carbon fibre fabric plies with 90° and 45° orientation. Photograph of the ply orientation is given in Figure 32.

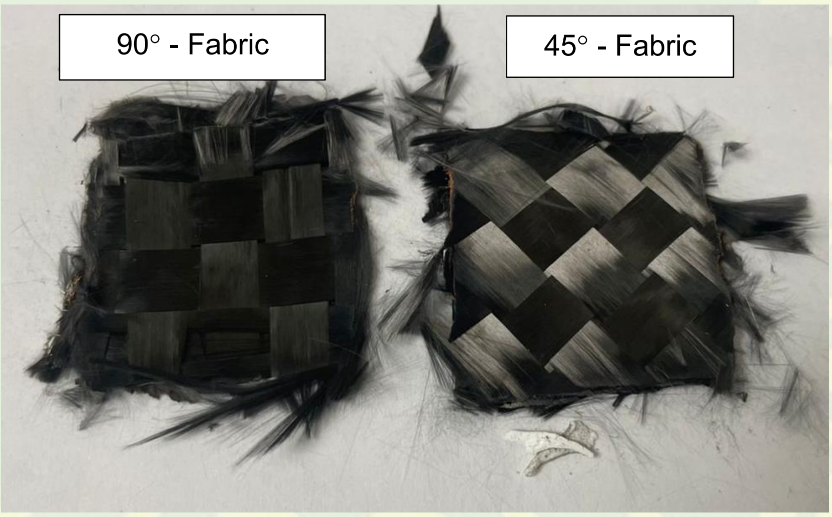

Figure 32. Orientation of Carbon Fibre Fabric

Cross-sectioned view for the ply orientation is given Figure 33, while that for calculation of void content and ply thickness are shown in Figures 34 and 35 respectively.

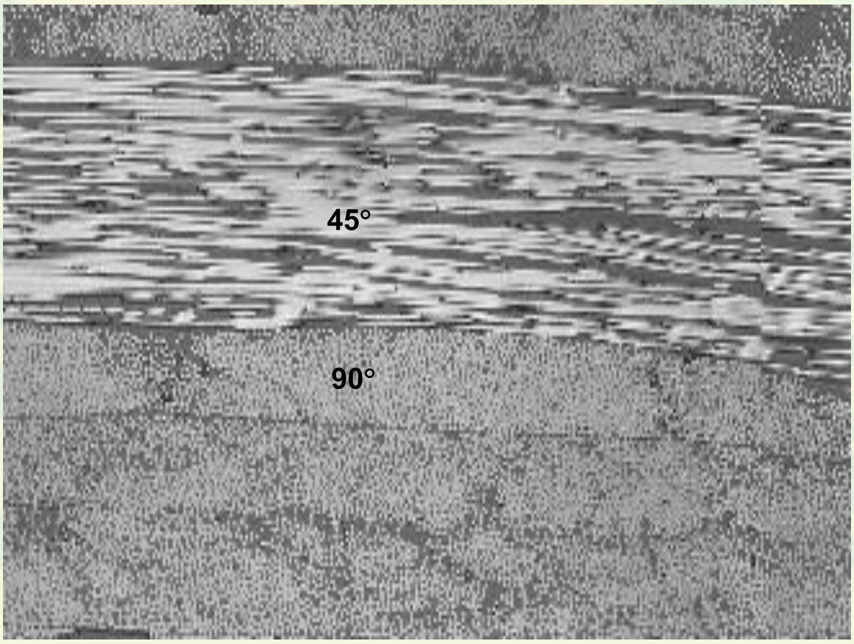

Figure 33. Laminate Cross-Section Indicating the Ply-Wise Variation in Fibre Orientation

SIRIM QAS International Sdn. Bhd.
CHEMICAL, POLYMER AND COMPOSITE SECTION (CPCT)

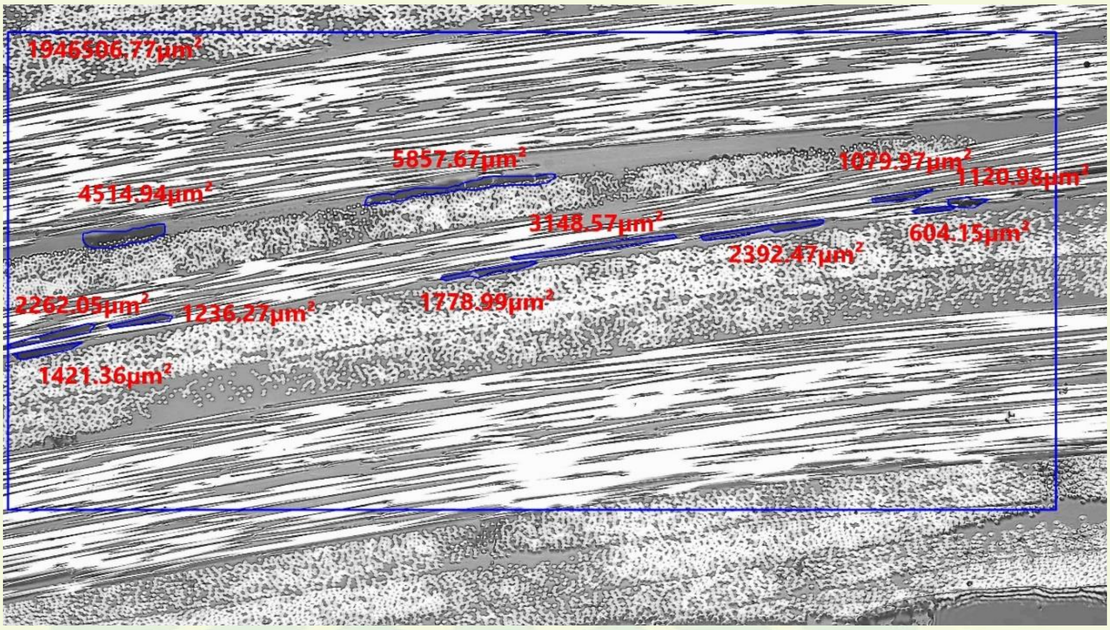

Figure 34. Area Used for the Calculation of Void Content

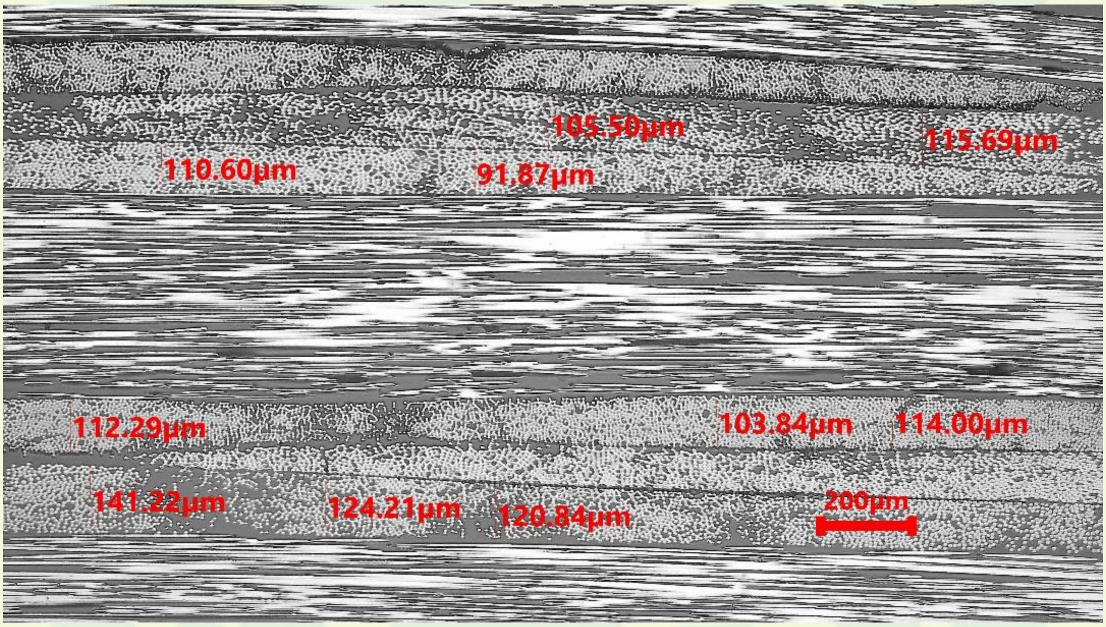

Figure 35. Image for Ply/Laminate Thickness Evaluation

For the area marked in blue rectangle the calculated void content is approximately 1.2% and the ply/laminate thickness for the 90° fibre orientation is approximately 114 μm (0.114 mm)

SIRIM QAS International Sdn. Bhd.
CHEMICAL, POLYMER AND COMPOSITE SECTION (CPCT)

3.3 Mechanical Testing

3.3.1. Results for Tensile Properties Testing

Results from the tensile properties testing conducted on CFRP composite samples cut from Site 1; Sample ID: BSKU/IPOOC/003(S1) - Left wing - near to the wheel well (Sample 1); Site 2; Sample ID: BSKU/IPOOC/004(S2) - Right wing - near to the wheel well (Sample 2), Site 3; Sample ID: BSKU/IPOOC/002(S3) - Right wing (upper skin) - near to the fuselage (Sample 3) and Site 4; Sample ID: BSKU/IPOOC/001(S4) - Left wing (upper skin) - near to the refuelling point (Sample 4) are given in Table 4 and Table 5.

Table 4. Tensile Strength of CFRP Composite Sample

Specimen No.	Tensile Strength (MPa)			
	Sample 1	Sample 2	Sample 3	Sample 4
1	89.8	108	15.4	22.1
2	248	113	14.5	11.2
3	234	123	18.2	11.1
4	121	91.6	16.5	25.9
5	133	120	14.9	20.6
Average	**165**	**111**	**15.9**	**18.2**

Table 5. Tensile Modulus of CFRP Composite Sample

Specimen No.	Tensile Modulus (MPa)			
	Sample 1	Sample 2	Sample 3	Sample 4
1	19,100	8,970	2,540	1,640
2	22,400	9,010	2,520	1,390
3	20,200	10,300	2,040	2,070
4	18,700	10,400	2,550	3,640
5	16,600	12,200	2,570	1,810
Average	**19,400**	**10,200**	**2,440**	**2,110**

SIRIM QAS International Sdn. Bhd. CHEMICAL, POLYMER AND COMPOSITE SECTION (CPCT)

General observations that can be made from the raw data reported in Table 4 and 5 are as follows:

i. Sample 1 exhibits both the highest tensile strength and modulus, making it the most mechanically robust.

ii. Samples 3 and 4 are the weakest in both strength and stiffness, which suggests they might have undergone further stages of degradation process (experienced more hydrolysis process) or have different material compositions or processing issues.

iii. Sample 2 shows moderate properties but with more consistency in the values, especially in the modulus data.

It can also be observed from the tensile properties data that there is a wide range of variability in tensile strength within the aircraft component samples, which could suggest variability in fibre distribution or bonding issue between the fibres and matrix.

An example of failure type due to fibre pullout as a result of tensile load on the tested sample is shown in Figure 36.

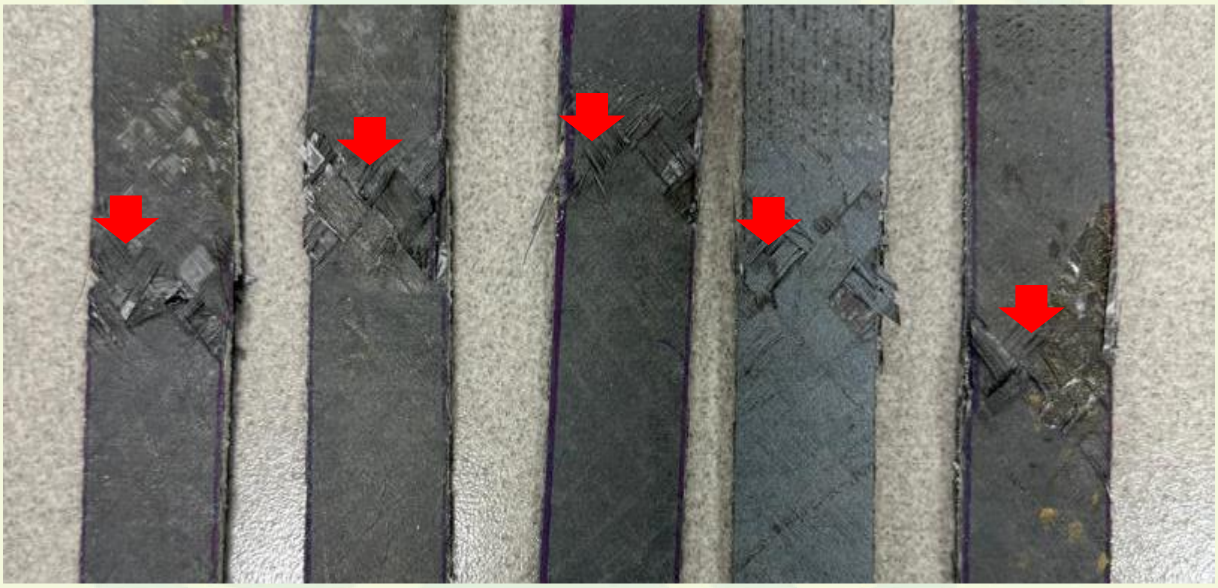

Figure 36. Photograph of Test Specimens after Tensile Properties Testing – Failure Type: Fiber Pullout (Red Arrows) Due to Tensile Loads

SIRIM QAS International Sdn. Bhd.
CHEMICAL, POLYMER AND COMPOSITE SECTION (CPCT)

The mode of failure observed in Figure 36 is similar to that observed on the component found at Site 2; Sample ID: BSKU/IPOOC/004(S2) - Right wing - near to the wheel well. For comparison purposes, photograph taken at ROI 1 indicating fibre pullout on the sample (see Table 2) are shown in Figure 37.

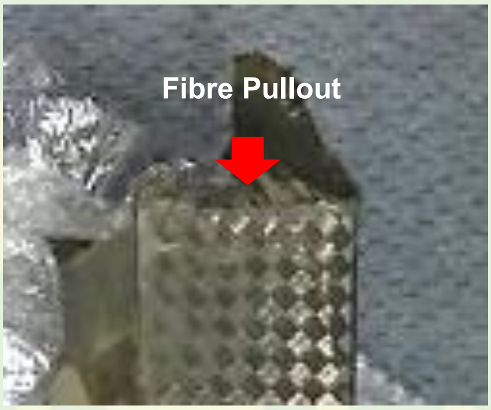

Figure 37. Fibre Pullout Found on ROI 1 of Component at Site 2; Sample ID: BSKU/IPOOC/004(S2) - Right wing - near to the wheel well

3.3.2. Results for Compressive Properties Testing

Results from the compressive properties testing conducted on CFRP composite samples from Site 1; Sample ID: BSKU/IPOOC/003(S1) - Left wing - near to the wheel well (Sample 1); Site 2; Sample ID: BSKU/IPOOC/004(S2) - Right wing - near to the wheel well (Sample 2), Site 3; Sample ID: BSKU/IPOOC/002(S3) - Right wing (upper skin) - near to the fuselage (Sample 3) and Site 4; Sample ID: BSKU/IPOOC/001(S4) - Left wing (upper skin) - near to the refuelling point (Sample 4) are given in Table 6 and Table 7.

Table 6. Compressive Strength of CFRP Composite Sample

Specimen No.	Compressive Strength (MPa)			
	Sample 1	Sample 2	Sample 3	Sample 4
1	18.1	19.0	11.8	17.7
2	10.1	18.2	14.6	20.1
3	10.5	19.1	16.1	13.1
4	31.6	19.7	11.2	14.5
5	17.5	19.6	15.1	13.0
Average	**17.6**	**19.1**	**13.7**	**15.7**

Table 7. Compressive Modulus of CFRP Composite Sample

Specimen No.	Compressive Modulus (MPa)			
	Sample 1	Sample 2	Sample 3	Sample 4
1	211	706	178	197
2	261	390	270	196
3	200	739	320	215
4	315	605	227	193
5	522	470	214	255
Average	**302**	**582**	**242**	**211**

General observations that can be made from the raw data reported in Table 6 and 7 are as follows:

i. Samples 3 and 4 exhibit both lower compressive strength and modulus, which could be indicative of hydrolysis effects. Hydrolysis could weaken the matrix and reduce bonding strength between fibres and the matrix, leading to lower mechanical performance.

ii. The variability in compressive strength and modulus, especially for Samples 1 and 4, suggests possible delamination issues. Delamination can cause localized weakness and reduce the overall stiffness of the composite, which is reflected in the lower modulus values.

iii. Sample 2 shows the highest compressive strength and modulus, with less variation in the data. This suggests that Sample 2 is in the best condition among the four.

These observations suggest that the samples might have suffered from some form of damage, either from hydrolysis or delamination or both, which would explain their reduced compressive properties.

SIRIM QAS International Sdn. Bhd.
CHEMICAL, POLYMER AND COMPOSITE SECTION (CPCT)

Photograph of test specimens after the compressive properties testing is shown in Figure 38.

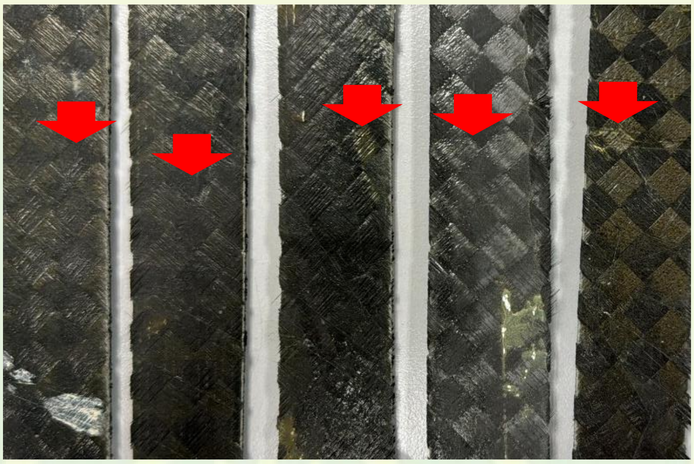

Figure 38. Photograph of Test Specimens after Compressive Properties Testing – Red Arrows Indicating Fibre Deformation

4. Executive Summary

i. The epoxy resin matrix used in the carbon fibre reinforced plastic (CFRP) composite material has most likely undergone significant degradation due to hydrolysis from exposure to a high-humidity environment, leading to increased moisture ingress.

ii. The glass transition temperature of the resin material was found to be higher than the reported value stated in Blackshape DOA No. EASA 215.550 – Compliance Report – Toray 2510 Series Resin Material Equivalency Test Results (Doc No BCV-04-64-02). This is most likely due to post-curing effects, thermal aging, and residual stress reduction.

iii. The tested CFRP composite component contains microcracks and voids that have likely weakened the overall structural integrity of the component. When exposed to extreme flight conditions, these defects can propagate, causing major cracking and delamination, further compromising the composite's mechanical properties.

iv. The man-made holes found on Site 1; Sample ID: BSKU/IPOOC/003(S1) - Left wing - near to the wheel well and Site 2; Sample ID: BSKU/IPOOC/004(S2) - Right wing - near to the wheel well, have induced severe cracking on the surface of the component (in the case of Site 1 sample) and across the thickness of the component, along with layer delamination (in the case of Site 2 sample). This has most likely significantly reduced the matrix's mechanical properties, leaving it unable to resist tensile forces during flight, as evidenced by fibre pullout in the tension mode at failed areas.

SIRIM QAS International Sdn. Bhd.
CHEMICAL, POLYMER AND COMPOSITE SECTION (CPCT)

v. The resin-to-fibre ratio of 3:2 in the composite matrix is consistent with the test results reported in Blackshape DOA No. EASA 215.550 – Compliance Report – Toray 2510 Series Resin Material Equivalency Test Results (Doc No BCV-04-64-02).

vi. The void content in the tested composite component, which is made up of alternating fabric plies with 90° and 45° orientations and about 114 µm (0.114 mm) ply thickness, was found to be about 1.2%. For comparison, the average void content for a single carbon fibre fabric reported in Blackshape DOA No. EASA 215.550 – Compliance Report – Toray 2510 Series Resin Material Equivalency Test Results (Doc No BCV-04-64-02) is around 0.5%.

vii. A wide range of variability in tensile and compressive properties (strength and modulus) was observed within the aircraft component samples of the same design structure. These results suggest that the CFRP composite samples may have suffered from damage, likely caused by hydrolysis, delamination, or both.

5. Conclusion

The comprehensive analysis indicated that the CFRP composite material has likely experienced significant degradation due to hydrolysis, thermal aging, and internal defects such as voids and microcracks. These factors have led to reduced structural integrity and variability in mechanical properties. The observed defects, including cracking and delamination, particularly around the man-made hole, highlighted the root cause of the failure under the operational stresses.

SIRIM QAS International Sdn. Bhd.
CHEMICAL, POLYMER AND COMPOSITE SECTION (CPCT)

CONDITIONS RELATING TO THE USE OF SIRIM QAS INTERNATIONAL TEST REPORT

1. A Test Report will be issued in respect of Testing Services conducted and shall relate only to the sample actually tested. SIRIM QAS International makes no warranty whatsoever and the Applicant shall not represent in any manner that any duplication or mass production of the Product is same as the sample actually tested or that SIRIM QAS International has tested any of the duplicated or mass-produced Product. Measurement uncertainty shall be included in the Test Report when there is no statement of conformity required. When a statement of conformity to a specification or standard is applied, the Simple Acceptance Rule is used. Unless otherwise stated, the Acceptance Rule with Guard Band is used.

2. For quantitative test results (with values), when a statement of conformity to a specification or standard is applied, the Simple Acceptance Rule shall be used. Unless otherwise stated, the Acceptance Rule with Guard Band is used, and additional charge will be incurred accordingly.

3. For qualitative test results (visual observation), when requested by applicant, a statement of conformity in the Test Report shall be reported. Should there is no request by applicant, a statement of conformity in the Test Report can be reported based on our discretion.

4. The Test Report shall not be misused, amended, changed, varied or modified in any manner whatsoever by the Applicant or otherwise.

5. If the Test Report is to be furnished to any third party or to the public, each such Test Report shall be furnished in full, legible and in its entirety.

6. The Test Report shall not be reproduced and shall not in any event be used for any advertising purposes or whatsoever without written approval from the Head of Quality, Occupational Safety and Health & Environment (QOSHE) of SIRIM QAS International of No 1, Persiaran Dato' Menteri, Building 8, Section 2, P.O. Box 7035, 40700 Shah Alam, Selangor Darul Ehsan.

7. Customer (Applicant/Manufacture/Factory,etc.) is not permitted to use any SIRIM QAS International, SIRIM or other SIRIM's subsidiaries logo or words on packaging, sample's manual, technical specification, items and products.

8. Subject to consent and written approval from the Head of Quality, Occupational Safety and Health & Environment (QOSHE) of SIRIM QAS International, the customer (Applicant/Manufacture/Factory,etc.) may use SIRIM QAS International logo or word on the promotional materials and the Applicant shall only include the phrase, "A sample of this product has been tested by SIRIM QAS International ...(Test Report No) ...(dated) ...(for what test) ...(to which standard)" or such similar words which stress that only the sample was actually tested. This phrase shall only be used for the purpose of product advertisement or product promotion (eg; brochures/flyers/official website). For avoidance of doubt, the statement shall not be used on the sample, packaging of the sample, items and products.

9. In the event there is an investigation from a Government Regulatory Agency concerning the Applicant's Test Report, SIRIM QAS International may disclose the information pertaining to the Test Report for purposes of such investigation.

10. In the event the Applicant is found in breach of this provision, SIRIM QAS International, SIRIM and/or other SIRIM's subsidiaries without prejudice to any other rights and remedies may take whatever action necessary including but not limited to:
    a) Informing and placing a notice in the media;
    b) Obtaining an injunction from Court (cost on a solicitor-client basis to be borne by the Applicant);
    c) Refusing to accept any further Product for Testing Services from the Applicant or whosoever related to the Applicant, whether subsidiary or otherwise;
    d) Instructing the Applicant to withdraw and recall the advertisement, statement or document in question and advertise a clarification and apology to SIRIM QAS International, SIRIM and/or other SIRIM's subsidiaries twice in a national publication of SIRIM QAS International's choice at the Applicant's sole cost; and
    e) Informing or lodging a report pertaining the Applicant's Test Report with the relevant authorities.

11. SIRIM QAS International is committed in supporting an environmentally-friendly business practices by reducing paper consumption, therefore we do not issue any hard copy of Test Report to the Applicant. However, additional certified true copy(ies) or softcopy of the Test Report may be issued upon request by the Applicant upon payment of the relevant fee. The certified true copy(ies) or softcopy of test report shall only be given for test report issued not more than three (3) years from the date of issuance.

12. Issuance of Amendment Report due to the following reasons are chargeable to the Applicant :
    a) Changes in details of the Applicant name and/or address;
    b) Changes in details of the Manufacturer's name and/or address;
    c) Changes in details of the Factory location name and/or address;
    d) Changes in details of the model and/or type designation

13. However, issuance of Supplementary Report due to the following reasons are FOC :
    a) Misprints and typo errors;
    b) Missing technical information as agreed in PP1 form;
    c) Test data not reported;
    d) Mistake in reporting of test data

14. Corrections to report shall only be allowed if the date of issuance of the original report has not exceeded 6 months and shall be limited to a maximum 3 times, after either case whichever occurs earlier, an Amendment or a Supplementary Report shall not be issued.

Appendix I

Aircraft Operations Outside Approved Flight Envelope

1. Exceeding Airspeed Limitations

Airspeed Exceeding V_{NE} (180 KIAS)										
S/N	**Date**	**Start Time (UTC)**	**End Time (UTC)**	**Duration (seconds)**	**Max Airspeed (KIAS)**	**Max Pitch (deg)**	**Max Roll (deg)**	**Max Load Factor (g)**	**Probable Ac Weight (kg)**	**Remarks**
1	10/12/2023	04:41:56	04:41:59	1.8	180.2	-4.7	2.0	1.68	887.6	Flt No 47 enroute ZZZZ to VTPP
2	10/12/2023	10:02:53	10:03:08	13.9	186.1	-12.8	-15.0	1.76	862.0	Flt No 49 enroute VTPH to VTSW
Total Duration (seconds)				**15.7**						

Table 1. Airspeed Exceeding V_{NE}

Airspeed Exceeding V_{NO} (155 KIAS)										
S/N	**Date**	**Start Time (UTC)**	**End Time (UTC)**	**Duration (seconds)**	**Max Airspeed (KIAS)**	**Max Pitch (deg)**	**Max Roll (deg)**	**Max Load Factor (g)**	**Probable Ac Weight (kg)**	**Remarks**
1	8/12/2023	04:45:39	04:45:45	6.7	155.2	-2.8	-1.7	1.02	869.4	Flt No 43 enroute VTBD to ZZZZ
2	8/12/2023	04:46:07	04:48:26	136.9	171.5	-4.9	-3.0	1.13	868.2	Flt No 43 enroute VTBD to ZZZZ
3	8/12/2023	04:58:37	05:02:04	206.2	174.2	6.8	13.3	1.95	862.6	Flt No 43 enroute VTBD to ZZZZ
4	8/12/2023	05:02:16	05:04:54	157.6	174.0	-8.3	-32.2	1.63	861.4	Flt No 43 enroute VTBD to ZZZZ
5	8/12/2023	05:05:02	05:05:22	20.2	159.8	-4.1	-3.2	1.12	861.2	Flt No 43 enroute VTBD to ZZZZ
6	8/12/2023	05:05:25	05:06:42	76.1	163.6	9.5	14.0	1.34	860.6	Flt No 43 enroute VTBD to ZZZZ
7	8/12/2023	05:08:57	05:09:00	3.3	155.5	0.7	-22.1	1.20	859.7	Flt No 43 enroute VTBD to ZZZZ
8	8/12/2023	05:11:00	05:11:29	28.2	172.8	25.3	-42.1	3.81	858.6	Flt No 43 enroute VTBD to ZZZZ
9	8/12/2023	10:09:48	10:10:20	31.5	168.3	37.1	40.1	3.17	und	Flt No 44 local ZZZZ
10	8/12/2023	10:11:12	10:11:28	13.9	161.5	27.2	-50.0	3.88	und	Flt No 44 local ZZZZ

S/N	Date	Start Time (UTC)	End Time (UTC)	Duration (seconds)	Max Airspeed (KIAS)	Max Pitch (deg)	Max Roll (deg)	Max Load Factor (g)	Probable Ac Weight (kg)	Remarks
11	8/12/2023	10:14:18	10:14:21	1.8	156.8	30.0	2.3	3.67	und	Flt No 44 local ZZZZ
12	9/12/2023	10:13:30	10:13:43	14.9	159.2	-5.3	22.8	1.54	und	Flt No 45 local ZZZZ
13	10/12/2023	04:23:29	04:26:45	197.9	163.5	-3.5	7.3	1.10	894.4	Flt No 47 enroute ZZZZ to VTPP
14	10/12/2023	04:38:57	04:40:46	109.9	170.1	-5.4	-15.3	1.43	888.2	Flt No 47 enroute ZZZZ to VTPP
15	10/12/2023	04:41:15	04:42:09	53.8	180.2	-7.2	15.8	1.68	887.6	Flt No 47 enroute ZZZZ to VTPP
16	10/12/2023	07:10:13	07:10:31	19.8	157.0	-4.6	-3.3	1.00	872.0	Flt No 48 enroute VTPP to VTPH
17	10/12/2023	07:11:01	07:11:55	51.9	158.4	-3.5	-4.7	1.04	871.4	Flt No 48 enroute VTPP to VTPH
18	10/12/2023	07:12:26	07:13:24	58.3	164.1	-4.4	-2.1	1.05	870.8	Flt No 48 enroute VTPP to VTPH
19	10/12/2023	07:13:43	07:18:06	260.8	179.9	-6.9	-17.3	1.52	868.9	Flt No 48 enroute VTPP to VTPH
20	10/12/2023	07:18:51	07:19:22	30.4	156.8	-5.8	-28.6	1.32	868.4	Flt No 48 enroute VTPP to VTPH
21	10/12/2023	09:56:52	09:57:05	11.0	158.3	-5.5	3.0	1.29	864.9	Flt No 49 enroute VTPH to VTSW
22	10/12/2023	09:58:36	09:58:52	15.3	162.1	-7.4	-2.7	1.10	864.2	Flt No 49 enroute VTPH to VTSW
23	10/12/2023	09:59:02	10:00:12	70.8	172.7	-8.3	37.6	1.29	863.6	Flt No 49 enroute VTPH to VTSW
24	10/12/2023	10:00:50	10:01:53	63.9	167.6	-14.2	57.6	1.93	862.9	Flt No 49 enroute VTPH to VTSW
25	10/12/2023	10:02:33	10:03:13	39.2	186.1	-13.3	-59.1	1.79	862.4	Flt No 49 enroute VTPH to VTSW
26	10/12/2023	10:25:12	10:25:22	8.9	158.2	21.1	-3.7	2.74	853.0	Flt No 49 enroute VTPH to VTSW
27	10/12/2023	10:27:16	10:27:24	8.2	164.3	9.6	-68.5	3.21	852.2	Flt No 49 enroute VTPH to VTSW
28	11/12/2023	07:00:14	07:00:19	4.1	161.3	22.8	-3.9	2.24	und	Flt No 50 local VTSW
29	11/12/2023	07:09:23	07:09:24	2.3	156.5	27.2	18.1	4.01	und	Flt No 50 local VTSW
30	11/12/2023	11:01:13	11:01:23	10.0	160.7	30.8	25.1	4.26	und	Flt No 50 local VTSW
31	11/12/2023	11:02:09	11:02:15	6.3	157.8	-11.0	46.6	2.49	und	Flt No 50 local VTSW
32	13/12/2023	00:35:49	00:35:53	4.0	158.8	31.7	12.6	4.59	913.5	Flt No 52 enroute VTSW to VTSS
33	13/12/2023	01:29:05	01:29:18	12.1	156.2	-3.9	-10.1	1.06	890.2	Flt No 52 enroute VTSW to VTSS
34	13/12/2023	01:29:43	01:30:31	45.7	173.9	-8.5	3.4	1.11	889.7	Flt No 52 enroute VTSW to VTSS
35	13/12/2023	01:31:16	01:32:34	79.7	167.1	-4.7	-10.3	1.23	888.8	Flt No 52 enroute VTSW to VTSS
36	13/12/2023	01:36:27	01:38:49	141.8	172.6	-7.3	-25.7	1.20	886.1	Flt No 52 enroute VTSW to VTSS
37	13/12/2023	01:39:16	01:39:45	25.4	157.4	-2.9	19.5	1.00	885.7	Flt No 52 enroute VTSW to VTSS
38	13/12/2023	01:40:31	01:41:27	55.7	162.3	-4.8	-20.7	1.48	884.9	Flt No 52 enroute VTSW to VTSS
39	13/12/2023	04:23:42	04:24:04	22.9	163.4	-5.6	-2.5	1.06	870.4	Flt No 53 enroute VTSS to WMSA

S/N	Date	Start Time (UTC)	End Time (UTC)	Duration (seconds)	Max Airspeed (KIAS)	Max Pitch (deg)	Max Roll (deg)	Max Load Factor (g)	Probable Ac Weight (kg)	Remarks
40	13/12/2023	04:24:16	04:30:43	385.6	179.3	-10.1	42.4	1.70	867.6	Flt No 53 enroute VTSS to WMSA
41	24/12/2023	02:32:41	02:32:49	9.6	160.1	-11.8	-15.3	1.28	und	Flt No 54 local WMSA
Total Duration (seconds)				2501.6						

Table 2. Airspeed Exceeding V_{NO}

Notes:

1. Probable aircraft weights are determined by subtracting the weight of fuel used (calculated from the average fuel flow data recorded by the Garmin G3X) from the probable take-off weights (TOW).
2. Duration (seconds) of occurrences is determined using the Power Timestamp (in milliseconds) data recorded by the Garmin G3X. (Recorded UTC times are not used to determine duration due to inconsistencies in time synchronisation caused by data buffering.)
3. Pitch direction: +ve values – pitch up; -ve values – pitch down.
4. Roll direction: +ve values – right roll; -ve values – left roll.
5. und – Undetermined.
6. ZZZZ – Chiang Mai Air Sports airfield.
7. VTSW – Phuket Airpark
8. Shaded rows: Occurrences of serious concern, where either V_{NE} (180 KIAS) was exceeded or V_{NO} (155 KIAS) was exceeded in combination with high angles of bank (>30°), high load factors (>2.9g), or both, including one instance of extended duration over 385 seconds with airspeed reaching 179.3 KIAS—near the V_{NE} of 180 KIAS—and a roll angle of 42.4°. (15 occurrences)

2. Exceeding Load Factor Limitations

Load Factor Exceeding +4.4 g / -2.0 g (Symmetric Flight) (Flap UP, Landing Gear UP)									
S/N	Date	Start Time (UTC)	End Time (UTC)	Duration (seconds)	Max/(Min) Load Factor (g)	Max Pitch (deg)	Max Roll (deg)	Probable Ac Weight (kg)	Remarks
1	13/12/2023	00:35:52	00:35:52	0.3	4.59	23.7	-3.0	913.5	Flt No 52 enroute VTSW to VTSS
			Total Duration (seconds)	0.3					

Table 3. Load Factor Exceeding +4.4 g / -2.0 g (Symmetric Flight)

Load Factor Exceeding 2.9 g / -0.0 g (Asymmetric / Rolling) (Flap UP, Landing Gear UP)									
S/N	Date	Start Time (UTC)	End Time (UTC)	Duration (seconds)	Max Load Factor (g)	Max Pitch (deg)	Max Roll (deg)	Probable Ac Weight (kg)	Remarks
1	8/12/2023	04:56:04	04:56:04	0.3	3.06	7.3	1.9	865.0	Flt No 43 enroute VTBD to ZZZZ
2	8/12/2023	04:56:09	04:56:10	0.8	3.19	-22.8	-20.3	865.0	Flt No 43 enroute VTBD to ZZZZ
3	8/12/2023	05:11:26	05:11:26	0.4	3.81	6.0	-0.1	858.6	Flt No 43 enroute VTBD to ZZZZ
4	8/12/2023	05:11:27	05:11:28	0.6	3.40	17.2	32.8	858.6	Flt No 43 enroute VTBD to ZZZZ
5	8/12/2023	05:11:29	05:11:33	3.7	3.42	20.2	86.2	858.6	Flt No 43 enroute VTBD to ZZZZ
6	8/12/2023	05:11:51	05:11:52	0.4	3.10	-12.9	73.6	858.5	Flt No 43 enroute VTBD to ZZZZ
7	8/12/2023	05:12:07	05:12:07	0.8	3.34	18.3	33.2	858.4	Flt No 43 enroute VTBD to ZZZZ
8	8/12/2023	10:10:18	10:10:18	0.6	3.17	6.0	0.1	und	Flt No 44 local ZZZZ
9	8/12/2023	10:10:19	10:10:20	0.7	3.17	23.4	1.8	und	Flt No 44 local ZZZZ
10	8/12/2023	10:11:26	10:11:27	0.9	3.88	9.1	14.7	und	Flt No 44 local ZZZZ
11	8/12/2023	10:12:06	10:12:06	0.7	2.95	5.1	-52.4	und	Flt No 44 local ZZZZ
12	8/12/2023	10:12:23	10:12:24	0.6	2.92	9.5	-7.5	und	Flt No 44 local ZZZZ
13	8/12/2023	10:12:38	10:12:39	1.6	2.94	-23.7	-62.7	und	Flt No 44 local ZZZZ
14	8/12/2023	10:14:20	10:14:21	1.7	3.67	3.7	2.3	und	Flt No 44 local ZZZZ
15	9/12/2023	10:09:11	10:09:13	2.0	4.30	-10.7	0.0	und	Flt No 45 local ZZZZ
16	9/12/2023	10:09:19	10:09:19	0.5	3.04	-5.1	7.5	und	Flt No 45 local ZZZZ

S/N	Date	Start Time (UTC)	End Time (UTC)	Duration (seconds)	Max Load Factor (g)	Max Pitch (deg)	Max Roll (deg)	Probable Ac Weight (kg)	Remarks
17	9/12/2023	10:09:44	10:09:45	1.3	3.46	9.2	-19.5	und	Flt No 45 local ZZZZ
18	9/12/2023	10:12:22	10:12:22	0.3	3.07	5.4	-0.6	und	Flt No 45 local ZZZZ
19	9/12/2023	10:12:49	10:12:50	0.7	3.45	-1.5	0.5	und	Flt No 45 local ZZZZ
20	9/12/2023	10:31:52	10:31:52	0.7	3.70	10.6	-27.2	und	Flt No 45 local ZZZZ
21	9/12/2023	10:31:53	10:31:54	0.7	3.04	25.4	-63.6	und	Flt No 45 local ZZZZ
22	9/12/2023	10:32:24	10:32:25	1.6	3.57	0.1	62.2	und	Flt No 45 local ZZZZ
23	10/12/2023	03:27:32	03:27:33	0.9	3.44	-4.7	-5.4	und	Flt No 46 local ZZZZ
24	10/12/2023	10:27:21	10:27:21	0.4	3.21	0.5	-19.9	852.2	Flt No 49 enroute VTPH to VTSW
25	10/12/2023	10:27:23	10:27:24	1.4	2.98	6.4	-68.5	852.1	Flt No 49 enroute VTPH to VTSW
26	11/12/2023	07:08:12	07:08:12	0.3	3.16	8.7	3.7	und	Flt No 50 local VTSW
27	11/12/2023	07:09:15	07:09:16	0.3	3.11	-8.1	54.0	und	Flt No 50 local VTSW
28	11/12/2023	07:09:24	07:09:25	1.3	4.01	6.5	1.9	und	Flt No 50 local VTSW
29	11/12/2023	11:01:21	11:01:23	1.2	4.26	5.5	3.6	und	Flt No 51 local VTSW
30	11/12/2023	11:02:16	11:02:16	0.4	3.11	10.4	-7.4	und	Flt No 51 local VTSW
31	13/12/2023	00:35:52	00:35:53	0.3	4.59	5.4	-3.0	913.5	Flt No 52 enroute VTSW to VTSS
32	24/12/2023	02:22:05	02:22:07	0.6	4.20	15.6	0.1	und	Flt No 54 local WMSA
			Total Duration (seconds)	**27.8**					

Table 4. Load Factor Exceeding +2.9 g (Asymmetric / Rolling)

Note:

1. Shaded rows: Occurrences of serious concern, where either the load factor (n) exceeded the limit of +4.4g/-2.0g (symmetrical flight), or n exceeded the limit of 2.9 g (asymmetrical/rolling) with the aircraft roll exceeding 30-degree angle of bank. (11 occurrences)

3. 360-Degree Rolls

360-Degree Rolls									
S/N	Date	Start of Roll Time (UTC)	End of Roll Time (UTC)	Duration (seconds)	Roll Direction	Max Airspeed (KIAS)	Max/(Min) Load Factor (g)	Probable Ac Weight (kg)	Remarks
1	8/12/2023	04:55:36	04:55:44	7.6	Left (-)	136.7	2.74	865.2	Flt No 43 enroute VTBD to ZZZZ
2	8/12/2023	04:56:03	04:56:10	6.8	Right (+)	154.4	3.19	865.0	Flt No 43 enroute VTBD to ZZZZ
3	9/12/2023	10:09:12	10:09:19	6.4	Left (-)	135.5	3.27	und	Flt No 45 local ZZZZ
4	9/12/2023	10:09:46	10:09:55	8.5	Right (+)	122.7	-0.12	und	Flt No 45 local ZZZZ
5	9/12/2023	10:12:21	10:12:29	7.9	Left (-)	133.7	3.07	und	Flt No 45 local ZZZZ
6	9/12/2023	10:12:51	10:12:56	5.5	Left (-)	134.3	2.89	und	Flt No 45 local ZZZZ
7	10/12/2023	03:27:34	03:27:42	7.3	Left (-)	131.9	2.29	und	Flt No 46 local ZZZZ
8	10/12/2023	03:28:13	03:28:21	7.8	Right (+)	139.4	2.33	und	Flt No 46 local ZZZZ
9	11/12/2023	07:01:48	07:01:56	8.5	Left (-)	138.7	2.17	und	Flt No 50 local VTSW
10	24/12/2023	02:32:03	02:32:11	8.1	Left (-)	148.7	1.79	und	Flt No 54 local WMSA
Total Duration (seconds)				**74.1**					

Table 5. 360-Degree Rolls

Note:

1. For the non-aerobatic BK 160TR aircraft, 360-degree roll is prohibited because it can subject the aircraft to high stresses, especially if not performed correctly, as indicated by the 360-degree roll occurrences marked in the shaded rows in the Table 5 that also exceeded load factor (+2.9/-0.0g) asymmetric/rolling limitation. (4 occurrences)

4. Rolls Exceeding 60-Degree Angles of Bank (Steep Turns)

Roll Exceeding 60 Degrees									
S/N	Date	Start Time (UTC)	End Time (UTC)	Duration (seconds)	Max Roll (deg)	Max Airspeed (KIAS)	Max Load Factor (g)	Probable Ac Weight (kg)	Remarks
1	8/12/2023	04:55:38	04:55:41	3.4	(360 Roll)	130.7	1.45	865.2	Flt No 43 enroute VTBD to ZZZZ
2	8/12/2023	04:56:05	04:56:08	3.3	(360 Roll)	144.7	2.39	865.0	Flt No 43 enroute VTBD to ZZZZ
3	8/12/2023	05:11:28	05:11:33	4.7	93.0	159.5	3.42	858.6	Flt No 43 enroute VTBD to ZZZZ
4	8/12/2023	05:11:46	05:11:53	6.8	80.8	131.2	3.10	858.5	Flt No 43 enroute VTBD to ZZZZ
5	8/12/2023	05:12:08	05:12:10	1.7	66.9	128.4	2.81	858.3	Flt No 43 enroute VTBD to ZZZZ
6	8/12/2023	10:08:49	10:08:57	8.4	-74.1	121.6	2.78	und	Flt No 44 local ZZZZ
7	8/12/2023	10:09:02	10:09:03	1.5	-62.2	95.7	1.98	und	Flt No 44 local ZZZZ
8	8/12/2023	10:09:34	10:09:40	6.1	63.9	142.1	2.34	und	Flt No 44 local ZZZZ
9	8/12/2023	10:10:29	10:10:33	4.4	67.7	97.7	1.57	und	Flt No 44 local ZZZZ
10	8/12/2023	10:10:45	10:10:49	4.6	-79.2	120.4	2.10	und	Flt No 44 local ZZZZ
11	8/12/2023	10:12:06	10:12:09	2.8	-65.9	143.4	2.36	und	Flt No 44 local ZZZZ
12	8/12/2023	10:12:13	10:12:20	6.1	-70.9	133.0	2.37	und	Flt No 44 local ZZZZ
13	8/12/2023	10:12:34	10:12:38	3.6	-71.2	130.6	2.94	und	Flt No 44 local ZZZZ
14	8/12/2023	10:12:50	10:12:51	1.5	-60.7	140.7	2.70	und	Flt No 44 local ZZZZ
15	8/12/2023	10:12:52	10:13:06	14.2	-69.7	138.5	2.69	und	Flt No 44 local ZZZZ
16	8/12/2023	10:13:30	10:13:32	1.4	-61.8	93.9	1.14	und	Flt No 44 local ZZZZ
17	8/12/2023	10:14:05	10:14:11	5.2	-76.2	143.0	2.11	und	Flt No 44 local ZZZZ
18	8/12/2023	10:14:24	10:14:28	5.8	76.7	130.3	1.35	und	Flt No 44 local ZZZZ
19	8/12/2023	10:14:47	10:14:53	7.0	70.8	105.4	2.17	und	Flt No 44 local ZZZZ
20	9/12/2023	10:07:01	10:07:05	4.1	-68.1	113.3	2.15	und	Flt No 45 local ZZZZ
21	9/12/2023	10:07:43	10:07:44	1.1	62.3	102.4	1.71	und	Flt No 45 local ZZZZ
22	9/12/2023	10:07:52	10:07:53	1.5	62.9	101.3	1.68	und	Flt No 45 local ZZZZ
23	9/12/2023	10:07:56	10:07:59	3.3	61.9	107.6	1.93	und	Flt No 45 local ZZZZ
24	9/12/2023	10:08:08	10:08:11	4.2	62.5	110.6	1.67	und	Flt No 45 local ZZZZ
25	9/12/2023	10:09:14	10:09:18	3.8	(360 Roll)	120.3	1.19	und	Flt No 45 local ZZZZ

S/N	Date	Start Time (UTC)	End Time (UTC)	Duration (seconds)	Max Roll (deg)	Max Airspeed (KIAS)	Max Load Factor (g)	Probable Ac Weight (kg)	Remarks
26	9/12/2023	10:09:24	10:09:28	4.1	-75.0	112.0	2.04	und	Flt No 45 local ZZZZ
27	9/12/2023	10:09:47	10:09:52	5.0	(360 Roll)	104.0	0.43	und	Flt No 45 local ZZZZ
28	9/12/2023	10:10:05	10:10:13	8.4	62.3	137.2	1.82	und	Flt No 45 local ZZZZ
29	9/12/2023	10:12:25	10:12:28	3.7	(360 Roll)	126.0	1.52	und	Flt No 45 local ZZZZ
30	9/12/2023	10:12:52	10:12:55	3.5	(360 Roll)	125.2	1.89	und	Flt No 45 local ZZZZ
31	9/12/2023	10:13:09	10:13:15	6.2	-85.2	134.0	2.62	und	Flt No 45 local ZZZZ
32	9/12/2023	10:31:52	10:31:56	3.9	-96.8	132.6	3.04	und	Flt No 45 local ZZZZ
33	9/12/2023	10:32:04	10:32:11	6.4	68.6	105.6	2.06	und	Flt No 45 local ZZZZ
34	9/12/2023	10:32:24	10:32:24	0.7	62.2	131.6	3.31	und	Flt No 45 local ZZZZ
35	10/12/2023	03:26:15	03:26:19	3.5	-75.2	119.7	2.74	und	Flt No 46 local ZZZZ
36	10/12/2023	03:26:43	03:26:47	3.6	74.6	118.2	2.29	und	Flt No 46 local ZZZZ
37	10/12/2023	03:26:49	03:26:56	6.9	75.8	117.2	2.52	und	Flt No 46 local ZZZZ
38	10/12/2023	03:27:35	03:27:40	4.0	(360 Roll)	122.6	2.03	und	Flt No 46 local ZZZZ
39	10/12/2023	03:28:16	03:28:19	3.9	(360 Roll)	120.2	0.85	und	Flt No 46 local ZZZZ
40	10/12/2023	09:11:19	09:11:19	0.6	-64.0	130.0	1.22	und	Flt No 46 local ZZZZ
41	10/12/2023	10:00:45	10:00:49	3.9	61.4	152.8	1.68	und	Flt No 46 local ZZZZ
42	10/12/2023	10:03:49	10:03:52	4.3	64.7	138.4	1.86	und	Flt No 46 local ZZZZ
43	10/12/2023	10:03:54	10:03:54	0.6	60.3	126.6	1.85	und	Flt No 46 local ZZZZ
44	10/12/2023	10:25:44	10:25:46	1.8	-61.9	122.3	1.73	und	Flt No 46 local ZZZZ
45	10/12/2023	10:26:00	10:26:09	8.7	-67.9	138.2	2.38	und	Flt No 46 local ZZZZ
46	10/12/2023	10:26:55	10:26:59	3.7	-67.7	140.4	2.85	und	Flt No 46 local ZZZZ
47	10/12/2023	10:27:11	10:27:11	0.6	-60.1	146.7	1.80	und	Flt No 46 local ZZZZ
48	10/12/2023	10:27:22	10:27:24	2.3	-68.5	163.2	2.98	und	Flt No 46 local ZZZZ
49	11/12/2023	06:57:40	06:57:45	4.8	-63.1	133.2	2.15	und	Flt No 50 local VTSW
50	11/12/2023	06:57:48	06:57:55	7.4	-64.5	135.2	2.15	und	Flt No 50 local VTSW
51	11/12/2023	07:00:21	07:00:27	5.9	-85.9	129.6	1.15	und	Flt No 50 local VTSW
52	11/12/2023	07:00:49	07:00:56	7.2	69.3	130.6	1.62	und	Flt No 50 local VTSW
53	11/12/2023	07:01:50	07:01:54	4.0	(360 Roll)	123.3	1.38	und	Flt No 50 local VTSW
54	11/12/2023	07:02:06	07:02:10	3.6	-67.4	135.9	1.36	und	Flt No 50 local VTSW

S/N	Date	Start Time (UTC)	End Time (UTC)	Duration (seconds)	Max Roll (deg)	Max Airspeed (KIAS)	Max Load Factor (g)	Probable Ac Weight (kg)	Remarks
55	11/12/2023	07:05:02	07:05:03	0.9	63.7	122.6	1.07	und	Flt No 50 local VTSW
56	11/12/2023	07:08:14	07:08:16	1.1	70.4	137.7	2.41	und	Flt No 50 local VTSW
57	11/12/2023	07:08:18	07:08:20	2.6	68.5	118.1	1.47	und	Flt No 50 local VTSW
58	11/12/2023	07:08:42	07:08:44	2.1	60.9	134.8	2.29	und	Flt No 50 local VTSW
59	11/12/2023	07:08:45	07:08:45	0.5	60.5	134.8	2.31	und	Flt No 50 local VTSW
60	11/12/2023	07:08:47	07:08:50	4.2	67.3	132.7	2.04	und	Flt No 50 local VTSW
61	11/12/2023	07:09:05	07:09:12	6.8	79.5	125.1	2.25	und	Flt No 50 local VTSW
62	11/12/2023	07:09:17	07:09:18	1.4	62.3	145.9	2.25	und	Flt No 50 local VTSW
63	11/12/2023	07:09:26	07:09:32	5.6	81.5	140.9	2.05	und	Flt No 50 local VTSW
64	11/12/2023	10:51:30	10:51:35	5.8	63.7	134.7	1.97	und	Flt No 51 local VTSW
65	11/12/2023	11:01:25	11:01:30	4.8	71.1	136.6	1.81	und	Flt No 51 local VTSW
66	11/12/2023	11:01:32	11:01:33	1.1	61.1	116.1	1.55	und	Flt No 51 local VTSW
67	11/12/2023	11:02:05	11:02:06	0.6	61.0	154.8	2.19	und	Flt No 51 local VTSW
68	11/12/2023	11:02:19	11:02:24	5.5	-67.7	134.2	1.41	und	Flt No 51 local VTSW
69	11/12/2023	11:02:45	11:02:49	4.7	-66.5	139.9	2.50	und	Flt No 51 local VTSW
70	11/12/2023	11:02:49	11:02:57	8.4	-66.5	139.9	2.50	und	Flt No 51 local VTSW
71	13/12/2023	00:35:57	00:35:58	1.3	63.3	112.3	0.59	913.4	Flt No 52 enroute VTSW to VTSS
72	13/12/2023	00:35:59	00:36:00	1.5	61.9	97.5	0.59	913.4	Flt No 52 enroute VTSW to VTSS
73	13/12/2023	00:36:05	00:36:07	2.8	62.3	120.4	2.00	913.4	Flt No 52 enroute VTSW to VTSS
74	24/12/2023	02:32:04	02:32:09	4.6	(360 Roll)	131.6	1.53	und	Flt No 54 local WMSA
75	24/12/2023	02:32:28	02:32:31	1.8	-62.5	110.9	1.01	und	Flt No 54 local WMSA
Total Duration (seconds)				299.5					

Table 6. Rolls Exceeding 60-Degree Angles of Bank

Note:

1. Shaded rows: Rolls exceeding 60° combined with maximum load factor exceeding 2.9 g (asymmetric/rolling) limitation. (6 occurrences)

Appendix J

Operating Limitations – BK 160TR[1]

BLACKSHAPE

BCV-00-38-05

Section 2
OPERATING LIMITATIONS

BK 160TR

SECTION 2
OPERATING LIMITATIONS

2.1 INTRODUCTION

Section 2 includes operating limitations, instrument markings, and basic placards necessary for safe operation of the aeroplane, its engine, standard systems and standard equipment.
The limitations included in this section have been approved by European Aviation Safety Agency.

2.2 AIRSPEED LIMITATIONS

Airspeed limitations and their operational significance are shown below:

	SPEED	KIAS	REMARKS
V_A	Design Maneuvering Speed	128	Do not make full or abrupt deflection of any flight control surface above this speed.
$V_{FE\text{-}LND}$	Max. Flaps Extended Speed	105	Do not exceed this speed with the flap in LND position.
$V_{FE\text{-}T/O}$	Max. Flaps T/O Speed	115	Do not exceed this speed with the flap in TO position.
V_{LE}	Max. Landing Gear Extended Speed	115	Do not exceed this speed with landing gear extended.
V_{LO}	Max. Landing Gear Operating Speed	115	Do not exceed this speed to operate the landing gear.
V_{NE}	Never Exceed Speed	180	Do not exceed this speed in any operation.
V_{NO}	Max. Structural Cruising Speed	155	Do not exceed this speed except in smooth air and then only with caution.

Table 2-1 Airspeed limitations

Rev. 0 10-Jun-2022 2-1

[1] BK 160TR Aircraft Flight Manual (Doc. No.: BCV-00-38-05), pages 2-1 and 2-10.

2.14 APPROVED MANEUVERS

The aircraft is certified in normal category in accordance with EASA CS-VLA regulation. Non-aerobatic operation includes:

(a) Any maneuver pertaining to "normal" flight
(b) Stalls (except whip stalls)
(c) Lazy Eights
(d) Chandelles
(e) Steep turns, in which the angle of bank does not exceed 60°

Recommended entry speeds for each approved maneuver are as follows:

Manoeuvre	Speed (KIAS)
Lazy eight	128
Chandelle	128
Steep turn (max 60°)	128
Stall	Slow deceleration (1 kts/s)

WARNING
Aerobatics maneuvers, including spins and turns with angle of bank of more than 60°, are not approved.

WARNING
Full or abrupt deflection of any flight control surface above V_A (=128 KIAS) could exceed limit loads and lead to damage of the aircraft structure.

WARNING
Avoid prolonged slip ball out. Max. 1 minute.
After slip ball out maneuver return in coordinated flight for at least 1 additional minute.

WARNING
Training stalls to be performed with a minimum entry altitude of 5000 ft AGL, Day VMC.

Appendix K

Flight Parameter Plots for Selected I-POOC Flights[2]

(Manoeuvres Outside Approved Flight Envelope)

1. Flight No 43 enroute to Chiang Mai Air Sports airfield on 08/12/2023.

Manoeuvres: Pull-up at 172 KIAS, n = 3.8 g, then roll to 90°, under high load factor.

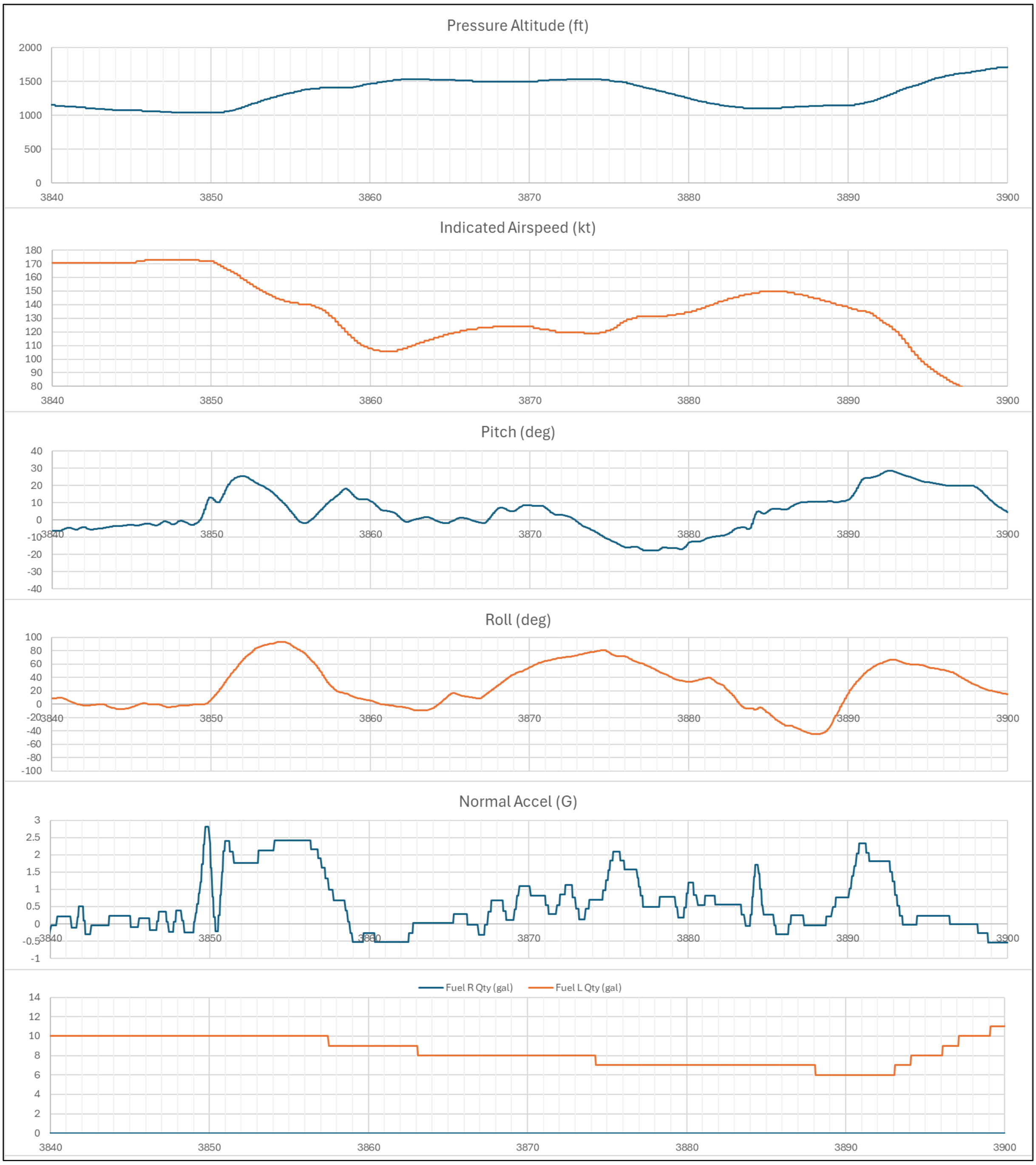

Figure 1

[2] Charts provided courtesy of Blackshape S.p.A.

2. Flight No 45 at Chiang Mai Air Sports airfield on 09/12/2023.

Manoeuvres: Dive from 85 to 137 KIAS, then pull-up to n = 4.3 g plus aileron roll (full aileron with n=3.3). This maneuver was repeated several times in different flights, at speeds below 140 KIAS. Two 360° rolls in this segment (left roll, then right roll).

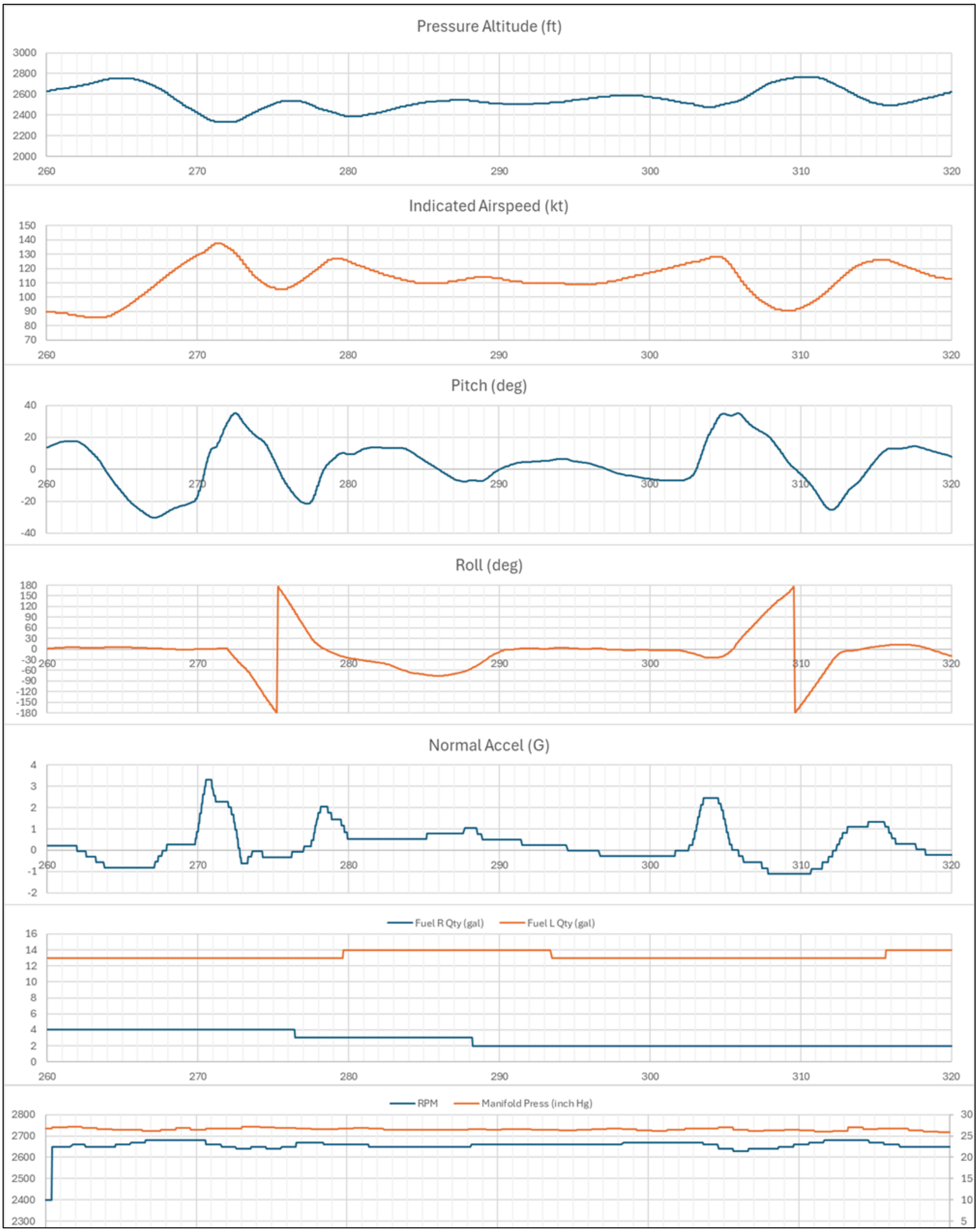

Figure 2

3. Flight No 45 at Chiang Mai Air Sports airfield on 09/12/2023.

Manoeuvres: Dive from 80 to 132 KIAS, then pull-up to n = 3.1 g plus aileron roll. Two 360° rolls in this segment (both, left roll).

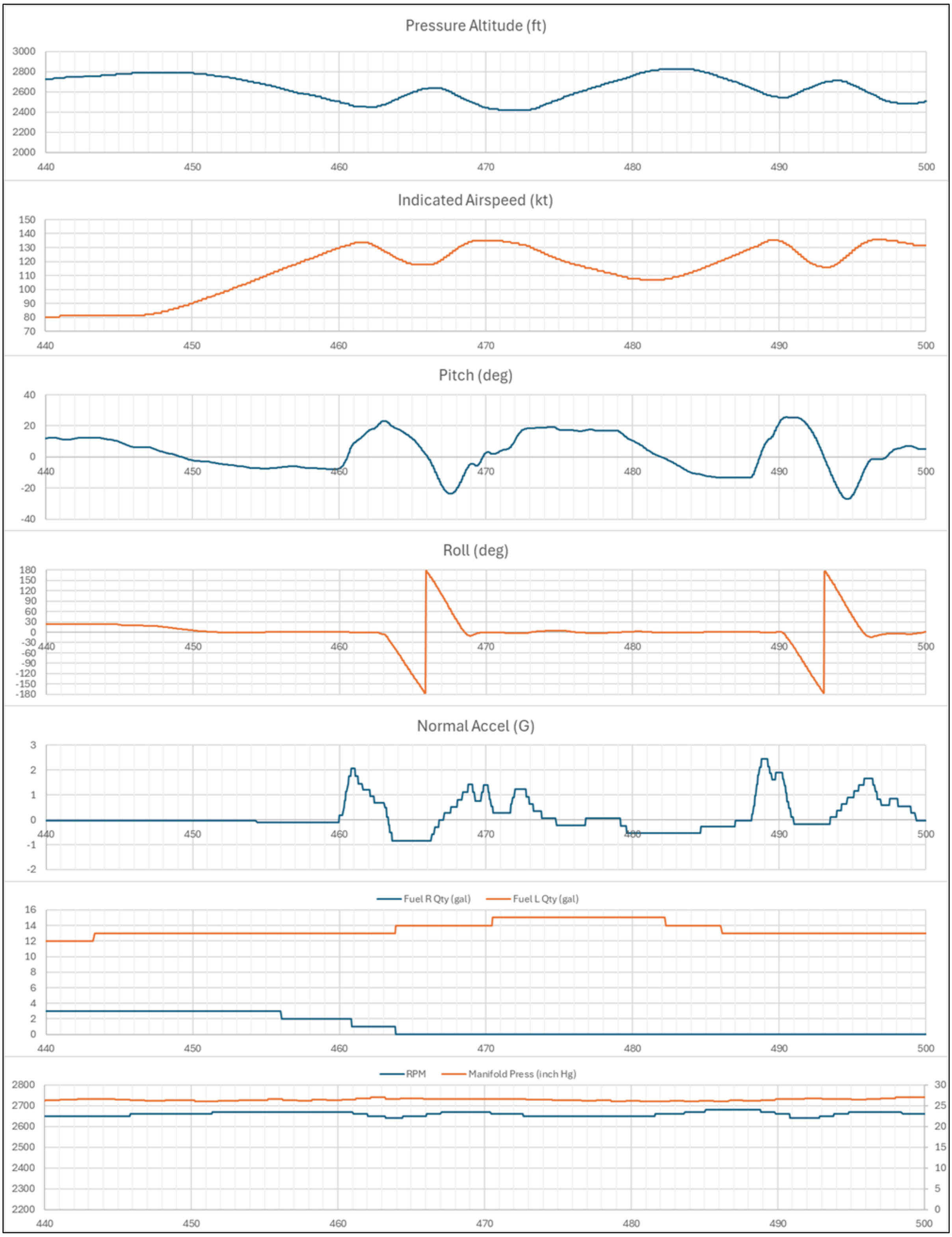

Figure 3

4. Flight No 45 at Chiang Mai Air Sports airfield on 09/12/2023.

Manoeuvres: Dive from 107 to 135 KIAS, then pull-up to n = 3.7 g, then roll to 90° under high load factor.

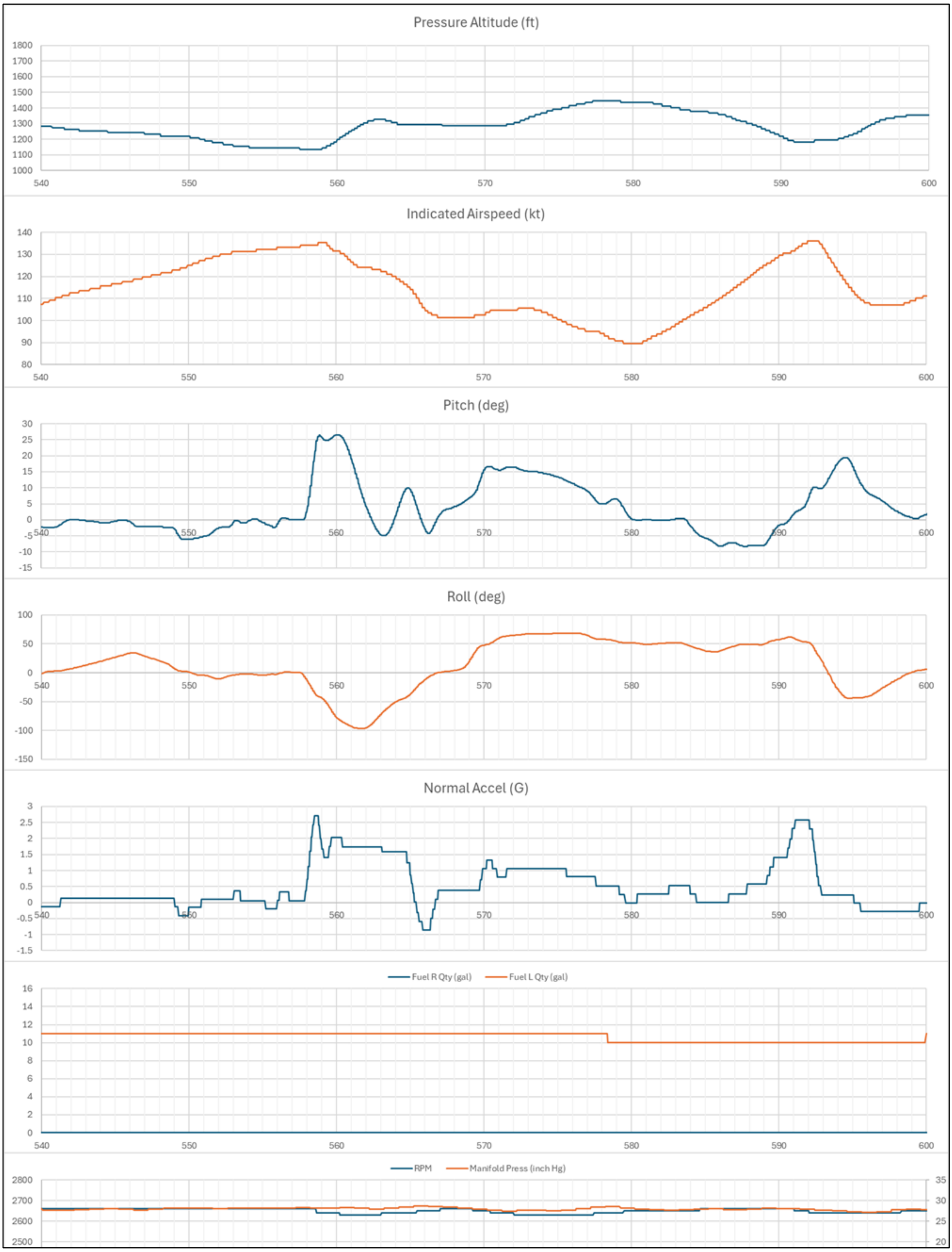

Figure 4

5. Flight No 46 at Chiang Mai Air Sports airfield on 10/12/2023.

Manoeuvres: Dive from 85 to 138 KIAS, then pull-up to n = 3.5 g plus aileron roll. Two 360° rolls in this segment (left roll, then right roll).

Figure 5

6. Flight No 50 at Phuket Airpark on 11/12/2023.

Manoeuvres: Dive from 103 to 157 KIAS, then pull-up to n = 4.0 g.

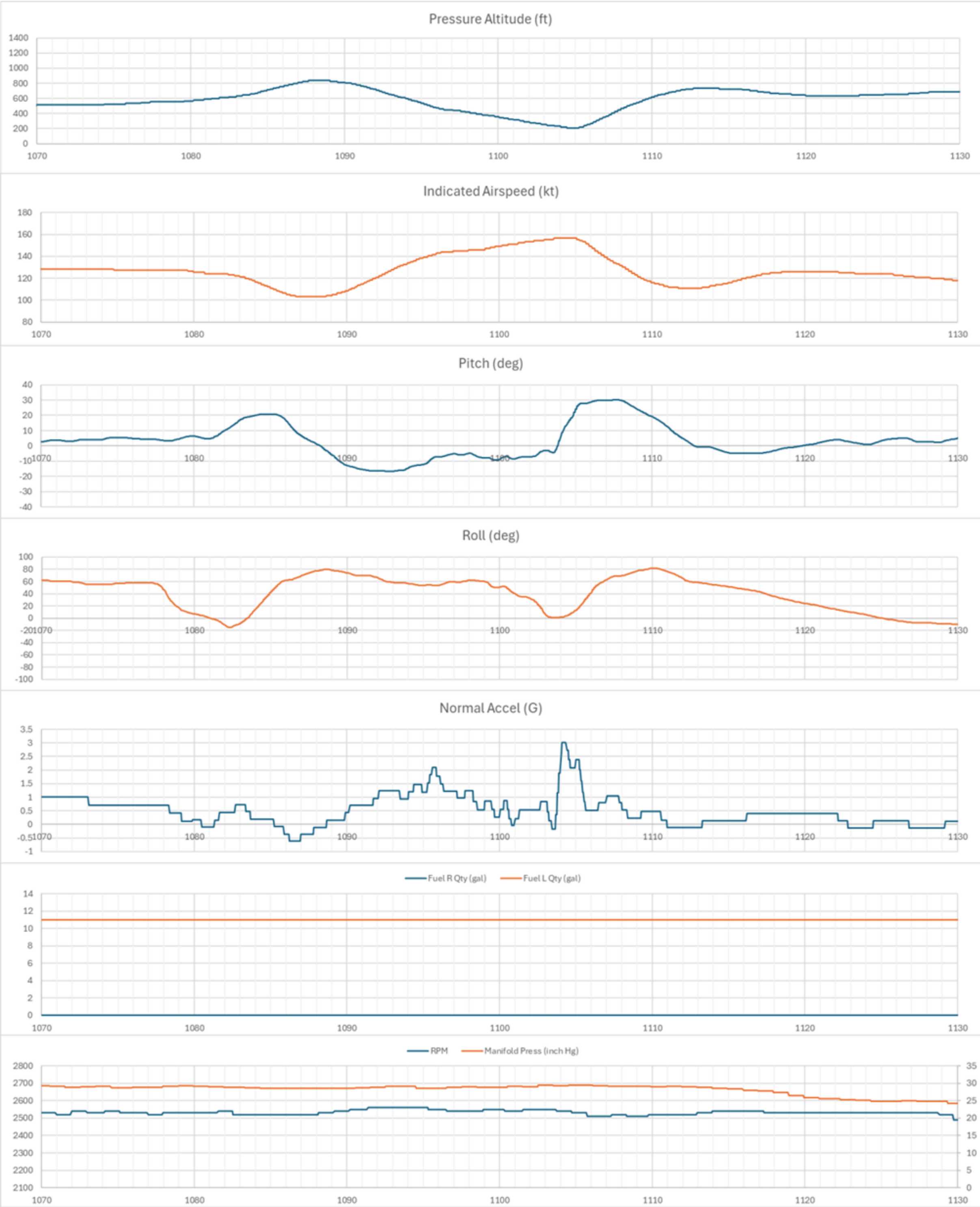

Figure 6

7. Flight No 51 at Phuket Airpark on 11/12/2023.

Manoeuvres: Pull-up at 161 KIAS, n = 4.3 g.

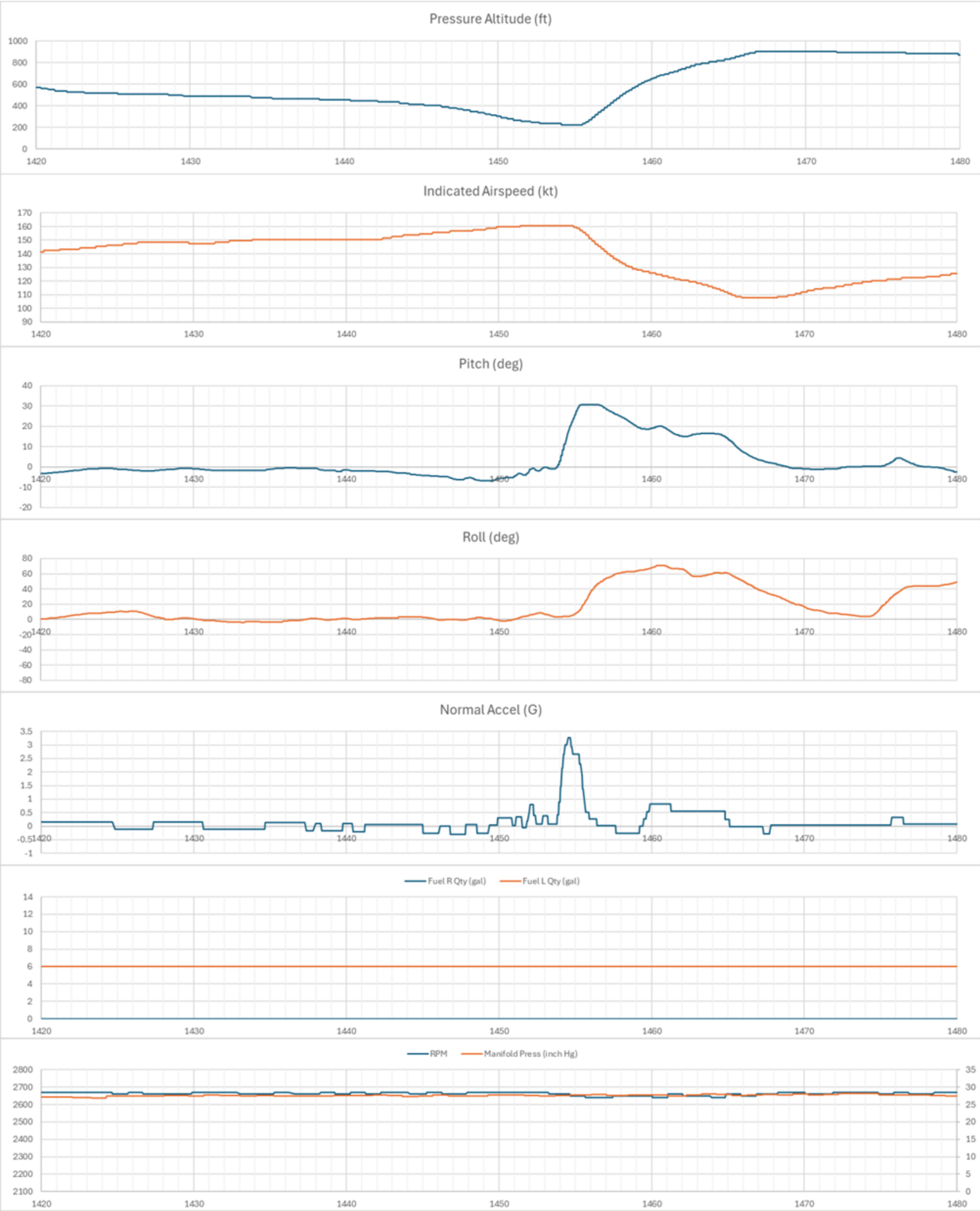

Figure 7

8. Flight No 52 enroute from Phuket Airpark to VTSS on 13/12/2023.

Manoeuvres: Dive from 115 to 158 KIAS, then pull-up to n = 4.6 g.

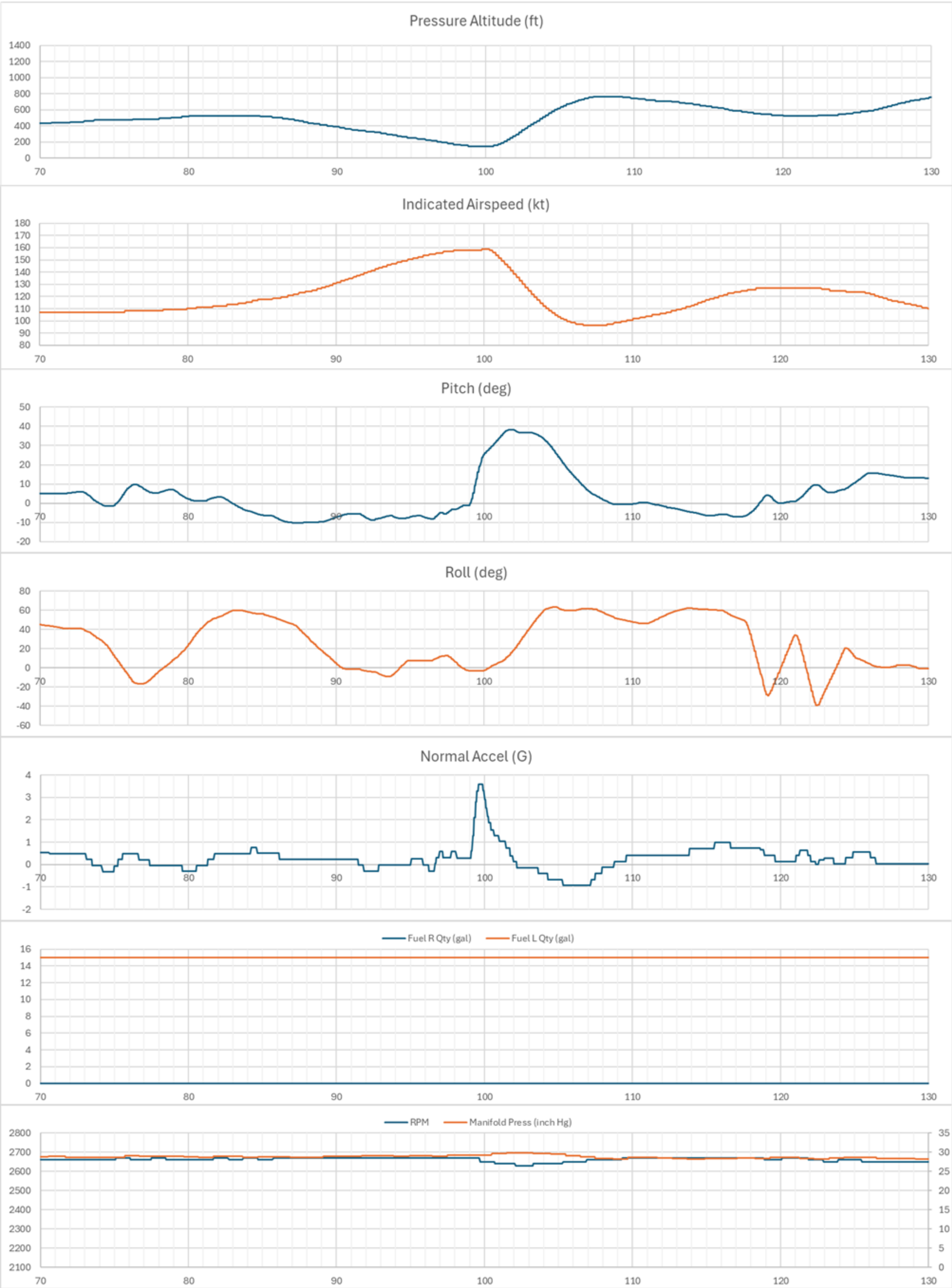

Figure 8

9. Flight No 54 in local area near WMSA on 24/12/2023.

Manoeuvres: Pull-up at 132 KIAS, n = 4.2 g.

Figure 9

Appendix L

BK 160TR – S/N BCV.21010 I-POOC Root Causes Analysis Report[3]

BLACKSHAPE	*APPENDIX* *Root Cause Analysis Report* **BK 160TR - S/N BCV.21010 I-POOC**	Doc. N° OAC-01-2024 Rev. 2 Date 15.04.2024 Page 1 of 31

APPENDIX

Root Cause Analysis Report

BK 160TR - S/N BCV.21010 I-POOC
Root Causes Analysis

[3] Blackshape S.p.A. report issued on 15 April 2024. This appendix includes only excerpts relevant to this investigation, specifically from pages 24 to 28.

	APPENDIX Root Cause Analysis Report BK 160TR - S/N BCV.21010 I-POOC	Doc. N° OAC-01-2024 Rev. 2 Date 15.04.2024. Page 24 of 31

4.6 Calculation of Aileron Loads in case of loss of left-wing lift caused by skin loss.

The aileron load condition was calculated in relation to the failure mode of the aileron as per wreckage inspection report NT/DO – 24001, and taking into account the following contributions due to a scenario of left-wing lift loss:

- Left roll rate due to asymmetric lift.
- Full aileron deflection opposite to the roll rate (stick full right)

The roll rate was calculated at 160 knots (peak speed reported in the radar data), considering the lift on the right wing and no lift on the left wing due to wing skin detachment.
The roll rate generated by the rolling moment is calculated considering the roll damping (ref. BCV-10-52-02):

$$C_{l\frac{pb}{2V}} = -0.485\ 1/rad$$

$$Rolling\ Moment = q\ S'\ b\ C_{l\frac{pb}{2V}}\ \frac{pb}{2V}$$

Where S' is 75% of the wing surface area, to account for left wing skin separation and assuming that some aerodynamic damping is still provided by the left wing remaining structure (spars, ribs, flap).

The resulting roll rate is:

$$p = \frac{Rolling\ Moment}{q\ S'\ b\ C_{l\frac{pb}{2V}}\ \frac{b}{2V}}$$

The aileron load and hinge moment were then calculated as:

$$F_{Ail} = qS_{Ail}\left(C_{FAil_0} + C_{FAil_\alpha}(\alpha + \Delta\alpha) + C_{FAil_{\delta Ail}}\delta_{Ail}\ K_a\right)$$

Where:
$C_{FAil_0} = 0.3096$: aileron force coefficient at zero angle of attack and zero aileron deflection (extracted from BCV-04-51-06)
$C_{FAil_\alpha} = 0.0233\ 1/deg$: aileron force coefficient due to angle of attack (extracted from BCV-04-51-06)
$C_{FAil_{\delta Ail}} = 0.0427\ 1/deg$: aileron force coefficient due to aileron deflection (extracted from BCV-04-51-06)
$S_{Ail} = 0.33\ m^2$: aileron surface
$c_{Ail} = 0.24\ m$: aileron mean geometric chord
$K_a = 0.99$: aileron effectiveness (extracted from USAF TR 5180 Figure 9-16)
$\delta_{Ail} = 13°\ (down)$
$\Delta\alpha = \sin^{-1}\left(\frac{arm\ p}{V}\right)$: increase of angle of attack due to roll rate
$arm = 3.33\ m$, distance between the aircraft centerline and the aileron centerline

All quantities were calculated for increasing angle of attack due to increasing pull-up combined with full right stick. The results of the calculation are reported in the Table 4-3:

Table 4-3 Aileron load calculation in case of left-wing lift loss and increasing local angle of attack due to incremental pull-up

V [kts]	α [deg]	Rolling moment [Nm]	Roll rate p [rad/s]	Δα [deg]	Aileron load F_{Ail} [N]	% Limit Load
160	-1.76	-6562	-0.86	1.99	1184	**137%**
160	0.70	-13361	-1.74	4.04	1328	**154%**

160	3.17	-20160	-2.63	6.11	1473	**171%**
160	5.63	-26958	-3.52	8.19	1618	**187%**

The above results show that the loads occurred to the left aileron being deflected fully down approaches the ultimate load during the incremental pull-up. This means that the load at full stick pull-up would be higher than the ones calculated above, which would have exceeded the ultimate load.

IMPORTANT NOTE: In case of left-wing skin loss, the torsion stiffness is greatly reduced, and the rear "C" shaped spar is exposed to higher deformations (in plane, out of plane, torsion) that would have led to additional stress to the aileron hinges attachment points. Under the loads reported in the table above, this could have caused the complete aileron detachment.

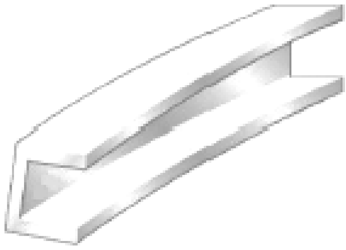

Figure 4-8 Sketch showing deformation of a C shaped spar

From the above evaluations, based on the data available so far, the hypothesis of aileron loss following a full right stick deflection to recover from the left-wing skin loss is considered a plausible scenario.

4.7 Calculation of RH Wing loads after loss of control

The calculation of RH wing loads is made with the hypothesis that after the LH wing skin loss, no lift is produced by the left wing, which would induce a rolling acceleration due to the unbalanced lift. The pilot would then attempt to recover control by applying full aileron RH (to oppose the LH rotation) and by pulling the stick (to recover from loss of altitude). The pull up would have caused a further rolling acceleration to the LH due to the increased lift asymmetry.
The aerodynamic model used for the loads computation is the same used for certification (ref. BCV-10-52-02).
The flight conditions analysed are the following:

- V = 160, 170, 180 kts ref. **NOTE 1**
- RH wing angle of attack $\alpha = \alpha_{stall}$ = 15 deg (taken from BCV-10-52-02) ref. **NOTE 2**
- $\delta_{aileron}$ = 14 deg UP (full stick RH)

In Figure 4-9 is shown a schematic representation of the RH wing condition and its span corresponding to the break-up location for which the load is calculated:

[1] With reference to the radar ground speed data of Figure 2-2 the value has been increased incrementally in the hypothesis that the aircraft accelerated beyond 160 kts due the rapid loss of altitude as recorded by the altitude radar data of Figure 2-1.
[2] It is supposed that the pull-up brought the RH wing to the maximum angle of attack (maximum lift coefficient), while the LH wing was stalled due to the loss of the skin.

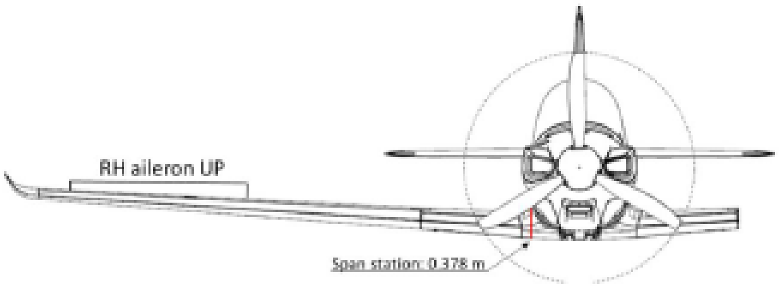

Figure 4-9 Schematic representation of the RH wing condition and its span corresponding to the break-up location for which the load is calculated

Aerodynamic contributions

Two separate aerodynamic contributions are considered in conjunction: angle of attack and aileron deflection. The aerodynamic coefficients to calculate the loads of are taken from BCV-10-52-02 at table 7, table 9, table 11 at span of 0.378 m of the RH wing.

Table 4-4 Separate aerodynamic contributions to the RH wing load

Airspeed [EAS]	Wingspan station [m]	Angle of attack contribution			Aileron deflection contribution			Aerodynamic Total		
		Shear [N]	Bending [Nm]	Torsion [Nm]	Shear [N]	Bending [Nm]	Torsion [Nm]	Shear [N]	Bending [Nm]	Torsion [Nm]
160 kts	0.378 (RH wing)	28340	47672	-16421	-3274	-6315	2548	25066	41357	-13873
170 kts	0.378 (RH wing)	31994	53817	-18537	-3696	-7129	2877	28298	46688	-15661
180 kts	0.378 (RH wing)	35868	60334	-20782	-4144	-7992	3225	31725	52342	-17558

	APPENDIX	Doc. N° OAC-01-2024
BLACKSHAPE	*Root Cause Analysis Report*	Rev. 2 Date 15.04.2024.
	BK 160TR - S/N BCV.21010 I-POOC	Page 27 of 31

Inertial contribution

The inertial contribution is given by the rolling acceleration, generated by the unbalanced lift (100% lift on the RH wing / 0% lift on the LH wing) and the aileron deflection RH (opposite to the rotation).

The unbalanced lift generates a rolling moment as shown in Figure 4-10, while the aileron deflection generates a rolling moment in the opposite direction. Both contributions are considered to calculate the rolling acceleration as shown below:

$$\dot{p} = \frac{Roll\ mom + qSbC_{l\delta_{all}}\delta_{all}}{I_{xx}}$$

Where:
I_{xx} = 1146 kgm², is calculated considering full fuel in both tanks
The coefficient $C_{l\delta_{all}}$ is taken from BCV-10-52-02

The roll moment is calculated considering the difference between the lift of the RH wing and the lift of LH wing, considered equal to 0 for the loss of the skin.

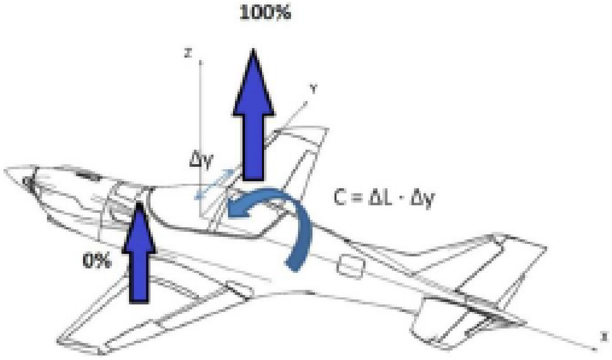

Figure 4-10 Rolling moment generated by unbalanced lift

The rolling acceleration inertial coefficients to calculate the inertial loads of Table 4-5 are taken from BCV-10-52-02 at table 3.

Table 4-5 Inertial RH wing load

Airspeed [EAS]	Rolling acceleration $\dot{p}$ [rad/s²]	Wingspan station [m]	Inertial contributions due to rolling acceleration		
			Shear [N]	Bending [Nm]	Torsion [Nm]
160 kts	23.9	0.378 (RH wing)	-2061	-4259	1724
170 kts	26.9	0.378 (RH wing)	-2327	-4808	1947
180 kts	30.2	0.378 (RH wing)	-2609	-5390	2182

The sum of the aerodynamic and inertial contributions give the total net load on the RH wing as reported in the Table 4-6 at the span equal to 0.378 m, i.e. the RH wing root. The computed loads corresponding to the RH wing root are then compared with the limit loads at the same wing-span station taken from BCV-10-52-02.

Table 4-6 Net RH wing load

Airspeed [EAS]		Limit Load (ref. BCV-10-52-02)	Calculated RH wing Load	% Limit Load
160 kts	Shear [N]	13505	23005	170%
	Bending [Nm]	23945	37098	155%
	Torsion [Nm]	-7013	-12148	173%
170 kts	Shear [N]	13505	25970	192%
	Bending [Nm]	23945	41880	175%
	Torsion [Nm]	-7013	-13714	196%
180 kts	Shear [N]	13505	29116	216%
	Bending [Nm]	23945	46952	196%
	Torsion [Nm]	-7013	-15375	219%

As shown in the Table 4-6 **the computed loads approach and exceed the ultimate loads of the certification, which is compatible with the occurred in-flight break-up.**

Appendix M

Comments on the Draft Final Report [4]

Comments from ANSV

Draft Final Report Section/Paragraph	Comments	AAIB's Response
2.2.4 Composite Material Analysis Page 53, paragraph 2.2.4: "**Material Degradation**. FTIR and TGA analyses indicated hydrolytic degradation in the epoxy resin matrix of the CFRP material, likely due to prolonged exposure to high humidity. This degradation weakened the resin's structure, potentially reducing its load-bearing capacity."	We propose the following modification (ref: NT-DO-24/2002 Rev.1 The wreckage has been found contaminated by water. The presence of hydrolysis is more likely to be attributable to water contamination that occurred after the crash, during the wreckage's cleaning process and subsequent conservation.): "FTIR and TGA analyses indicated hydrolytic degradation in the epoxy resin matrix of the CFRP material, likely due to prolonged exposure to high humidity. This occurred mainly in the aftermath of the accident during cleaning and conservation of the wreckage. This degradation weakened the resin's structure."	Partially agreed. The substance of the agreed portion is incorporated into the report. The proposed revision regarding hydrolytic degradation is acknowledged, particularly the consideration that wreckage cleaning and post-accident conservation may have contributed to the material's condition. However, hydrolysis cannot be attributed solely to post-accident factors, as multiple pre-existing conditions could have facilitated moisture ingress before the accident. The I-POOC composite structure was subjected to significant operational overload, potentially causing microcracking in the resin matrix and delamination, creating pathways for moisture ingress. Stress concentration areas, particularly at joints and load-bearing sections, are known to be prone to such degradation, further increasing susceptibility. Additionally, man-made holes in the structure would have compromised its protective barrier, providing direct entry points for moisture and accelerating hydrolytic effects.

[4] In accordance with paragraph 6.3 of ICAO Annex 13, comments to the Final Report are appended if desired by the commenting State. Only non-editorial-specific, technical aspects upon which no agreement could be reached are appended. ANSV has requested that its disagreed comments be appended.

Draft Final Report Section/Paragraph	Comments	AAIB's Response
		While post-accident wreckage handling may have contributed to hydrolytic degradation, it is not the sole cause. The combined effects of operational overload and structural compromise strongly indicate that hydrolysis was already occurring before the accident. A balanced assessment should consider both pre- and post-accident factors.
2.2.4 Composite Material Analysis Page 54, paragraph 2.2.4 "The analysis of the I-POOC airframe's composite materials identified several factors that compromised its structural integrity, including material degradation due to hydrolysis and thermal aging, variability in mechanical properties, and internal defects such as voids and microcracks in critical areas. These weaknesses were compounded by stress concentrations from uncertified modifications, such as the tie-down rings installed through man-made holes, and operational overload. Together, these factors likely accelerated the failure of critical components, ultimately contributing to the inflight separation and the accident."	We propose deleting this above indicated part: the reason is that the SIRIM lab test results are based on samples not representative of the airframe status before the crash, since the wreckage and its parts have been contaminated by water. For this reason, they cannot definitively be used to conclude that the airframe presented defects that could have contributed to the inflight separation.	Partially agreed. The substance of the agreed portion is incorporated into the report. While the significance of post-accident exposure on the wreckage is acknowledged, the findings related to material degradation due to hydrolysis, thermal aging, and mechanical variability should not be disregarded. Degradation mechanisms such as hydrolysis and aging can develop over time, potentially affecting the material's structural integrity. It is agreed that the SIRIM test samples were subjected to environmental factors, crash impact damage, and operational overload, which complicate the interpretation of the results. Therefore, it is necessary to retain this paragraph with amendments to more accurately reflect the influence of post-accident conditions on the material analysis. The amended paragraph recognises that while the observed degradation may have been exacerbated by post-accident exposure, further investigation is required to determine the extent to

Draft Final Report Section/Paragraph	Comments	AAIB's Response
		which these factors influenced the pre-crash structural condition.
2.2.4 Composite Material Analysis Page 54, paragraph 2.2.4 "It is important to note that the SIRIM composite material test samples, taken from accident wreckage, were exposed to operational overload, crash impact damage, and environmental factors before and after the crash. These conditions contributed to material degradation that may not be present in factory-prepared samples used for qualification testing. While the SIRIM results offer insights into the I-POOC composite material's real-world durability before and they may not fully reflect the properties of pristine samples used in the manufacturer's qualification tests. Additionally, structural damage from man-made perforations in the aircraft wings, including cracking and delamination, further complicates direct comparison with factory qualification results."	We propose the following modification (ref: NT-DO-24/2002 Rev.1): "It is important to note that the SIRIM composite material test samples, taken from accident wreckage, were exposed to operational overload, crash impact damage, and environmental factors after the crash. Since these conditions are not present in the factory, where the manufacturing process of composite structures is under strict control and carried out in accordance with approved process specifications, it is not possible to conclude that the test samples taken from the wreckage are representative of the aircraft structure before the accident. Additionally, structural damage from man-made perforations in the aircraft wings, including cracking and delamination, further complicates direct comparison with factory qualification results."	Partially agreed. The substance of the agreed portion is incorporated into the report. The influence of post-accident exposure is acknowledged. While crash impact, operational overload, and environmental factors affected the test samples, they do not invalidate the material analysis. The SIRIM test offers valuable insights into real-world degradation, making its results relevant to understanding the composite material's durability. Factory-prepared samples undergo strict controls and are not exposed to such conditions. However, wreckage samples still provide a realistic perspective on how the material performed under operational stresses. While the results require cautious interpretation, they remain useful for assessing in-service degradation. Additionally, structural damage from man-made perforations, including cracking and delamination, significantly affected airframe integrity. These defects, regardless of post-accident conditions, must be considered when comparing with factory qualification results. Thus, while careful interpretation is warranted, the test data remains essential for a comprehensive assessment, with appropriate caveats.

Draft Final Report Section/Paragraph	Comments	AAIB's Response
2.3.5 Composite Material Integrity and Possible Defects Page 58, paragraph 2.3.5 "Prolonged exposure to excessive loads accelerates fatigue in composite structures, highlighting the importance of adhering to operational limits for structural longevity and safety. Repeated prohibited manoeuvres and operational exceedances placed undue stress on the I-POOC's composite structure, accelerating fatigue in the CFRP material. While CFRP is generally resilient, excessive loading can lead to delamination, microcracking, and other fatigue-related damage, as identified in SIRIM's analysis. Notwithstanding the finding that the I-POOC's composite material was compromised due to operational stress, it is important to exercise caution. Some of the observed structural degradation may have resulted from factors unrelated to operational stress. While the SIRIM test samples were taken from accident wreckage and may not fully reflect the properties of factory-prepared material, there are valid concerns regarding potential manufacturing defects—such as incomplete curing or voids in the laminate layers—that could introduce weak points, making the material more susceptible to stress-related damage. Given this uncertainty, it is crucial to	We propose the following modification (the reason is that the SIRIM lab test results are based on samples not representative of the airframe status before the crash since the wreckage and its parts have been contaminated by water. For this reason, they cannot definitively be used to conclude that the airframe presented defects that could have contributed to the inflight separation.): "Prolonged exposure to excessive loads accelerates fatigue in composite structures, highlighting the importance of adhering to operational limits for structural longevity and safety. Repeated prohibited manoeuvres and operational exceedances placed undue stress on the I-POOC's composite structure, accelerating fatigue in the CFRP material. Excessive loading can lead to delamination, microcracking, and other fatigue-related damage, as identified in SIRIM's analysis. In summary, excessive loads accelerate fatigue in composite materials, and repeated operational exceedances contributed to the degradation of the I-POOC's CFRP material."	Partially agreed. The substance of the agreed portion is incorporated into the report. The importance of excessive loading as a primary factor in the degradation of the composite material is acknowledged and remains central to the findings. The revised text maintains this emphasis while ensuring a balanced assessment. The concern that the SIRIM test samples were taken from wreckage exposed to post-accident environmental conditions, including water contamination, is recognised. This factor has been reflected in the report, with caution in interpreting the results. While these conditions complicate direct comparisons with factory-prepared material, they do not invalidate the observations, as they provide insights into real-world degradation mechanisms. Regarding potential manufacturing defects, the revised text reflects that these cannot be entirely ruled out, but operational exceedances were the primary contributors to material degradation. This cautious approach ensures all plausible factors are considered without overstating manufacturing-related issues. Thus, while ANSV's emphasis on operational stresses as the dominant factor is acknowledged, the final wording appropriately accounts for the complexities introduced by post-accident conditions and the slight possibility of material inconsistencies. The revised text provides a fair and balanced reflection of the available evidence.

Draft Final Report Section/Paragraph	Comments	AAIB's Response
conduct a thorough review to address any doubts regarding potential internal defects in the material of the BK 160TR aircraft type and ensure the integrity of the composite structure in the existing flee. In summary, excessive loads accelerate fatigue in composite materials, and repeated operational exceedances contributed to the degradation of the I-POOC's CFRP material. While operational stress played a major role, the possibility of manufacturing defects, however slight, should not be overlooked. Given the limitations of the SIRIM test samples, further review is essential to ensure the integrity of the composite structure in the existing BK 160TR fleet."		
3.0 Conclusion (Organisation) Page 74, paragraph 3.1.4.1	We propose the following modification (the reason is that is important to emphasize that the disputes over the transfer of ownership of the aircraft arose exclusively from Sky Media's indecisiveness over the company that would have registered the aircraft in its own name and, as a consequence, cannot be attributed to Blackshape S.p.A.'s willful misconduct or negligence. According to ENAC regulations, and as argued by Blackshape S.p.A, the aircraft could only be registered in the name of the purchaser, Sky Media, which received the aircraft and paid for it in full. The issue arose from Sky Media's reluctance to register the aircraft in its own name in Singapore, accordingly to the contract signed and the payment received by Blackshape. Instead, Sky Media proposed or to register the aircraft in Romania in the name of the Company owned by [identities of persons	Partially agreed. The substance of the agreed portion is incorporated into the report. The proposed revision is acknowledged, but the original finding is retained with a slight modification of the text to align with the safety-focused objectives of the investigation. While the investigation does not address the specifics of the unresolved disputes, the original finding highlights their impact on operational safety. The focus is on how these disputes created gaps in accountability for the aircraft's maintenance and condition, which are directly relevant to safety concerns. As an Annex 13 safety investigation, the report identifies factors compromising safety, not issues

Draft Final Report Section/Paragraph	Comments	AAIB's Response
"Blackshape S.p.A. failed to ensure the aircraft's operational safety due to unresolved disputes with Sky Media and did not facilitate a proper transfer of ownership, creating gaps in accountability for its maintenance and condition."	redacted] (possibility not legally actionable, as confirmed by the Blackshape notary involved on several occasions by our Company to try to resolve the problem of the transfer of ownership) or to register the aircraft in the name of AST, so creating uncertainties regarding accountability for the maintenance and condition of the aircraft. These uncertainties were further increased, as correctly reported in section 1.17.3. above, by (i) Sky Media's decision to appoint AST as subject entitled to provide marketing and promotional services and (ii) the circumstance that AST was identified or implied as the owner and/or operator of the aircraft in various documents.): "Blackshape S.p.A. experienced difficulties in transferring ownership of the aircraft due to unresolved disputes with Sky Media."	of blame or liability. The lack of a proper transfer of ownership and resulting uncertainties regarding accountability were significant to the aircraft's safety, and the original wording accurately reflects this. Therefore, while the disputes are outside the scope of the investigation, the finding remains relevant in addressing organisational factors that contributed to gaps in accountability, crucial for the ongoing safety of the fleet.
4.0 Safety Recommendations Page 78, paragraph 4.4.1 "Blackshape is recommended to adopt a cautious approach in reviewing the structural integrity of the BK 160TR aircraft, particularly concerning the composite material used in the I-POOC. While the likelihood of material issues may be low, a thorough assessment of potential airworthiness concerns is essential to ensure the continued structural integrity of the existing fleet."	We propose deleting the above Safety Recommendation: the ANSV is in disagreement with the fore mentioned Safety Recommendation, for the reason that this statement has no technical related function since it does not identify specific issues that could provide the manufacturer with specific actions to elevate the airplane safety.	Disagreed. The recommendation remains relevant and necessary based on the investigation's findings and conclusions. While operational stresses were identified as the dominant factor in the composite material's degradation, the investigation highlights the need for a cautious approach to the structural integrity of the BK 160TR fleet. The potential for long-term operational risks and possible material inconsistencies warrants further assessment to ensure continued airworthiness.

Draft Final Report Section/Paragraph	Comments	AAIB's Response
		The recommendation does not at all imply a widespread fleet issue but advocates for a proactive review of the aircraft's structural integrity, with particular focus on the composite material used in the I-POOC. Given evidence of fatigue and degradation under exceedance conditions—as well as the slight possibility of manufacturing defects—a cautious, ongoing approach is warranted. This provides the manufacturer with actionable guidance to monitor and manage the fleet's composite integrity, helping to prevent undetected degradation that could affect airworthiness over time. In summary, the recommendation serves as a precautionary measure aligned with the broader objective of ensuring the continued safety of the BK 160TR fleet. Retaining it reinforces the importance of structural monitoring and proactive risk management.